NMR STUDIES OF CARBOHYDRATES IN THE SOLID STATE

by

TANG KUAN LIM

B.Sc. (Hons.), University of Malaya, Malaysia, 1977

A THESIS SUBMITTED IN PARTIAL FULFILMENT OF

THE REQUIREMENTS FOR THE DEGREE OF

DOCTOR OF PHILOSOPHY

in

THE FACULTY OF GRADUATE STUDIES

(Department of Chemistry)

We accept this thesis as conforming

to the required standard

THE UNIVERSITY OF BRITISH COLUMBIA

November 1985

In presenting this thesis in partial fulfilment of the requirements for an advanced degree at the University of British Columbia, I agree that the Library shall make it freely available for reference and study. I further agree that permission for extensive copying of this thesis for scholarly purposes may be granted by the head of my department or by his or her representatives. It is understood that copying or publication of this thesis for financial gain shall not be allowed without my written permission.

Department of CHEMISTRY

The University of British Columbia
1956 Main Mall
Vancouver, Canada
V6T 1Y3

Date 17/12/85

ABSTRACT

The work described herein entails the application of solid-state n.m.r. methods to both mono- and polysaccharide carbohydrates. Two major n.m.r. methods have been evaluated for studying these substances, namely, the carbon-13 cross-polarization-magic angle spinning method and the deuterium quadrupole echo method.

Heptakis-(2,6-di-O-methyl)-β-cyclodextrin and β-cyclodextrin peracetate were prepared and, together with α- and β-cyclodextrins as hosts, were used to encage a variety of organic guest molecules.

A number of metal sugar conjugates were prepared according to the procedures documented in this laboratory. Firstly, chelate coordination complexes were synthesized by forming salicylaldimine ligands derived from combinations of amino sugars (methyl 3,4,6-tri-O-acetyl-2-amino-2-deoxy-β-D-glucopyranoside or 1,3,4,6-tetra-O-acetyl-2-amino-2-deoxy-β-D-glucopyranose) and salicylaldehyde, with subsequent complexation of these to copper(II), zinc(II), and cobalt(II) ions. Similarly, chitosan Schiff's bases were prepared and complexed to copper(II) ion.

Application of the ^{13}C-cross-polarization-magic angle spinning method in the spectral assignment of cyclodextrin inclusion complexes and metal sugar conjugates in the solid state has been demonstrated. In all cases, recourse to solution spectra was necessary for correct assignments of individual carbon resonances. The sugar resonances of

cyclodextrins are relatively broad and are complicated by the substantial splittings. The rationales for such observations were drawn from comparative studies, based on closely related guest molecules. The smaller guest molecules were least affected by the cavity size of the host molecule heptakis-(2,6-di-O-methyl)-β-cyclodextrin and the isotropic chemical shift values were similar to those measured for solutions. These values suggest that the guest molecules undergo anisotropic motion, which can be detected by the use of the dipolar dephasing technique. Studies of metal sugar conjugates by ^{13}C n.m.r. revealed that paramagnetic ions have profound effects on the resolution obtained. The high concentrations of these ions result in broad featureless spectra. On the other hand, the diamagnetic ions proved to have little effect on the isotropic chemical shifts of the sugar chelates.

The deuterium quadrupole echo method has been used specifically to study the mobility of the guest molecules encaged in cyclodextrins. The "powder-type" spectra obtained were then compared with results reported in the literature in order to define the types of molecular motion.

TABLE OF CONTENTS

LIST OF TABLES

Table

LIST OF FIGURES

Figure

CHAPTER II

ACKNOWLEDGEMENT

I express my gratitude to Dr. L. D. Hall for his guidance and constant encouragement throughout the course of this work.

While it is impossible to thank all those who contributed to the completion of this thesis, I am truly indebted to Dr. A. Naito for many helpful discussions. It is also a pleasure to thank Messrs. L. Talagala, V. Rajanayagam, K. Holme and S. Luck for proof-reading the manuscript.

Finally, special thanks are due to Mr. K. Sukul and others in the electrical shop of this department for their expert technical back-up.

Dedication

To my late Father

INTRODUCTION

Carbohydrates are amongst the most abundant types of molecule in nature, and they play a vital role in every form of life. In recent years, many new examples of their important biomedical and industrial applications have been unravelled; these include the development of new pharmaceuticals[1] and chromatography materials,[2] and their use in oil recovery.[3] These and other areas (not mentioned here) would benefit from the development of general methodologies in which carbohydrates can be chemically modified. In turn, this requires the development of new spectroscopic tools for evaluating the physical and chemical properties of what are frequently intractable materials. In this thesis, emphasis was placed on the latter area, and n.m.r. spectroscopy has been used extensively throughout the course of the work.

Proton and carbon-13 nuclear magnetic resonance (^{1}H-n.m.r. and ^{13}C-n.m.r.) spectroscopy have previously been shown to be useful for the characterization of carbohydrates[4] in solution. Both mono- and poly-saccharide chemistry have benefited from both these methods for studying the structure and function of the "natural" and "modified" forms of these materials. Unfortunately, ^{1}H-n.m.r. spectroscopy as a method for studying polysaccharides suffers because the resonances are excessively broad.[5] Fortunately, this problem is somewhat less severe for ^{13}C n.m.r., and the wide range of chemical shifts (>200 parts per million) for the carbon resonances

generally allows assignments to be made for the resolvable, individual peaks in most spectra.[6] A minor shortcoming of this method is that the ^{13}C-n.m.r. spectrum of a saccharide cannot be directly interpreted without comparison with spectra of known compounds. This is compensated by the wealth of information provided for molecular structure, especially on the nature of the anomeric linkages for the specific types of residues.

Unfortunately, there are many instances where the structural characterization of carbohydrates cannot be aided by the normal high-resolution Fourier transform (F.t.) ^{1}H- and ^{13}C-n.m.r. approaches. This is the situation for samples which cannot be dissolved under conditions that would retain their structural integrity, or where there is the possibility that solvent-solute interactions could completely change the molecular structure or conformation. Finally, high-resolution n.m.r. methods are ill-suited for studies of polysaccharides that are of low solubility or that are insoluble. In the latter situation, no resonance signal is observed by normal F.t. n.m.r. techniques for the following practical reasons: "line-broadening", caused by anisotropic dipole-dipole interactions and chemical shift anisotropy, and "low-sensitivity" associated with the extremely long ^{13}C spin lattice relaxation times.

It is now well known that such problems can be largely overcome by the combined use of high power decoupling[7] (to remove ^{13}C-^{1}H dipolar coupling), magic angle spinning[8] (to

remove chemical shift anisotropy), and cross-polarization[9] (to overcome ^{13}C sensitivity problems). As a result, ^{13}C n.m.r. measured in the solid state can prove useful for chemical and structural investigations of organic molecules in the solid state. Many modifications[10] of the basic methods have been reported, which further facilitate solid-state studies. The methodology of solid-state n.m.r. spectroscopy complements single-crystal structural analysis in that it is capable of confirming the correctness of existing X-ray structures. The growing popularity of this method is dominated by the ease of sample handling, and the reduced time needed to acquire a spectrum.

The main theme of this Thesis consists of the application of solid-state n.m.r. methods to both mono- and poly-saccharide carbohydrates. Two major n.m.r. methods have been evaluated for studying these substances; these are the carbon-13 cross-polarization-magic angle spinning (^{13}C-c.p.-m.a.s.) method[11] referred to above, and the deuterium (^{2}H) quadrupole echo method.[12] The latter method is used specifically to study the anisotropic motion of molecules. The resolution, sensitivity, as well as the theory of the c.p. and c.p.-m.a.s. methods, will be discussed in some detail in the first part of Chapter I; the second part describes briefly the theory of solid-state ^{2}H n.m.r. pertinent to randomly oriented samples.

Our initial motivation was to study the molecular mobilities of some saccharide systems which might have

potential practical use as pharmaceuticals. Cyclodextrins were the obvious initial choice because of their known ability to form inclusion complexes,[13] and their selective catalytic activity.[14] These substances are macrocyclic glucose polymers produced by the action[15] of Bacillus macerans amylase on starch. Interestingly, complexes of drugs and insecticides with cyclodextrins often exhibit physicochemical and biochemical properties, which are not shown in the absence of the cyclodextrin. For that reason, extensive studies by solution-state n.m.r. spectroscopy of both "inclusion" and "catalysis" of cyclodextrins have been described[16] in the last decade. However, no such studies had been made in the solid state and it was decided to focus our attention on the molecular reorientation of the inclusion complexes of α- and β-cyclodextrins in the solid state. Considerable advances in the formulation of theories on the effect of various dynamic modes on ^{2}H-n.m.r. lineshapes had already been made, and more were anticipated, which would enable us to analyze our results qualitatively. As will be seen, the preparation of suitable complexes has involved a number of deuterated guest molecules, aromatic or otherwise, with cyclodextrins and some of their derivatives. Overall, the series of compounds prepared has been used to establish a relationship between motion, structure, and stability.

We were enticed into making further explorations with solid-state n.m.r. by the slow growth in early 1981 of the

application of c.p.-m.a.s. methods to chemical problems. At that time, most of the literature reports were centered on the techniques themselves, or on investigations of a more physical nature. In contrast, it was decided that this thesis should encompass a broad discussion, from an organic chemist's viewpoint, of the types of chemical information that may be derived from the ^{13}C spectra of carbohydrates. Elucidation of the structures and motion of cyclodextrin inclusion complexes would, besides constituting an important and interesting chemical problem in its own right, help illustrate broader opportunities. Chapter II of this Thesis is devoted mainly to solid-state n.m.r. studies of cyclodextrins and their inclusion complexes.

It was felt that it was desirable to make comparative studies with another class of inclusion complexes and Dianin's compound was chosen because complexes analogous to those of cyclodextrins could be readily synthesized.[17] This will be discussed as a sub-section of Chapter II.

Chapter III, summarizes the application of solid-state n.m.r. methods to another area which has previously been of interest at U.B.C., namely, metal-sugar conjugates. The interaction of various metals and sugars has previously been studied in solution by n.m.r., and by electron spin resonance (e.s.r.) in both solution and solid state. The work described in this Thesis represents an initial effort to adapt some of the experience previously gained during the work of Chapter II to the use of metal ions for partial

assignment of ^{13}C-c.p.-m.a.s. spectra. Schiff's bases formed from amino derivatives of mono- and poly-saccharides were the main focus of those studies since an extensive knowledge of their chelating properties had been previously established.[18] Since copper(II) complexes were used, this work led to the evaluation of the paramagnetic effects of copper(II) ion on the sugars in the solid state. The syntheses of the specific metal-sugar compounds involved extensions of procedures previously documented in this laboratory.

References

1. H. H. Baer, J. L. Strominger, The Amino Sugars, The Chemistry and Biology of Compounds Containing Amino Sugars, Academic Press, New York, IA, 1969; R. L. Whistler, Industrial Gums, Polysaccharides and Their Derivatives, Academic Press, New York, 1973.

2. H. F. Hixson, E. P. Goldberg, Polymer Grafts in Biochemistry, Dekker, New York, 1976.

3. R. L. Whistler, Industrial Gums, Academic Press, New York, 1973; C. T. Githens, J. W. Burnham, Society of Petroleum Engineers Journal, 17, 5(1977); R. Tiner, Southwestern Petroleum Short Course Proceedings, 23, 1976; B. Sandiford, Energy Communications, 4, 53(1978); H. E. Gilliland, ibid., 4, 83(1978).

4. A. S. Perlin, G. K. Hamer, ACS Symp. Ser. No. 103, 1979, 123.

5. A. S. Perlin, B. Casu, G. R. Sanderson, L. F. Johnson, Can. J. Chem., 48, 2260(1968).

6. A. Darke, E. G. Finer, R. Moorhouse, D. A. Rees, J. Mol. Biol., 99, 477(1975).

7. F. Bloch, Phys. Rev., 111, 841(1958); L. R. Sarles, R. M. Cotts, ibid., 111, 853(1958).

8. E. R. Andrew, Prog. Nucl. Magn. Reson. Spectrosc., 8, 1(1971).

9. S. R. Hartmann, E. L. Hahn, Phys. Rev., 128, 2042(1962).

10. D. A. Torchia, J. Magn. Reson., 30, 613(1978); J.

Tegenfeldt, U. Haeberlen, ibid., 36, 453(1979); S. J. Opella, M. H. Frey, J. Am. Chem. Soc., 101, 5854(1979).

11. J. Schaefer, E. O. Stejskal, ibid., 98, 1031(1976).
12. J. Davis, K. Jeffrey, M. Bloom, M. Valic, T. Higgs, Chem. Phys. Lett., 42, 390(1976).
13. F. Cramer, Chem. Ber., 86, 1576(1953).
14. F. Cramer, W. Saenger, H.-Ch. Spatz, J. Am. Chem. Soc., 89, 14(1967).
15. D. French, Adv. Carbohydr. Chem., 12, 189(1957); F. Schardinger, Zentralbl. Bakteriol. Parasitenkd. Infektionskr. Hyg. II, 29, 188(1911).
16. J. P. Behr, J. M. Lehn, J. Am. Chem. Soc., 98, 1743(1976); M. Komiyama, M. L. Bender, Proc. Nat. Acad. Sci. U.S.A., 73, 2969(1976).
17. D. D. MacNicol, J. J. McKendrick, D. R. Wilson, Chem. Soc. Rev., 7, 65(1978).
18. R. A. A. Muzzarelli, Chitin, Pergamon, Oxford, 1977; M. J. Adam, L. D. Hall, J. Chem. Soc. Chem. Comm., 1979, 234; L. D. Hall, M. Yalpani, Carbohydr. Res., 83, C5(1980).

CHAPTER I

GENERAL BACKGROUND

Solid-State N.M.R. Methods

I.1. High-Resolution ^{13}C N.M.R.

I.1.1. Introduction

The development of high-resolution, pulse Fourier transform ^{13}C n.m.r. as a routine tool during the early 1970's constituted a major advance in the analysis of organic liquids. More recently, there has been an increasing interest in the application of n.m.r. techniques to problems involving organic solids. In solids, the lack of molecular motion allows the dipolar- and anisotropic-magnet interactions between spins to dominate the absorption spectrum which is, therefore, very much broader than that of liquid. If those interactions could be effectively removed, the resultant high-resolution n.m.r. spectrum would be of great value in the structural and dynamical analysis of molecules, since the solid-state ^{13}C-n.m.r. spectroscopy would then provide a direct link between n.m.r. studies in solution and X-ray data from the solid state. The two techniques necessary for obtaining the required high-resolution n.m.r. spectra from solids are now well established; they are generally referred to as "cross-polarization" (c.p.) and "magic-angle-spinning" (m.a.s.).

The sensitivity-enhanced, cross-polarization n.m.r. experiment was first introduced by Hartmann and Hahn[1] in 1962, but was not applied to natural-abundance ^{13}C studies of organic solids by Pines et al.[2] until some ten years later. Independently of that approach, in the late fifties,

Andrew[3] and Lowe,[4] each introduced a different design for magic angle spinning, each with its own unique advantages. However, it was only by combining these two techniques, that Schaefer and Stejskal[5] became the first workers in 1975, to report high-resolution ^{13}C-n.m.r. spectra of polymers in the glassy state. The combination developed by them has gained widespread popularity because of its simplicity, the ease of interpretation of the spectra, and the fact that the observed linewidths can be less than 0.1 parts per million (p.p.m.) in exceptional cases.

The ^{13}C-c.p.-m.a.s. method has already been successfully applied to a wide diversity of materials, ranging from crystals of simple organic molecules, to oil shales and coals.[6] Although the method has been available for almost a decade, its application to the carbohydrate field is still fairly new, and during the course of the present work, only a few ^{13}C-c.p.-m.a.s. spectra have been reported for high-molecular-weight polysaccharides[7] of limited solubility and high solution-viscosity. This Laboratory has also demonstrated the use of this method for studying the primary structure of polysaccharides.[8]

In order to understand the ^{13}C-c.p.-m.a.s. method, it is necessary to discuss the dual problems of resolution and sensitivity, and the principles which have led to their solution, in some detail.

I.1.2. Line-Broadening Mechanisms

I.1.2.1. Proton Dipolar Broadening

Classically, the energy of interaction between two isolated magnetic point dipoles μ_1 and μ_2 is given by (Fig. I-1)[9]

$$E_m = \left\{ \frac{\mu_1 . \mu_2}{r^3} - 3 \frac{(\mu_1 . r)(\mu_2 . r)}{r^5} \right\} \frac{\mu_0}{4\pi} \qquad (1)$$

where the vector r is the distance between μ_1 and μ_2, and μ_0 is the permeability constant ($4\pi \times 10^{-7}$ kg m $s^{-2}A^{-2}$). The appropriate Hamiltonian for the dipolar interaction of a substance containing two different magnetic species, I and S, of magnetogyric ratio γ_I and γ_S, is

$$H_D = H_{II} + H_{SS} + H_{IS} \qquad (2)$$

In the discussion that follows only the last term of Eq. (2) is involved; by substituting $\hat{\mu} = \gamma \hbar \hat{I}$ into Eq. (1), H_{IS} may be written as

$$H_{IS} = \gamma_I \gamma_S \hbar^2 \left\{ \frac{\hat{I}_I \hat{I}_S}{r^3} - 3 \frac{(\hat{I}_I . r)(\hat{I}_S . r)}{r^5} \right\} \frac{\mu_0}{4\pi} \qquad (3)$$

When the scalar products are expanded and the equation is tranformed to spherical polar coordinates (Fig. I-2), the following expression is obtained:

$$H_{IS} = \frac{\gamma_I \gamma_S}{r^3} \hbar^2 \, [A + B + C + D + E + F] \, \frac{\mu_0}{4\pi} \qquad (4)$$

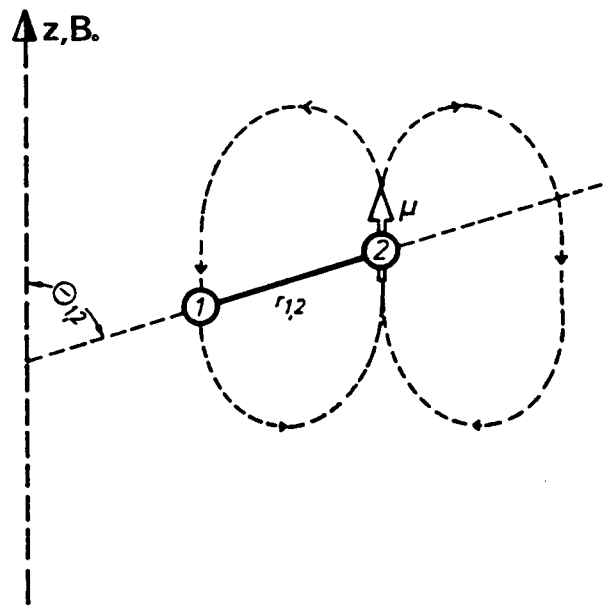

Fig. I-1. Interaction between two isolated magnetic point dipoles at a distance $r_{1,2}$.

The expressions for the six terms, A to F, can be found in standard texts[9-11] and are summarized in Appendix I. Each of them contains a spin factor and a geometric factor, and their values are averaged to zero for rapid isotropic motion.

In the absence of interactions involving scalar coupling and chemical shift anisotropy, the total spin Hamiltonian for the IS (heteronuclear) system is reduced to the sum of Zeeman and dipolar terms, that is,

$$h^{-1}H = -(\nu_I \hat{I}_{I_z} + \nu_S \hat{I}_{S_z}) + h^{-1}H_d$$

where ν_I and ν_S are the Larmor frequencies, and H_d is given

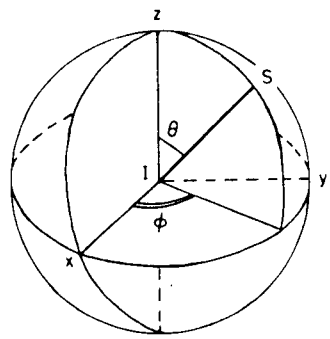

Fig. I-2. Axis system and polar coordinates for I-S dipolar coupling.

by Eq. (4). Since the dipole energies are very much smaller than the Zeeman energies, only the A term commutes with the Zeeman operator and the truncated Hamiltonian[12] becomes

$$h^{-1}H = -(\nu_I \hat{I}_{I_z} + \nu_S \hat{I}_{S_z}) + R\hat{I}_{I_z}\hat{I}_{S_z}(1 - 3\cos^2\theta) \quad (5)$$

where θ is the angle between r_{IS} and the applied static magnetic field, B_o, and $R = (\mu_o/4\pi)r^{-3}\gamma_I\gamma_S(\hbar/2\pi)$ (in frequency units) is sometimes referred to as the dipolar coupling constant. The corresponding energy levels calculated are

$$E_m = h^{-1}E_m = -(\nu_I m_I + \nu_S m_S) + Rm_I m_S(1 - 3\cos^2\theta) \quad (6)$$

The usual selection rules apply ($\Delta M_I = \pm 1, \Delta M_S = 0$ and

$\Delta M_I = 0, \Delta M_S = \pm 1$ for allowed I and S transitions, respectively) so that for the case of two isolated spin-1/2 nuclei, I and S, in a single crystal with only one orientation for r_{IS}, there are two S transitions at

$$\nu = \nu_S \pm 1/2R(1 - 3\cos^2\theta) \qquad (7)$$

and two corresponding I lines. The splitting of the doublet, $\Delta\nu_{IS}$, is given by $R(1 - 3\cos^2\theta)$, and its variation with orientation in the magnetic field will yield both R and the relation of θ to the crystal setting.

For an organic solid, the major source of line broadening in the ^{13}C spectrum is the dipolar broadening from nearby (e.g., directly bonded) protons. The z-component, B_z^H, of the local field which ^1H exerts on the ^{13}C magnetic moment is obtained from the expression derived earlier for the splitting (in Hertz):[13]

$$\Delta\nu_{CH} = \frac{\gamma_C}{\pi} \left| B_z^H \right| \frac{\mu_o}{4\pi} \qquad (8)$$

with

$$B_z^H = \pm \frac{\mu_z^H}{r_{CH}^3} (1 - 3\cos^2\theta)$$

in which $\mu_z^H = \gamma_H \hbar/2$ is the magnetic moment. In a powder sample, there exist many pairs of spins with different values of r_{CH} and θ, which results in a broad resonance line. Typical ^{13}C-^1H dipolar interactions can be very

large; for a C-H bond parallel to B_o, $\Delta\nu_{CH}$ of 40 kilohertz (kHz) would be expected.[14]

The expression for the dipolar splittings as shown above, is derived from the coupling between ^{13}C nuclei and "static" proton magnetic moments. It has been demonstrated that these splittings are generally reduced experimentally by the "flip-flop" spin motion of dipolar-coupled protons which have antiparallel moments.[15] This process, called spin diffusion, is particularly important because it provides an efficient path for the spin-spin relaxation of protons. Thus, it limits the lifetime of the spin state, leading to uncertainty in broadening of the resonance. The ^1H-^1H dipolar splitting ($\Delta\nu_{HH}$) is approximately equal to the flip-flop rate, and the spin fluctuations average the ^{13}C-^1H interaction to $\Delta\nu_{CH}$ ($\Delta\nu_{CH}/\Delta\nu_{HH}$).[16] Since $\Delta\nu_{HH} > \Delta\nu_{CH}$ for most organic solids, the ^{13}C dipolar linewidth may therefore be scaled by the factor ($\Delta\nu_{CH}/\Delta\nu_{HH}$). Still, the reduced linewidth is in the order of kilohertz.

The dipolar interaction is largely removed by continuously irradiating the ^1H spin system with a strong radiofrequency (r.f.) field set to the appropriate Larmor frequency. This means that B_z^H is suppressed via a reduction of the effective magnetic moment, μ_z^H. The effect of the r.f. irradiation is to induce rapid rotation of proton spins, that effectively makes $< \mu_z^H > = 0$ (Fig. I-3). Normally, spin decoupling fields of 40 kHz or more are needed to remove the ^{13}C-^1H dipolar interactions. However

substantial broadening still remains, due to chemical shift anisotropy interactions (c.s.a.) and ^{13}C-^{13}C homonuclear interactions, which cannot be removed by high power decoupling.

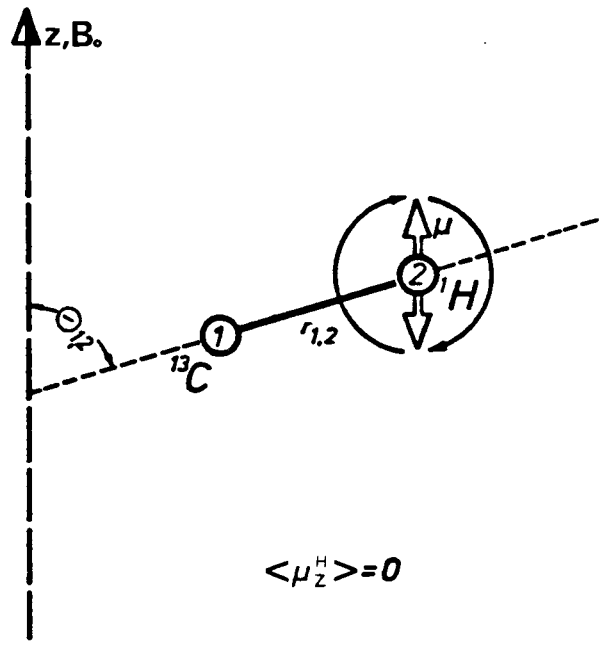

Fig. I-3. Rapid rotation of proton spin 2, effected by high power decoupling.

I.1.2.2. Chemical Shift Anisotropy

With dipolar decoupling, the resolution of the ^{13}C spectrum is improved, but the spectral lines still exhibit an anisotropic lineshape. The maximum chemical shift anisotropy for carbon resonances (e.g., of aromatic and carbonyl carbons) in neutral molecules can cover a spectral range of 200 p.p.m.,[17] or of the order of 10 kHz (at

50.3 MHz). This line-broadening arises from the nonsymmetrical electron density around the ^{13}C nuclei in the molecule. Thus these carbons, which experience different shieldings of the magnetic field depending upon the orientation of molecular-fixed axes with respect to the applied field,[10] would have different chemical shifts.

For sufficiently simple systems involving only a few chemically different types of carbons, resolved or partially resolved chemical shift anisotropies are a rich source of new information about the geometry and electronic structure of the solids. The lineshape for a carbon resonance (Fig. I-4) is generally "tent-like", and it can be described by the three principal components (i.e., σ_{11}, σ_{22}, and σ_{33}) contained in the chemical shift tensor, $\boldsymbol{\sigma}$. However, in most cases, it is impossible to extract the anisotropy information because of the extensive overlap of the different signals originating from the many kinds of carbon atoms in the molecule.

The resonance frequency can be expressed as

$$\nu_o = \left|\frac{\gamma_c}{2\pi}\right| B_o (1 - \sigma_{zz}) \qquad (9)$$

where σ_{zz} is the shielding constant measured along B_o. σ_{zz} can be related to the three principal components by the direction cosines:[11]

$$\sigma_{zz} = \sum_{j=1}^{3} \sigma_{jj} \cos^2\theta_j \qquad (10)$$

where the angles, θ_j, are those between the j direction and B_0. The convention $\sigma_{11} \leq \sigma_{22} \leq \sigma_{33}$ is usually adopted. In

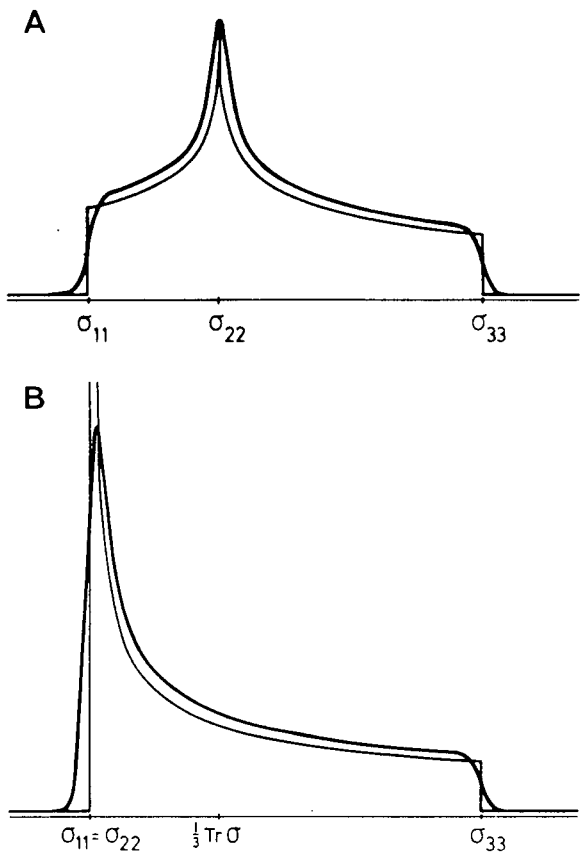

Fig. I-4. Chemical shielding powder pattern: (A) arbitrary second rank tensor ($\sigma_{11} \neq \sigma_{22} \neq \sigma_{33}$); (B) axially symmetric second rank tensor ($\sigma_{11} = \sigma_{22} \neq \sigma_{33}$) (from Ref. [9]).

solution, molecular motion averages the anisotropic part of this chemical shift tensor, that is, the shielding constant is independent of orientation in B_0. Thus, the effective isotropic chemical shift (σ_i) is given by

$$\sigma_i = 1/3 \mathrm{tr}\sigma = 1/3(\sigma_{11} + \sigma_{22} + \sigma_{33}) \qquad (11)$$

where the isotropic average of each $\overline{\cos^2\theta_j}$ term is 1/3. If a rigid specimen is mechanically spun with angular velocity ω_r about an axis inclined at angle β to B_o, and at angles χ_j to the principal axes of σ as shown in Fig. I-5, we have

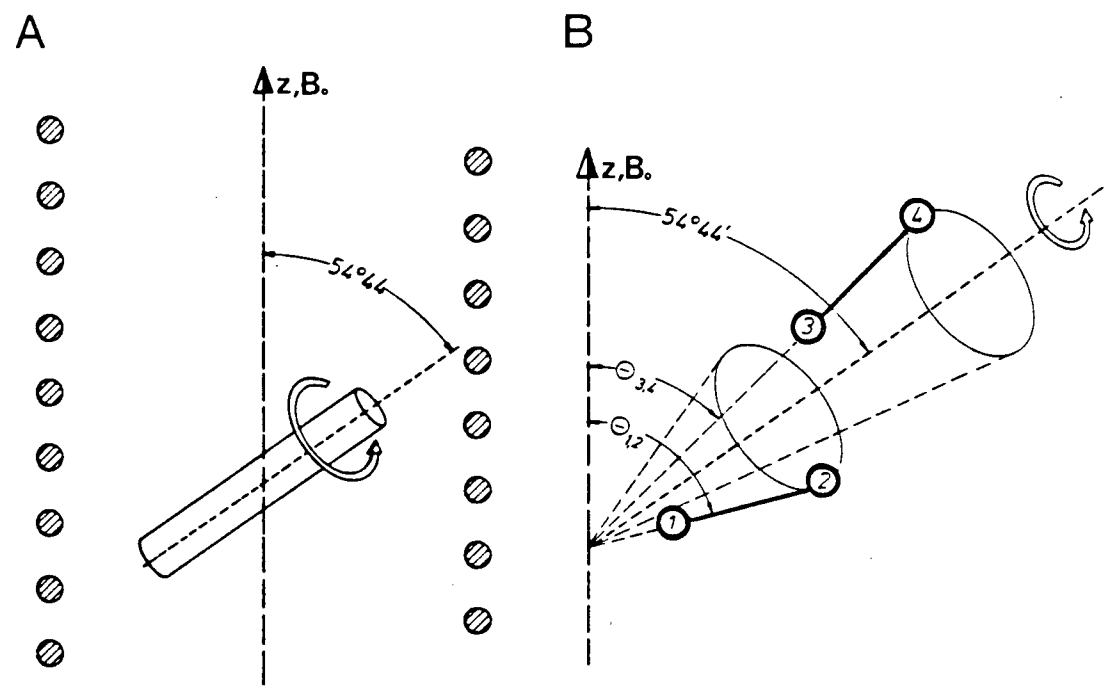

Fig. I-5. Magic angle spinning of a specimen: (A) by rotating in a field of a solenoid under the magic angle of 54°44'; (B) the time averaged value of all the binding vectors becomes 54°44', i.e. $\langle\theta_{1,2}\rangle = \langle\theta_{3,4}\rangle = 54°44'$ in spite of $\theta_{1,2} \neq \theta_{3,4}$.

(see Appendix II)

$$\cos\theta_j = \cos\beta\cos\chi_j + \sin\beta\sin\chi_j\cos(\omega_r t + \psi_j) \qquad (12)$$

where ψ_j is the azimuthal angle of the jth principal axis of σ at t = 0. Substituting (12) into (10) and taking the time average, the shielding constant for each kind of nucleus is written as

$$\overline{\sigma_{zz}} = 3/2(\sin^2\beta\sigma_i) + 1/2(3\cos^2\beta - 1) \sum_j \sigma_{jj} \cos^2\chi_j \quad (13)$$

In general this latter term produces a powder pattern when summed over all possible nuclear orientations. However, when $\beta = 54.7^\circ$, then $\cos^2\beta = 1/3$, and $\sin^2\beta = 2/3$ and Eq. (13) reduces to the expression

$$\overline{\sigma_{zz}} = \sigma_i \quad (14)$$

This means that in a polycrystalline sample only a single sharp line will be observed for each set of inequivalent nuclei, provided that the rotational rate is sufficiently fast. If the spinning rate is less than the chemical shift anisotropy, the spectrum is broken up into a complex profile of sidebands (Fig. I-6), which trace out a tent-like pattern related to the spatial anisotropy, centered around each isotropic shift.[18] This complicates structural assignments and also results in a loss of sensitivity. Increasing the magnetic field, B_o, does not necessarily increase the resolution of the spectrum because the chemical shift anisotropy is field dependent, and thus higher field strengths require higher spinning rates.

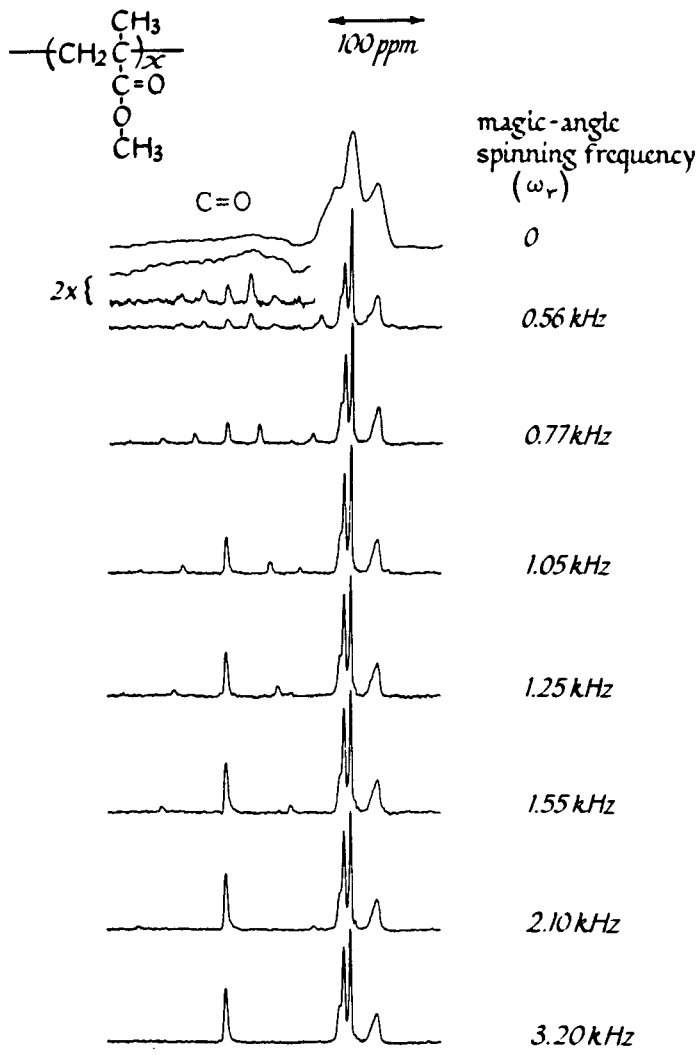

Fig. I-6. ^{13}C-N.m.r. spectra of poly(methyl methacrylate) as a function of spinning frequency (from Ref. [18]).

I.1.3. Sensitivity Enhancement

In solution n.m.r. studies of "dilute spins" such as ^{13}C and ^{15}N, nuclear Overhauser enhancement (n.O.e.),[19]

Fourier transform and signal averaging techniques can be employed to improve the signal-to-noise ratio. In solids, poor spectral resolution and long spin-lattice relaxation times may pose serious problems for signal detection, thereby making conventional solution techniques difficult to study. These problems have been largely overcome by the ingenious technique of cross-polarization, developed by Pines et al..[2]

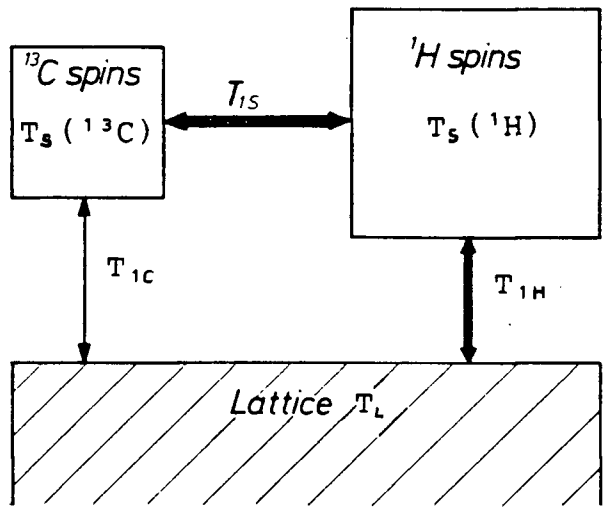

Fig. I-7. ^{13}C-^{1}H Cross-polarization experiment (spin temperature concept).

As shown in Fig. I-7, the ^{13}C-c.p. n.m.r. experiment involves the tranfer of polarization (hence signal intensity) from the "more abundant" ^{1}H spins to the "dilute" ^{13}C spin system. This technique is also called "proton enhanced nuclear induction spectroscopy" (p.e.n.i.s.); it provides a new relaxation path for ^{13}C

spins, so that their effective relaxation time is drastically reduced. It is a particularly effective version of double resonance in the rotating frame,[1] based on the dynamics and thermodynamics of nuclear spin systems. Thus, the language of spin thermodynamics is well suited to the discussion of these phenomena, and will be used.

I.1.3.1. Spin Temperature

When a solid sample containing ^1H and ^{13}C nuclei is placed in a magnetic field B_o, the energy levels of these nuclei are split into two levels, $\pm(\gamma/2\pi)B_o/2$, corresponding to spin alignment parallel and antiparallel to B_o (Fig. I-8A). The population ratio, n_1/n_2, of these two levels 1 and 2 of a spin system is given by the Boltzmann law:[9]

$$n_1/n_2 = \exp -\Delta E/RT_s \qquad (15)$$

where ΔE is the energy difference between the two levels, and T_s is the spin temperature. A small population difference implies a high spin temperature T_s (in the limit, $n_1 = n_2$ means $T = \infty$); conversely, a large population difference signifies a low temperature T_s. Protons, which are part of a large spin system, can interact with each other by the process of spin diffusion, as mentioned previously in Section I.1.2.1.

Consider now a single proton which changes Zeeman

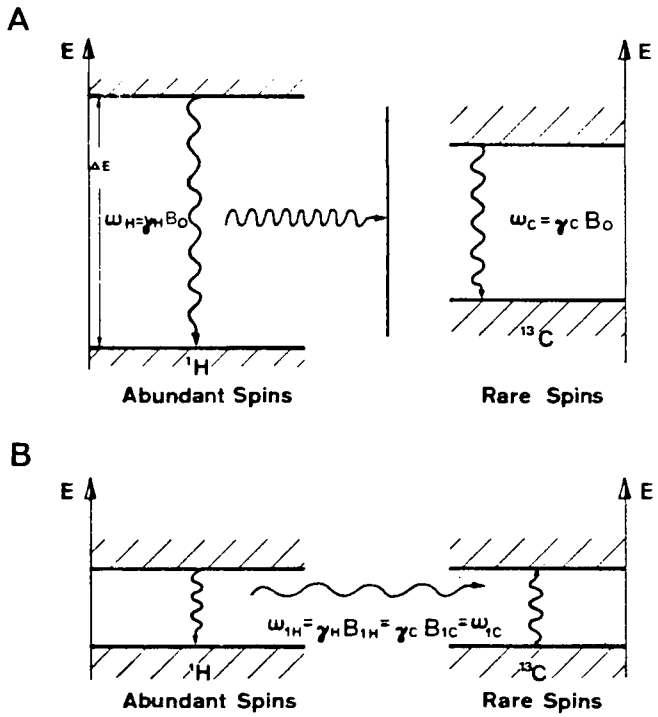

Fig. I-8. Representation of energy levels: (A) in the laboratory frame; (B) in the rotating frame (from Ref. [6]).

levels by exchanging energy with the lattice. This information is conveyed in a short time (<100 μs) to a large number of neighboring protons by their mutual spin flips. As a result, during that time all the protons achieve a state of internal equilibrium, and hence can be considered as a single thermodynamic reservoir, as represented by Eq. (15). After a lapse equivalent to several spin-lattice relaxation times, $T_1(^1H)$, the proton reservoir will come to equilibrium with the lattice, and $T_S(^1H)$ will be equal to the lattice temperature T_L. The ^1H magnetization produced in the laboratory frame is then given by the Curie Law as

$$M_0(^1H) = C_H B_0/T_L \qquad (16)$$

where $C_H = 1/4(\gamma_H^2\hbar^2N_H)/k$ is the proton Curie constant, in which N_H is the number of protons and k is the Boltzmann constant. Similarly, the small ^{13}C magnetization can be represented as

$$M_0(^{13}C) = C_c B_0/T_L \qquad (17)$$

I.1.3.2. Cross-Polarization

With those concepts on hand, the c.p. experiment can be explained. The first step involves transfer of the ^1H magnetization to the rotating frame by spin-locking along the direction of the r.f. field, B_{1H}. Initially, the protons are perturbed (since $B_{1H} <<< B_0$), but shortly, they regain their internal equilibrium. The population of these states is again governed by the Boltzmann distribution, which is characterized by T_S in the rotating frame. Thus, the ^1H magnetization is given by

$$C_H B_0/T_L = C_H B_{1H}/T_S$$

i.e.

$$T_S = (B_{1H}/B_0)T_L \qquad (18)$$

Since $B_{1H} <<< B_0$, the proton spins are effectively at a very low spin temperature; for a sample at room temperature, T_S is approximately 3 K[13] and the total spin

energy is $-C_H B_0^2/T_S$. At this juncture, the ^1H spins are brought into thermal contact with the ^{13}C spins by irradiating the carbons on resonance. Albeit that the ^{13}C magnetization is small along the B_0 direction at the start of the pulse, the carbon nuclei will still precess about the r.f. field, B_{1C}, at the frequency $\omega_{1C} = \gamma_C B_{1C}$. Hence, there are two oscillating components along the z direction in the rotating frame, one for the ^1H magnetization at frequency $\omega_{1H} = \gamma_H B_{1H}$, and the other for the ^{13}C magnetization. If the amplitude of B_{1C} is adjusted so that the Hartmann-Hahn condition is satisfied (Fig. I-8B), then the frequencies of the oscillatory components will be identical, that is,

$$\gamma_C B_{1C} = \omega_{1C} = \omega_{1H} = \gamma_H B_{1H} \qquad (19)$$

The above condition implies that the effective energies of protons and carbons are comparable, and polarization transfer now occurs between the proton and carbon pools via proton-carbon spin flips. This is maintained for a time constant, T_{CH} (typically 0.5-5 ms), during which the spin energy is redistributed between the proton- and the carbon-pools so that a common spin temperature, T'_S, is achieved:

$$C_H B_{1H}^2 / T_S = (C_H B_{1H}^2 + C_C B_{1C}^2)/T'_S \qquad (20)$$

Since $C_C << C_H$ (i.e., $N_C \sim 10^{-2}N$), this temperature will

be approximately equal to that of the spin-locked proton magnetization. During this process the protons lose only a very small amount of their total magnetization (remember, $T_{1\rho}^{H} >> T_{CH}$), and the resulting ^{13}C magnetization is given by

$$M(^{13}C) = C_C B_{1C} / T_S' = C_C B_{1C} / T_S \qquad (21)$$

Substituting Eqs. (18) and (19) into (21) gives the relationship

$$M(^{13}C) = (\gamma_H / \gamma_c) \, C_C B_0 / T_L \qquad (22)$$

$$= 4 M_0(^{13}C)$$

where $M_0(^{13}C)$ is the magnetization which would be generated in B_0 after waiting for the equivalent of 3-5 T_{1C} period. In this way, a fourfold enhancement[2] in ^{13}C signal-intensity can be obtained from a single cross-polarization process.

I.1.4. The ^{13}C-C.P.-M.A.S. Experiment

The experimental detail shown in Fig. I-9 represents the timing sequence for the c.p. experiment. Essentially the procedure can be divided into four parts: 1) polarization of the ^{1}H spin system, 2) spin locking in the rotating frame, 3) thermal contact between the ^{1}H and ^{13}C

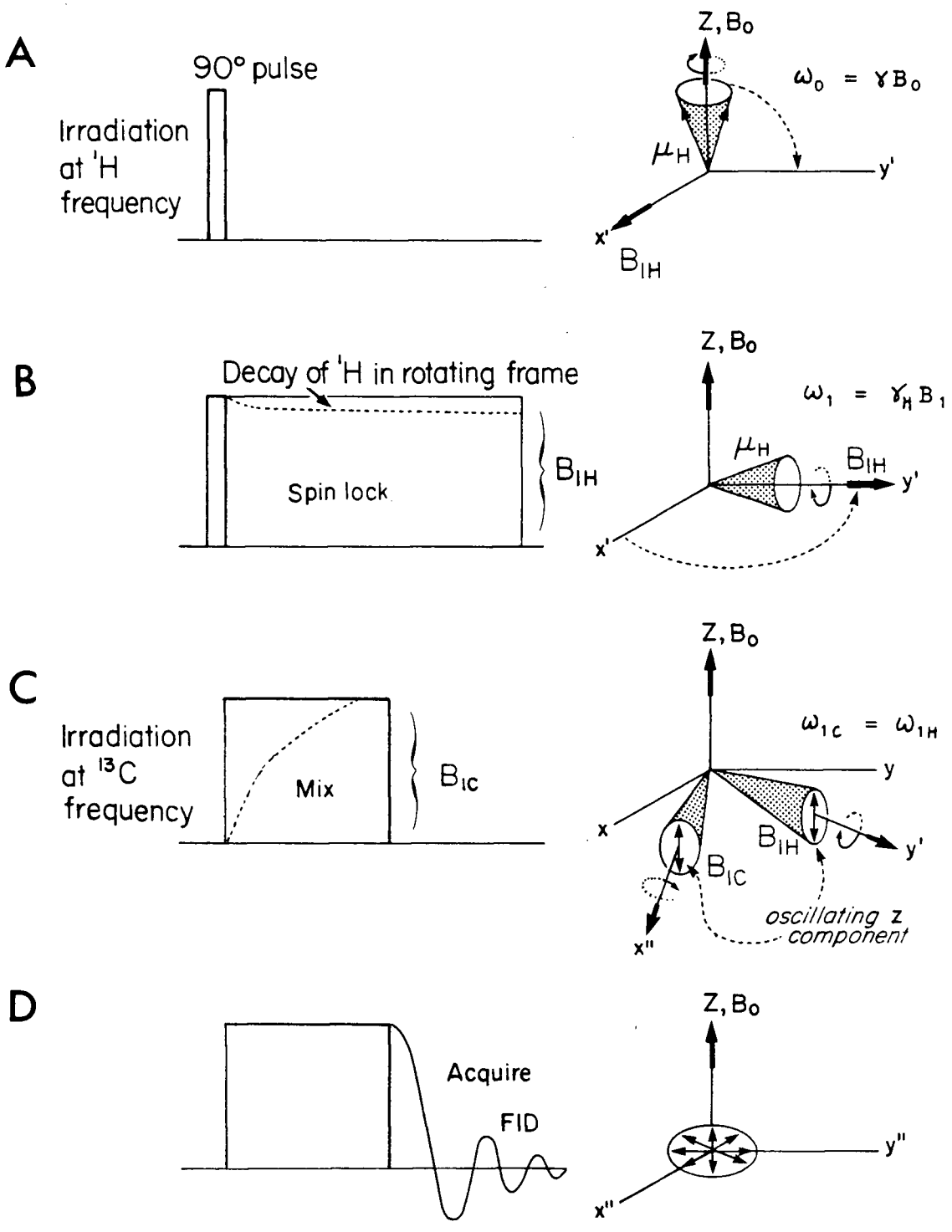

Fig. I-9. Timing sequence for cross-polarization experiment: (A) polarization of the ^{1}H spin system; (B) spin locking in the rotating frame; (C) thermal contact between the ^{1}H and the ^{13}C spin systems; (D) observation of the ^{13}C free induction decay (from Ref. [6]).

spin systems, and 4) observation of the ^{13}C free induction decay (f.i.d.). During the whole c.p. experiment, spinning of the sample is maintained at the magic angle.

I.1.4.1. Polarization of ^{1}H

Initially, the ^{1}H magnetization is allowed to build up along B_0, with the population difference governed by ΔE as shown in Eq. (15). This magnetization is then brought by a 90° pulse into the x'y' plane, along y'. The ^{1}H and ^{13}C spins are assumed to be rotating about B_0 at their respective Larmor frequencies, that is, the ^{1}H coordinate system x'y' precesses at $\omega_{oH} = \gamma_H B_0$, and the ^{13}C system x"y" at $\omega_{oc} = \gamma_C B_0$.

I.1.4.2. Spin Locking

Immediately after the 90° pulse (in microseconds), the phase of the r.f. field, B_{1H}, is electronically shifted by 90° to the y' direction, so that it is colinear with the ^{1}H magnetization. In this way a state of low spin temperature is prepared; the strong magnetization produced in the high B_0 field is now parallel to the small B_{1H} field, which results in a high level of polarization in the rotating frame. At this time the ^{13}C magnetization is zero in the x"y" plane, which corresponds to an infinite spin temperature.

In the presence of the strong B_0 field, this "spin-

locked" condition cannot be maintained indefinitely. In practice, this magnetization eventually decays to zero by spin-lattice relaxation in the rotating frame, with a time-constant denoted by $T_{1\rho}(^1H)$.

I.1.4.3. ^{13}C-^1H Thermal Contact

During the spin-lock condition, B_{1C} is applied along the x" direction. It is adjusted to the Hartmann-Hahn condition, and maintained for a time, t_{CP}, which is preferably equal to, or slightly longer than, T_{CH}. The transfer of magnetization via cross-polarization now occurs, resulting in a rapid increase in the ^{13}C magnetization and a very small decrease in the ^1H magnetization.

I.1.4.4. Observation of ^{13}C Free Induction Decay

The last step of the c.p. experiment is to switch off the ^{13}C r.f. field and then to observe the "proton enhanced" ^{13}C f.i.d.. During the ^{13}C observation time, the ^1H r.f. field is still maintained in order to provide the high-power decoupling field. In practice, the entire sequence has to be repeated until a suitable signal-to-noise (S/N) ratio is obtained. Finally, the resultant f.i.d. is Fourier transformed to give the frequency domain spectrum.

I.1.4.5. Optimization of the Cross-Polarization Experiment

The success of c.p. depends on several experimental conditions, which can be met in most cases. These include the requirement that the magnitudes of B_{1C}, B_{1H} be greater than the natural linewidths of the ^1H and ^{13}C resonances and that $T_{1C} > T_{1H} \geq T_{1\rho}(^1H) > t_{cp} > T_{CH}$. If the above conditions are not fulfilled, optimum gain in the ^{13}C signal intensity cannot be achieved. The best combination of parameters from the point of view of c.p. experiments is a short T_{1H} associated with a very long $T_{1\rho}(^1H)$. These conditions are often satisfied in molecules with reorienting methyl groups.[20]

The actual c.p. rate, $1/T_{CH}$, results from a summation over all possible ^{13}C-^1H spin interactions of the molecular system. A number of parameters are involved; the most important one is the second moment of the ^{13}C-^1H bond, ($T_{CH}^{-1} \propto M_2^{CH}$), which is written as[15]

$$M_2^{CH} = \frac{1}{2}\gamma_C \gamma_H h \frac{\mu_o}{4\pi}^2 \sum_k \left(\frac{1 - 3\cos^2\theta_{jk}}{r_{jk}^3} \right)^2 \qquad (23)$$

where the sum, $\sum_k [(1 - 3\cos^2\theta_{jk})/r_{jk}^3)]^2$, includes all relevant proton nuclei, k, in relation to the considered carbon nucleus j. Based on this expression, it can be seen that the magnitude of available cross-polarization is dependent on the ^{13}C-^1H dipolar interactions; these vary as

r_{CH}^{-3}, where r_{CH} is the distance separating the nuclei. In general then, nonprotonated carbons are expected to become magnetized via this mechanism much more slowly than protonated carbons, providing that there is no rapid molecular motion that can average the static intramolecular interactions. Accordingly, the relative c.p. rates of carbons are as follows: CH_3(static) > CH_2 > CH ≥ CH_3(rotating) > C(nonprotonated).[13]

Quantitatively accurate c.p. spectra, in which the relative signal intensities agree with the known carbon ratios, have been obtained for highly protonated, organic diamagnetic solids.[21] For this to be possible, it is mandatory for the chemical system to be homogeneous, so that all the spin-locked ^1H magnetization can be characterized by the same rate of decay, $T_{1\rho}(^1H)$. Also, the $T_{1\rho}(^1H)$ should be much longer than T_{CH} to ensure complete polarization of all carbons, particularly the nonprotonated ones, before relaxation in the rotating reference frame dominates the ^1H magnetization.

I.1.4.6. Experimental Aspects of Magic Angle Spinning

Adjustment of the magic angle is carried out to minimize the observed linewidths of the sample under study. Any missetting of the angle is reflected in the shape and width of the resulting lines. Since the shielding constant, $\bar{\sigma}_{zz}$, contains the reduction factor $|1/2(3\cos^2\beta - 1)|$ [Eq. (13)], the resolution of each line should be sensitive

to small deviations in the actual angle from the magic angle value. In practice, the increase in linewidth is equivalent to approximately 2.5 % of its static linewidth for every degree of deviation from the magic angle.[22] The static linewidth refers to the width obtained when the intended spinning axis is parallel to B_0. It has been shown experimentally[23] that a high level of accuracy in setting the magic angle can be attained if adequate precautions are taken.

Many types of high-speed sample spinners have been employed in solid-state n.m.r.; they are essentially modifications of either the conical[24] (Fig. I-10A) or the cylindrical[25] spinner. The former is referred to as the Andrew-type rotor, which has the principle advantage of simplicity of construction. However, its disadvantage is related to the difficulty of routinely obtaining stability, especially with inhomogeneous samples, spinning at high rates. The cylindrical rotor was first described by Lowe, but it too has its own share of problems.

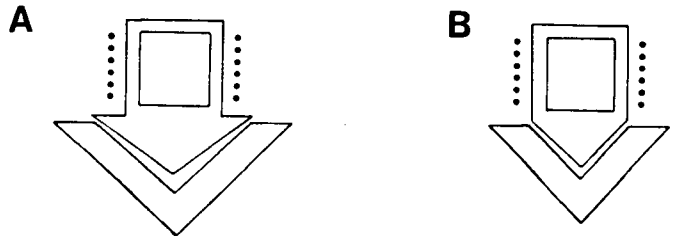

Fig. I-10. Schematic representation of high-speed sample spinners: (A) Andrew-Beams; (B) bullet (from Ref. [10]).

Bartuska and Maciel[26] have designed a bullet-shaped rotor (Fig. I-10B), which can favorably withstand spinning rates up to ca. 3.5 kHz. Since it resembles the Andrew spinner, their relative merits have been discussed. Yannoni et al.[27] have developed a variable-temperature (v.t.) spinning apparatus to address a variety of interesting chemical problems (Fig. I-11); their rotor can sustain 3-4 kHz at liquid nitrogen temperature with helium as the propellant gas.

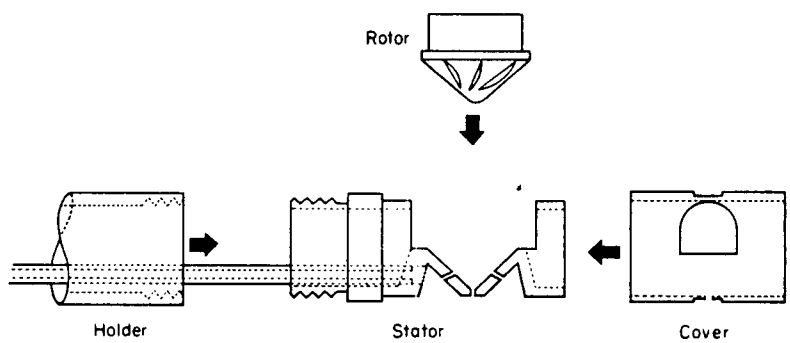

Fig. I-11. A spinner system suitable for variable temperature magic angle spinning studies (from Ref. [27]).

A number of materials have been used to construct the spinners. They include Kel-F (polytrifluorochloroethylene), Delrin [poly(oxymethylene)], Teflon, Plexiglas [poly(methyl methacrylate)], boron nitride,[28] and aluminium oxide. Delrin and Kel-F rotors are commonly used by most research groups; the former is stronger and can achieve a spinning rate of about 4.5 kHz. Unfortunately, Delrin itself has a large ^{13}C resonance; fortunately this can be suppressed[29]

from the spectrum of interest. For rotation rates up to ca. 5 kHz, the turbine may be driven with compressed air of about 3 atmospheres pressure. Compressed helium or hydrogen gas must be used if higher rotation rates are needed.

I.1.4.7. Spectral Resolution

Even under optimal conditions for high-power proton decoupling and magic angle spinning, static and/or dynamic effects can limit the resolution attainable from some organic solids. It has been found for amorphous materials, that the lack of a fixed, single conformation may lead to a distribution of isotropic chemical shifts for individual carbons.[30] Usually this gives rise to substantial line-broadening, of the order of several p.p.m., that may result in a "featureless" spectrum. In other cases, splittings of resonance lines are caused by magnetic inequivalences[13] which are present in the solid state but not in solution. Other mechanisms[22] which can affect the resolution include motional modulation of both the ^{13}C-^{1}H dipolar decoupling and of the chemical shift anisotropy. As a result, the ^{13}C-n.m.r. linewidths of solids are 10 to 100 times broader than those measured in solution.

I.1.5. Useful Pulse Sequences and Related Techniques

To an organic chemist, the ideal outcome of a solid-state n.m.r. measurement is the complete assignment of all

the carbon resonances. This goal continues to provide a compelling reason for exploration of both the technical and chemical aspects of this area. It has already been shown that pulse techniques can be employed to remove spinner-signals and spinning-sidebands,[31,32] to increase S/N ratio, and to distinguish different classes of carbons.[33] Also, chemical modification of the samples by introduction of metal ions, of deuterons,[34] or of ^{13}C-enriched nuclei[35] can assist in spectral assignments. Generalization of these preliminary findings would encourage more routine application of solid-state ^{13}C n.m.r. to structural analysis of important organic compounds; indeed such studies will probably not occur until such auxillary methods are widely available.

As mentioned earlier, Delrin is still a very convenient material for the manufacture of high-speed spinners, except that its ^{13}C signal, centered at 89.11 p.p.m. conceals a region of the spectrum which is vitally important, especially for carbohydrates. To expose this spectral region, a method is used which is analogous to the solvent suppression routines that are familiarly applied to solution-state n.m.r. spectroscopy; in the present context, it involves the suppression of the resonance signal from the sample-spinner. It depends on the fact that the magnetization of the protons of Delrin usually decays far more rapidly than that of the organic substrate; this occurs because the polymeric material is

probably quite mobile in the solid state.[30] Thus, the introduction of an appropriate delay immediately following the 180° pulse (at position 1 in Fig. I-12), ensures that the subsequent cross-polarization sequence transfers proton magnetization only to the carbons of the organic substrate.

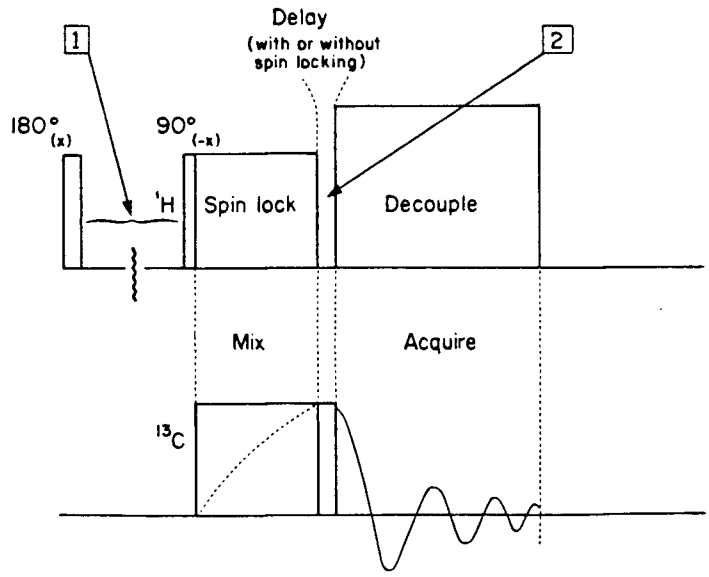

Fig. I-12. Pulse sequence used to suppress the Delrin signal, and signals from protonated-carbon atoms in solids.

Consideration of the time course for nuclear relaxation has led to another useful pulse sequence which assists in assignment. This was first tested by Alla and Lippmaa[36] and provides, in principle at least, an unequivocal means for discriminating between the resonances of carbon atoms that bear protons from those that bear none. In this case, advantage is taken of the fact that, without spin locking, the magnetization of the protonated carbon atoms decays more rapidly than that of those which are nonprotonated. Thus insertion of a suitable delay time

at position 2 in the pulse sequence ensures that, even though all carbon atoms are magnetized to the same extent at the end of the mixing time, only those having relatively longer ^{13}C relaxation times retain a measurable magnetization at the start of the carbon acquisition-time.

The overall repetition time of the c.p. experiment is essentially determined by the shorter T_{1H}. If $T_{1\rho}(^1H)$ is long compared with "T_{CH} plus the acquisition time for the observation of the ^{13}C f.i.d." (typically 50-100 ms), then a substantial amount of proton polarization will still remain at the end of the first observation period. Thus, it is possible to carry out multiple-contact cross-polarization before the proton polarization requires replenishment. Although this procedure produces a further gain in sensitivity, generally it is not used in practice because it requires the B_{1H} field to be on for a long time, and substantial problems of heat dissipation may result.

Recently, a pulse sequence[37] has been introduced which shortens the overall waiting period between successive spin-locking sequences. The resultant process involves flipping the proton magnetization back along the B_0 direction; thus, a 90° pulse reversed in phase with respect to the initial pulse, $90°_x$, is applied at the end of the spin-locking pulse (Fig. I-13). A delay time is then set to the minimum consistent with the avoidance of heat dissipation problems. This technique is not suitable for systems having very short $T_{1\rho}(^1H)$ and long T_{1H} values.

Importantly, however, the experiment is user-friendly in that there will never be a decrease in S/N ratio in comparison with the standard single-contact experiment.

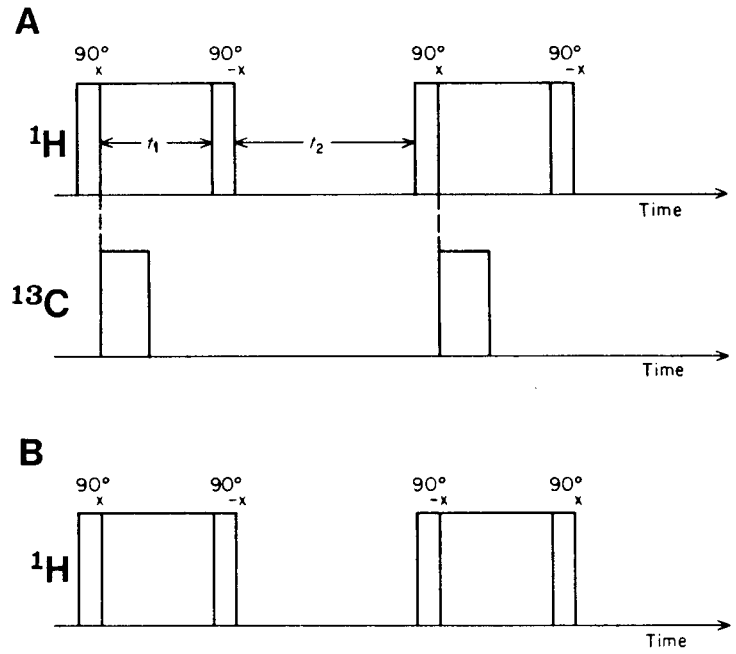

Fig. I-13. Cross-polarization with flip-back of ^{1}H-spin magnetization: (A) pulse timing for the cross-polarization; (B) phase-alternated version of the flip-back experiment (from Ref. [10]).

It is possible for the ^{1}H spin-lattice relaxation time to be very long (greater than 100 s) in the extreme correlation limits of $\omega_{0H}\tau >> 1$ for very slow, and $\omega_{0H}\tau << 1$ for very fast motion, respectively. This is characteristic of the correlation time for the particular motion involved, and it is necessary to devise an effective method for retrieving ^{13}C-c.p.-m.a.s. spectra of such specimens. It is well known that the introduction of paramagnetic impurities into a host lattice can reduce its

relaxation times.[38] Because this effect depends on the inverse sixth power of the distance, the T_1 values are expected to be reduced most for those protons and carbons that are located closest to the paramagnetic centers. Since all the protons are involved in mutual spin flips with their neighbors, the overall T_1 of the entire proton pool is reduced. However, such interactions are very weak for carbons at natural abundance, and hence only those that are closer to the paramagnetic centers are significantly affected. Low concentrations of paramagnetic impurity do not alter the space group symmetry or the crystal structure of the host molecules, nor produce any observable isotropic shift or broadening of the ^{13}C resonances.

The effects of metal ions on the isotropic shifts of stoichiometric metal complexes have been reported recently.[39] In the case of paramagnetic complexes, the resonances of the carbons closest to the metal center are broadened or not visible at all. By binding suitable metal ions to selective sites of large molecules, partial assignments of the spectra are made possible.

Quadrupole nuclei, such as nitrogen-14[40] and deuterium, can also be very useful in spectral assignments. The asymmetric doublet pattern and broadening of the resonances from carbons directly bonded to nitrogen-14 can be easily seen in the spectrum (Fig. I-14). This lineshape is caused by the ^{13}C-^{14}N dipolar interaction, which is not averaged by magic angle spinning. Selective deuteration of

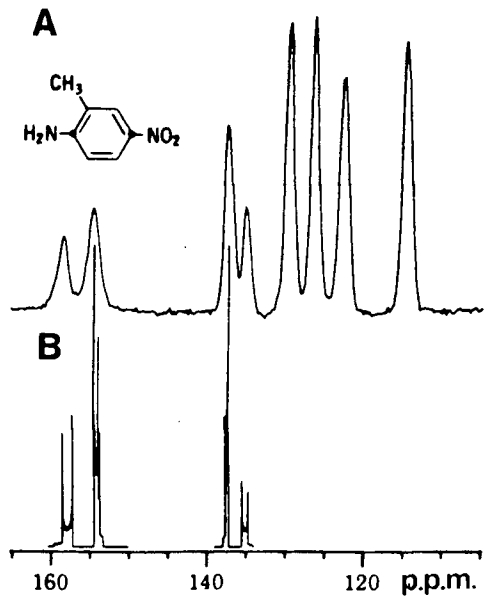

Fig. I-14. ^{13}C-N.m.r. spectra of 2-methyl-4-nitroaniline: (A) normal c.p.-m.a.s.; (B) theoretical spectrum, calculated as described in Ref. [40].

organic molecules has been widely explored, and it is a great asset to solid-state studies. Albeit that ^{13}C enriched samples can be used, such syntheses may not be that straightforward, and this limits the applicability of the method.

I.2. ^2H N.M.R.

I.2.1. Introduction

Deuterium n.m.r. represents a powerful tool for probing both the static and dynamic properties of organic solids and solid polymers. This is because the properties of the spectrum are dominated by the spin-electric quadrupole interaction;[41] the internuclear magnetic dipolar interactions, which are relatively weak, do not affect the lineshape analysis. However, three obstacles, each of which lowers the overall signal-to-noise, had to be overcome in order to make ^2H n.m.r. an attractive method: (1) the low natural abundance (0.0156 %) of ^2H, (2) the low magnetogyric ratio, which is smaller by a factor of 6.51 by comparison with ^1H, and (3) the quadrupole splitting which can result in a spectral width >250 kHz for rigid solids.

Recent developments of experimental solid-state n.m.r. techniques,[42,43] plus the use of ^2H-enriched compounds, have paved the way for this method. The low natural abundance of ^2H can be used to an advantage, since selective labelling up to 100 % is fairly simple, and the negligible level of background signal at natural abundance does not complicate the overall spectrum. Furthermore, analysis of the experimental lineshapes can be performed for some mobile systems where formulation of theories of the dependence on motional dynamics has been established.[44]

Deuterium n.m.r. spectra of rigid solids show the characteristic "Pake-doublet" pattern.[45] The magnitude of

the quadrupole coupling is determined by the orientation of the molecule in the magnetic field. Any reorientational processes result in changes of the Pake pattern, and by measuring the changes in the shape of the pattern, it is possible to characterize both the rate and the mechanism of the molecular reorientation.

I.2.2. N.M.R. of Quadrupolar Nuclei in the Solid State

In an applied magnetic field B_0, the total spin Hamiltonian for a spin $I \geq 1$ is given by

$$H = H_Z + H_Q + H_D + H_{CSA} + H_{SC} \qquad (24)$$

where H_Z, H_Q, H_D, H_{CSA}, and H_{SC} are the Zeeman, quadrupole, dipole, chemical shift anisotropy, and scalar coupling Hamiltonians, respectively. For deuterons which have nuclear spin $I = 1$, H_D, H_{CSA}, and H_{SC} are essentially negligible and hence, the truncated Hamiltonian may be written as

$$H = H_Z + H_Q \qquad (25)$$

At conventional nuclear resonance frequencies (i.e., "high field" cases), the quadrupole interaction in solids is much weaker than the Zeeman interaction, thus, only a first-order perturbation is required for description of the

the energy levels. The Zeeman interaction Hamiltonian is given by

$$H_z = -\gamma\hbar B_0 I_z = -h\nu_0 I_z \qquad (26)$$

with B_0 along the z-axis of the laboratory coordinate frame, and the Larmor frequency $\nu_0 = \gamma B_0/2\pi$. The Zeeman levels will then have energies

$$E_m = -mh\nu_0 \qquad (27)$$

where m is the magnetic quantum number. For a spin 1 nucleus, m takes values of 1, 0, -1.

Since the magnetic field (rather than the electric field) determines the direction of quantization, the first-order theory will give rise to the energy levels[41]

$$\bar{E}_m = \frac{E_m}{h} = -m\nu_0 + \frac{\nu_Q}{4}\left[3m^2 - I(I+1)\right]\left[\frac{3\cos^2\theta - 1}{2} + \eta\frac{\sin^2\theta\cos^2\psi}{2}\right] \qquad (28)$$

where θ and ψ are the Euler angles defining the orientation of the principal axis of the electric field gradient (e.f.g.) tensor (usually along the C-D bond direction) with respect to the laboratory coordinates. ν_Q is the quadrupole coupling constant, and η is the asymmetry parameter which

provides the measure of the deviation of the e.f.g. from axial symmetry. For the case of C-D bonds, η is usually less than 0.05 according to the theoretical calculations and crystal studies.[46-49] Using the assumption of axial symmetry (i.e. $\eta = 0$) to eliminate ψ dependence, as is certainly true for deuterons in sp^3 bonds to carbon, the three energy levels for a single deuteron (Fig. I-15) may be written as

$$\begin{aligned} \bar{E}_{-1} &= \nu_0 + \frac{\nu_Q}{4}\,\frac{3\cos^2\theta - 1}{2} \\ \bar{E}_0 &= -\frac{\nu_Q}{2}\,\frac{3\cos^2\theta - 1}{2} \\ \bar{E}_1 &= -\nu_0 + \frac{\nu_Q}{2}\,\frac{3\cos^2\theta - 1}{2} \end{aligned} \qquad (29)$$

The allowed transitions are governed by the selection rule $\Delta m = \pm 1$; the resonance frequency ν_t (for $\Delta m = -1$ transition) is given by

$$\begin{aligned} \nu_+ &= \bar{E}_{-1} - \bar{E}_0 = \nu_0 + \frac{3}{4}\,\nu_Q\,\frac{3\cos^2\theta - 1}{2} \\ \nu_- &= \bar{E}_0 - \bar{E}_{+1} = \nu_0 - \frac{3}{4}\,\nu_Q\,\frac{3\cos^2\theta - 1}{2} \end{aligned} \qquad (30)$$

Thus, two resonance lines of equal intensity are observed, and their separation results in the "quadrupole splitting".

$$\Delta\nu_Q = \nu_+ - \nu_- = \frac{3}{2}\,\nu_Q\,\frac{3\cos^2\theta - 1}{2} \qquad (31)$$

$$= \frac{3}{2}\,\frac{e^2qQ}{h}\,\frac{3\cos^2\theta - 1}{2}$$

The term e^2qQ/h is generally referred to as the static quadrupole coupling constant, where eQ is the nuclear quadrupole moment, eq is the e.f.g. at the deuterium nucleus, and h is Planck's constant.

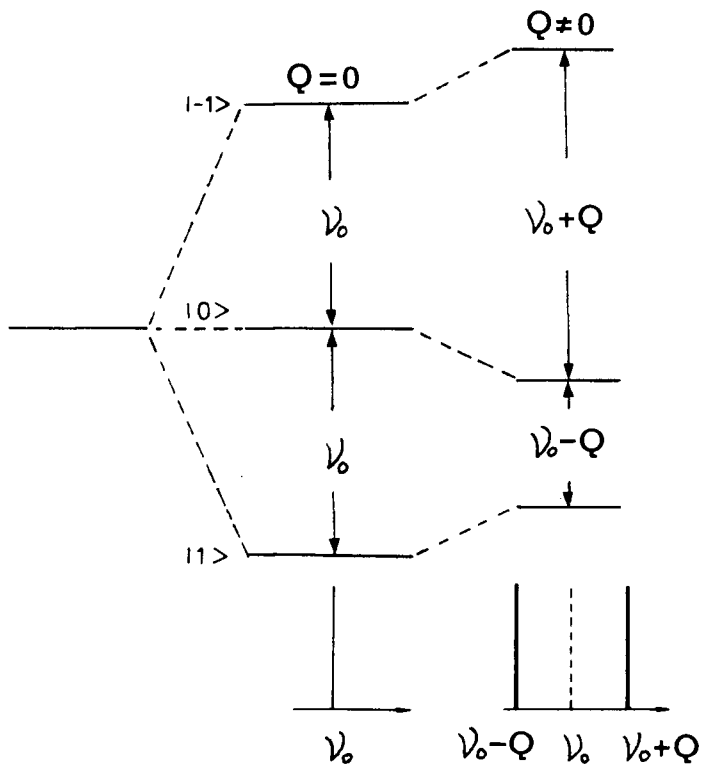

Fig. I-15. Energy level diagram for spin, I = 1, showing the effect of a weak electric quadrupole interaction, Q, on the Zeeman levels.

I.2.3. Electric Field Gradient Effects

The e.f.g. is characterized by a symmetric second rank tensor, $\hat{V}$, with principal elements given by V_{xx}, V_{yy}, and V_{zz}. These three parameters are not independent, that is,

$$V_{xx} + V_{yy} + V_{zz} = 0$$

where

$$V_{xx} = -\frac{1}{2}(1 - \eta)V_{zz}$$

$$V_{yy} = -\frac{1}{2}(1 + \eta)V_{zz} \qquad (33)$$

Conventionally, the e.f.g. principal axes are chosen such that $V_{zz} > V_{xx} > V_{yy}$ where V_{zz} is along the C-D bond, V_{yy} is perpendicular to the plane of the bond, and V_{xx} is orthogonal to these two axes. Therefore,

$$\eta = \frac{V_{xx} - V_{yy}}{V_{zz}} \qquad (34)$$

which assures that its value lies between 0 and 1.

In general, it is usually not possible to give a simple analytical expression for the quadrupolar energy to include the effects of field gradient asymmetry. However, the following equations hold true for the spin 1 case:

$$\Delta\nu_1 = \frac{3}{4}\nu_Q(1 - \eta)$$

$$\Delta\nu_2 = \frac{3}{4}\nu_Q(1 + \eta) \qquad (35)$$

$$\Delta\nu_3 = \frac{3}{2}\nu_Q$$

The effect of η on the lineshape is to split the singularity (which corresponds to $\theta = 90^\circ$) into two parts.[50] A shoulder grows out of the singularity and moves away from ν_o with increasing η (Fig. I-16). At the same time, the singularity itself shifts an equal amount away from its original ($\eta = 0$) position back towards ν_o. Evidently, as η approaches zero, the Ψ dependence is eventually eliminated to yield Eq. (31).

I.2.4. Deuterium N.M.R. of Liquid Crystals

In the liquid or gaseous state, where molecular reorientation is rapid relative to the reciprocal of the quadrupole coupling constant, the term $(3\cos^2\theta - 1)$ in Eq. (31) is averaged to zero. The quadrupole splitting collapses to yield a single peak at ν_o.

Some materials are known to form liquid crystals, in which certain domains exist where there is considerable ordering of the molecules. In the presence of B_o, some liquid crystalline phases tend to become aligned, with the long axis of the liquid crystal-forming molecules oriented approximately parallel to the field. Due to rapid

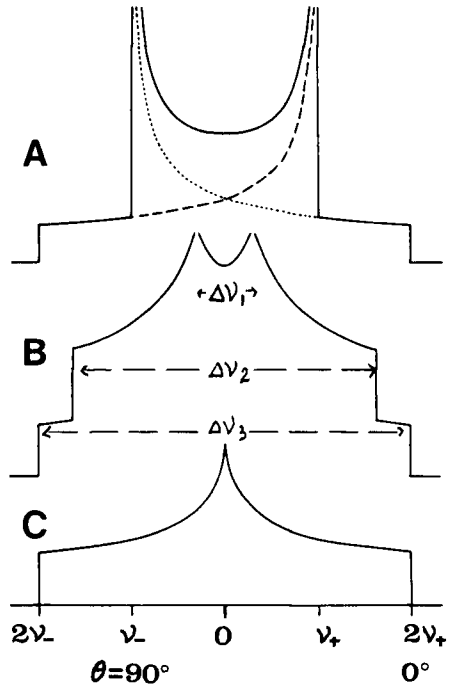

Fig. I-16. Calculated powder pattern for spin, I = 1, in the following electric field gradients: (A) η = 0.0; (B) η = 0.67; (C) η = 1.0 (from Ref. [50]).

reorientation of the molecules (about an axis of at least C_3 symmetry) within the liquid crystal, only a partial ordering of the molecules exists, and the time-average "order parameter", S_{CD}, is related to the observed quadrupole splitting according to the expression[51]

$$\Delta\nu_Q = \frac{3}{2}\frac{e^2qQ}{h} S_{CD} \qquad (36)$$

$$S_{CD} = \left\langle \frac{3\cos^2\theta - 1}{2} \right\rangle$$

where θ is the angle between the C-D vector and B_o. If the long axis is not parallel to the field direction but makes

an angle Ω with this axis (Fig. I-17), the observed doublet spacing may be written as:

$$\Delta\nu_Q(\Theta,\Omega) = \frac{3}{2}\frac{e^2qQ}{h}\left\langle\frac{3\cos^2\Theta_n - 1}{2}\right\rangle\left\langle\frac{3\cos^2\Omega - 1}{2}\right\rangle \quad (37)$$

$$= \frac{3}{2}\frac{e^2qQ}{h}S_{CD_n}\left\langle\frac{3\cos^2\Omega - 1}{2}\right\rangle$$

where Θ_n is the angle between the C-D bond direction and the normal $\underset{\sim}{n}$. The quadrupole splitting collapses if the long axis is inclined at the "magic angle" ($\Omega = 54.7^\circ$) with respect to B_o.

For a lipid bilayer consisting of a lyotropic liquid crystal derived from a deuterated long-chain hydrocarbon, S_{CD_n} is a measure of the time-average fluctuation of the C-D bond axis with respect to $\underset{\sim}{n}$ to the bilayer surface.

Rowell et al.[52] have shown that the deuterium n.m.r. spectra of aromatic compounds dissolved in a nematic matrix always give rise to a doublet which is split by the quadrupole interaction. Such molecules participate in the anisotropic motion of the solvent, and the analysis of their n.m.r. spectra is quite straightforward.

I.2.5. Deuterium N.M.R. of Polycrystalline Samples

I.2.5.1. Static Orientation of a C-D bond

For rigid polycrystalline (or powder) samples where many small crystals are randomly oriented with respect to

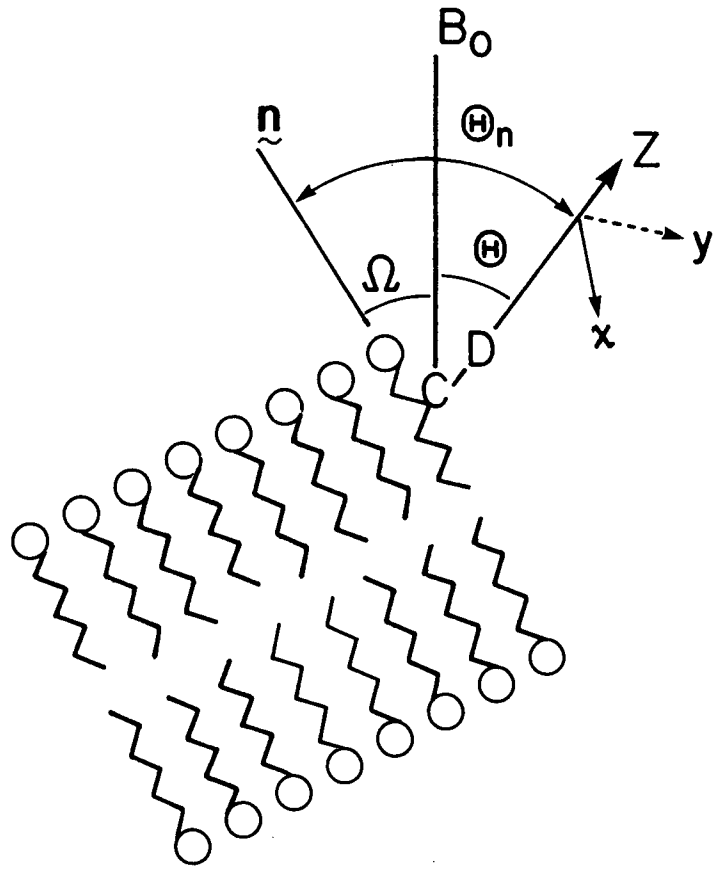

Fig. I-17. Schematic representation of a lipid bilayer. [$\underset{\sim}{n}$ is the normal to the bilayer. Ω is the angle between the magnetic field B_0 and $\underset{\sim}{n}$, Θ is the angle between the C-D vector and B_0, and Θ_n is the angle between the C-D vector and $\underset{\sim}{n}$.]

B_0, the deuterium resonance is observed as a broad envelope. The shape of the "powder-type" spectrum is then the average over the resonances of all values of θ of the nuclear spins. Each of the individual orientations in the polycrystalline sample gives two resonances, and each orientation must be given equal statistical weight.

For a uniform distribution of N nuclei over a surface of a sphere of radius r, the number of nuclei per unit area is $N/4\pi r^2$. The fraction dN of nuclei oriented between θ and $\theta + d\theta$ with respect to B_0 (Fig. I-18) is given by the area

of a zone of the sphere, $2\pi r^2 \sin\theta d\theta$, multiplied by the spin surface density:[51]

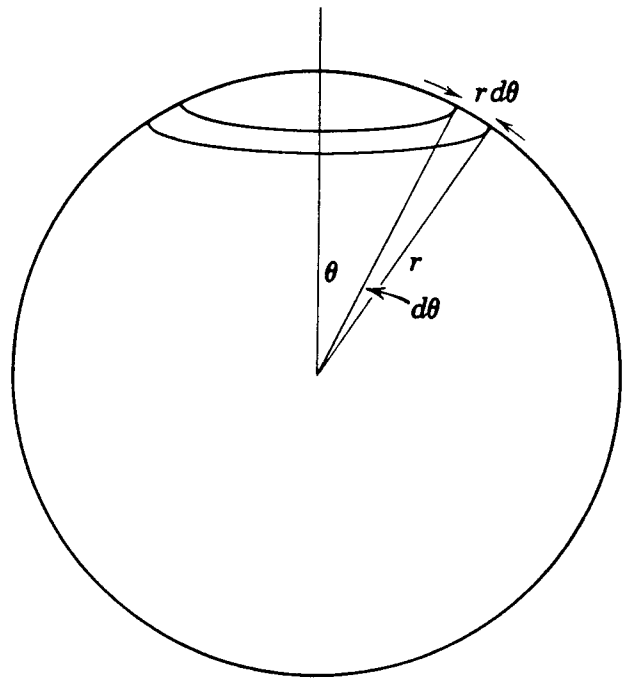

Fig. I-18. Annular ring between θ and $d\theta$ with area $2\pi r^2 \sin\theta d\theta$.

$$dN = (N/4\pi r^2)2\pi r^2 \sin\theta d\theta \qquad (38)$$

$$= (N/2)\sin\theta d\theta$$

The probability density $p(\theta)$ is then given by

$$p(\theta) = 1/2(\sin\theta) \qquad (39)$$

$$\int_0^\pi p(\theta)d\theta = 1 \qquad (40)$$

According to Eq. (30), the resonance frequency $\nu_{\pm}$ is dependent on the orientation angle θ:

$$\nu_{\pm} = \nu_o \pm \frac{3}{2}\nu_Q \frac{3\cos^2\theta - 1}{2}$$

For convenience, a "reduced" resonance frequency $\xi_{\pm}$ is defined as

$$\xi_{\pm} = \frac{\nu_{\pm} - \nu_o}{\frac{3}{4}\nu_Q} = \pm \frac{3\cos^2\theta - 1}{2} \qquad (41)$$

where $1 \geq \xi_+ \geq -1/2$ and $-1 \leq \xi_- \leq +1/2$. The probability function $p(\xi)$ is defined such that $p(\xi)d\xi$ describes the fraction of spins between ξ and $\xi + d\xi$. The two probability densities $p(\theta)$ and $p(\xi)$ are related to each other by

$$p(\xi) = p(\theta)\frac{d\theta}{d\xi} = \frac{1}{2}\sin\theta\frac{d\theta}{d\xi} = -\frac{1}{2}\frac{d\cos\theta}{d\xi} \qquad (42)$$

Now the deuterium spectrum can be expressed in terms of the two resonances ξ_+ and ξ_-, so that

$$p(\xi) = p(\xi_+) + p(\xi_-) \qquad (43)$$

Combining Eqs. (41) and (42), the probability densities are given by the following relationship.

$$p(\xi_{\pm}) \propto \frac{1}{\sqrt{\pm 2\xi_{\pm} + 1}} \qquad (44)$$

A typical powder spectrum (Fig. I-19) is obtained by plotting the probability densities $p(\xi_+)$, $p(\xi_-)$, and $p(\xi)$ against ξ. Because $p(\xi)$ diverges at frequencies $\xi = \pm 1/2$, a peak separation corresponding to $\theta = 90^\circ$ and a shoulder separation corresponding to $\theta = 0^\circ$ are observed. For $\eta = 0$, their respective separations are given by

$$\Delta\nu_Q = \frac{3}{4}\frac{e^2qQ}{h}$$

and (45)

$$2\Delta\nu_Q = \frac{3}{2}\frac{e^2qQ}{h}$$

These expressions assume that there are no fast ($>10^5$ s^{-1}), large-amplitude motions of the C-D vectors in the solid sample. It should be noted that the experimental spectrum is slightly different from its theoretical counterpart due to the dipolar broadening, and the measured peak to peak value is less than the actual splitting.[53] As an empirical experimental correction, peak positions are usually taken slightly to the outer-side of the spectral peaks.

I.2.5.2. Reorientational Motions for a C-D Bond

In the case of "fast" reorientational motion, with a correlation time $\tau_c < 1/\Delta\nu_Q$, it is necessary to make a time average of the field gradient tensor.[44] This motion should

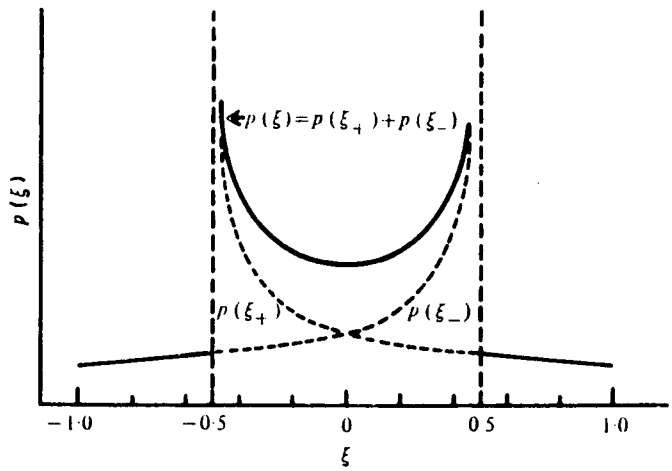

Fig. I-19. Theoretical powder pattern for a deuteron in a symmetric electric field gradient ($\eta = 0$). The dashed lines indicate the individual components of the m = -1 <--> m = 0 (ξ_+) and m = 0 <--> m = +1 (ξ_-) transitions, while the solid line represents the sum of the two components (from Ref. [51]).

be uniform about an arbitrary axis z' (Brownian motion, or planar jumps between equivalent sites of symmetry higher than, or equal to, C_{3v}) in order that partial averaging of the original quadrupole tensor to an effective axially symmetric tensor, with its principal axis along z', would occur. Using the notation of Fig. I-20, it can be shown that the motionally averaged splitting, $\Delta\nu_{Q_1}$, is

$$\Delta\nu_{Q_1} = \frac{3}{2}\,\frac{e^2qQ}{h}\,\frac{(3\cos^2\theta' - 1)(3\cos^2\beta - 1)}{2} \qquad (46)$$

where θ' is the angle between the axis of motional averaging and the magnetic field direction, and β is the angle between the principal axis of the e.f.g. tensor and

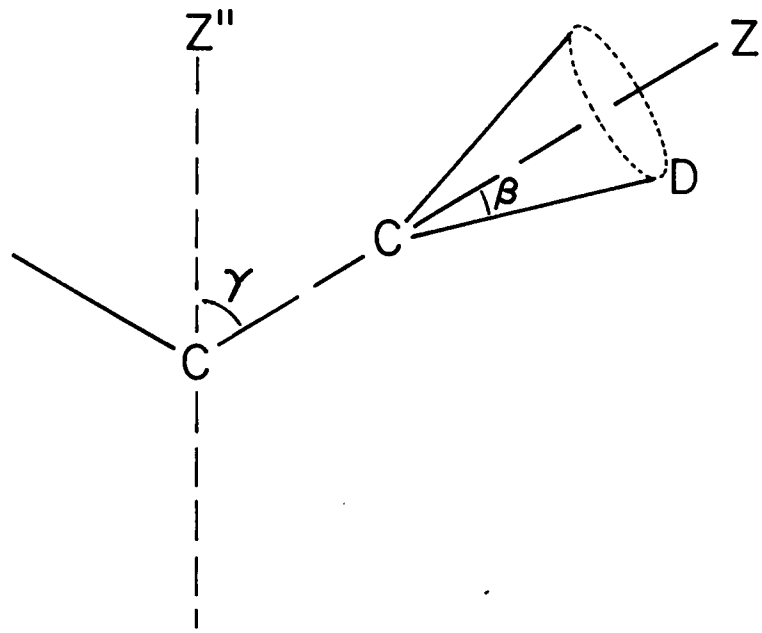

Fig. I-20. Illustration of reorientational motions for a C-D bond inclined at β degrees with respect to an axis of motional averaging, z', which in turn is inclined at γ degrees with respect to another axis of motional averaging, z''.

the axis of the motional averaging. From the experimental value of $\Delta\nu_{Q_1}$, the angle β can thus be obtained. Any other rapid motion occurring about a second diffusion axis z" would further reduce the quadrupole splitting, by further shrinking of the effective quadrupole tensor. By measuring the corresponding values $\Delta\nu_{Q_1}$ and $\Delta\nu_{Q_2}$, the angle γ between z' and z" can be derived from

$$\Delta\nu_{Q_2} = \Delta\nu_{Q_1} \frac{(3\cos^2\gamma - 1)}{2} \qquad (47)$$

It is possible to compute the lineshape corresponding to the presence of any other type of motion by considering the angles, amplitudes, and the rates involved. Different types of models for molecular reorientation have been investigated, however, this is usually difficult, time consuming, and arbitrary.[54] In general, the problem is simpler for fast motion where the angles involved are the only parameters required for the calculations of spectra for well-defined motional models.

I.2.6. Spin Echoes in Solids

The first example, of what is now a whole family of ingenious experiments which have been designed to remove the effect of the applied field inhomogeneity, was first reported by Hahn in 1950.[55] Initially, a 90° pulse is applied along x' at time zero to a spin system (Fig. I-21). The magnetization that has decayed in the rotating x'-y' plane due to external field inhomogeneity can be refocussed into an echo by an appropriate pulse (which can be 90° out of phase, although this is not mandatory). An inverted spin echo is obtained when a 180° pulse is applied along the x' axis. Also, an echo can be observed following a 90° pulse (90° out of phase); that this can only be a dipolar echo demonstrates the existence of an average static

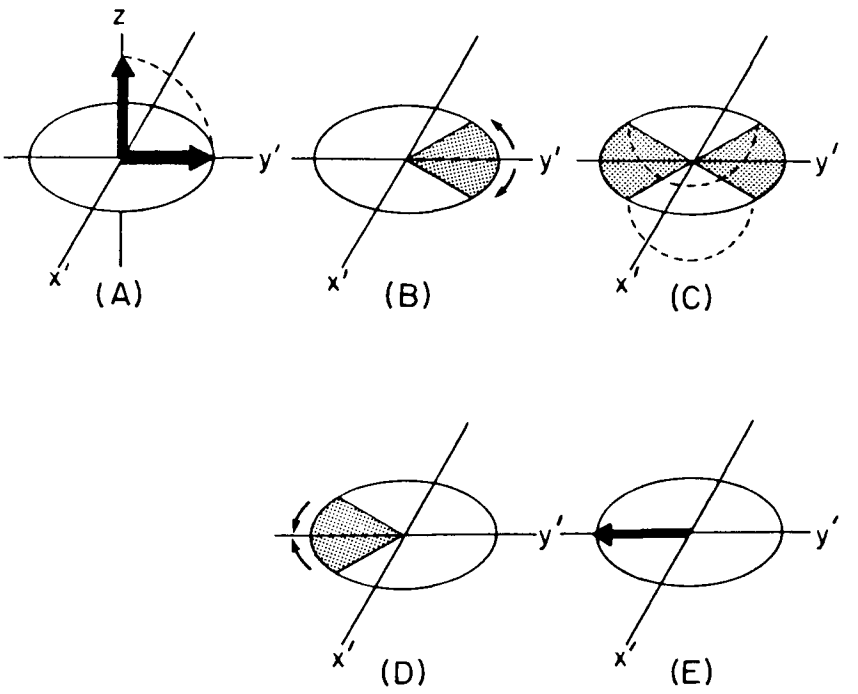

Fig. I-21. Rotating frame representation of the spin isochromats in a Hahn echo sequence.

interaction. The (180^{0}_{x}) Hahn echo cannot be formed for dipolar coupled solids because the local field is not static; now the second pulse simply inverts all spins and, consequently, the local fields as well.

Quadrupole echoes were first observed from solids by Solomon[56] for the I = 5/2 species ^{127}I in KI. The calculations were carried out for a $90\text{-}\tau\text{-}\beta_{0^\circ}$ (XX) sequence, where β is the variable width of the second pulse, and the notation β_{0° indicates a zero-degree phase-shift between the initial, 90° pulse and the second, β pulse. The analysis was based on the assumption that the dipolar interactions were negligibly small in comparison with the

quadrupolar terms. According to the author, no spin-echo response for any rotation angle, β, in the solid state for spins I = 1 is anticipated, using this pulse sequence.

Deuterium n.m.r. spin echoes were subsequently observed by applying the $90\text{-}\tau\text{-}\beta_{0^\circ}$ sequence[57] to perdeuterated organic solids, under the conditions such that $\beta \neq k.90^\circ$, and $k = 0,1,2,...$ This experimental observation proves that dipolar interactions between deuterons in these systems cannot be neglected, since such echoes arise only in their presence. This theory predicts that the echo-amplitude is dependent on β and τ, the width of the second pulse and the interpulse spacing, respectively.

The deuteron spin echo response for a $90^\circ\text{-}\tau\text{-}\beta_{90^\circ}$ (XY) sequence is given by the expression:[57]

$$E_{XY}(\beta,\tau) = a(\tau)\sin^2\beta + b(\tau)\sin^2\beta\cos^2\beta \qquad (48)$$

The $\sin^2\beta$ component dominates $E_{XY}(\beta,\tau)$ at short τ, but it decays much faster than the $\sin^2\beta\cos^2\beta$ component. Thus, the maximum echo amplitude shifts to $\beta < 90^\circ$ with increasing τ. In the absence of dipolar interactions, the second term vanishes. Theoretically, only the first term of the XY echo is predicted for the isolated spin I = 1 subjected to quadrupole interactions.

For the XX sequence, in the presence of dipolar interactions between spins, the dependence is

$$E_{xx}(\beta,\tau) = -c(\tau)\sin^2\beta\cos^2\beta \qquad (49)$$

This term vanishes if there are no dipolar interactions. In these expressions, a, b, and c are constants for a given τ value, since they are independent of β. Apart from a change of sign, the theory also predicts that the echo shape is the same for the two pulse sequence.

I.2.7. Deuterium N.M.R. Experiments

The usual experimental procedure for a pulse F.t. n.m.r. measurement involves the accumulation of the f.i.d. following application of a 90° pulse which is applied at a frequency, ν, set close to the sample's resonant frequency, ν_0. The frequency spectrum of this sample is then obtained by Fourier transformation of the f.i.d.. This same technique is also applicable to deuterium quadrupolar systems, in which the spectrum of a given deuteron is a doublet with lines at $\nu_0 \pm \nu$. However, such powder spectra are often very broad, which presents some serious problems for pulsed F.t. n.m.r.. For example, it is difficult to excite the sample uniformly across the whole spectral range using a r.f. pulse of finite power. Furthermore, the total decay time of the f.i.d. following a single excitation pulse is only a few tens of microseconds; this is shorter than the recovery time of the probe following the pulse. Since much of the information is contained in the very early part of the f.i.d., it is mandatory to circumvent the

"dead-time" of the receiver.[42,43]

Largely because of the latter problem, the application of F.t. methods to deuterium n.m.r. in high fields enjoyed little success until the development in 1976, of the F.t. solid echo method, which is now routinely used to overcome the receiver dead time. This involves a two-pulse, quadrupole echo sequence as shown below: An initial pulse,

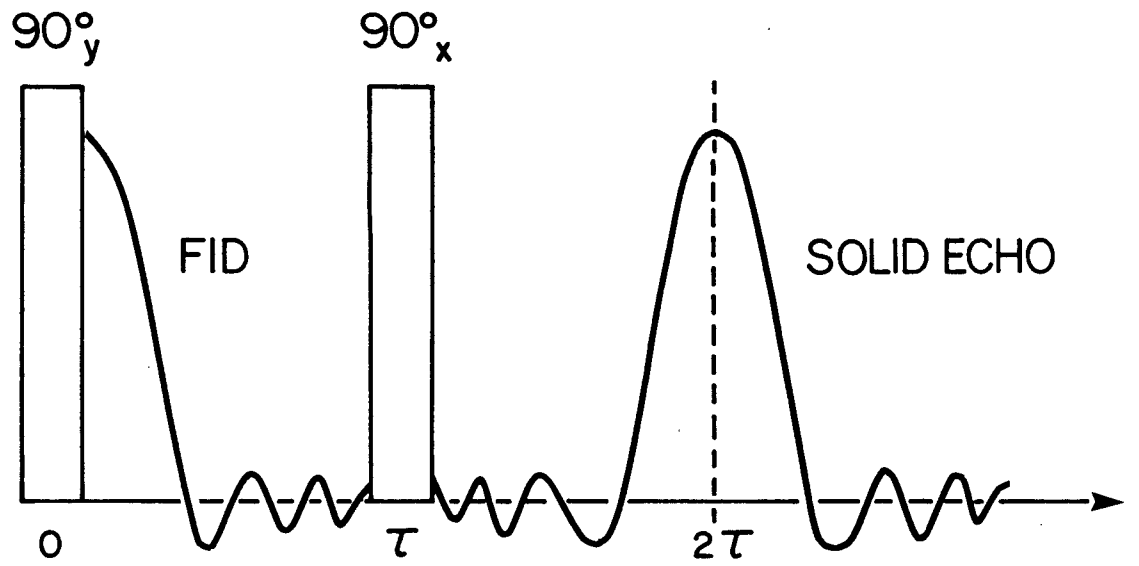

Schematic representation of a ^2H solid echo pulse sequence.

which rotates the magnetization by 90°, is followed at a time τ later by a second 90° pulse which is phase shifted by 90° with respect to the first. A characteristic signal called the "quadrupole solid-echo" is observed at $t = 2\tau$, which has maximum amplitude when the flip angle of these pulses is exactly 90°. If τ is set large, the probe will have sufficient time for full recovery from the effect of

the excitation pulses, and the signal may be accumulated with zero time set at the top of the echo. The refocussing of the nuclear magnetization is complete under these conditions, aside from the effects of relaxation and static magnetic field inhomogeneities.

It should be noted that this echo method does not necessarily lead to an undistorted spectrum. In fact, the finite width of the second pulse greatly reduces the intensity in the wings of the spectrum.[58] Also, the appearance of the spectrum is affected if Fourier transformation of the signal does not start at the top of the quadrupolar echo.[58,59] The bandwidth of the probe,[43] receiver,[60] and transmitter may also lead to distortions of the spectrum. Another kind of distortion occurs when the time scale for molecular reorientation is comparable to the echo refocussing time.[61] Thus, it is essential to recognize these effects in order to interpret the spectra correctly.

In an actual experiment, the pulse lengths are usually not exactly 90°, and the phases do not bear exactly the correct relation to the receiver phase. Since the second pulse not only produces an echo, but also a f.i.d. (90° out of phase to the echo), it is necessary to eliminate the latter by alternating the phase at the first pulse between 0° and 180° and that of the second pulse between 90° and 270°.

The use of pulses shorter than 90° may generate problems when quadrature phase detection is used, since the

quadrature component containing the f.i.d. following the second pulse would result in a serious distortion of the spectrum on Fourier transformation. In order to resolve this problem, τ is set as long as 240 μs to ensure that the f.i.d. has decayed at the time the echo maximum occurs.[43] This also effectively eliminates any remnant of the free induction signal arising from the first pulse, that is not refocussed by the second pulse.

For a broad deuterium n.m.r. spectrum, the spectral wings are progressively suppressed relative to the center as the pulse length is increased. This occurs as a result of the precession of the nuclear spins due to the quadrupolar interactions, during the r.f. pulse. This effect can be reduced by decreasing the pulse length, but only for spectra with good signal-to-noise ratio, since drastic reduction in intensity occurs when the flip-angle of the pulse, θ, is significantly shorter than $\pi/2$.

References

1. S. R. Hartmann, E. L. Hahn, Phys. Rev., 128, 2042(1962).
2. A. Pines, M. G. Gibby, J. S. Waugh, J. Chem. Phys., 59, 569(1973).
3. E. R. Andrew, Arch. Sci.(Geneva), 12, 103(1959).
4. I. J. Lowe, Phys. Rev. Lett., 2, 285(1959).
5. J. Schaefer, E. O. Stejskal, J. Am. Chem. Soc., 98, 1031(1976).
6. F. P. Miknis, Magn. Reson. Rev., 7, 87(1982).
7. H. Saitô, R. Tabeta, T. Harada, Chem. Lett., 1981, 571.
8. L. D. Hall, M. Yalpani, Carbohydr. Res., 91, C1(1980).
9. M. Mehring, NMR Basic Principles and Progress, Vol. 11, Springer-Verlag, Berlin, 1976; R. K. Harris, Nuclear Magnetic Resonance Spectroscopy, Pitman, London, 1983.
10. R. E. Wasylishen, C. A. Fyfe, Annu. Rep. NMR Spectrosc., 12, 1(1982).
11. E. R. Andrew, Prog. Nucl. Magn. Reson. Spectrosc., 8, 1(1971).
12. J. H. Van Vleck, Phys. Rev., 74, 1168(1948).
13. C. S. Yannoni, Acc. Chem. Res., 15, 201(1982).
14. R. G. Griffin, G. Bodenhausen, R. A. Haberkorn, T. H. Huang, M. Munowitz, R. Osredkar, D. J. Ruben, R. E. Stark, H. van Willigen, Phil. Trans. R. Soc. Lond. A, 299, 475(1981).
15. A. Abragam, The Principles of Nuclear Magnetism, Oxford University Press, London, 1961.

16. G. Sinning, M. Mehring, A. Pines, Chem. Phys. Lett., 43, 382(1976).

17. A. Pines, M. G. Gibby, J. S. Waugh, ibid., 15, 373(1972).

18. E. O. Stejskal, J. Schaefer, R. A. McKay, J. Magn. Reson., 25, 569(1977).

19. J. H. Noggle, R. E. Schirmer, The Nuclear Overhauser Effect, Academic Press, New York, 1971.

20. H. W. Bernard, J. E. Tanner, J. G. Aston, J. Chem. Phys., 50, 5016(1969).

21. L. B. Alemany, D. M. Grant, R. J. Pugmire, T. D. Alger, K. W. Zilm, J. Am. Chem. Soc., 105, 2133(1983).

22. D. L. VanderHart, W. L. Earl, A. N. Garroway, J. Magn. Reson., 44, 361(1981).

23. W. L. Earl, D. L. VanderHart, ibid., 48, 35(1982).

24. E. R. Andrew, A. Bradbury, R. G. Eades, Nature, 182, 1659(1958).

25. I. J. Lowe, Phys. Rev. Lett., 2, 285(1959).

26. V. J. Bartuska, G. E. Maciel, J. Magn. Reson., 42, 312(1981).

27. C. A. Fyfe, H. Mossbruger, C. S. Yannoni, ibid., 36, 61(1979).

28. G. R. Hayes, R. Huis, A. D. H. Clague, Bull. Magn. Reson., 2, 120(1981).

29. N. Zumbulyadis, J. Magn. Reson., 49, 329(1982).

30. J. Schaefer, E. O. Stejskal, R. Buchdahl, Macromolecules, 10, 384(1977).

31. W. T. Dixon, J. Magn. Reson., 44, 220(1981).

32. M. A. Hemminga, P. A. De Jager, K. P. Datema, J. Breg, ibid., 50, 508(1982).

33. S. J. Opella, M. H. Frey, J. Am. Chem. Soc., 101, 5854(1979).

34. L. D. Hall, T. K. Lim, Carbohydr. Res., 124, C1(1983).

35. P. E. Pfeffer, K. B. Hicks, M. H. Frey, S. J. Opella, W. L. Earl, J. Magn. Reson., 55, 344(1983).

36. M. Alla, E. Lippmaa, Chem. Phys. Lett., 37, 260(1976).

37. J. Tegenfeldt, U. Haeberlen, J. Magn. Reson., 36, 453(1979).

38. S. Ganapathy, A. Naito, C. A. McDowell, J. Am. Chem. Soc., 103, 6011(1981).

39. V. P. Chacko, S. Ganapathy, R. G. Bryant, ibid., 105, 5491(1983).

40. S. J. Opella, J. G. Hexem, M. H. Frey, T. A. Cross, Phil. Trans. R. Soc. A, 299, 665(1981).

41. R. G. Barnes, Adv. Nucl. Quadrupole Reson., 1, 335(1974).

42. J. H. Davis, K. R. Jeffrey, M. Bloom, M. I. Valic, T. P. Higgs, Chem. Phys. Lett., 42, 390(1976).

43. D. Hentschel, H. W. Spiess, J. Magn. Reson., 35, 157(1979).

44. E. Meirovitch, I. Belsky, S. Vega, J. Phys. Chem., 88, 1522(1984) and references therein.

45. G. E. Pake, J. Chem. Phys., 16, 327(1948).

46. J. R. Hoyland, J. Am. Chem. Soc., 90, 2227(1968).

47. W. Derbyshire, T. Gorvin, D. Warner, Mol. Phys., 17, 401(1969).

48. B. M. Fung, I. Y. Wei, J. Am. Chem. Soc., 92, 1497(1970); B. M. Fung, Nat. Acad. Sci., 1974, 436.

49. R. G. Barnes, J. W. Bloom, Mol. Phys., 25, 493(1973).

50. R. G. Barnes, J. W. Bloom, J. Chem. Phys., 57, 3082(1972).

51. J. Seelig, Q. Rev. Biophys., 10, 353(1977).

52. J. Rowell, W. Phillips, L. Melby, M. Panar, J. Chem. Phys., 41, 3442(1965).

53. M. Bloom, E. E. Burnell, S. B. W. Roeder, M. I. Valic, ibid., 66, 3012(1977).

54. C. M. Gall, J. A. DiVerdi, S. J. Opella, J. Am. Chem. Soc., 103, 5039(1981).

55. E. L. Hahn, Phys. Rev., 80, 580(1950).

56. I. Solomon, Phys. Rev., 110, 61(1958).

57. N. Boden, S. M. Hanlon, Y. K. Levine, M. Mortimer, Mol. Phys., 36, 519(1978).

58. M. Bloom, J. H. Davis, M. I. Valic, Can. J. Chem., 58, 1510(1980).

59. J. H. Davis, Biochim. Biophys. Acta, 737, 117(1983).

60. D. E. Barnaal, I. J. Lowe, Rev. Sci. Instrum., 37, 428(1966).

61. H. W. Spiess, H. Sillescu, J. Magn. Reson., 42, 381(1981).

CHAPTER II

CYCLODEXTRINS AND THEIR INCLUSION COMPLEXES

Chemistry of Cyclodextrins

II.1. Introduction

Cyclodextrins (CDs) were first isolated as degradation products of starch in the last century by Villiers (1891),[1] and were subsequently characterized as cyclic-oligosaccharides in 1904 by Schardinger.[2,3] In 1938 Freudenberg et al.[4] reported procedures for preparing pure cyclodextrins, and also the elucidation of their chemical structures. By the mid-fifties, many of the earlier conflicts on their physical and chemical properties had been resolved, and recently the chemistry of cyclodextrins has been updated in review articles[5,6] and books.[7,8] They are now correctly described as cyclic, non-reducing oligosaccharides containing between six and twelve $\alpha(1\rightarrow4)$-linked glucopyranose units. Cyclodextrins are also referred to as cycloamyloses, cycloglucans, Schardinger dextrins, and sometimes simply as dextrins. The most common ones that can be obtained in large scale are the α-, β-, and γ-cyclodextrins that consist of six, seven, and eight glucose units, respectively. Alternatively, they may be designated by the names cyclohexa-, cyclohepta-, and cycloctaamyloses, which are more descriptive of the structures. They have torus-like macrorings that are capable of forming inclusion compounds with smaller "guest" molecules which fit into their 6-10 Å cavity (Fig. II-1). However, the rings of the higher homologues are highly flexible; their wide cavities may not enclose the guest molecules tightly

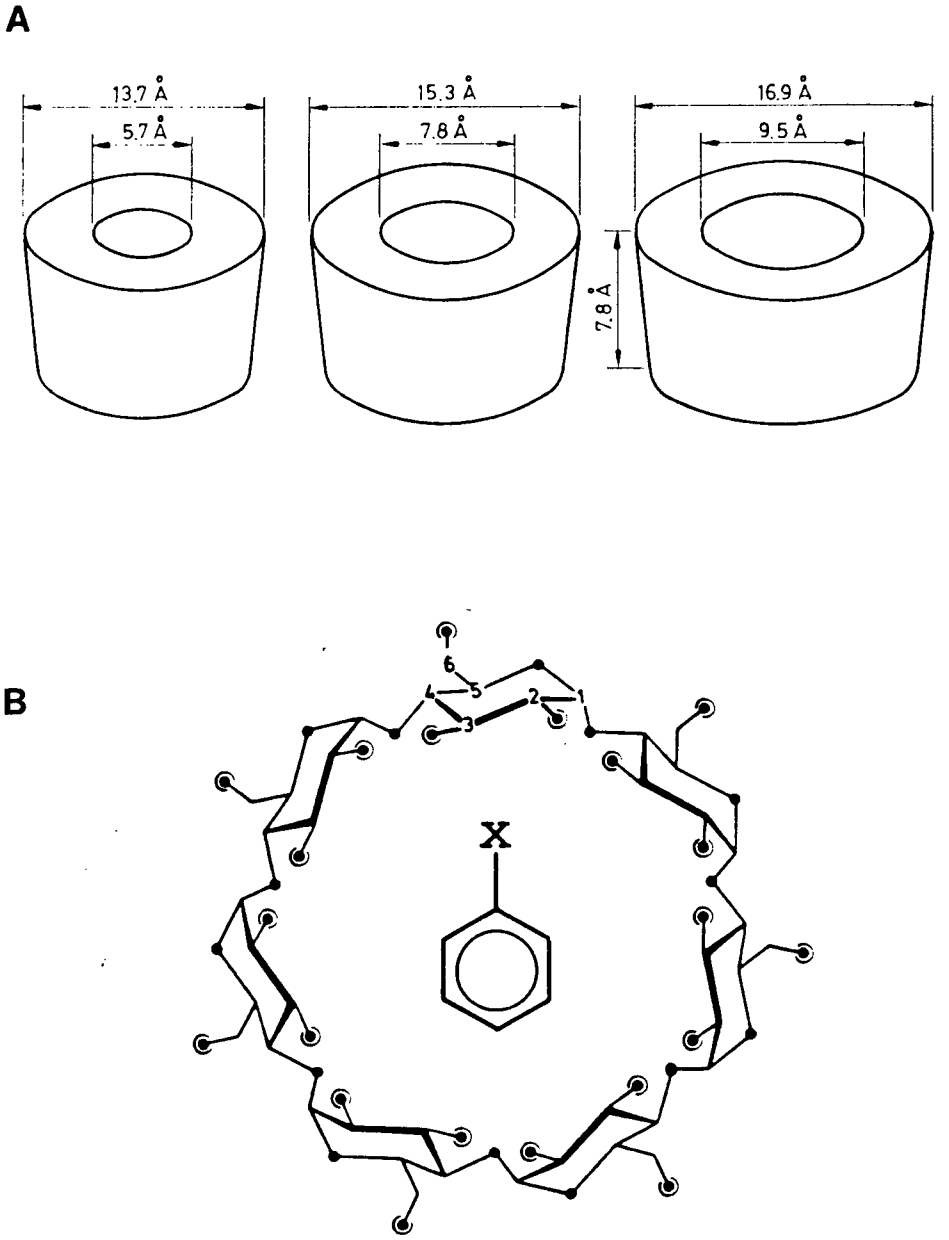

Fig. II-1. Cyclodextrins: (A) dimensions of α-, β-, and γ-cyclodextrins; (B) structure of β-cyclodextrin (from Ref. [8]).

enough to promote complex formation.

A great deal of attention has been focussed on them as excellent models[9] of hydrolytic enzymes, both in terms of substrate complexation and reactivity. They are most outstanding in facilitating chemical reactions amongst heterogeneous and homogeneous reagents. Cyclodextrins are also used in the production of pharmaceuticals, pesticides, foodstuffs, and toilet articles; the sensitive substances enclosed within them are protected from the effects of light and the atmosphere, thereby enabling easy handling and storage in the powder form. By complexation, the irritant effects of some substances can be suppressed (e.g. treatment of iodine poisoning with starch), and many unpleasant tastes or odors may be reduced or even eliminated completely. The cyclodextrin-iodine complexes[10] also serve as models for the investigation of the more complicated polymeric starch-iodine reaction. Cyclodextrins have been employed in gel inclusion[11] and affinity chromatography[12] by binding chemically to a polymer carrier and as selective synthetic membranes[13] by merely incorporating them into the polymer matrix. Selective chemical modification[14] of cyclodextrins provides opportunities to influence their complexing behavior by introducing various groups or compounds either by ionic or covalent bonding into the macroring. Methylated cyclodextrins have been prepared[15] and shown to be versatile complexing agents, in both aqueous and organic

solvents. The stability of their crystalline complexes depends on the shape and size of the encaged molecule. Acetylated cyclodextrins may also serve as host for smaller-size organic molecules; this has been demonstrated in this thesis, using β-cyclodextrin peracetate.

II.1.1. The Structure of Cyclodextrins

It is necessary to have an accurate understanding of the nature of the cavity of the cyclodextrins in order to establish the forces that stabilize inclusion complexes. The intermolecular interactions responsible for complex formation have been discussed for known complexes, and some suggestions on the cavity of the cyclodextrins have been proposed.[6]

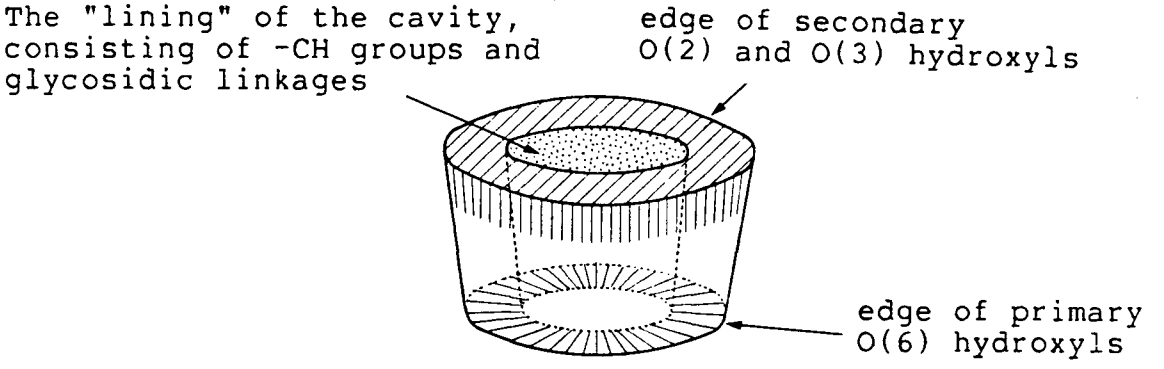

Fig. II-2. Characteristic structural features of cyclodextrins (from Ref. [8]).

The conformation of the cyclodextrins has an important bearing on the physical and chemical properties. From the evidence accumulated by X-ray crystallographic and n.m.r.

studies,[16,17] a more or less undistorted C1(D)-chair conformation of the glucose units is favored. The narrower opening of these toroidal-shaped molecules (Fig. II-2) contains the primary O(6) hydroxyl groups whereas the wider opening is occupied by the secondary O(2) and O(3) hydroxyls. Hence, the outside of the cavity is hydrophilic in character, while, the inside is hydrophobic as the lining consists of -CH groups and glycosidic linkages. The C(6)-O(6) bonds are preferentially directed away from the cavity except for hydrogen bonding occurring between the hydroxyl groups and the included guest molecules, which are mainly held by close contacts to the -CH hydrogen atoms lining the cavity. It was observed that cyclodextrins always adopt a "round" structure, with intramolecular hydrogen bonds O(3)-H..O(2) and O(3)..H-O(2) existing between adjacent glucopyranose units.[6] These interactions stabilize the macrocycle and at the same time significantly influence its solubility in water. Deuterium exchange studies[18,19] of the hydroxyl groups have been followed by n.m.r. spectroscopy, and the equilibrium constants are 0.75 and 0.65 for α- and β-cyclodextrins, respectively; these values are smaller than that for amylose (0.85). This indicates that the interactions are strongest for β-cyclodextrin whose flexibility is the weaker of the two cyclodextrins. It is therefore reasonable to assume that the structural features derived from the crystalline state will be largely retained in solution, because of the

conformational restraints imposed on them by their looped arrangement.

II.1.2. The Driving Force for Complexation

There has been relatively little emphasis placed on the understanding of the interactions responsible for substrate binding. A number of suggestions as to the origins of these driving forces have been made, and the three major ones are as follows: release of cyclodextrin strain energy, release of high-energy cavity water, and van der Waals and London dispersion forces. Verification of these binding forces would require some knowledge of the complexes in solution.

Recently, Bergeron et al.[20] were able to show that release of strain energy could only play a minor role in complexation. In the "empty" α-cyclodextrin-water complex, Manor and Saenger[21] pointed out that the two water molecules, with a van der Waals radius of 3.8 Å, are located in a fixed position within the 5.0 Å wide cavity that is slightly collapsed. This can be achieved by the rotation of one of the six glucopyranose units, thereby, resulting in a snug fit with the small molecules. However, this would disrupt the intramolecular hydrogen bonding of the secondary hydroxyl groups and also would impose steric strain at the glycosidic linkages. Upon complex formation, the strain is relieved together with a drop in potential energy, but this driving force is of little importance to

"empty" β- and γ- cyclodextrins which are not strained.

Crystallographic studies[22] of cyclodextrins and their inclusion complexes, reveal that water molecules occupy the hydrophobic cavity in the absence of a guest molecule. These water molecules are thought to be unstable (high in enthalpy) due to their inability to form hydrogen bonds with the bulk water molecules and the groups lining the cavity. However on complexation, a guest molecule would displace the water before occupying the cavity and at the same time strip off its own hydration sphere. The former would result in a favorable decrease in enthalpy, and this driving force may be considered to be nonspecific. When the released water molecules are taken up by the bulk water, this increases the stability of the complex due to an increase in entropy. For a relatively apolar guest molecule, this process is expected to generate a favorable binding force which dominates when electrostatic or coordination interactions are less important.[8]

The interactions between the substrate and the surrounding cyclodextrin are usually weak and are mainly due to van der Waals and dispersion forces.[6] Thus, small molecules are usually disoriented within the cavity, even in the presence of hydrogen bonding with the O(6) hydroxyl groups. More recent experiments and theoretical considerations have indicated that these forces probably dominate in clathration. The other forces discussed above may also be involved to a certain extent, depending on the

nature of the encaged molecule.

II.1.3. Cyclodextrin Inclusion Complexes

Inclusion complexes are molecular compounds having the characteristic structure of an adduct, in which the "host" molecule spatially encloses the "guest". The latter is situated in the cavity that often remains practically unaltered, beyond a slight deformation. Research on carbohydrate inclusion complexes has been reviewed by several authors,[22,23] and cyclodextrins have drawn the most attention.

The most interesting feature of these cyclodextrins is their ability to form complexes with a variety of guest molecules in their cavity. These guest molecules range from polar reagents such as acids, amines, small ions such as ClO_4^-, SCN^-, and halogen anions,[24] to highly apolar aliphatic and aromatic hydrocarbons and, even, rare gases.[25] The stability of these complexes varies with the size of the guest and the host, and the obvious requirement is a mutual fit between them. Large substrates will not be able to penetrate into the cavity and therefore no binding will occur. On the contrary, small subtrates will move freely in and out of the cavity with little or no apparent binding. Thus, the "best fit" phenomenon[26] can be used in separating the cyclodextrins from each other. For example, α-, β-, and γ-cyclodextrins are effectively precipitated from aqueous solution by benzene. However, only γ-

cyclodextrin can form insoluble complex with anthracene, while the other two remain in solution because the substrate will not effectively penetrate their cavities. Similarly for β-cyclodextrin, bromobenzene is a better precipitant than benzene, whereas the reverse is true for α-cyclodextrin.

In some instances, the extent of complexation depends on the polarity of the guest molecule. Partial penetration by certain groups or side chains into the channel may also promote complex formation. According to Cohen and Lach,[27] geometric factors are decisive in determining the type of substrates that will form inclusion complexes.

Cramer and Henglein[28] carried out the first systematic study of 54 guest components within cyclodextrins and realized that the law of constant proportions applies to the inclusion. Complexes with a constant guest/cyclodextrin ratio always crystallized out regardless of their molar ratios in aqueous solution; this is indicative of a real inclusion phenomenon. In the crystalline state, Lammars[29] showed that the guest molecules can be accomodated not only in the cavities of the host molecules, but also in their intermolecular cavities formed by the crystal lattice. The crystal lattice of these cyclodextrins is stable even when the cavities of some of the cyclodextrin molecules are not occupied or contain water molecules. Therefore, the molar ratios of crystalline cyclodextrin complexes are usually nonstoichiometric, but in solution the ratios are usually

1:1. A notable exception[30] is with long-chain alkanes and fatty acids (with n > 4), where the cyclodextrins may form channel structures in solution in order to accommodate the chains.

The encaged molecules are preferably oriented in a position such that maximum contact between the hydrophobic part of the guest and the cyclodextrin cavity is achieved. On the other hand, the hydrophilic part of the guest molecule will remain at the outer face of the complex to ensure close proximity with both the solvent and the hydroxyl groups of the host (Fig. II-3). In solution, steric requirements are less stringent and complexes which are not crystallizable may be formed. α-Cyclodextrin can form a 1:1 complex with benzoic acid, however, only the β-cyclodextrin-benzoic acid complex can be crystallized readily.

The fact that the guest molecule was actually contained in the cavity was first shown by X-ray studies.[31] Depending on the size and ionic or molecular character of the guest, two different forms of inclusion complexes, namely, "channel" or "cage" structures can be formed. Channel structures develop when cyclodextrin molecules are "stacked-like-coins-in-a-roll" to yield endless channels, in which the guest molecules are included. Cage structures are a result of a displaced arrangement of cyclodextrins in a "herring-bone" pattern, in which the guest molecules are located in discrete, small cavities. The crystal structures

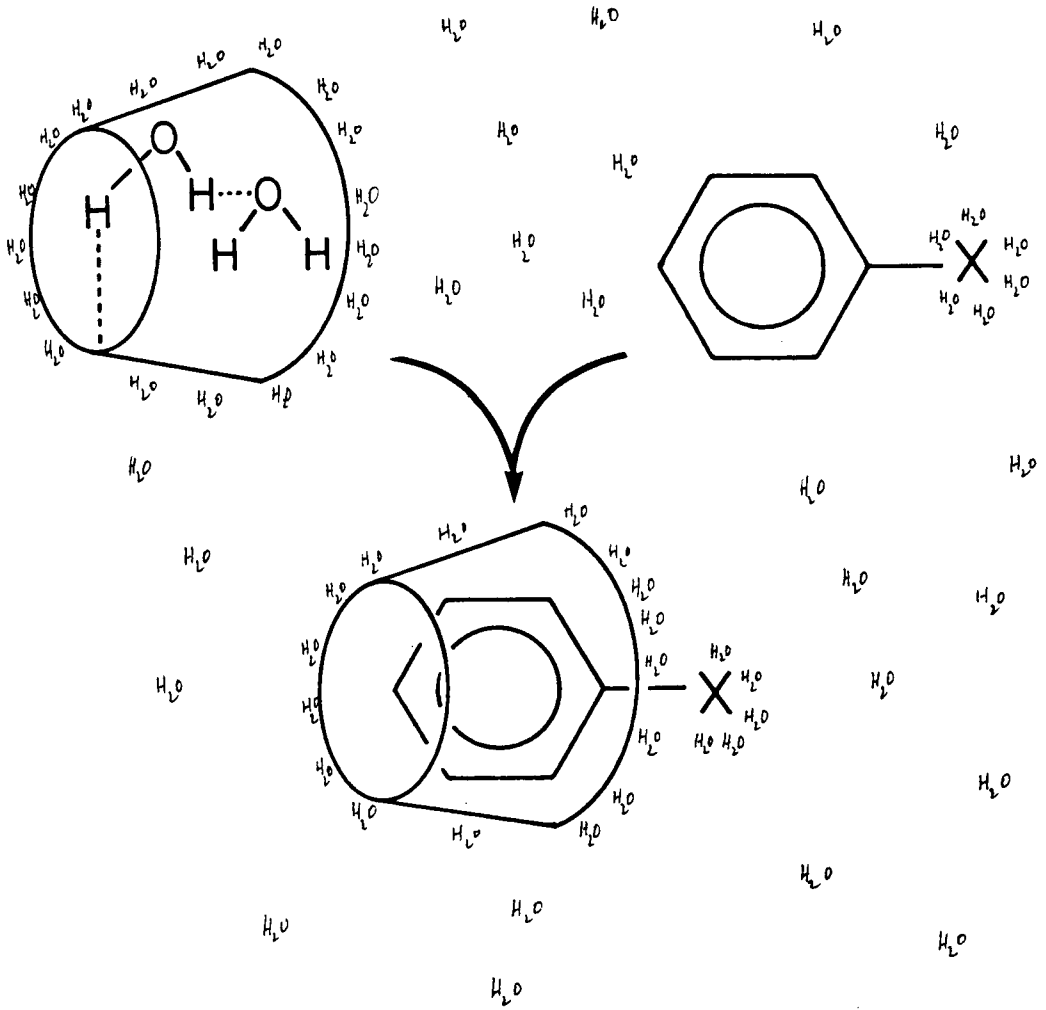

Fig. II-3. Schematic representation of the formation of cyclodextrin inclusion complexes.

of α-cyclodextrin complexes that have been analyzed include the following guests:[6] water, methanol, iodine, polyiodide, krypton, 1-propanol, p-iodoaniline, dimethyl sulfoxide and methanol, m-nitrophenol, methyl orange, and potassium acetate. In the case of β-cyclodextrin, its complexes with water, 1-propanol, p-iodophenol, 2,5-diiodobenzoic acid, and p-nitroacetanilide have been determined. Recently, two structures of γ-cyclodextrin complexes with 1-propanol/water and water have been described.

II.1.4. Cyclodextrins as Enzyme Models

In recent years, cyclodextrins have drawn much attention as models for enzyme-catalyzed reactions.[7] The hydrophobic interaction between the substrate and the cavity contributes significantly to the hydrophobic recognition by cyclodextrins. Here, they participate not only in complexation; covalent bonds are actually being broken and formed. Cyclodextrins have been suggested as excellent models of hydrolytic enzymes. The hydrolyses[32] of esters and amides involve the following stages: binding, acylation, and deacylation, which are consistent with those involved by hydrolytic enzymes. Furthermore, the cyclodextrin-accelerated cleavage of these substrates exhibits many of the kinetic features shown by enzymatic reactions, including substrate-specificity and competitive-inhibitions. The first observation[33] of an α-cyclodextrin-accelerated reaction was the hydrolysis of ethyl p-

chloromandelate. The addition of 1.32×10^{-3} M α-cyclodextrin caused an acceleration in the hydrolysis of the ester by a factor of 1.38.

The hydrolysis of phenyl esters in the presence of cyclodextrins has been extensively investigated. Most of the information obtained from these systems is applicable to other covalent catalyses[7] by cyclodextrins (Fig. II-4). The geometry of the guest molecule within the annulus does play an important role in the deacylation of esters.[3,4] Both α- and β-cyclodextrins accelerate the cleavage[8] of p-nitrophenyl acetate at pH 7.5; their acceleration factors are 2-3- and 5-fold, respectively. Here, the guest molecule is situated in the cavity of α-cyclodextrin, with the molecular axes of the two being aligned coaxially. In this way, the ester group is not favorably oriented with respect to the secondary hydroxyl groups of cyclodextrin that initiate the acylation process. Although this orientation is possible within the cavity of β-cyclodextrin, now the high mobility of the guest results only in a moderate acceleration. The hydrolysis of m-nitrophenyl acetate shows an acceleration of about 70 fold by α-cyclodextrin.[8] Presumably, the ester-function is located very close to the secondary hydroxyl groups, thereby, achieving a close contact. The larger β-cyclodextrin ring, which is unable to secure the substrate tightly, produces only a 20-fold acceleration.

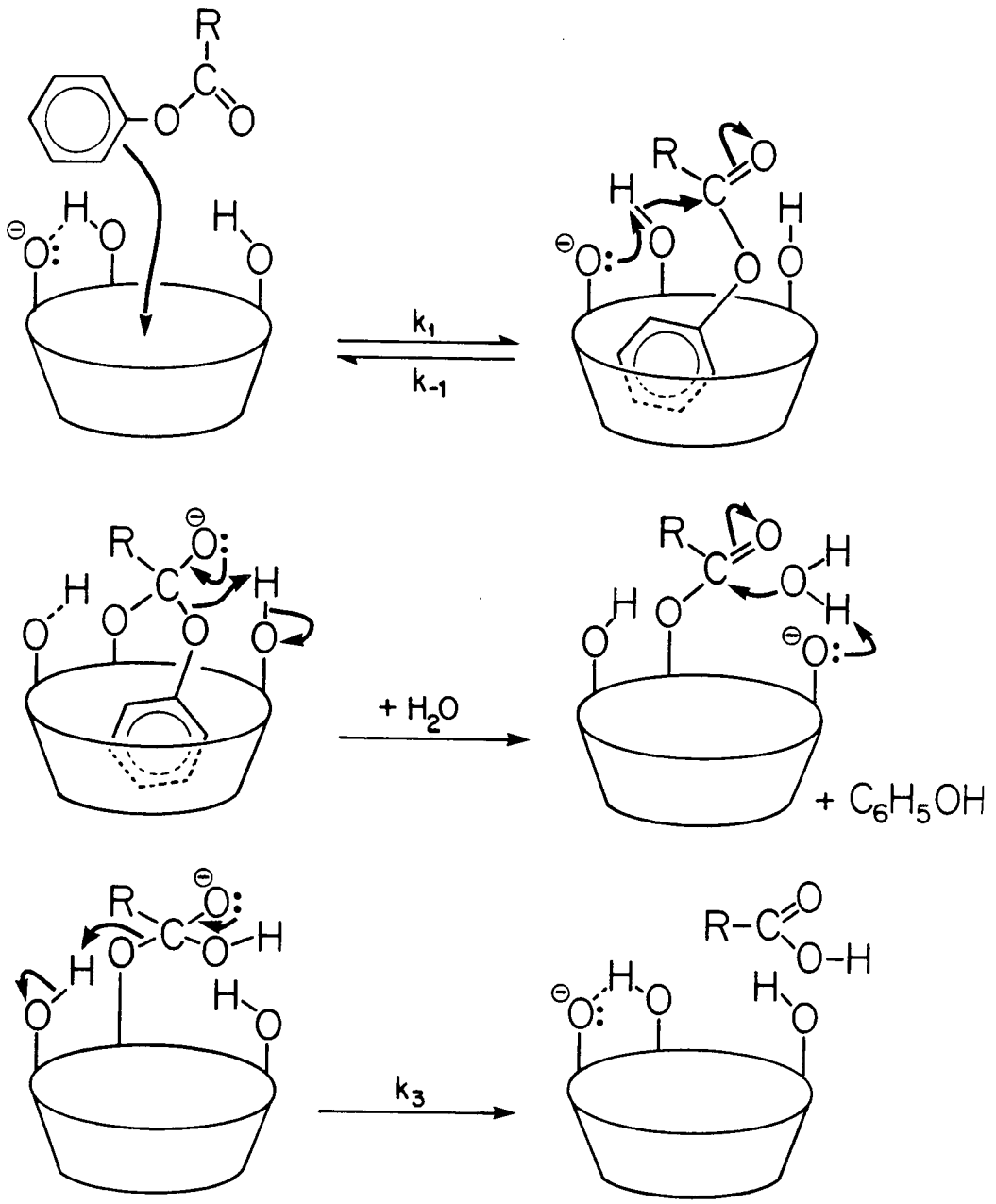

Fig. II-4. Schematic representation of the catalytic hydrolysis of phenyl acetate by cyclodextrin (from Ref. [6]).

II.1.5. Cyclodextrins as Models for Starch

Conformationally, cyclodextrins may be regarded as a projection of part of a starch helix down the cylindrical axis. Both molecules exhibit similar C1-glucopyranose conformation, and therefore the spatial arrangements of atoms lining their cavities resemble each other. It is then obvious that cyclodextrins could be used as models for starch since the X-ray diffraction studies on fibers of iodine-starch complex gave no explicit description of the structure of the iodine chain in the complex, or the iodine-starch interactions.[35] Hence, the *a*-cyclodextrin-iodine-iodide system has been the most extensively studied of the cyclodextrin inclusion systems, because the "finite columns" of the stacked cyclodextrin molecules mimic the starch helix. A cage-type complex of composition *a*-CD.I_2.$4H_2O$ crystallizes as reddish needles from an aqueous solution of *a*-cyclodextrin and molecular iodine.[36] In the presence of metal iodides, almost black, channel-type complexes are formed. From a series of complexes studied, it was concluded that the deep color is a result of charge transfer within the iodine chains. Thus, the charge transfer between iodine and oxygen atoms of the surrounding *a*-cyclodextrin molecules previously proposed,[37] can be ruled out. The dominant interactions between them are merely van der Waals contact between iodine and the inwardly directed H atoms at C(3) and C(5).

II.1.6. Chemical Modification of Cyclodextrins

Chemical modification of the hydroxyl groups in order to affect the complexation properties and/or to attach reactive functional groups, either by ionic or covalent bonding into the macroring, is a major area of interest. The solubility of inclusion complexes formed with apolar guest molecules is generally low.[8] This is especially unfavorable in the case of complexes of pharmaceuticals, since readily water-soluble complexes are highly desirable. Partial methylation of the cyclodextrins increases their solubility, presumably due to the disruption of intramolecular hydrogen bonds. The water-solubility of partially methylated β-cyclodextrin containing seven methyl groups is approximately four fold higher than that of non-substituted parent cyclodextrin.[8] According to Casu et al.[38] the methylated cyclodextrins increase the solubility and stability of the complexes formed with less suitable, apolar guests. Concomitantly, the methyl groups are not expected to obstruct the macrorings, and thus would allow a direct comparison of their complexing properties with those of the parent molecules.

Cyclodextrins may serve as better enzyme models if one side of the cavity, preferably the primary hydroxyl side, is more or less closed. Derivatization at this end would also provide a more apolar continuation of the cavity.

Selective and efficient modification of cyclodextrins, especially polysubstitutions, poses many synthetic and

structural problems because of the large number of hydroxyl groups. Furthermore, in the process of substitution, the steric interactions developed may offset the ongoing selectivity.

One practical way of preparing cyclodextrin derivatives is to react all primary hydroxyl groups with p-toluenesulphonyl or mesitylenesulphonyl, chloride. By suitable nucleophilic substitution,[39] the products can be further converted to 6-azido- or 6-deoxy-6-halogenocyclodextrin and other products. Methylation[40] of heptakis(6-bromo-6-deoxy)-β-cyclodextrin with dimethyl sulphate/barium hydroxide affords the 2-O-methyl derivative which, after replacement of the 6-bromo moiety with benzoate and hydrolysis, can be converted to 2-O-methyl-β-cyclodextrin.

II.1.7. Cyclodextrin Polymers

High molecular weight derivatives of cyclodextrins are called cyclodextrin polymers. The special properties of cyclodextrins are largely retained when they are incorporated into the polymer chain as a definite structural unit. Several polymers containing cyclodextrins have been synthesized[41] to investigate the role portrayed by the attached sugar moieties in binding and catalysis. The polymerization of β-cyclodextrin acrylate yields a water-soluble homopolymer (molecular weight 10^4-10^5), which exhibits almost the same properties as the free

cyclodextrin. Cyclodextrin copolymers are produced by the reaction of cyclodextrins with some di- or poly-functional reagents. Since the former are also polyfunctional, branching sites may be formed in the process of polymerization. These polymers are only soluble up to a certain molecular weight; crosslinking and sufficiently high degree of polymerization result in insoluble gels.[42]

The complexing behavior can be different for monomeric and polymer-fixed cyclodextrins. Both hosts show 1:1 stoichiometry for small substrates (gas molecules), but the latter afford a weaker binding. For larger guest molecules that can accommodate two macrorings, the polymer complexes were shown to be more stable; the high local concentration of the cyclodextrin within the polymer allows such cooperative binding.

N.M.R. Studies of Inclusion Complexes

II.2. Introduction

To date, the complex formation of cyclodextrins has been mostly investigated in solution. Inclusion of substrates in the cyclodextrin cavity can be followed by the following spectroscopic methods; nuclear magnetic resonance, ultraviolet absorption, fluorescence, and optical rotation. The n.m.r. methods[43] provide the most direct evidence for the inclusion of any kind of guest molecules, by monitoring the shifts in their resonances. The other methods are confined to molecules possessing

certain functionalities which are sensitive to those specific detection techniques.

The dynamics of inclusion complexes in solution and in the solid state can best be described by n.m.r. measurements. In solution, molecular motions of the guest molecules have been investigated by ^{2}H and ^{13}C nuclear relaxation studies;[44] the analogous solid-state studies of molecular reorientation form part of this thesis.

For crystalline samples, X-ray structure analysis is the best method for determining their stoichiometry, and visualizing the included guest molecules. However this technique is too time-consuming for routine analysis, and the X-ray data offer no information on the mobility, if any, of the guest molecules. An evaluation of the n.m.r. techniques on these aspects in the solid state will be discussed in great detail, later in this thesis.

II.2.1. Solution-State N.M.R. Studies

The ^{1}H- and ^{13}C-n.m.r. methods have been used extensively to study complexes of unsubstituted cyclodextrins. However, the spectra obtained are usually unsatisfactory because of the low solubility of the complexes in deuterated water. Therefore, most of the results obtained so far involve complexes of polar guest molecules that are relatively soluble in this solvent. By observing the complexation-induced shifts in ^{1}H- and ^{13}C-n.m.r. spectra of both the guest and the host, it is

possible to determine the binding and the geometry of the complex. The complex formation with aromatic guest molecules is indicated by the "upfield shift" of the hydrogen atoms at C(3) and C(5) due to the anisotropic shielding effect of the aromatic ring. On the other hand, the hydrogens of C(1), C(2), and C(4), situated on the exterior of the cavity, will not be affected by the penetration of the guest molecules. Sunamoto et al.[45] have suggested that the observed changes in the shifts may not be caused by the anisotropic effect, but rather by the microsolvent effect. This involves the expulsion of water molecules, which increases the hydrophobic character of the cavity on complexation.

Bergeron and Channing[19] employed ^{13}C n.m.r. as a probe in the determination of cyclodextrin substrate conformations. By measuring the changes in the chemical shift values of the guest molecule, its orientation can be determined; the carbons most intimately associated with the cavity should be shifted most. They concluded that at least four of the following parameters may account for the observed ^{13}C shifts of the complexed cyclodextrin: removal of water from the cavity, shielding by the π-cloud of the aromatic guest molecule, conformational changes, and steric interactions.

Inclusion complexes in solution are not static species; the system is usually in the fast-exchange limit from a n.m.r. point of view.[7] That is, the substrate

resonances appear at the average of their free and bound forms, which can have different orientations within the cavity, weighted by the fractional population of the molecules in each environment. According to the results obtained from ^{13}C-n.m.r. relaxation studies,[44] the dynamic coupling between the mononuclear aromatic compounds and *α*-cyclodextrin is weak and the aromatic ring is rapidly rotating within the annulus of the host.

II.2.2. Solid-State N.M.R. Studies

Solid-state n.m.r. techniques have recently been used to study clathrates, weakly hydrogen-bonded complexes, and polymorphic forms[46] of the same material that are difficult or impossible to relate in solution. High-resolution ^{13}C-n.m.r. spectroscopy detects not only chemical distinctions, but also magnetic inequivalences present in the solid complexes. The latter may be confirmed by X-ray data based on crystallographic inequivalence in the unit cell. Hence, the solid-state ^{13}C-n.m.r. spectra can be used to provide an immediate indication of the presence of any configurational or conformational multiplicity that may exist, prior to undertaking the more time-consuming crystal structure analysis. On the other hand, deuterium n.m.r. is a useful tool for the study of molecular motion in solids.

As mentioned earlier, previous studies of inclusion complexes of cyclodextrins using n.m.r. methods have provided valuable insight, however, those studies have been

confined to soluble complexes. Prompted by the rapidly growing interest in the use of modified cyclodextrins as model enzymes, and also by commercial use of solid cyclodextrins to sequester a variety of organic substances, we have evaluated two n.m.r. methods for studying these substances. As will be seen, the cross-polarization-magic angle spinning method allows individual resonances to be assigned to the specific carbon atoms in the sample and also provides a direct measure of the extent of complexation. Furthermore, the deuterium quadrupole echo method gives insight concerning the anisotropic motion of the guest-substrate within the annulus of the cyclodextrin ring.

II.3. Synthesis

II.3.1. Previous Work

The ability of the cyclodextrins to form inclusion complexes relies upon the size and nature of the substrates which must fit entirely, or at least partially, into the cavity. Depending on the properties of the guest molecules, the following general methods have been adopted by several research groups in the synthesis of these complexes:[6]

1) At least an equimolar proportion of a water-soluble substance is dissolved directly in a concentrated, hot, aqueous solution of the cyclodextrin. The inclusion complex generally crystallizes out on slow cooling.

2) Water-insoluble substances are dissolved in non-

complexing solvents such as ether, chloroform, etc. and the solutions are shaken with, or layered over or underneath, a concentrated cyclodextrin solution. For liquid-guest substances, solvent is not necessary for the preparation. Precipitates are usually obtained; however, very slow cooling may allow crystals to form at the interface.

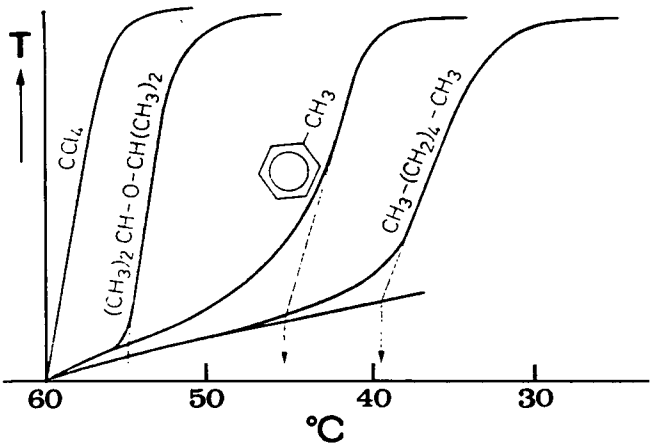

Fig. II-5. Turbidity curves for 3 %, aqueous β-cyclodextrin solutions + 5 % of the corresponding solvent (from Ref. [8]).

The crystallization of β-cyclodextrin and its inclusion complexes from aqueous solution has been studied[47] by following the turbidity as a function of temperature (Fig. II-5). Certain solvents such as benzene, toluene, n-hexane, carbon tetrachloride, isopropyl ether, dichloroethane, amongst others can affect precipitation of crystalline complexes at relatively high temperatures. In general, higher concentrations of guest would result in the onset of turbidity at higher temperatures.

A series of complexes formed with water-immiscible liquids has been reported by Cramer and Henglein.[28] The

liquid component was added to an aqueous solution of cyclodextrin and the mixture allowed to stand for 5-8 d, with occasional stirring. The resulting precipitate was washed with water, acetone, and finally with ether to remove any adhering molecules. Then, it was allowed to dry overnight in a desiccator.

a-Cyclodextrin is known to form complexes with dimethyl sulfoxide (DMSO) and methanol. Crystals of *a*-cyclodextrin-methanol pentahydrate have been prepared[48] from a methanolic solution. Similarly, *a*-cyclodextrin-DMSO-methanol (1:1:2) dihydrate can be obtained[49] from a DMSO-methanol solution containing *a*-cyclodextrin hexahydrate.

Selective chemical modification of cyclodextrins is necessary to increase the molar ratio of guest/cyclodextrin. Methylation and acetylation of cyclodextrins have been reported;[15,50] the substituent groups are expected to affect the cavity size to a certain degree. In particular, the syntheses of heptakis-(2,6-di-O-methyl)-β-cyclodextrin (2,6-di-O-Me-β-CD) and β-cyclodextrin peracetate (2,3,6-tri-O-Ac-β-CD) are relevant to the work reported in this thesis.

Theoretically, there are three possible isomeric heptakis-di-O-methyl-β-cyclodextrins. Only the synthesis of 2,6-di-O-Me-β-CD has been reported, but the structure was initially identified as being that of the 3,6-isomer. Using spectroscopic methods, Casu et al.[15] proved that on methylation with dimethyl sulphate in the presence of BaO

and $Ba(OH)_2.8H_2O$, the 2,6-isomer was the product. However, its yield and the details of the procedure were not included in the report. Recently, Szejtli et al.[51] repeated the same experiment and attempts were made to optimize the reaction and isolation conditions. They noted that successful selective reaction of the fourteen 2,6-hydroxyl groups depended crucially on the ability to keep the reaction below 20°C since the large amount of heat which is evolved rather unpredictably in the process of methylation can cause 3-O-methylation to occur. After stirring for 4 d at room temperature, a homogeneous suspension was formed. The excess reagent was quenched with ammonium hydroxide, and the mixture was suspended in a small volume of chloroform and filtered. Petroleum ether was added to induce crystallization, and the crude material was further recrystallized from hot water.

β-Cyclodextrin peracetate can be obtained in high yield by adapting the synthetic procedures described in Refs. 52 and 53. In the first procedure, peracetylation of this compound was carried out at room temperature in acetic anhydride with dry pyridine as the catalyst. The crude product was precipitated by pouring the solution with stirring into ice and water. The second method involved the addition of β-cyclodextrin to boiling acetic anhydride containing anhydrous sodium acetate. The mixture was heated under reflux for thirty minutes, allowed to cool to room temperature and poured with stirring into ice and water.

The crude product was then crystallized from toluene.

II.3.2. Synthesis of Cyclodextrin Inclusion Complexes

The experimental results above encouraged us to synthesize α- and β-cyclodextrin ([1] and [2]) complexes with deuterated DMSO-d_6 in aqueous or methanolic solution. Thereafter, attempts were made to synthesize some of those known complexes (using the method of Cramer and Henglein[28]) with apolar aromatic substrates, but with little success. Presumably, the guest components merely aggregated to the outside of the cyclodextrin molecule in the process of fast precipitation. Thorough washings could well remove these molecules, and reduce the molar ratio of guest/cyclodextrin. Therefore these complexes, which are seldom of stoichiometric composition, are not suitable for solid-state ^{13}C-n.m.r. studies.

It was decided to synthesize 2,6-di-O-Me-β-CD [3] and 2,3,6-tri-O-Ac-β-CD [4] because of the following:

1) They are soluble in less-polar organic solvents, even in water for the methylated derivative.

2) The influence of cavity size on complexation with a series of guest molecules, and their molar ratios can be compared.

It is known[8] that methylation or acetylation of the sugar should increase the hydrophobic environment around the cavity, and at the same time, the hydrophobic interaction with the guest molecules is expected to be

enhanced. Hence, the types of substituent groups attached to the substrates should play an important role in complex formation. The presence of polar moieties such as amino, nitro, carbonyl, and hydroxyl groups on the substrate should lower the stability of the complex. These polar molecules are very soluble in the crystallizing solvent, methanol, and will therefore prefer to remain in the bulk solvent. Alkyl substituents should greatly increase the hydrophobic character of the guest molecules; a methyl or ethyl substituent that is ortho to a carbonyl group has a shielding effect on the latter, thereby increasing the hydrophobic character of the whole molecule and its stability.[8] A similar group placed at the para position should have a relatively weak effect on the molecule, and the hydrophobic effects should increase in the order para < meta < ortho.

These anticipated substituent effects were verified in our studies by the results obtained with compound [3] (Table II-1). An exception is p-bromotoluene, in which its complex-forming ability is lower than that of bromobenzene. It should be noted that the crystallization of the latter derivative with the host molecule [3] was done with great difficulty. Another observation is that larger molecules such as durene and naphthalene failed to form inclusion complexes. The inability of these molecules to penetrate deeply into the cavity could have affected the molecular packing, caused by the large protruding segments.

Table II-1. Crystalline complexes formed by cyclodextrins

Complex no.	Substrate	Host	Molar ratio*
	with apolar compounds		
[5]	benzene.....	[3]	1:1
[6]	toluene.....	[3]	1:1
[7]	ethylbenzene.....	[3]	1:1
[8]	p-xylene.....	[3]	1:1
[9]	chlorobenzene.....	[3]	1:1
[10]	bromobenzene.....	[3]	1:1
[11]	cyclohexane.....	[3]	1:1
[12]	methylcyclohexane.....	[3]	1:1
[13]	biphenyl.....	[3]	2:1
[14]	4,4'-dimethylbiphenyl...	[3]	1:1
[15]	p-di-tert.-butylbenzene.	[3]	1:1
[16]	bromotoluene.....	[3]	1:0.2
[17]	durene.....	[3]	1:0.1
[18]	naphthalene.....	[3]	1:0.2
	with polar compounds		
[19]	pyridine.....	[3]	1:0.2
[20]	p-hydroxytoluene.....	[3]	1:0.2
[21]	p-toluidine.....	[3]	1:0.1
[22]	benzoic acid.....	[3]	1:0.1
	with apolar compounds		
[23]	benzene.....	[4]	1:1
[24]	toluene.....	[4]	1:1
[25]	p-xylene.....	[4]	1:1

* molar ratio of cyclodextrin:substrate.

Inclusion complexes of host [3] were prepared by crystallizing the sugar from a solvent that could also function as a guest, or from a solution of the guest in a non-complexing solvent such as chloroform or methanol. ^{1}H-N.m.r. and u.v. methods were then used to confirm the inclusion of guest molecules, and to estimate the stoichiometry of the complexes.

A literature search for a known, crystalline β-cyclodextrin peracetate did not reveal any complex formed between the solvent and the cyclodextrin molecules. To our knowledge, no inclusion complexes of this molecule with any organic substrates have been reported before. It was decided to investigate this compound by ^{1}H-n.m.r. spectroscopy, and produce a limited series of inclusion complexes.

The permethylated α-cyclodextrin was also prepared, but with much difficulty following the method of Lehn et al..[14] The crude product showed more than one spot on thin-layer chromatography plates, and purification on a column did not give a completely pure compound. Since a large quantity of this reasonably expensive material was needed for the synthesis of its inclusion complexes, it was decided not to choose this as the potential host molecule.

II.4. ^{13}C-N.M.R. Studies - Some Specific Examples

Because the α- and β-cyclodextrins can be obtained easily, they are best suited for n.m.r. studies. A number

of modified cyclodextrins have been fully characterized in solution by Lehn et al..[14] According to Szejtli et al.,[51] their ^{13}C-n.m.r. solution investigations revealed that the assignments given by Lehn for the C-3 and C-5 atoms of 2,6-di-O-Me-β-CD should be interchanged. There was no ambiguity for the case of 2,3,6-tri-O-Ac-β-CD, which was first studied by Takeo et al..[50] Owing to the simple symmetry of these cyclodextrins and their derivatives, all the constituent glucopyranose residues in the dextrins are expected to be chemically and physically indistinguishable, in the absence of conformational isomerism. Supporting evidence also comes from the work reported in this thesis on the solution ^{13}C-n.m.r. spectra of compounds [1] to [4], which are shown in Fig. II-6. The complex formation of many compounds, especially aromatics, with hosts [3] and [4] will be the main focal point of discussion in the latter part of this chapter.

There is a common misconception that chemical shifts measured in high-resolution experiments for the solid state and for solutions are the same for a particular compound. Lippmaa et al.[54] carried out experiments with some representative groups of organic compounds to illustrate the solid-state effects on the chemical shifts and splittings of ^{13}C resonances. Several rather general conclusions about the ^{13}C chemical shifts can be drawn from the results put forward by several other research groups.[46,54-58] In the absence of specific solid-state

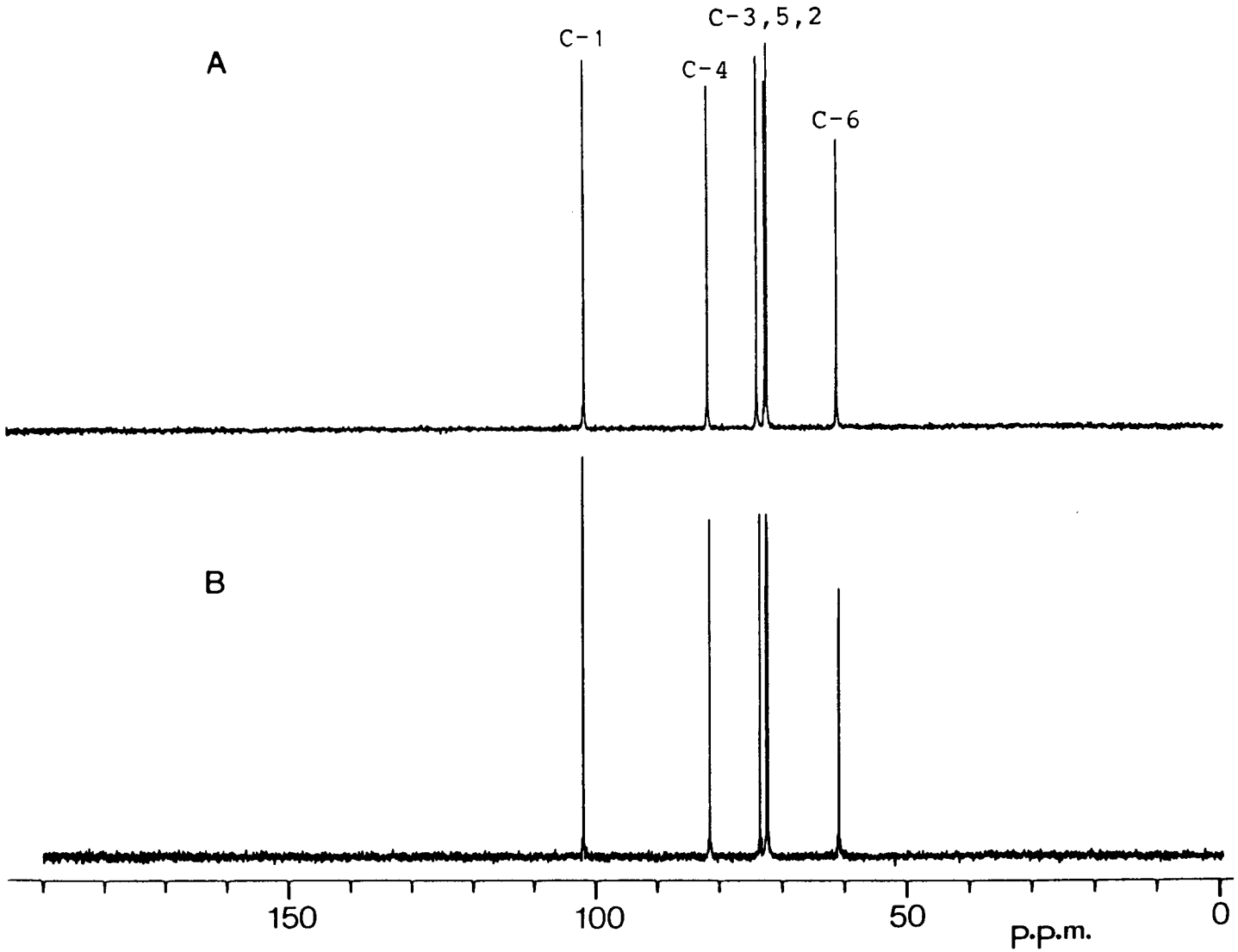

Fig. II-6. ^{13}C-N.m.r. spectra of (A) [1] and (B) [2] in D_2O, (C) [3] in $CDCl_3$, and (D) [4] in $(CD_3)_2CO$ at ambient temperature.

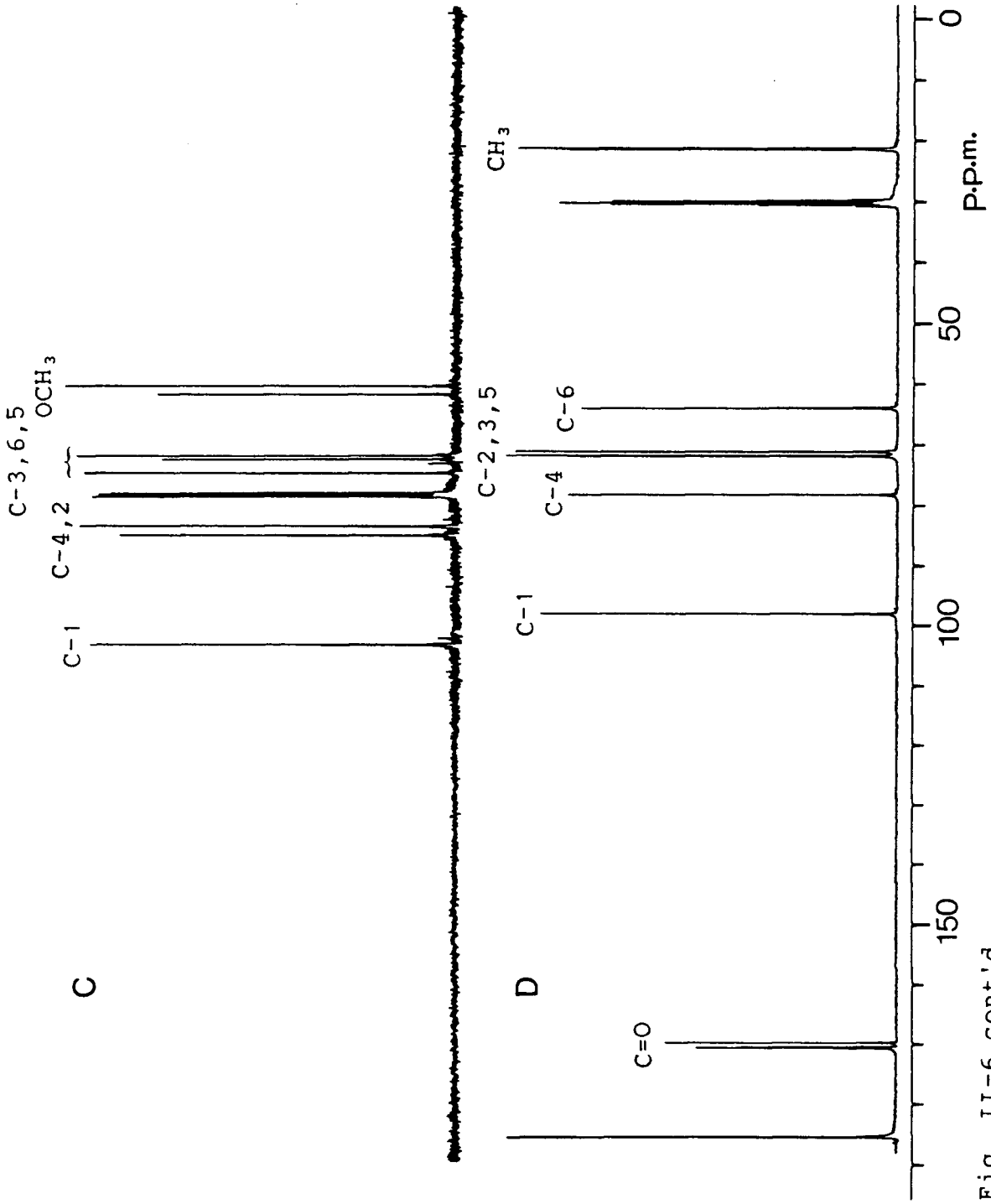

Fig. II-6 cont'd

effects, differences between the isotropic chemical shift values measured for the solution and pulverized crystalline samples are small and do not normally exceed the solvent effects.[46] Significant changes may arise from intramolecular (conformational) and intermolecular (crystallographic) effects, which determine the actual magnetic environment of nuclei in solid samples. Hence, it is of interest to find examples where the solid-state chemical shift data can be explained in terms of those effects separately.

There are many ways in which the molecular structure in the solid state can differ from that in solution. These commonly include molecular conformation, hindered intramolecular motion, tautomerism, intramolecular hydrogen bonding, and intramolecular nonbonded interactions. Specific examples are chosen here to highlight some of these areas that are relevant to later discussion on cyclodextrin inclusion complexes.

Studies of cellulose polymorphs[55,56] have shown very definite solid-state n.m.r. splittings of the signals of C-1 and C-4 atoms, which anchor the glycosidic linkages between the glucopyranose units. These splittings provide direct evidence for the presence of two types of glucose monomer. Subsequent studies on the conformations of oligo- and poly-saccharides, viz. cycloamyloses and amylose, have been reported by Saitô and Tabeta.[57] They have shown that the ^{13}C chemical shifts of α-cyclodextrin are very similar

to those of high molecular weight crystalline amylose, by comparing the resonances of carbons at the glycosidic linkages which are very sensitive to conformational changes. Their spectra do not reflect the presence of different conformations, and the linewidths of these signals are significantly narrow. In contrast, ^{13}C signals of β- and γ-cyclodextrins are split into at least two sets of signals, suggesting that there are two or more different conformers present in the solid state.[57] This could be explained by the less symmetrical nature of "empty" cyclodextrins, having distorted glycosidic linkages.

Processes such as internal rotation and ring inversion are expected to occur much more slowly in the solid state than in solution at the same temperature.[58] The solid state may induce magnetic inequivalence in a pair or pairs of carbon atoms, which are equivalent in solution. This kind of restricted motion is normally observed for internal rotation about single C-C bonds at ambient temperature in the solid. By increasing the temperature, it is possible to render these atoms equivalent, provided the rotation rates are greater or comparable to the frequency separation of the signals. Garroway et al.[59] have investigated a piperidine-cured epoxy, based on a resin from the diglycidyl ether of bisphenol A. The resonances for the C-3,C-3' carbons (Fig. II-7) appear as two distinct peaks that finally coalesce to a sharp peak, over the temperature range of -123 to 77°C.

As mentioned previously, the splittings of ^{13}C

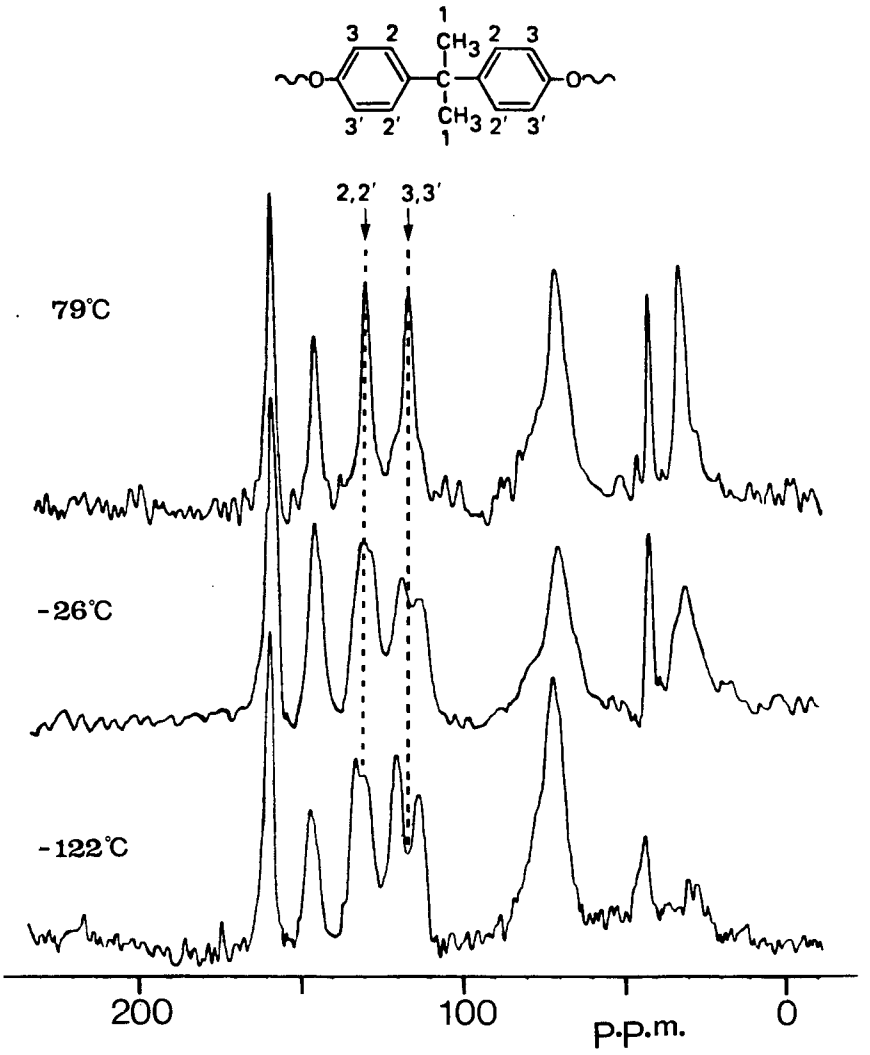

Fig. II-7. ^{13}C-C.p.-m.a.s. spectra of an epoxy resin, diglycidyl ether of bisphenol A (DGEBA) recorded over a 200°C temperature range (from Ref. [59]).

resonances can arise from a mixture of intramolecular and intermolecular effects. If the average shifts are close to those observed in solution, then it is reasonable to conclude that intramolecular interactions predominate over the other effects. In the case of p-dimethoxybenzene, the 1,4-nonbonded intramolecular interaction between the

substituent group and the aromatic ring leads to a splitting of about 6 p.p.m. for the signals of the ortho carbons.[54] This kind of magnetic inequivalence results from the methyl groups located on the plane of the ring, thereby generating a conformation of minimum energy, in which they are closer to one of the two ortho carbons.

Nuclei which are crystallographically inequivalent in the solid may give rise to separate n.m.r. absorptions. The importance of such intermolecular effects has been illustrated recently[60] for 2,4-dinitrotoluene, whose spectrum shows a splitting of about 3 p.p.m. for the methyl peak. This suggests that there are two non-congruent molecules in the unit cell, and a subsequent X-ray report has confirmed the finding. However, the aromatic region of the spectrum does not show any sign of splitting. Therefore the effects of local environment would appear to be largest for the methyl groups.

Evaluation of a number of clathrates and polymorphic forms of hydroquinone has also yielded line splittings that can be related to crystal structures.[46] The author has shown that the intermolecular interactions may induce isotropic chemical shift differences as large as 4 p.p.m., and this magnitude of dispersion could be important in the study of more complex systems.

II.5. X-ray Studies

It is pertinent to have some knowledge of the crystal

structures of cyclodextrins and their inclusion complexes, before trying to extract any useful information from the solid-state ^{13}C-n.m.r. spectra. The crystal structures of several cyclodextrin complexes have been extensively investigated by X-ray analysis. Harata et al.[61] have shown the structures of several cyclodextrin complexes with mono- and di-substituted benzenes; the substrates are bound inside the cavity or situated within a column formed by the stack of cyclodextrin rings. In the case of monosubstituted benzenes, the phenyl group is located inside the host cavity, while the substituent group protrudes from the secondary-hydroxyl side of the cavity. When disubstituted benzenes are included, the bulkier group is thrust into the ring instead of the smaller substituent, which has to be located outside the cavity. The inclusion geometry may be interpreted mainly in terms of the stereospecific relationship between the guest and the host.

Hexakis-(2,3,6-tri-O-methyl)-*a*-cyclodextrin (2,3,6-tri-O-Me-*a*-CD) also forms inclusion complexes, and their structures[62] have been compared with those of *a*-cyclodextrin complexes. As shown in Fig. II-8, the benzaldehyde and p-nitrophenol molecules are included in reverse orientation when the shape and size of the *a*-cyclodextrin cavity are altered. The introduction of methyl groups into the cyclodextrin ring enlarges the O(2),O(3) side of the cavity, so that the guest molecule appears to be loosely bound in it. At the same time, the large

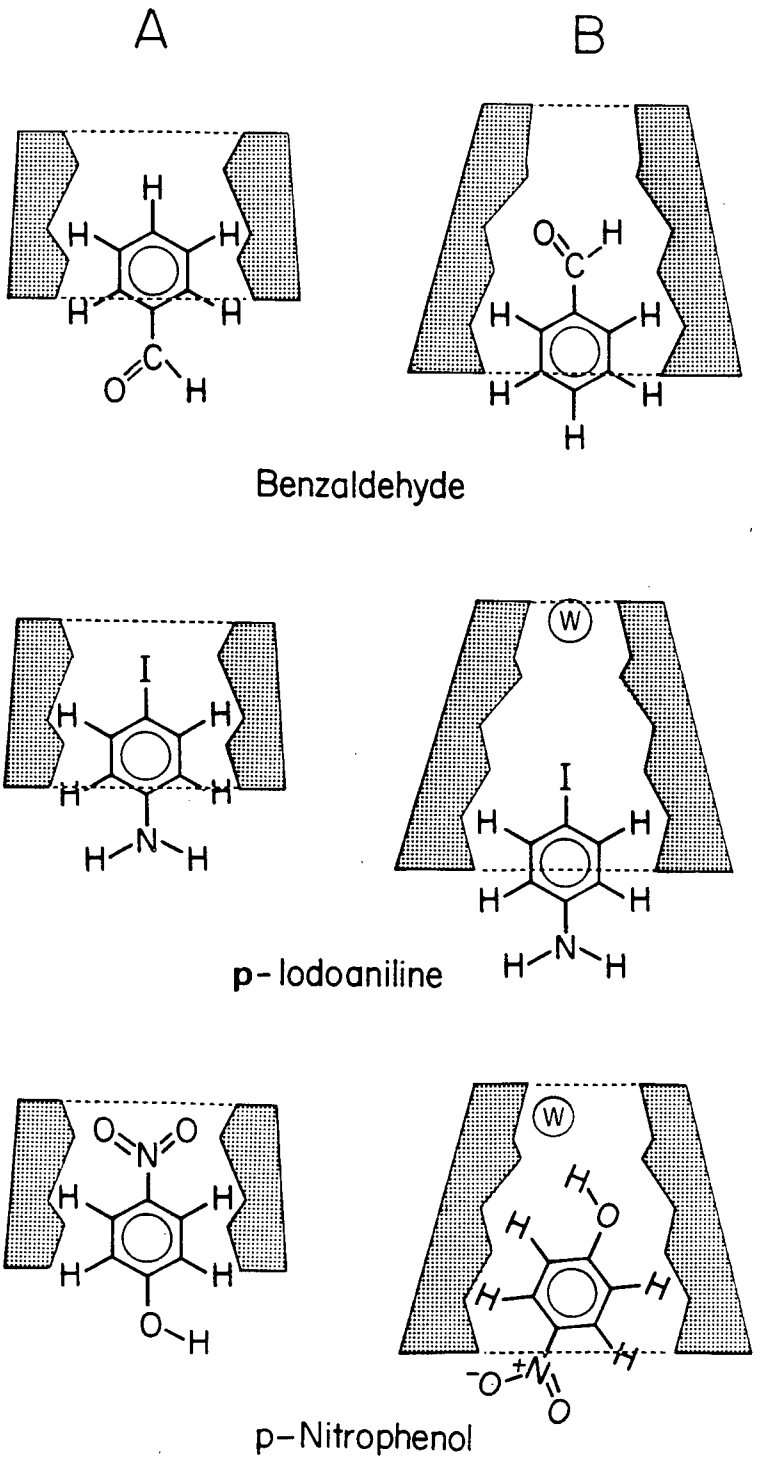

Fig. II-8. Schematic diagrams of the *a*-cyclodextrin (A) and 2,3,6-tri-O-Me-*a*-CD (B) complexes. Water molecules are indicated by W (from Ref. [62]).

inclination of the 2,3,6-tri-O-methylglucopyranose residues makes the primary-hydroxyl side of the cavity so narrow that the nitrophenyl group cannot be deeply inserted. Thus, the choice of substituent group to be included is mainly determined by the steric effect. The water molecule in this complex may also play a part in fixing the substrate inside the cavity by hydrogen bonding. The rationale for the similar inclusion pattern observed in the benzaldehyde complex is that the whole molecule may be more able to fill the cavity. In contrast to those two complexes, the orientation of p-iodoaniline within the cavity is the same as that in *a*-cyclodextrin. Although the inclusion of either the aminophenyl or the iodophenyl group is sterically possible, the latter is preferred because of its stronger van der Waals interaction with the hydrophobic cavity.

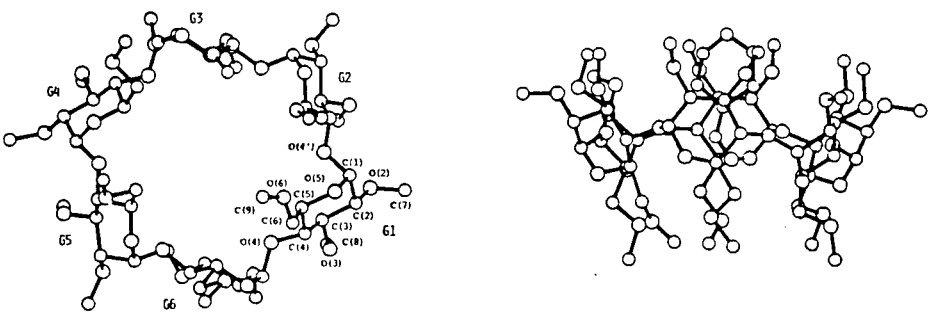

Fig. II-9. Structure and numbering scheme of 2,3,6-tri-O-Me-*a*-CD (from Ref. [62]).

Permethylation of the ring not only affects the position and orientation of the guest molecules, but also the macrocyclic conformation of the host.[62] The C(6)-O(6)

bonds in the G4 and G5 residues (Fig. II-9) are in a gauche-gauche conformation, while the others have a gauche-trans conformation. The six glycosidic oxygen atoms form an elliptically distorted hexagon, which may change its macrocyclic conformation slightly to suit the shape of the included group or molecule. A large conformational change is restricted due to steric hindrance imposed by the C(8) methyl groups of the permethylated cyclodextrin.

To our knowledge, the crystal structures of 2,6-di-O-Me-β-CD and its inclusion complexes have not been analyzed. Thus, in this work we have had to use the X-ray data of the α-cyclodextrin complexes to enable comparative studies of the solid-state ^{13}C-n.m.r. results to be made.

II.6. Results and Discussion

II.6.1. ^{13}C-N.M.R. Experimental Methods

Application of dipolar dephasing and Delrin suppression methods[63,64] are included in this thesis as integral parts of the ^{13}C-n.m.r. solid-state studies. As stated in the introduction, these methods facilitate the potentially complex task of unravelling and assigning complex spectra of organic molecules.

Prior to the discussion on cyclodextrins and their inclusion complexes, we briefly introduce the tosylated sugar derivatives here to illustrate this point because their well-dispersed ^{13}C spectra could be readily obtained. Also, the syntheses[65] were easily accomplished giving pure

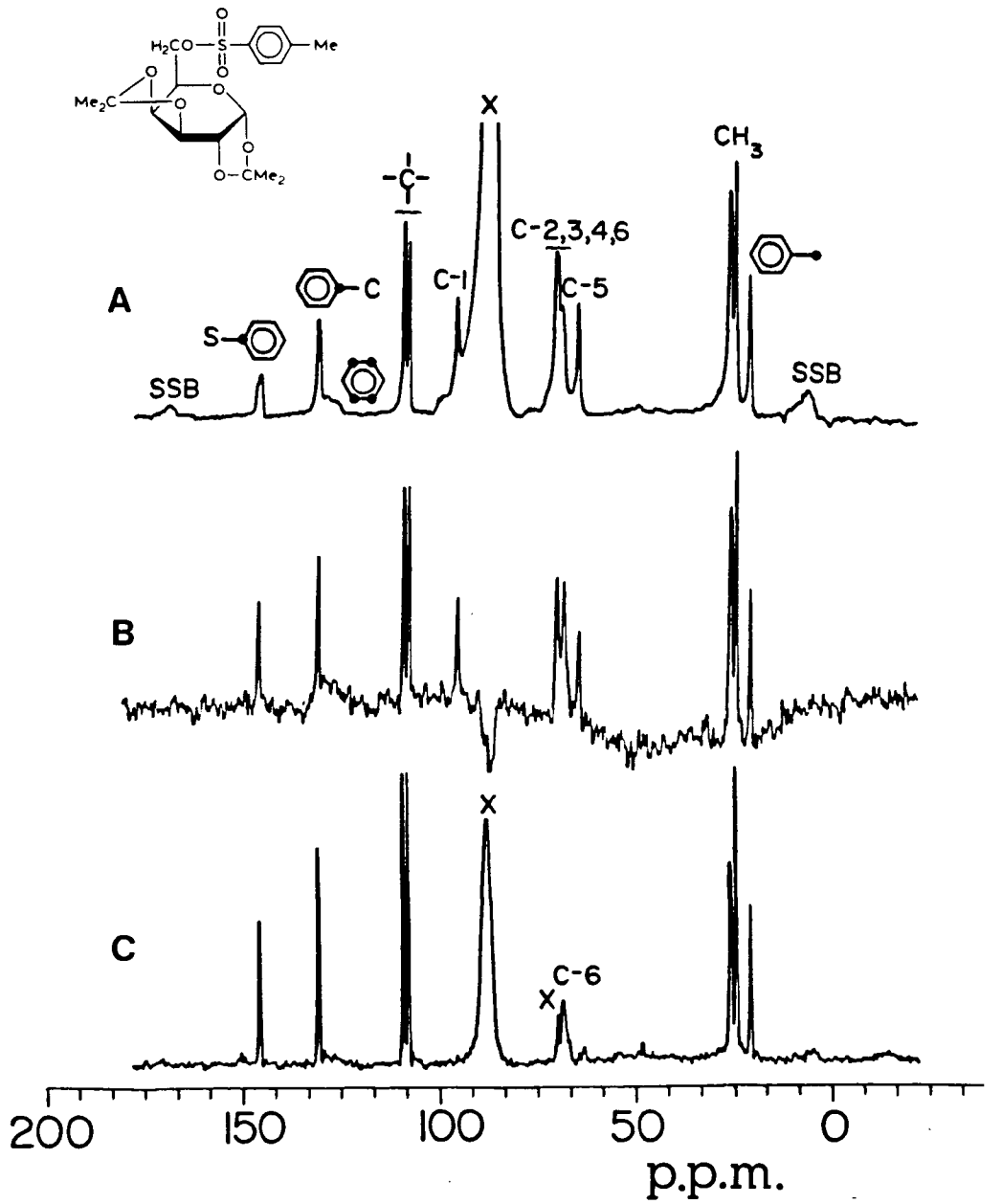

Fig. II-10. ^{13}C-N.m.r. spectra of 1,2:3,4-di-O-isopropylidene-6-O-p-tolylsulfonyl-α-D-galactopyranose. [(A) Normal ^{13}C-c.p.-m.a.s. spectrum, 5-ms contact time, and 3,350 scans. (B) Delrin-signal suppression, obtained by setting a delay time of 500 ms between the 180° and 90° pulses of ^{1}H. (C) Nonprotonated-carbon spectrum, obtained by setting a 40-μs period without proton decoupling, prior to ^{13}C data-acquisition. Deuteration at C-6 of the compound is recorded in (B) and (C). Delrin signals and spinning side-bands are indicated as X and SSB, respectively.]

crystalline compounds in high yield. Fig. II-10A shows a typical example of the ^{13}C-c.p.-m.a.s. spectrum of a crystalline sample, namely, 1,2:3,4-di-O-isopropylidene-6-tosyl-*α*-D-galactopyranose, in a Delrin rotor. The dipolar dephasing spectrum, obtained by setting a 40-μs period without proton decoupling prior to data acquisition is shown in Fig. II-10C. With the concomitant solution spectra, partial assignments of the ^{13}C resonances are made possible. Besides those of the nonprotonated carbons, methyl and deuterated-carbon resonances are discernible; the rapid methyl group rotations and large ^{13}C-^{1}H distances can reduce the proton-carbon dipolar coupling drastically.

The immense Delrin signal can be suppressed quite cleanly if the experimental conditions are favorable. Fig. II-10B indicates an incomplete suppression of the signal when the delay time between the two pulses ($180^{o}x$ and 90^{o}-x) was set at 500 ms; for a duration of 600 ms, a "cleaner" spectrum was observed. Still, a residual, Delrin signal is usually observed. This could be due either to r.f.-pulse imperfections or to physical inhomogeneity of the spinner material.

As a cautionary note, attention may be drawn to the fact that the signals of the four protonated carbon atoms of the tosyloxy moiety at 129.9 p.p.m. are so broad that they are barely detectable. This is characteristic of other tosylated sugars that we have studied, and several alternative explanations can be cited.[64]

II.6.2. ^{13}C-N.M.R. Studies of Cyclodextrin Inclusion Complexes with Liquid Guest Molecules

In this section we report studies of complexes of cyclodextrins in the solid state by ^{13}C n.m.r., using the c.p.-m.a.s. method. Interpretation of these ^{13}C-n.m.r. spectra is facilitated by comparison with the ^{1}H- and ^{13}C-n.m.r. studies of these complexes in solution, and with the X-ray data obtained in the solid state. Since the crystal structures of the host molecules [3] and [4], and their inclusion complexes have not been confirmed by X-ray crystallography, studies of a related series of guest molecules provide a basis for some interpretation.

Compound [3] was found to afford crystalline complexes of molar ratio 1:1 with many guest molecules and, therefore, provided a good series of complexes for studying their properties in the solid state. In contrast, compound [4] was shown to be less suitable as a host, probably due to space restriction at both ends of its cavity. Reported X-ray data[62] of 2,3,6-tri-O-Me-α-CD show that the six O(2)-C(7) bonds are directed outside the cyclodextrin ring, with the six O(3)-C(8) bonds turned inside the ring. Nevertheless, as compared to β-cyclodextrin we would expect a wider opening for the O(2),O(3) side of the cavity of compound [3], but probably not in the case of compound [4]. A list of guest molecules which were used to study the complexing behavior of these hosts is shown in Table II-1 (see Pg. 98).

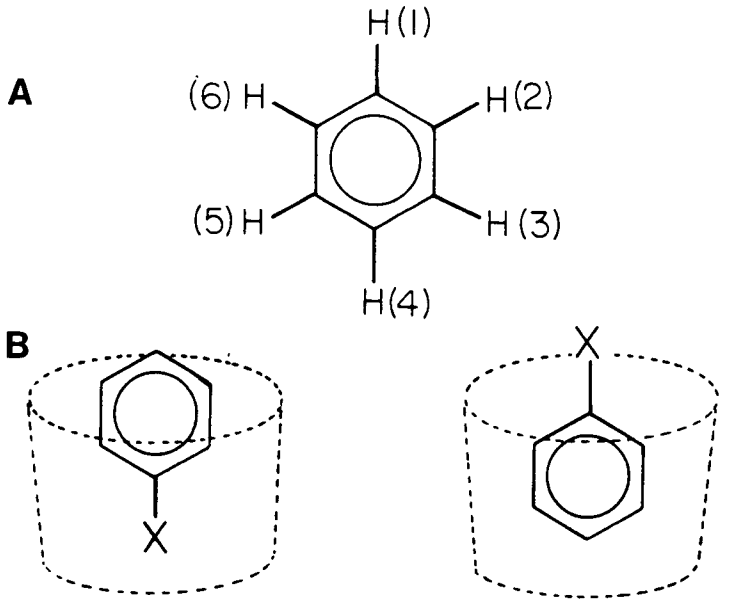

Fig. II-11. The dimensions of the benzene ring, taking into consideration the van der Waals radii of the aromatic hydrogens (A) and the molecular orientations of a monosubstituted benzene ring in cyclodextrin (B).

According to Van Hooidonk and Breebaart-Hansen,[67] the diameter of the β-cyclodextrin cavity is 7.5 Å and the size of the benzene ring is about 6.8 Å, that is the distance measured between H(2) and H(6) (Fig. II-11). One would expect a monosubstituted benzene ring to orient along its long axis in the cavity, rather than in a "crosswise" manner. However, the "upright" position allocated to the benzene ring could be either "head-first" or "head-last". As mentioned earlier,[61,62] the molecular dispositions of substituted benzenes may differ from one host to another, and their complexes may crystallize in "cage"- or "channel"-type structures, depending on the nature and size of the guest molecule. It may not be possible to distinguish the correct orientation solely by the ^{13}C-c.p.-

m.a.s. method in this complicated system. Such uncertainties will not seriously limit our discussion on other interesting static and motional aspects of the "guest-host" structure in the solid state.

The solid-state ^{13}C spectra of compound [3], with and without magic angle spinning, are compared to its solution spectrum in Fig. II-12. The linewidths of the spectra of the spinning solids are relatively broad, even at a spinning frequency of about 4.3 kHz. This is attributed to a dispersion of chemical shifts, along with smaller magnetic susceptibility contributions which survive the sample spinning. Surprisingly, the methoxyl groups show a reasonably large separation. Since the n.m.r. instrument is only capable of producing linewidths of 0.5 p.p.m. in favorable cases, the true splitting cannot be accurately measured. Nevertheless, the separation of ca. 2 p.p.m. far exceeds the chemical difference (0.9 p.p.m.) of the C(2) and C(6) methoxyl groups measured in solution. This can be explained in terms of a coexistence of crystalline and amorphous domains; the latter being caused by the partial "melting" of the crystalline sample in the sintered glass funnel during the process of suction filtration.[51] The broad shoulder at 68.2 p.p.m. also suggests such existence. Similar results were also obtained when complex [5] was heated to 170°C for 3 h to regenerate the free host [3]. Recrystallization of compound [3] from chloroform/pet. ether or methanol diminished the apparent splitting of the

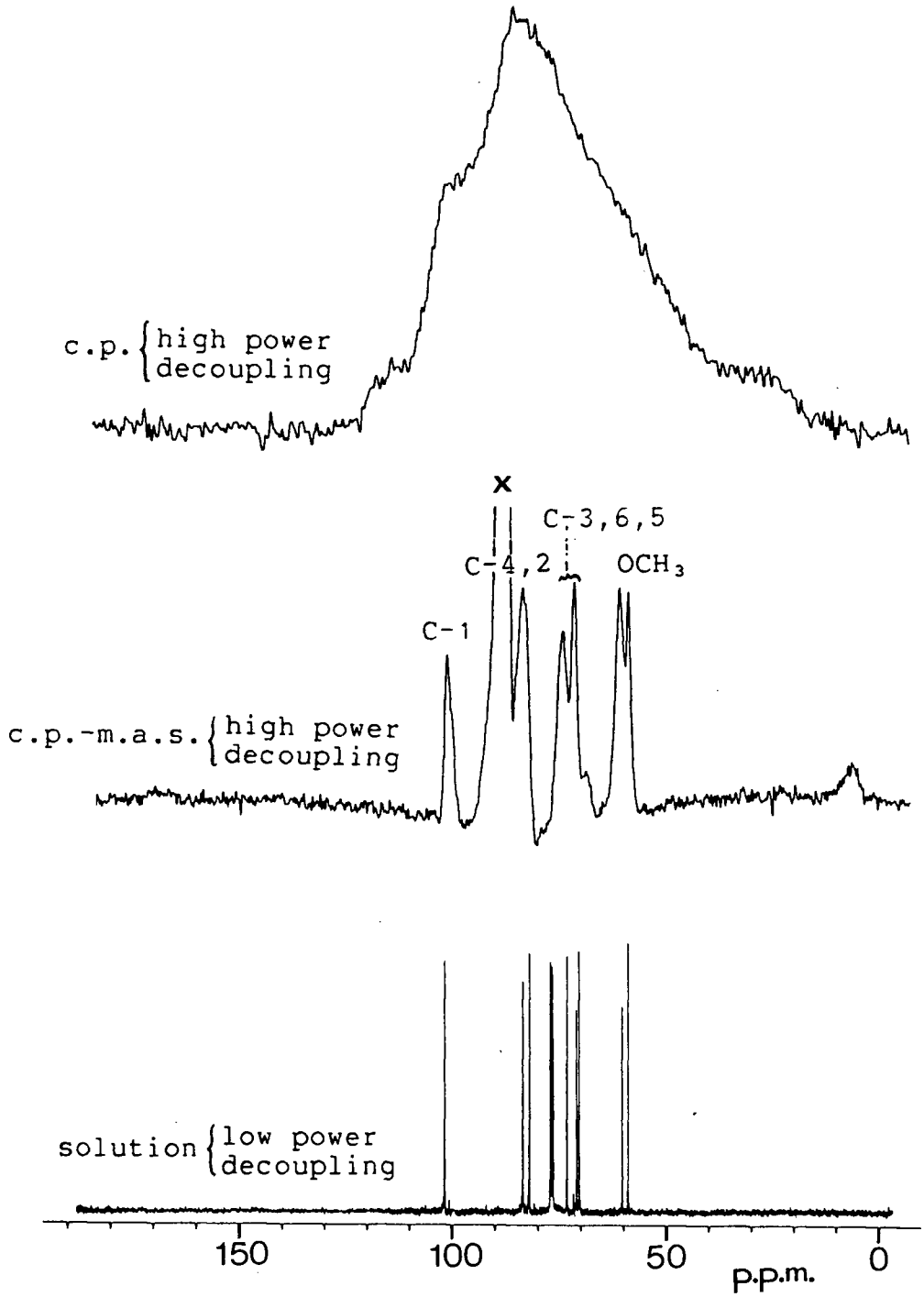

Fig. II-12. Dipolar-decoupled c.p. ^{13}C-n.m.r. spectra of [3], with and without magic angle spinning. These are compared to the solution-state spectrum of the same compound (in $CDCl_3$).

signals of the methoxyl moieties. It is known[57] that any slight irregularities in the crystal packing can distort the 2,6-di-O-methyl-glucopyranose monomer or change the hydrogen bonding in the solid, and thereby produce slightly different shifts for different monomers. However, there is no indication of the presence of more than one kind of different conformer in the lineshape of the C-1 resonance for any of these samples. This could be further verified if there were no overlapping of signals in the C-4 region for this molecule.

A genuine example of an amorphous sample is illustrated by a precipitated sample [4], which reveals an unoriented powder spectrum as shown in Fig. II-13. Heating the recrystallized sample [24] to 130°C for 1 d removed its guest molecule, toluene, and at the same time it destroyed the crystalline structure.

Fig. II-14 shows the ^{13}C-n.m.r. spectra obtained for several related inclusion complexes of 2,6-di-O-Me-β-CD. The gradual change in the lineshape patterns of the sugar resonances from complex [5] to [10], suggests the same "upright" orientation inside the host cavity for the benzene ring as has been found for other aromatic molecules.[8] Presumably, the long axis of the aromatic molecule lies almost parallel to the channel (cavity) axis of the cyclodextrin.

The splittings of the ^{13}C resonances of the host may be discussed in terms of the parameters which are known[19]

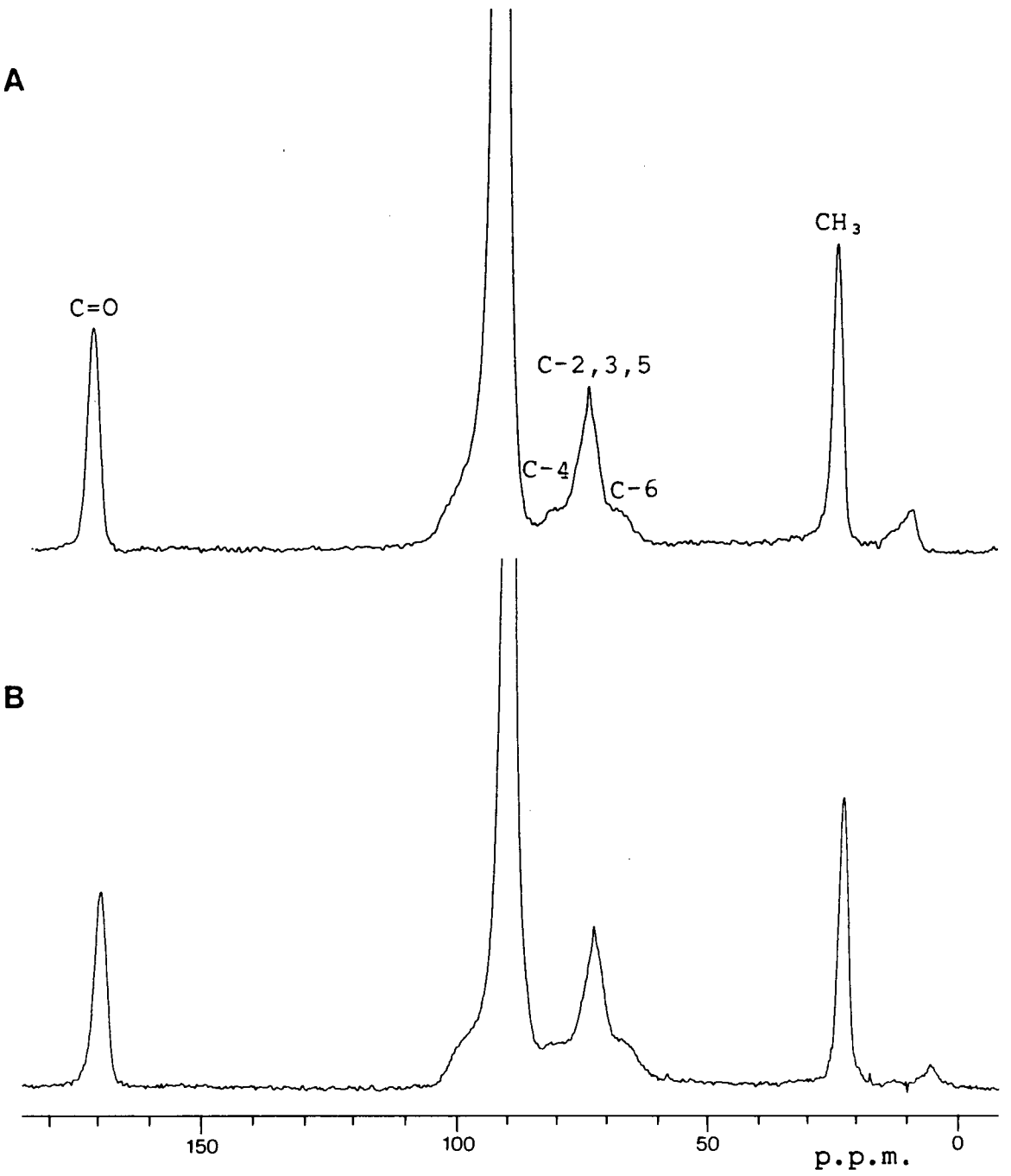

Fig. II-13. ^{13}C-N.m.r. spectra of the amorphous samples [4]: (A) precipitated sample; (B) recrystallized sample [24], with the guest (solvent) molecules removed by heating.

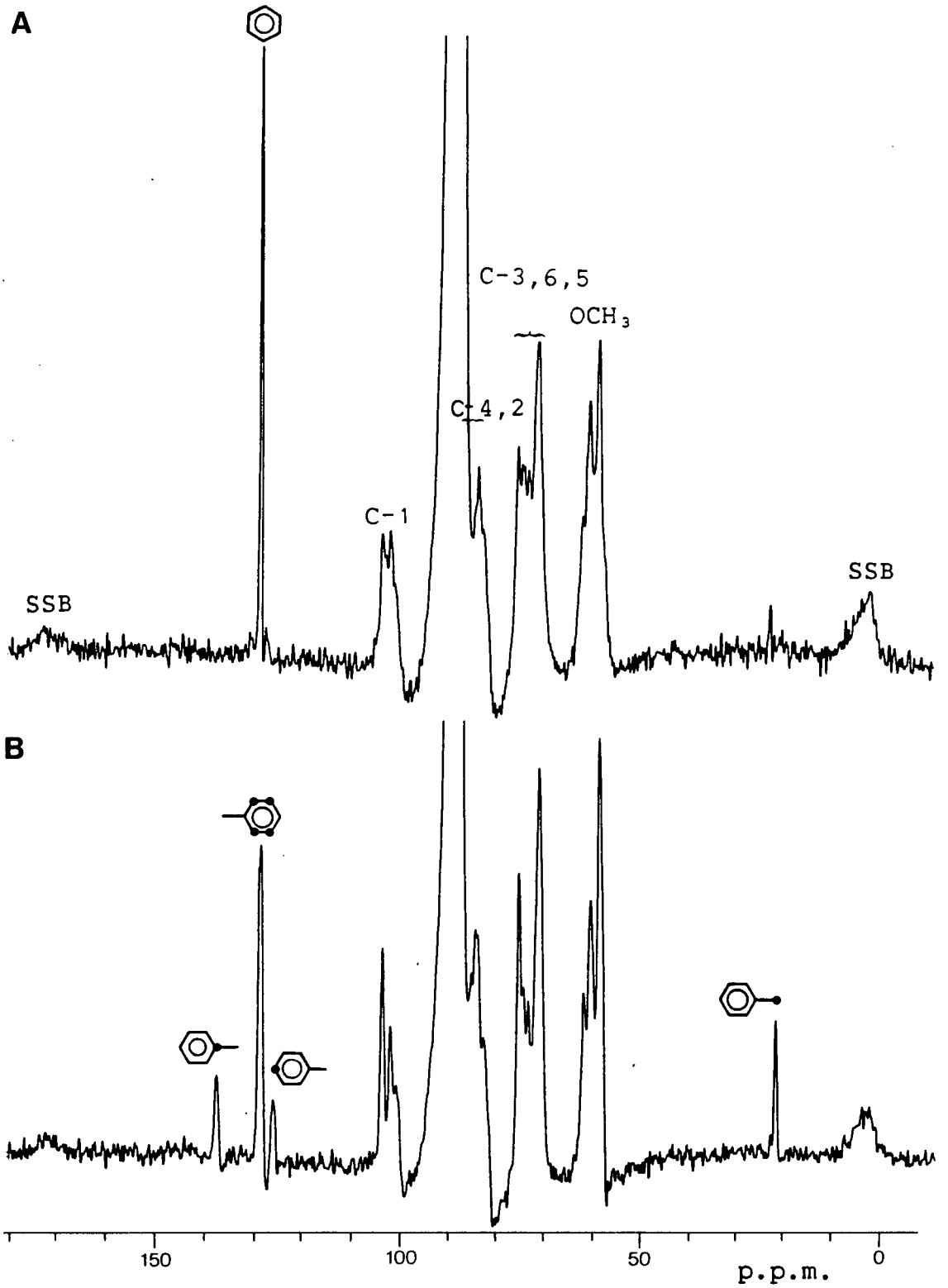

Fig. II-14. ^{13}C-N.m.r. spectra of 2,6-di-O-Me-β-CD inclusion complexes: (A) [5]; (B) [6]; (C) [7]; (D) [8]; (E) [9]; (F) [10]; (G) [11]; (H) [12].

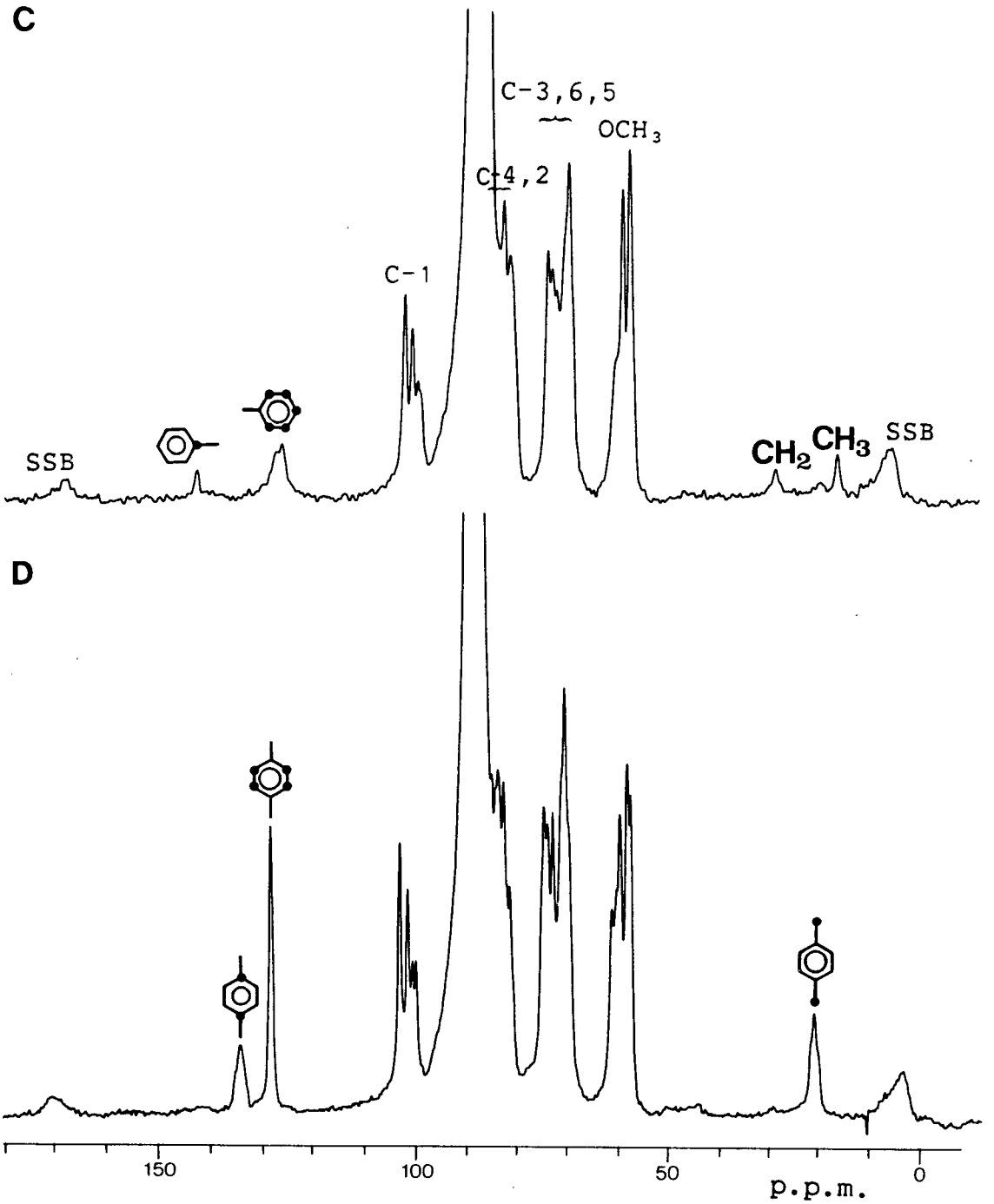

Fig. II-14 cont'd

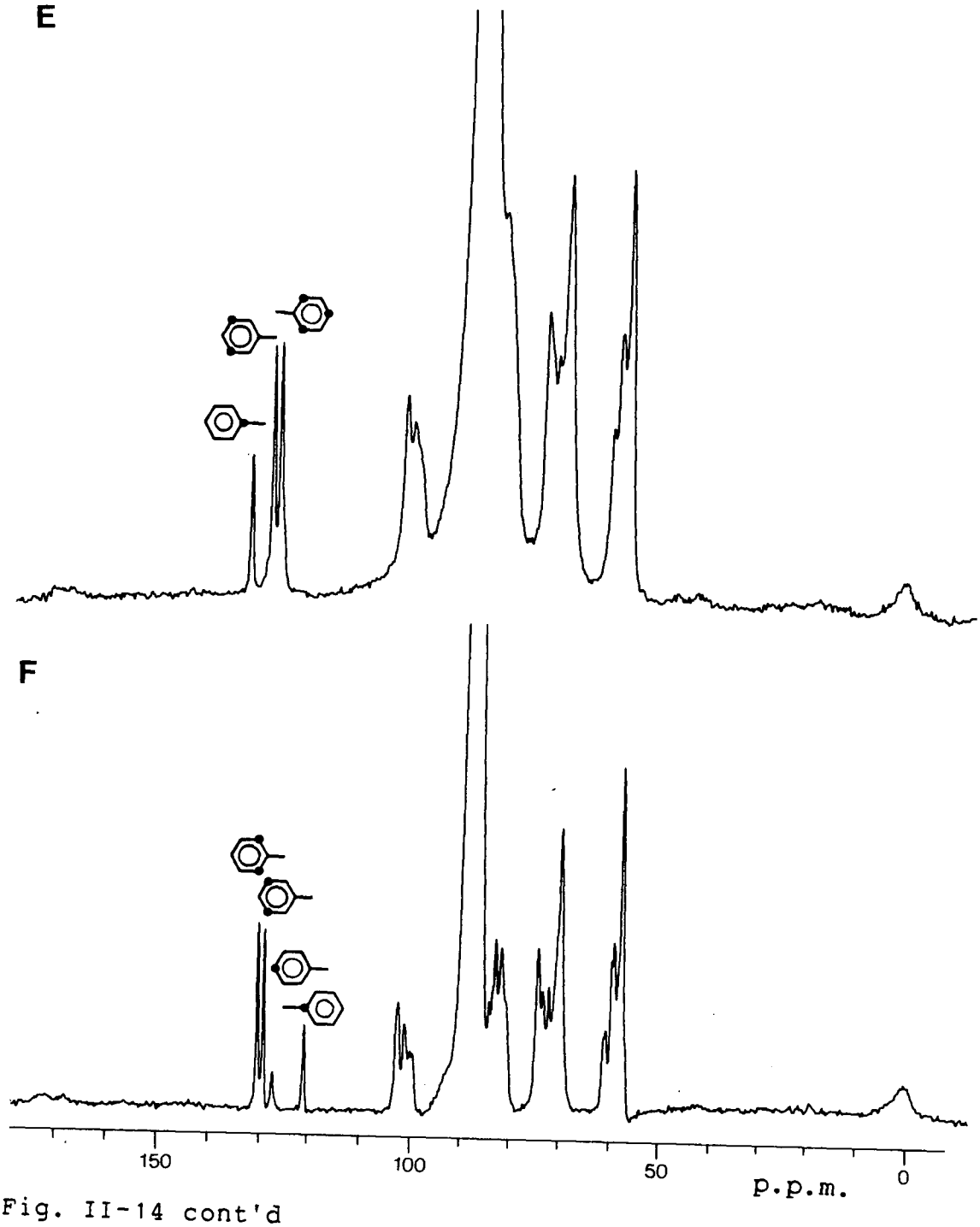

Fig. II-14 cont'd

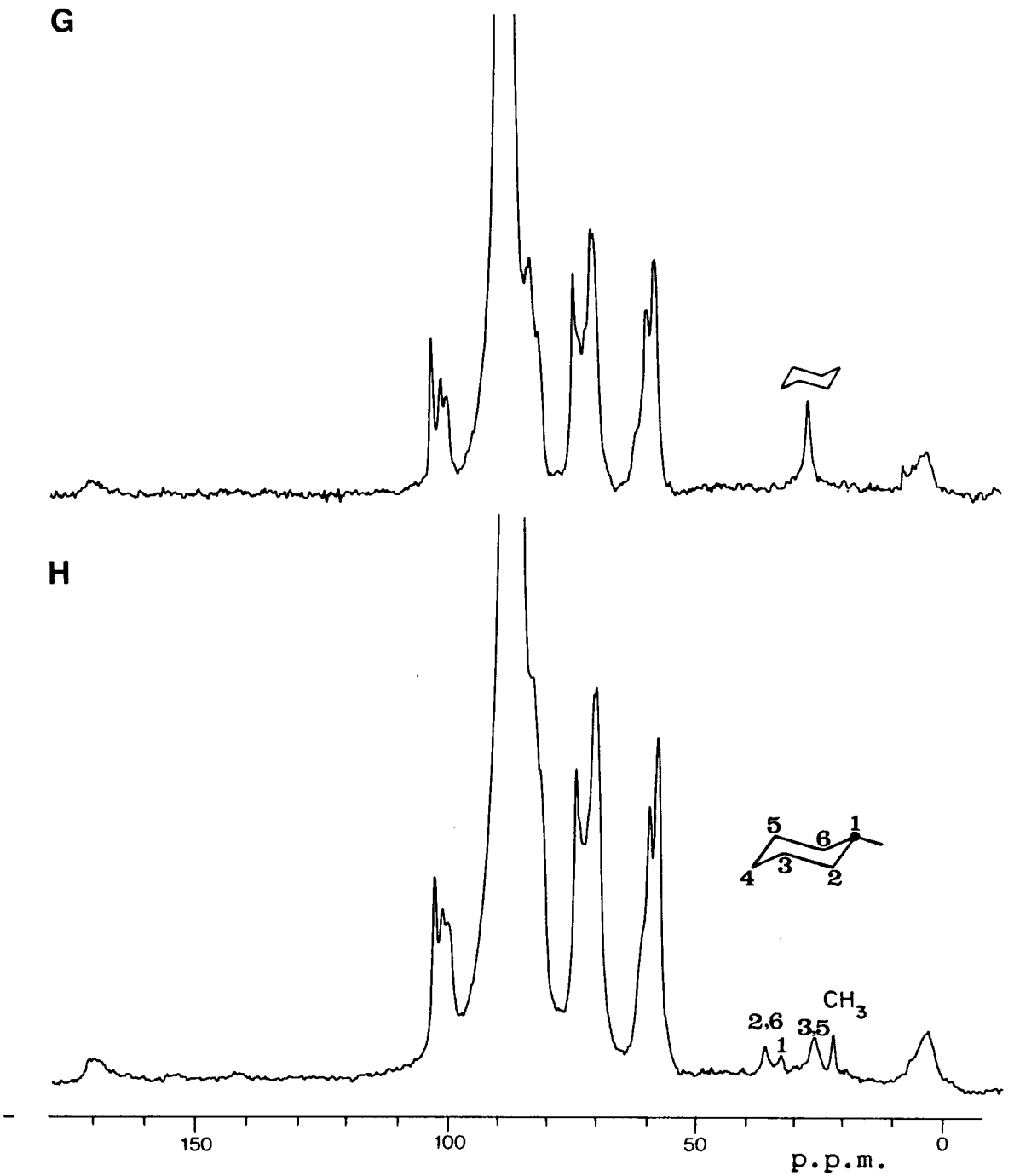

Fig. II-14 cont'd

to contribute to changes in the chemical shifts on complex-formation in solution. If the π-cloud deshielding effect was of significance in perturbing the carbon resonances, this perturbation should be slightly different for a given set of carbons due to restricted mobility of the guest molecule. As in solution, such an effect is unlikely because similar splitting patterns were observed for the host with smaller aromatic and nonaromatic guest molecules. Hence, the major contributions may well come from the steric interactions and conformational changes of the cavity on substrate complexation. It is obvious from the set of spectra above that the splittings become more complex with increasing size of the substituent groups in monosubstituted benzenes, and more so in the disubstituted benzenes. Here, the participation of conformational change may be considered large since the macrocyclic conformation of the host is relatively free of steric hindrance at the C-2,C-3 side of the cavity. This would provide a good fit between the guest and the host. On the other hand, the bulky acetyl groups of compound [4] may impose severe restriction on bond distortions, and also constriction of the opening at both ends of the truncated cone. Fig. II-15 reveals the complexity of the ^{13}C resonances of the host, even with benzene as the guest molecule. Again, a similar trend was observed in their splitting patterns; the effect is most pronounced for the complex with the largest substrate, p-xylene, that can be accommodated inside the

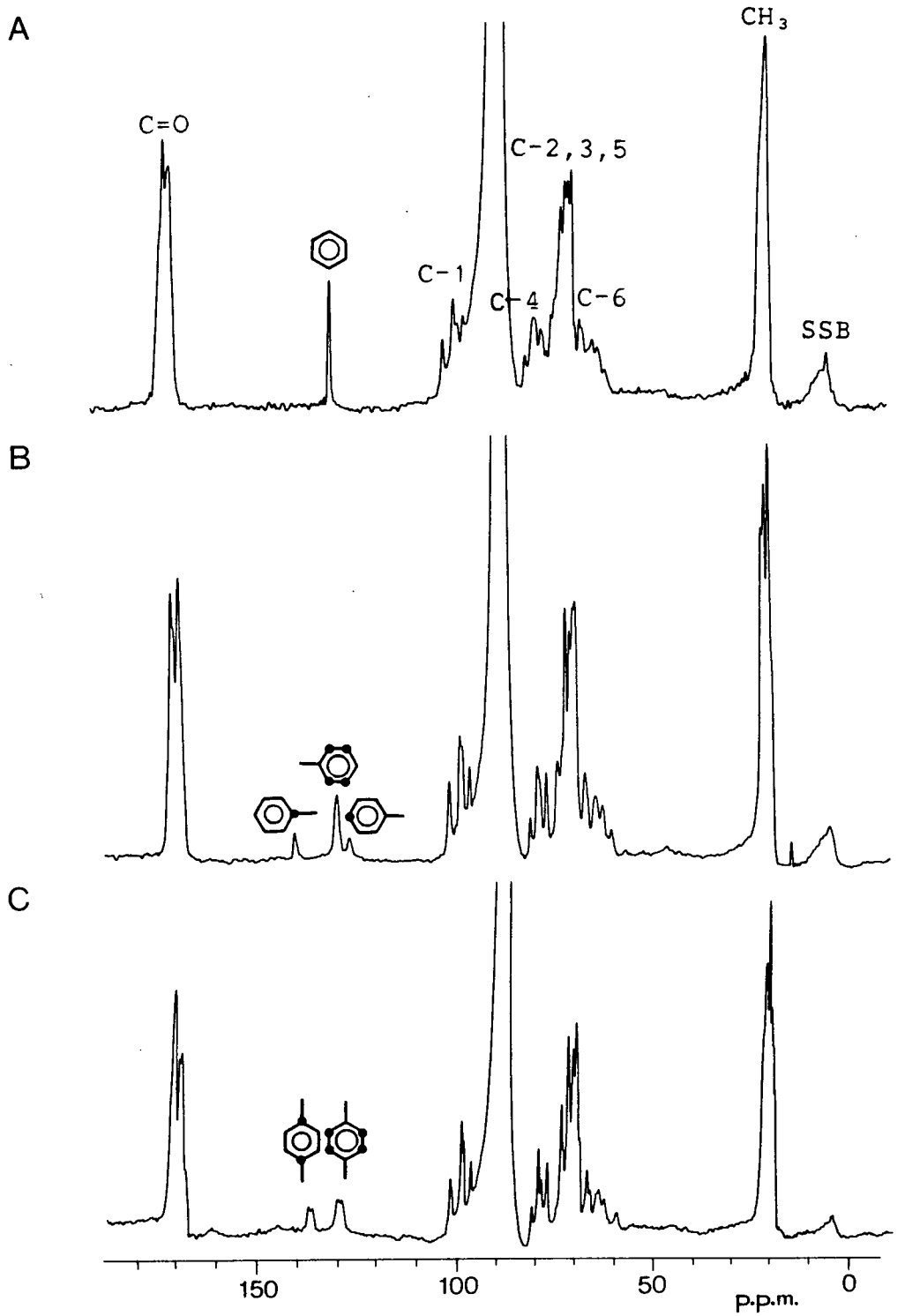

Fig. II-15. ^{13}C-N.m.r. spectra of 2,3,6-tri-O-Ac-β-CD inclusion complexes: (A) [23]; (B) [24]; (C) [25].

cavity.

Depending on the extent of the host-guest interactions, noticeable changes in the chemical shifts of the guest molecules can be anticipated. Table II-2 lists the chemical shift values of the ^{13}C resonances of the aromatic molecules as neat liquids and as encaged aromatic "solids". The isotropic chemical shift values of these molecules remain practically the same, on going from the free to the complexed forms with host molecule [3]. This indicates that the guest molecules have very weak van der Waals contacts with the interior surface of the cavity, and that they are essentially "free". In the case of β-cyclodextrin peracetate complexes, the isotropic chemical shift differences are greater than 1.0 p.p.m.; the maximum experimental drift in chemical shift for this n.m.r. instrument is estimated to be ±0.5 p.p.m.. Hence, the downfield shift of the guest resonances could be attributed to the small cavity of the host molecule, in which the acetyl groups bestow a strong deshielding effect on the guest molecule. An interesting observation is the splittings of the aromatic carbon resonances of p-xylene into doublets in complex [25]. We suggest that this may be caused by incomplete penetration of the rigid guest molecule into the cavity.

In the solid state, the aromatic ring of the guest molecules is not freely rotating about its two-fold axis within the annulus of the host. However, it can undergo

Table II-2. Chemical shifts (p.p.m.) for the liquid guest molecules

Substrate	Host	(unsub)	C_1	ortho	meta	para	CH_2	CH_3
benzene.....		128.5						
	[3]	128.7						
	[4]	129.7						
	[30]*	126.7						
toluene.....			137.7	129.2	128.6	125.6		
	[3]		138.0	(128.7)		126.2		
	[4]		140.5	(130.0)		126.6		
	[30]		134.1	(129.2)		(obscured)		
p-xylene.....			134.5	(129.1)				20.8
	[3]		135.0	(128.7)				21.6
	[4]		(137.5,136.5)	(130.3,129.1)				(obscured)
	[30]		132.2	(128.3)				20.7
ethylbenzene..			144.1	128.4	127.9	125.8	29.1	15.7
	[3]		144.5	128.8	127.7	(obscured)	29.5	17.1
chlorobenzene.			134.7	128.9	130.1	126.8		
	[3]		134.3	128.6	130.0	(obscured)		
bromobenzene..			123.0	131.9	130.5	127.3		
	[3]		122.0	131.5	130.3	128.5		

* Dianin's compound.

librational flip motion with a very small amplitude.[66] Large angle rotation by the aromatic ring about its long axis may be restricted in the cavity of compounds [3] and [4]; this is particularly true in the latter because of severe steric hindrance imposed by the acetyl groups. The perturbation from the rigid crystalline field may ultimately determine the differences in the time scale and mode of motion of the aromatic rings in solution and in the solid complexes.[66]

Supporting evidence for differential motion of individual segments of the guest stems from the ^{13}C-c.p.-m.a.s. measurements used to differentiate between the resonances of protonated and nonprotonated carbons. The dipolar dephasing technique[63] can be used to eliminate spectral signals from carbons strongly coupled to protons, leaving signals from nonprotonated carbons and weakly coupled carbons because of averaging of dipolar interactions by extensive molecular reorientation. In this way, the signals from their pendant substituents such as the methoxyl and acetoxyl moieties are retained. Substantial signals were obtained for all the resonances of the guest molecules within the crystalline matrix of compound [3] as depicted in Fig. II-16. However, the resonances of the aromatic carbons of complexes [24] and [25] are essentially suppressed because residual, or no, motion is allowed for the ring that is intimately associated with the cavity. Only the methyl groups give

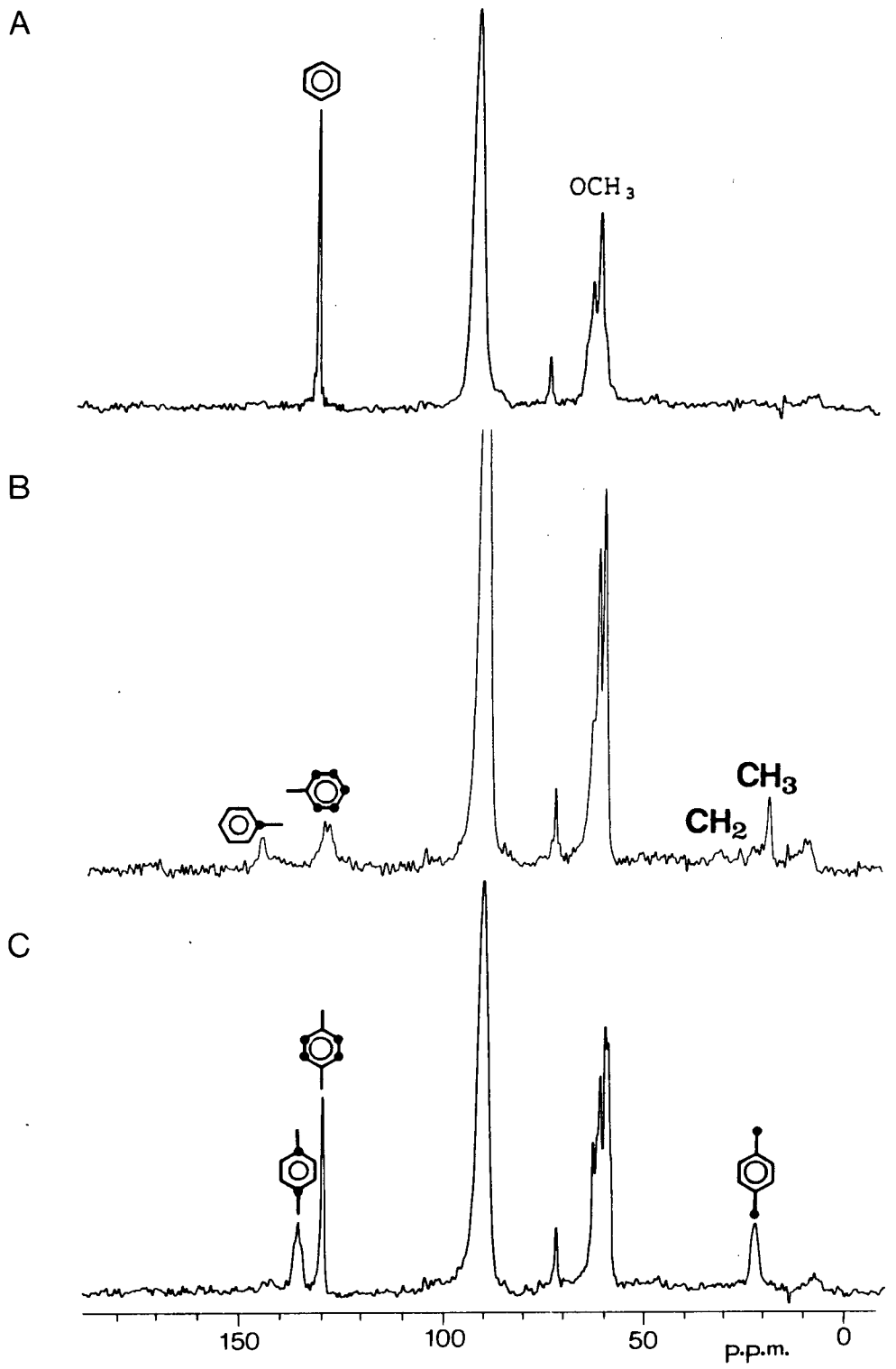

Fig. II-16. Dipolar-dephasing ^{13}C-n.m.r. spectra: (A) [5]; (B) [7]; (C) [8]; (D) [23]; (E) [24]; (F) [25].

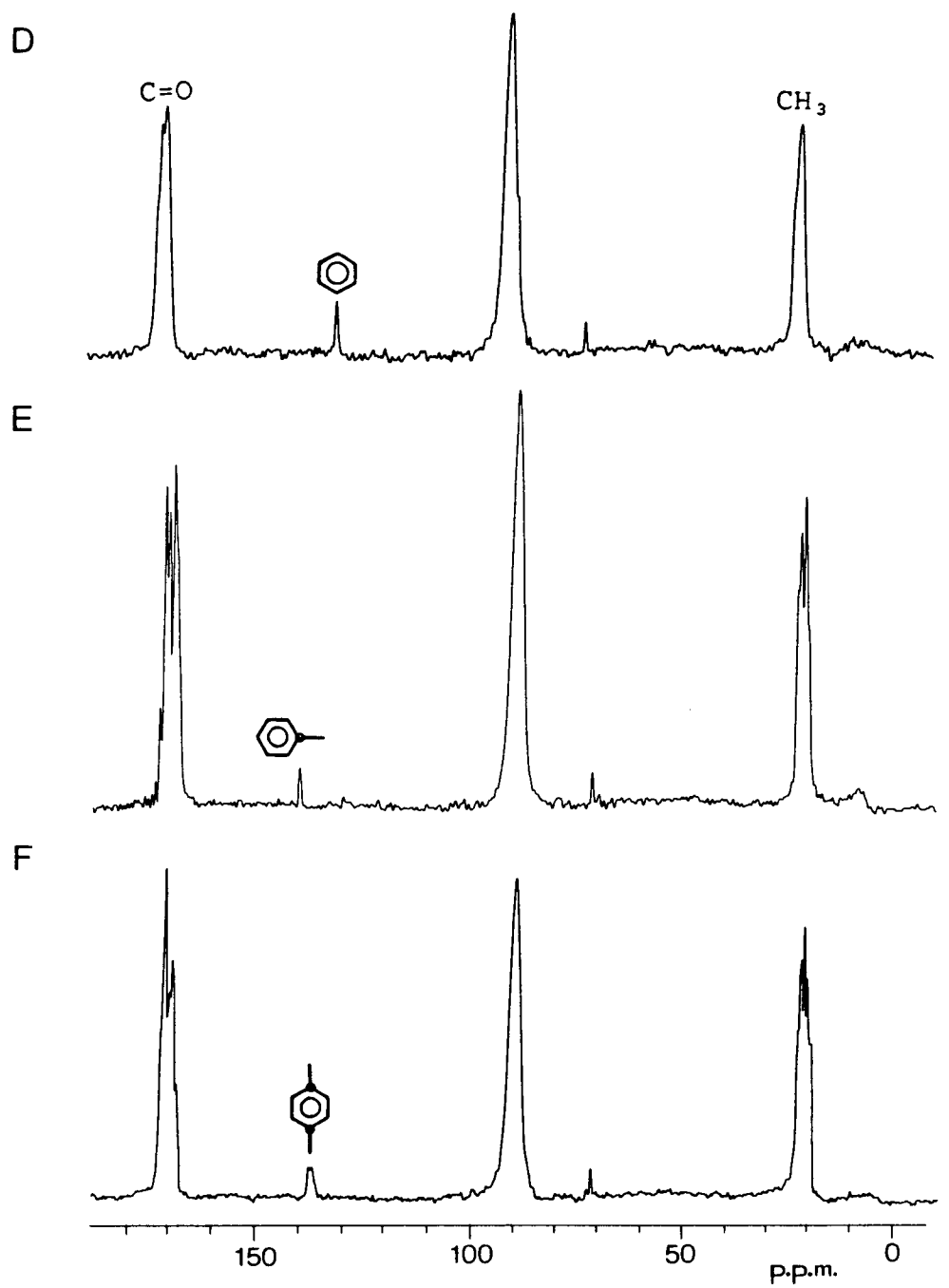

Fig. II-16 cont'd

substantial signals, that reflect the various additional degrees of freedom available to all these carbon atoms.

In principle, variable-temperature (v.t.) ^{13}C-c.p.-m.a.s. experiments[58] should provide valuable insight into the dynamics and compositions of inclusion complexes involving liquid substrates. Unfortunately, such studies were not possible at U.B.C. because of the unavailability of a v.t.-m.a.s. probe. Nevertheless, studies of temperature effects on crystalline complexes are presented by recording a series of spectra from samples which had been heated prior to each n.m.r. measurement, over a wide range of temperatures. Figs. II-17 and II-18 reveal the thermal stability of the complexes with benzene and toluene, respectively; these were gradually "distilled" from the cavity of the host molecule [3]. The splittings of the host resonances diminish gradually, and the peaks are progressively moved towards those of the free host at higher temperatures.

The importance of aroma-cyclodextrin complexes in the food industry has been extensively investigated by several research groups.[68] The preparation of these complexes is relatively simple, and the β-cyclodextrin complex of d-limonene has been reported by Suzuki and Ikura.[69] Compounds [2], [3], and [4] were used to encage this substrate, but with limited success. Only compound [3] afforded a complex with a guest/cyclodextrin molar ratio of 1:1; the ^{13}C chemical shifts of the guest resonances (Fig. II-19) are

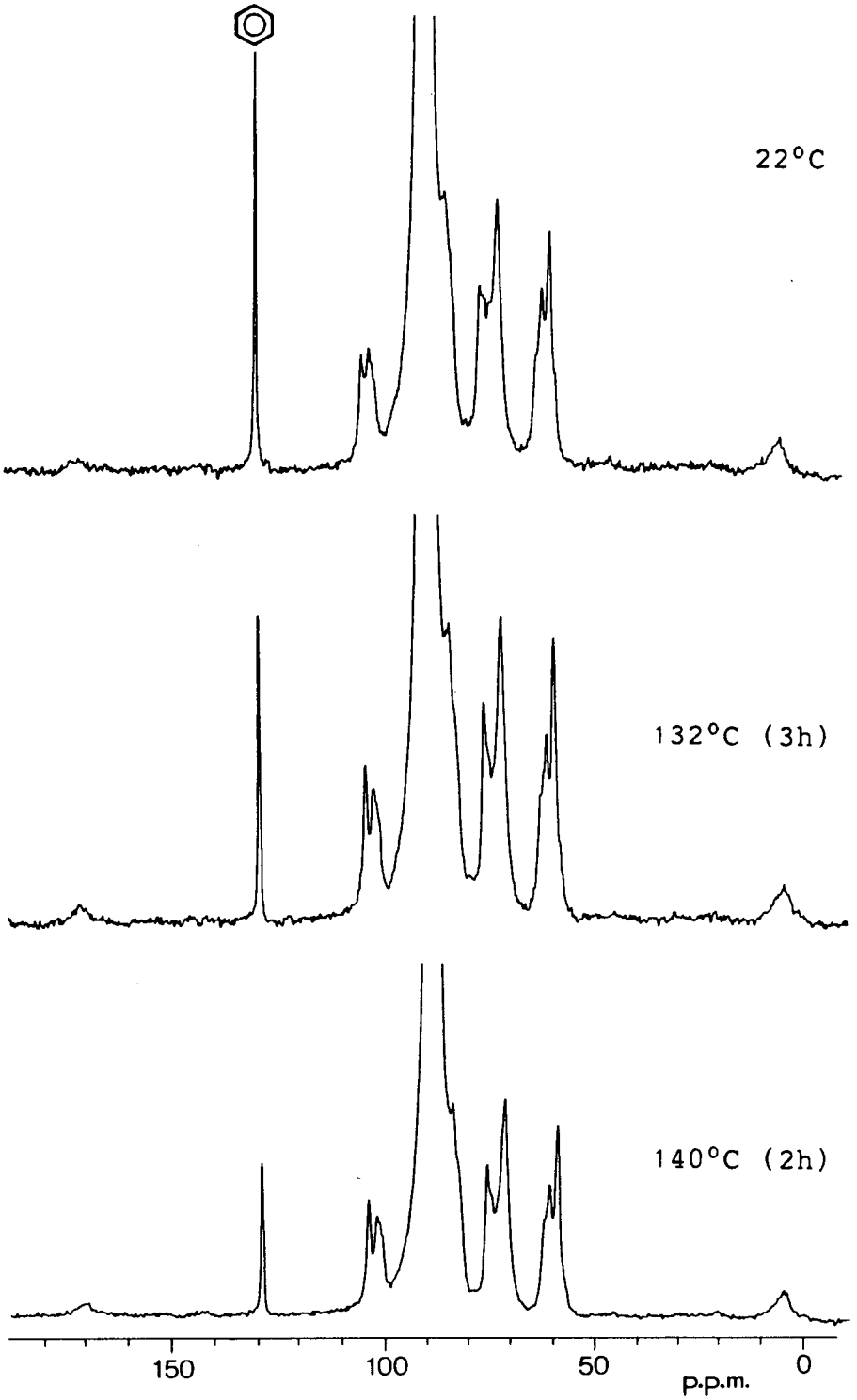

Fig. II-17. ^{13}C-N.m.r. spectra of [5], preheated at the temperatures indicated.

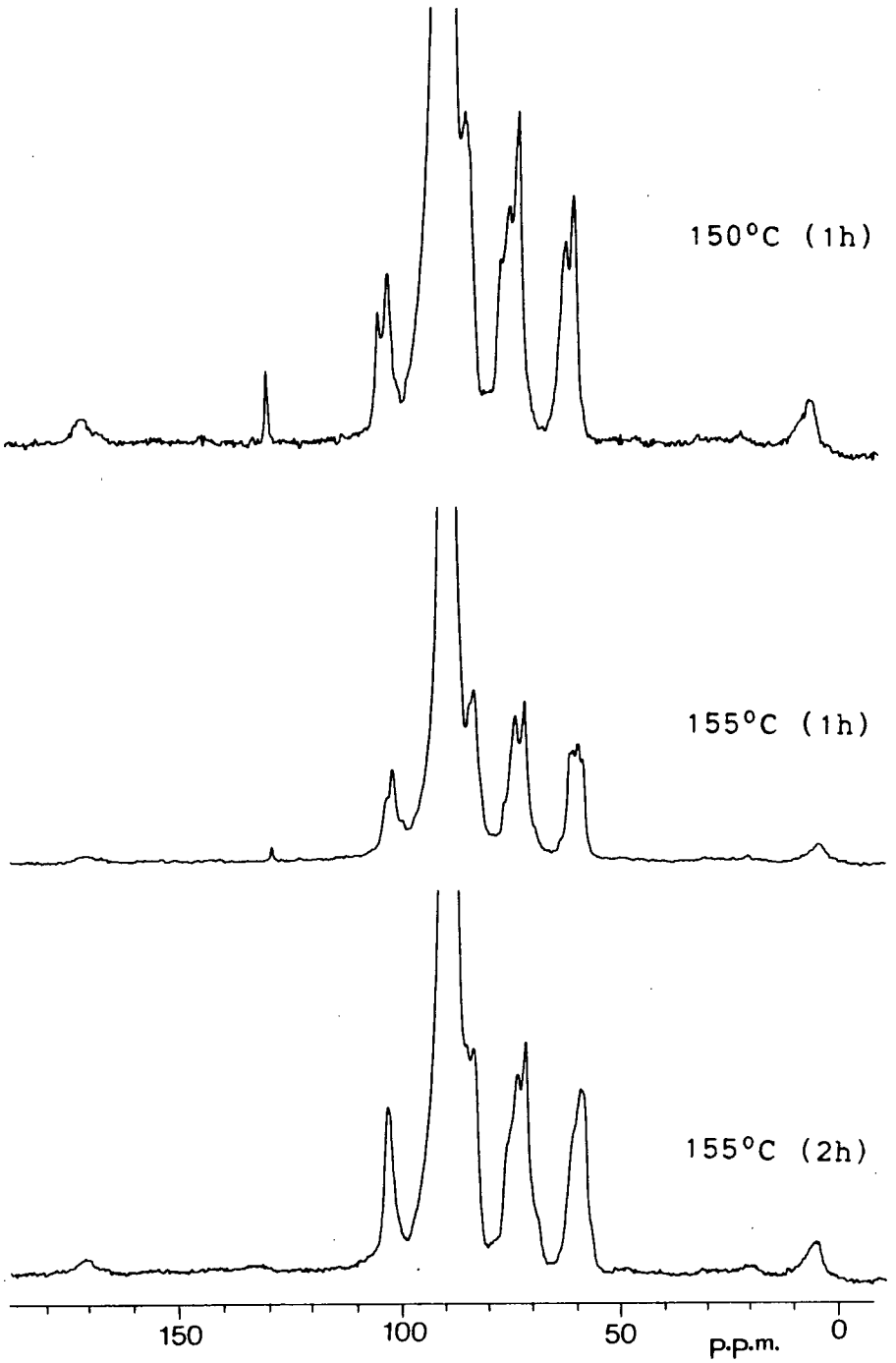

Fig. II-17 cont'd

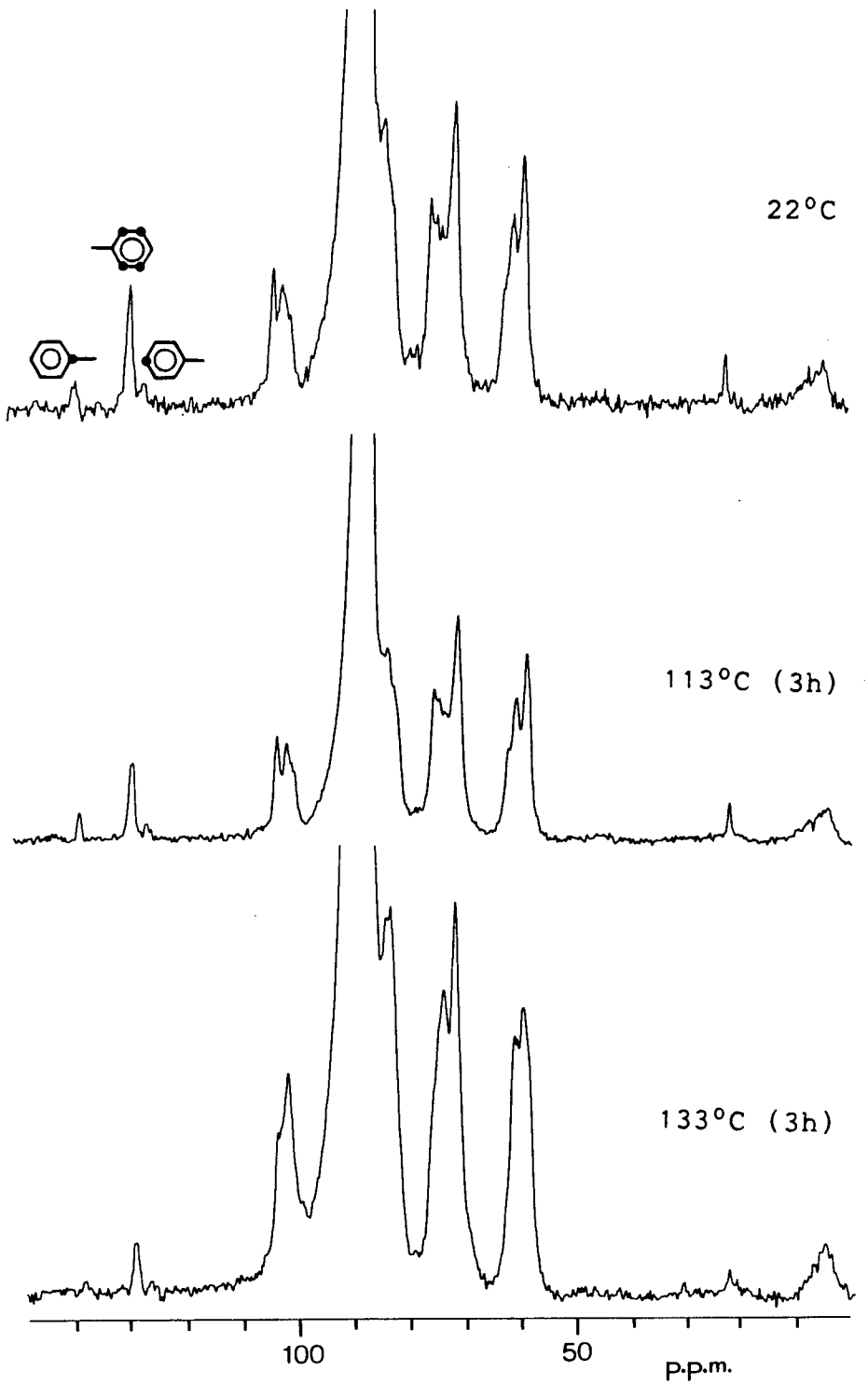

Fig. II-18. ^{13}C-N.m.r. spectra of [6], preheated at the temperatures indicated.

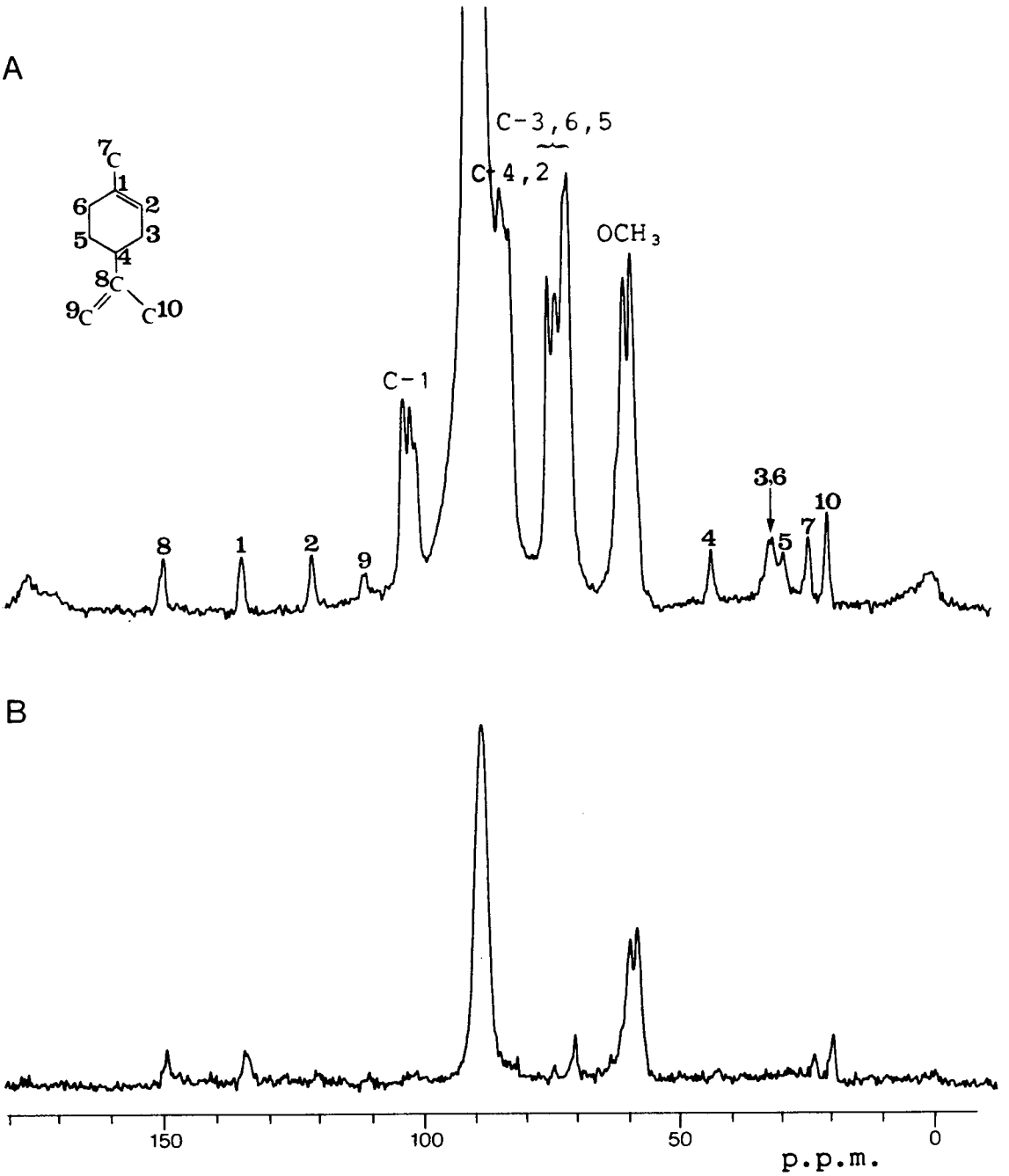

Fig. II-19. ^{13}C-N.m.r. spectra of 2,6-di-O-Me-β-CD-d-limonene complex: (A) normal c.p.-m.a.s.; (B) with dipolar dephasing.

quite close to those obtained in solution, except for C-4,C-5, and C-9. The differences in the isotropic chemical shift values of these carbons may be explained by the rigidity of the molecule within the cavity.

II.6.3. ^{13}C-N.M.R. Studies of Cyclodextrin Inclusion Complexes with Solid Guest Molecules

It was found that variations in crystalline field can alter the chemical shift dispersions of solid substrates between their free state, and complexed state with the host molecule [3]. This occurs when relatively large guest molecules are involved in the complexation; e.g., biphenyl, 4,4'-dimethylbiphenyl, and p-di-tert.-butylbenzene. One would expect their combining ratios of guest to host to be 1:2; this is only true for biphenyl, whereas the others yield 1:1 complexes. Since these guest molecules are elongated, their complexes may well crystallize in channel- or discontinuous "channel"-type structures.[61] In the former, one guest molecule is included within the cylinder, while the other is located outside the cyclodextrin ring to afford a molar ratio of 1:1. Alternatively, one guest molecule is assigned to a ring, thereby disrupting the channel-type structure of the host as illustrated in Fig. II-20.

Biphenyl crystals are known[70] to be monoclinic, with 2 molecules in the unit cell of space group $P2_1/a$. The

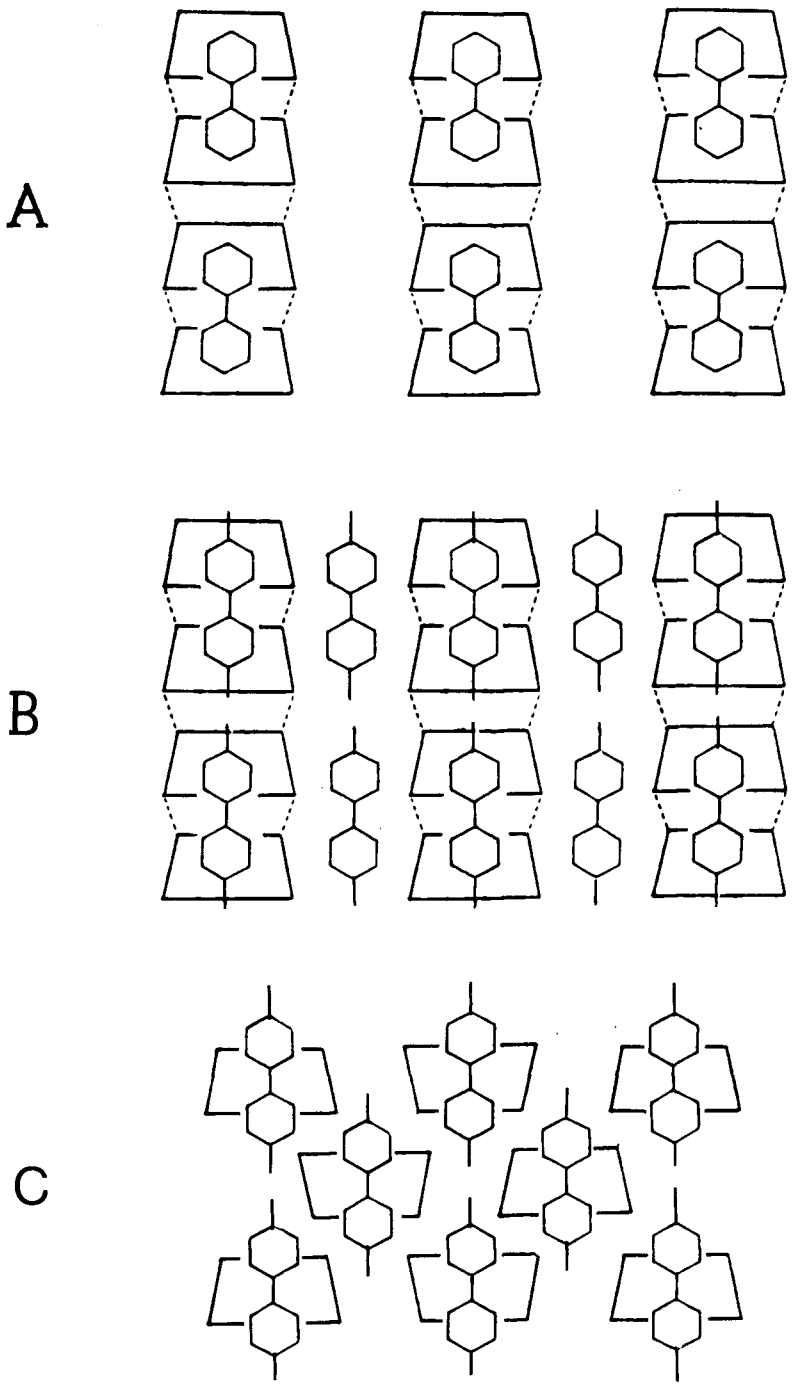

Fig. II-20. Schematic drawings of the inclusion possibilities for larger guest molecules (from Ref. [61]).

single, symmetry-independent molecule, which is situated on a center of symmetry, has a completely planar structure for the carbon skeleton. Albeit that the hydrogen atoms are situated in the plane defined by the carbon atoms of biphenyl, there are small in-plane displacements of the ortho hydrogen atoms from idealized positions, that reduce the steric strain. The gain in stabilization energy from attainment of planarity is probably of the same order as that required to compress the C and H atoms slightly;[71] thus, it is reasonable to suppose that planar or non-planar arrangements could occur in the crystal, depending on the packing. The behavior of the biphenyl molecule in other situations has been discussed in the literature;[72,73] the dihedral angle between the two rings is 40-50° in the vapor phase, and 20-25° in solution.

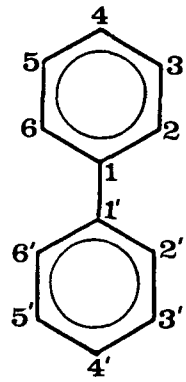

The ^{13}C-n.m.r. spectra of solid biphenyl and its complex with compound [3] are shown in Fig. II-21. The linewidths and chemical shifts of the carbon resonances

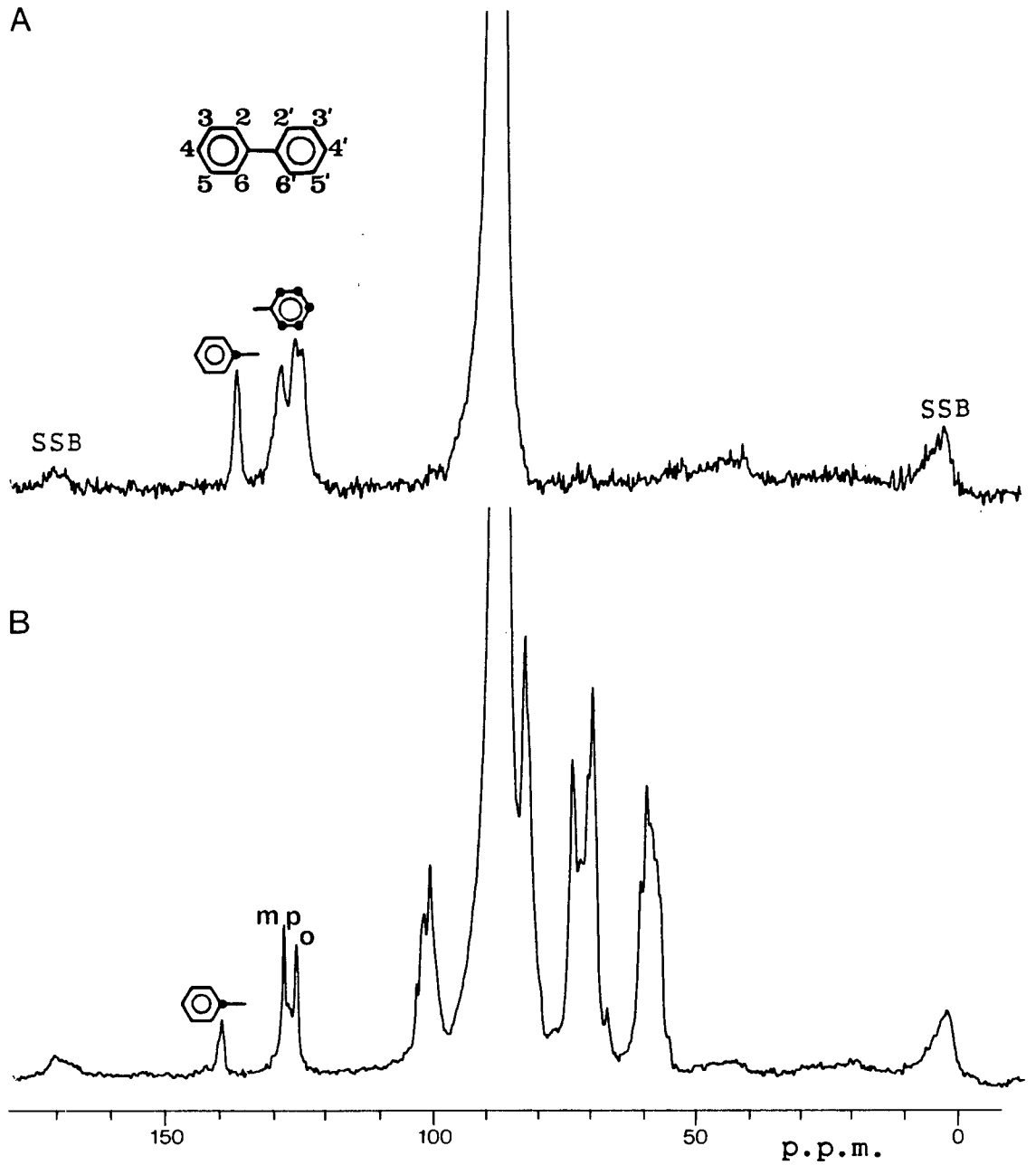

Fig. II-21. ^{13}C-N.m.r. spectra of (A) biphenyl and (B) 2,6-di-O-Me-β-CD-biphenyl inclusion complex, [13].

belonging to the guest molecule are affected by the change in its environment. Carbon atoms C-1,C-1' or C-4,C-4' probably have equivalent molecular and crystal environments since a single ^{13}C resonance was observed in the solid state for the C-1,C-1' pair of carbons. It should be noted that crystal symmetry does not require the ortho or meta carbon pairs to be equivalent.[74] In this case, the difference is not sufficiently large and, hence, only broad resonances were observed for the ortho and meta carbons. The in-plane displacements of the hydrogen atoms may not cause any broadening of the carbon resonances because the overall symmetry of the molecule is still retained. The encaged biphenyl molecule would probably adopt a coplanar structure within the annulus of the ring. This is evident from the narrower and well-resolved linewidths, and any slight magnetic inequivalence in the pairs of carbon atoms is now removed because the molecule is experiencing a "solution-like" environment. At the same time, the steric compressions[75] are relieved as indicated by the downfield shifts of the C-1 and ortho carbons, which are close to those values measured in solution. Librational motion of the molecule, about its long axis, is suggested from the dipolar dephasing spectrum.

Based on the X-ray data reported by Casalone et al.,[71] the solid-state spectrum of 4,4'-dimethylbiphenyl should be more complicated than that of biphenyl. The crystals are monoclinic, with 8 molecules in the unit cell of space

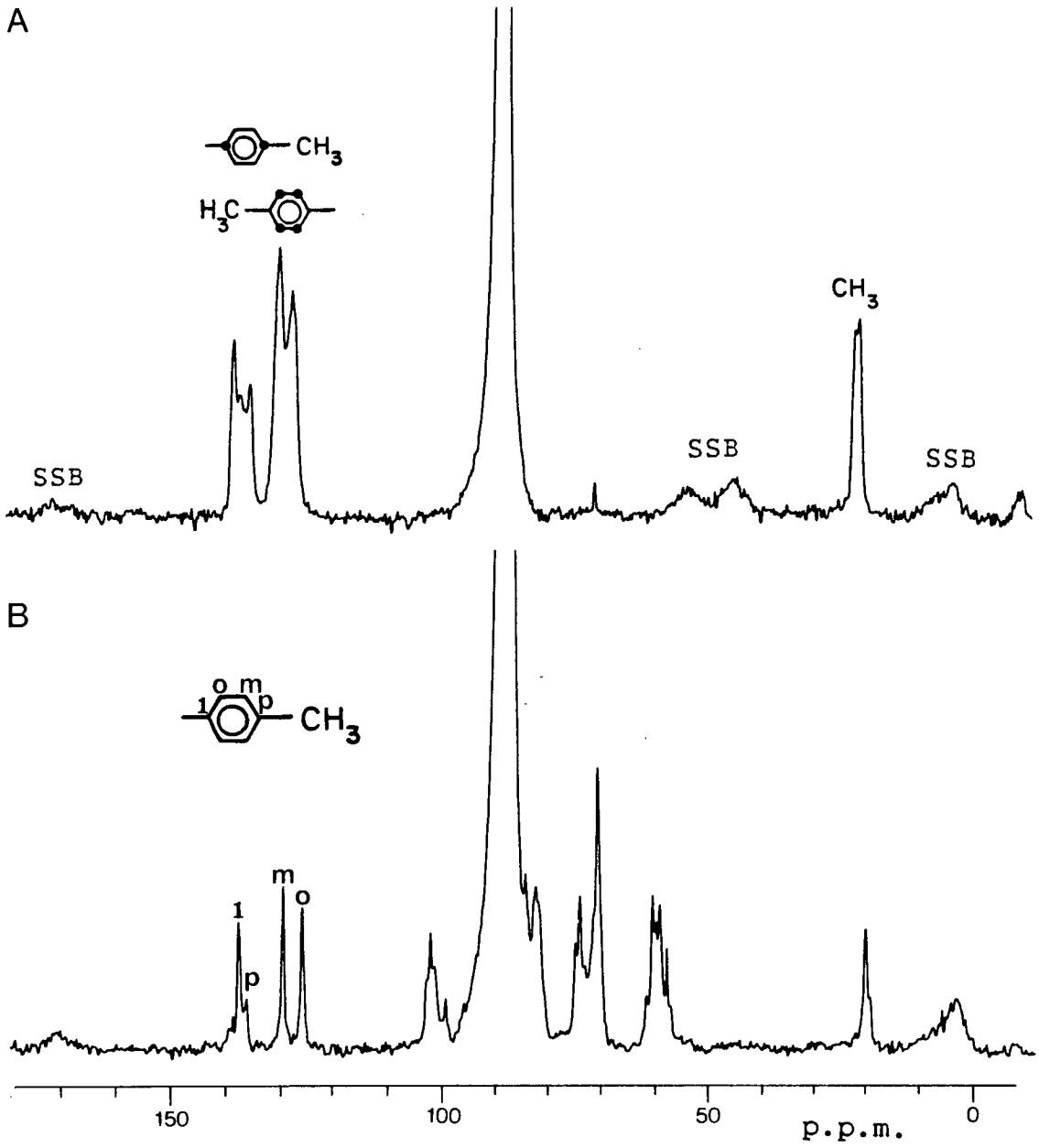

Fig. II-22. ^{13}C-N.m.r. spectra of (A) 4,4'-dimethylbiphenyl and (B) 2,6-di-O-Me-β-CD-4,4'-dimethylbiphenyl inclusion complex, [14].

group $P2_1/c$. There are 2 molecules in the asymmetric unit, with dihedral angles of 36° and 40°, respectively. Therefore, each carbon resonance is expected to split at least into a doubletted-doublet; instead, broad signals with fewer splittings were observed (Fig. II-22). The intramolecular and intermolecular effects may not be large enough to give resolvable splittings due to the small difference in the dihedral angles, yet considerable shifts are induced by the latter. The splittings and shifts in the carbon resonances can be removed by encaging the molecule inside the cavity of compound [3]. If this complex crystallizes in a channel-type structure, the chemical shifts of the guest molecule situated inside and outside the long column should differ. But sharp signals with isotropic chemical shifts close to those data obtained in solution were observed. Therefore the molecule is probably planar, and undergoing molecular reorientation within the discontinuous "channel"-type structure of the host.

The crystal structure of p-di-tert.-butylbenzene has been reported,[76] with no indication of inequivalent molecules in the unit cell of space group $P2_1/n$. The ^{13}C-n.m.r. spectrum shows two peaks for the ortho carbons, which are due to inequivalent molecular and crystal environments (as discussed earlier for the biphenyl molecule), while the other carbon signals appear as singlets. The asymmetric lineshape of the C-1 resonance arises because of the slight misset of the magic angle,

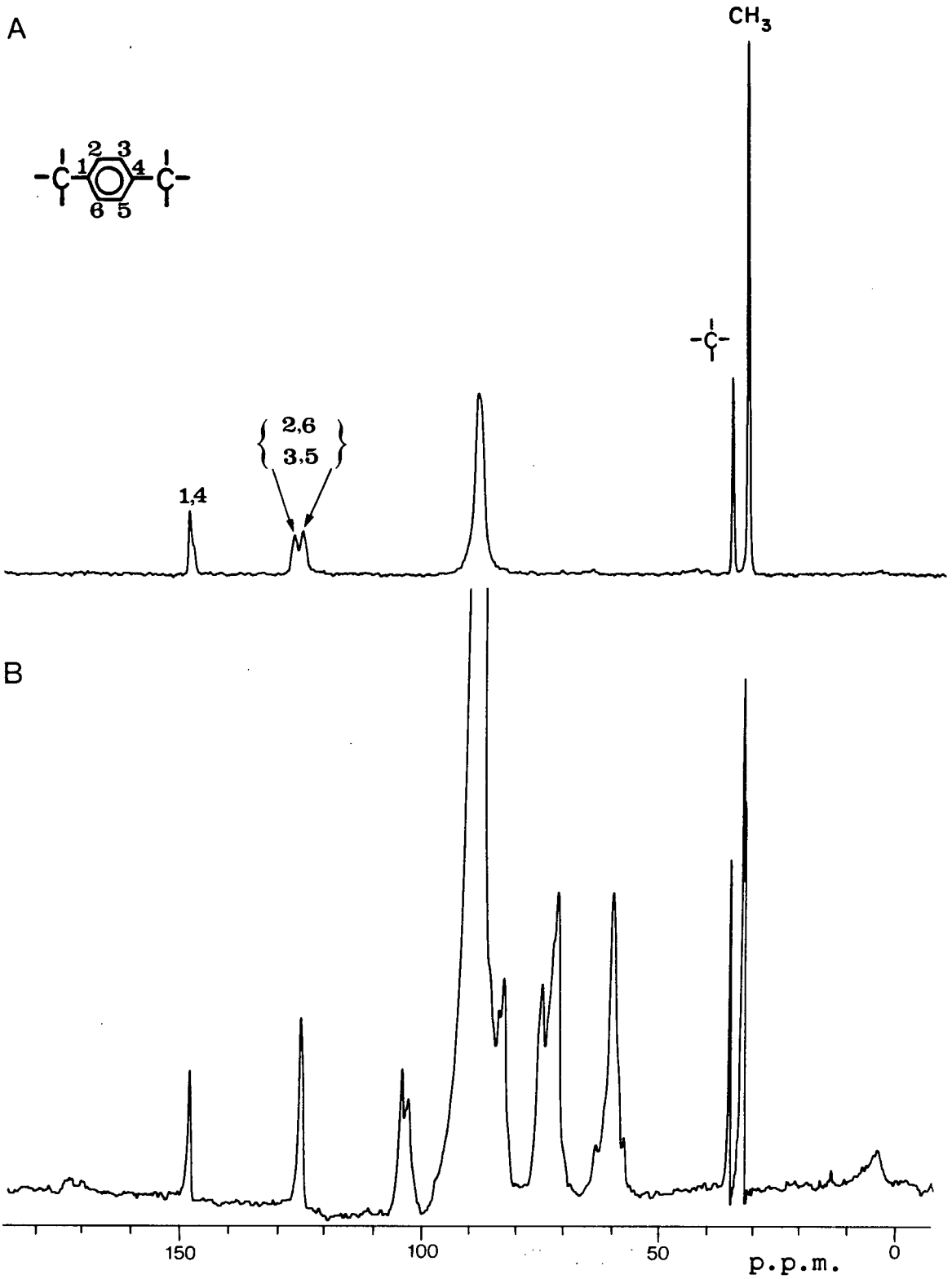

Fig. II-23. ^{13}C-N.m.r. spectra of (A) p-di-tert.-butylbenzene and (B) 2,6-di-O-Me-β-CD-p-di-tert.-butylbenzene inclusion complex, [15].

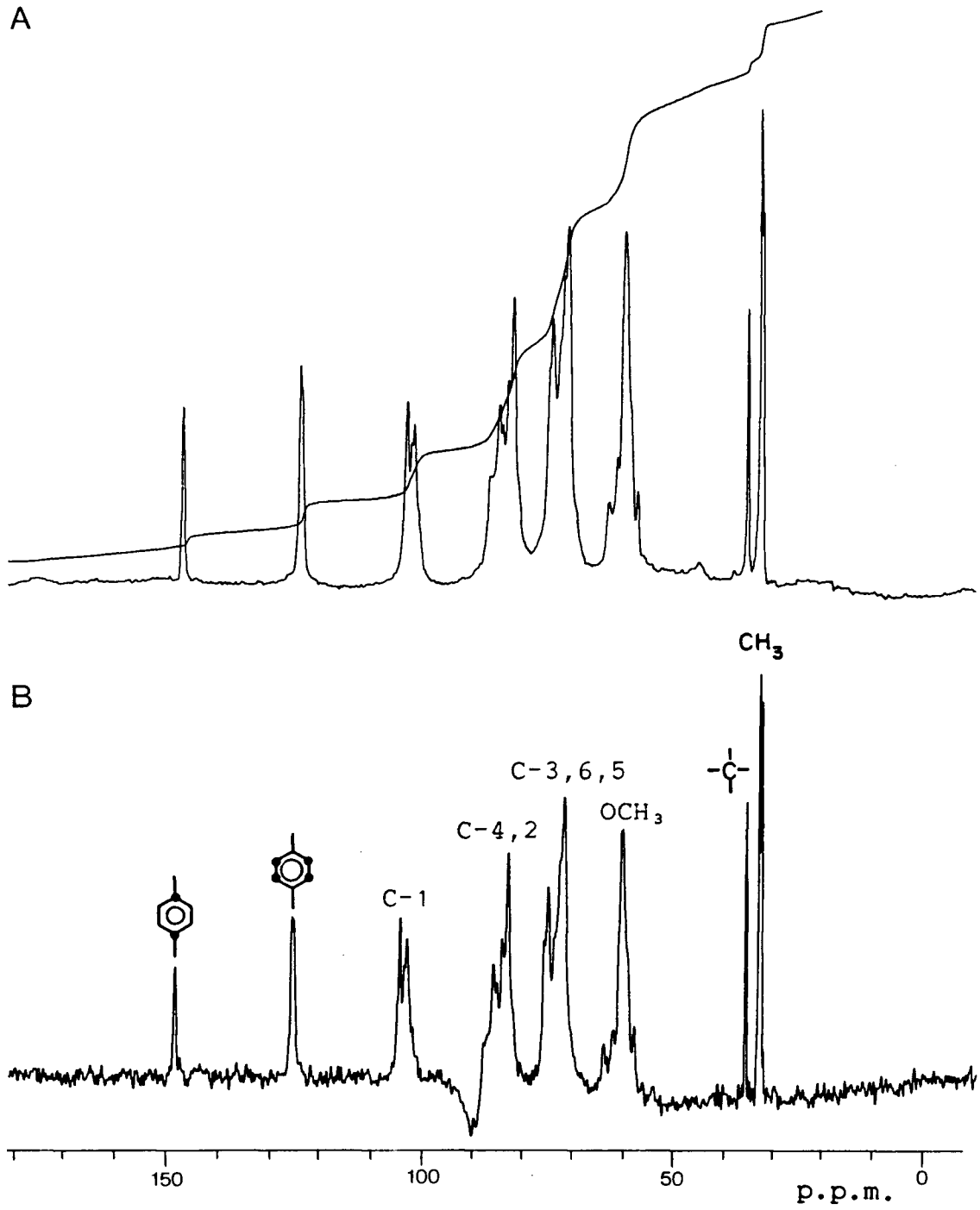

Fig. II-24. ^{13}C-N.m.r. spectra of [15]: (A) normal c.p.-m.a.s. (sample in a deuterated, plexiglas spinner); (B) Delrin-signal suppression; (C) dipolar dephasing spectrum (obtained by setting a 40-μs period without proton decoupling, prior to ^{13}C data-acquisition); (D) same as (C), but with a longer waiting period of 100 μs; (E) Delrin-signal suppression and dipolar dephasing.

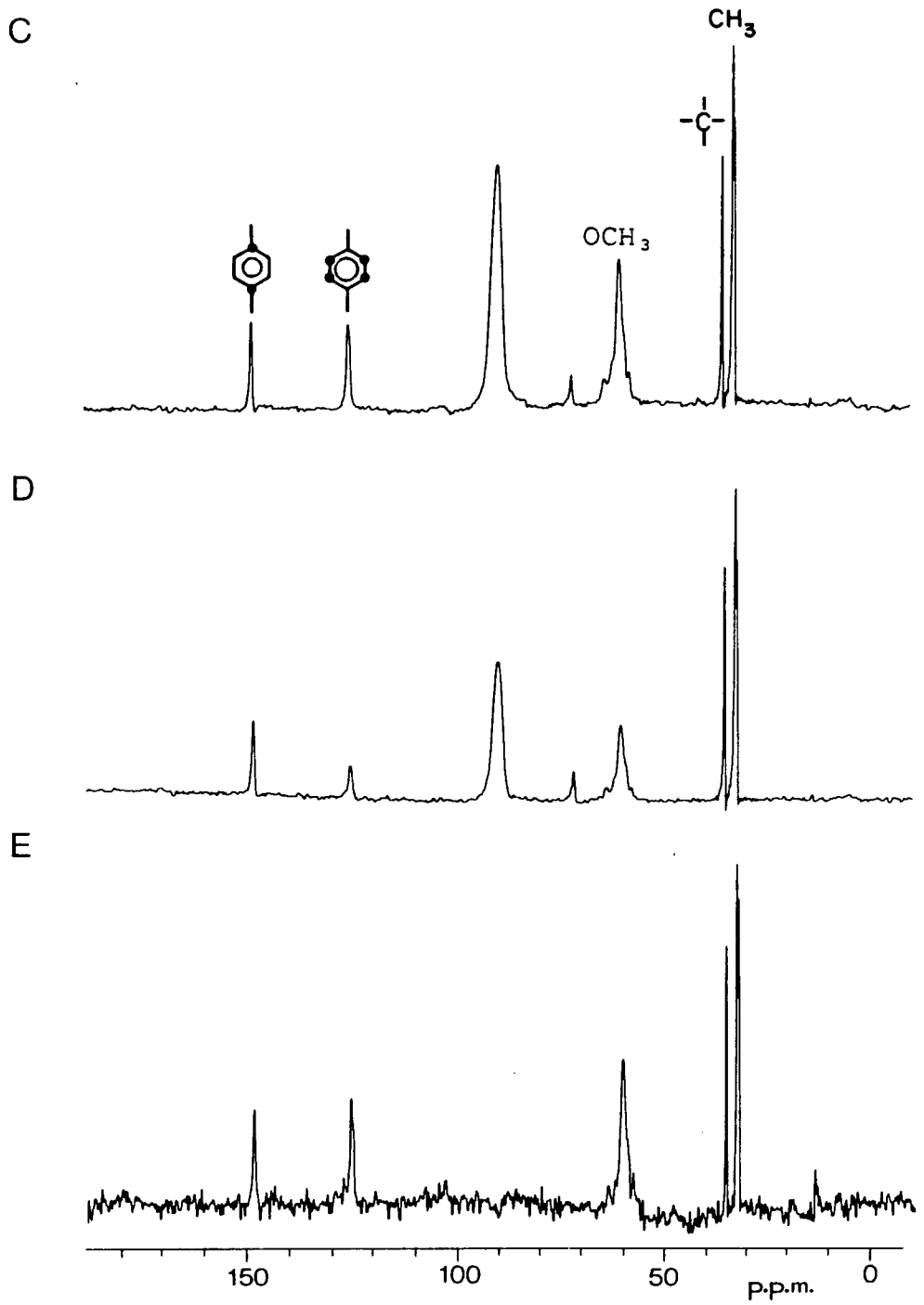

Fig. II-24 cont'd

resulting in incomplete averaging of its large chemical shift anisotropy. Similarly, molecular reorientation of the guest molecule within the cavity of the host affords sharp signals (Fig. II-23); a singlet for the ortho carbons and, surprisingly, a doublet of equal intensity for the methyl carbons. We conclude that the two tert.-butyl moieties probably experience different local environments that appear to be largest for the methyl groups. The subsequent spectra (Fig. II-24) summarize the results that are obtained from the dipolar dephasing and Delrin suppression methods.

II.6.4. ^{2}H-N.M.R. Studies of Cyclodextrin Inclusion Complexes

There has been an impressive number of deuterium n.m.r. spectroscopic studies of the dynamics of the "guest" molecules dissolved in liquid crystal systems,[77-79] and recently in solid clathrates[80-82] as well. Such spectra are profoundly simplified by the large and usually uncomplicated quadrupole splittings, and the lineshapes offer a critical test for models of anisotropic molecular rotation. Thus, the splittings can reveal new and direct information on the motion of a guest molecule within the host materials.

Recently, an X-ray study[49] of the complex of dimethyl sulfoxide with *a*-cyclodextrin, showed the guest molecule to be located in the host cavity nearest to the secondary

hydroxyl groups and with two hydrogen bonds to the adjacent α-cyclodextrin molecules. The complexes of DMSO with both α- and β-cyclodextrins, were prepared from solutions in DMSO/water or DMSO/methanol/water; however, only approximate stoichiometry of these complexes could be obtained from the microanalysis data. Fortunately, this did not compromise the present study of the effect of ring-size on the mobility of the $(CD_3)_2SO$ molecule.

As mentioned earlier (Chapter I, Pg. 56), the ^2H-n.m.r. spectrum of the polycrystalline powder of static C-D bearing dimethyl sulfoxide molecules will have a peak maxima separation of

$$\Delta\nu_Q = \frac{3}{2}\frac{e^2qQ}{h}\frac{(\cos^2\theta - 1)}{2} \qquad (1)$$

$$= \frac{3}{4}\frac{e^2qQ}{h} \quad ; \quad \text{for } \theta = 90^\circ,$$

where θ is the angle between the magnetic field, B_o, and the principal axis of the electric field gradient tensor (usually along the C-D bond direction). The quadrupole coupling constant of $(CD_3)_2SO$, e^2qQ/h, has been determined experimentally[83] to be 162 kHz. Due to the fast C_3 rotation of the methyl group, it is necessary to take the average over all directions of the C-D bond axis (Fig. II-25). In the case of sp^3 bonds, the asymmetry parameter is assumed to be zero, and the motionally averaged splitting is then given by

$$\Delta\nu_{Q_1} = \Delta\nu_Q\left(\frac{3\cos^2\beta - 1}{2}\right) \qquad (2)$$

where $\beta = 109°28'$ for a tetrahedral geometry of the methyl groups. The full rigid-lattice breadth of the deuterium n.m.r. spectrum would be reduced by the factor, $(3\cos^2 109°28' - 1)/2$, to give a splitting of 40.5 kHz.

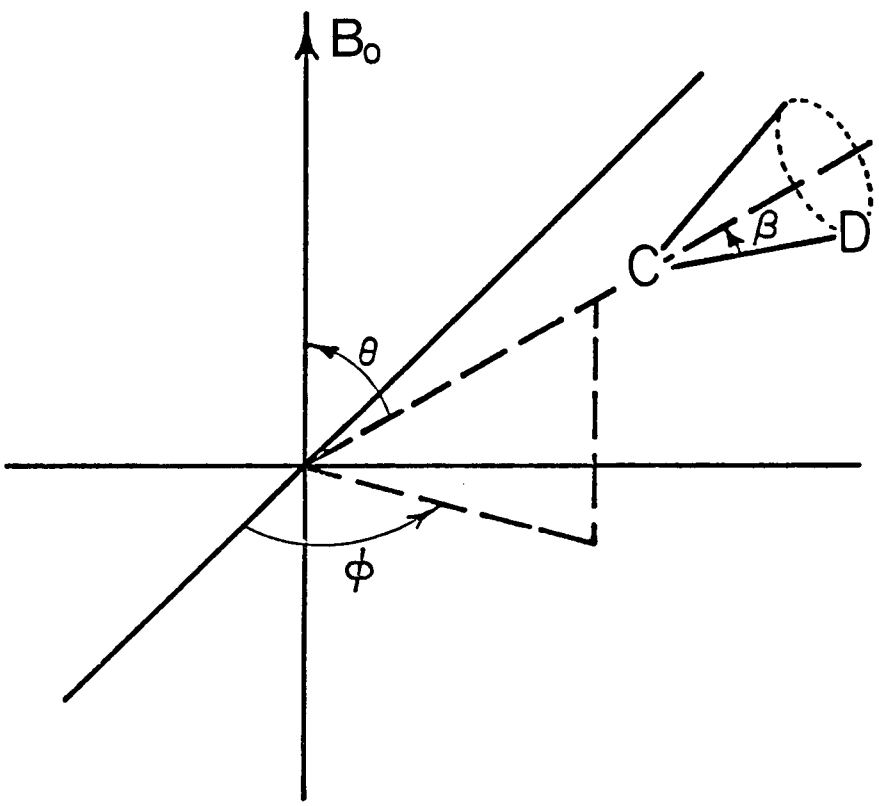

Fig. II-25. Illustration of an isolated methyl-d_3 group oriented with its C_3 axis inclined at the polar coordinates (θ,ϕ) with respect to the laboratory frame.

The deuterium n.m.r. spectra (see Figs. II-26 and II-27) of the β-CD-DMSO-d_6-H_2O complex [26] indicated that the molecular motion is not strictly confined to the methyl

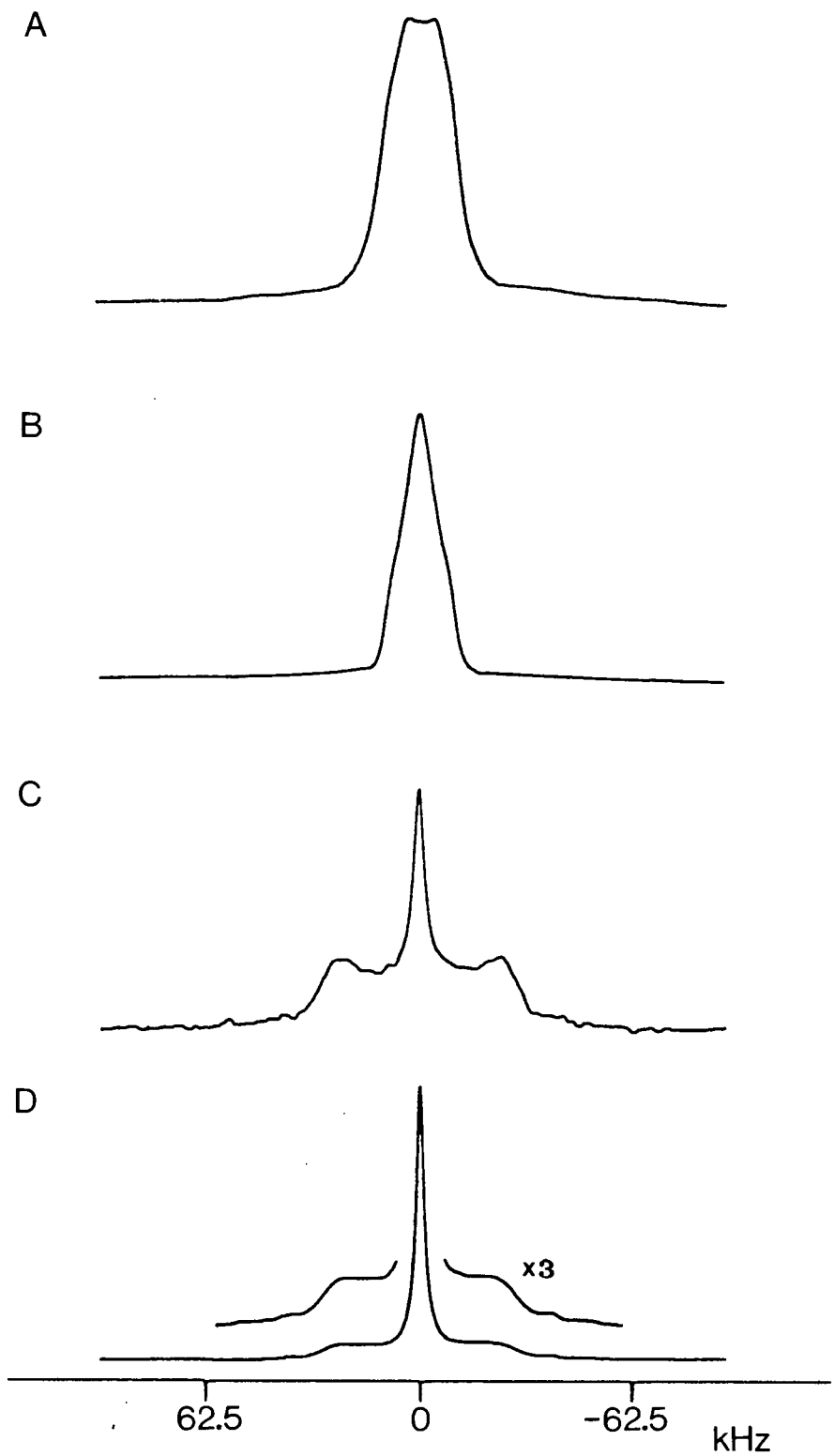

Fig. II-26. ^{2}H-N.m.r. spectra of (A) $(CD_3)_2SO$ in [26]; (B) $(CD_3)_2CO$ in [27]; (C) $(CD_3)_2SO$ in [28]; (D) $(CD_3)_2CO$ in [29]; (measured at 20°C).

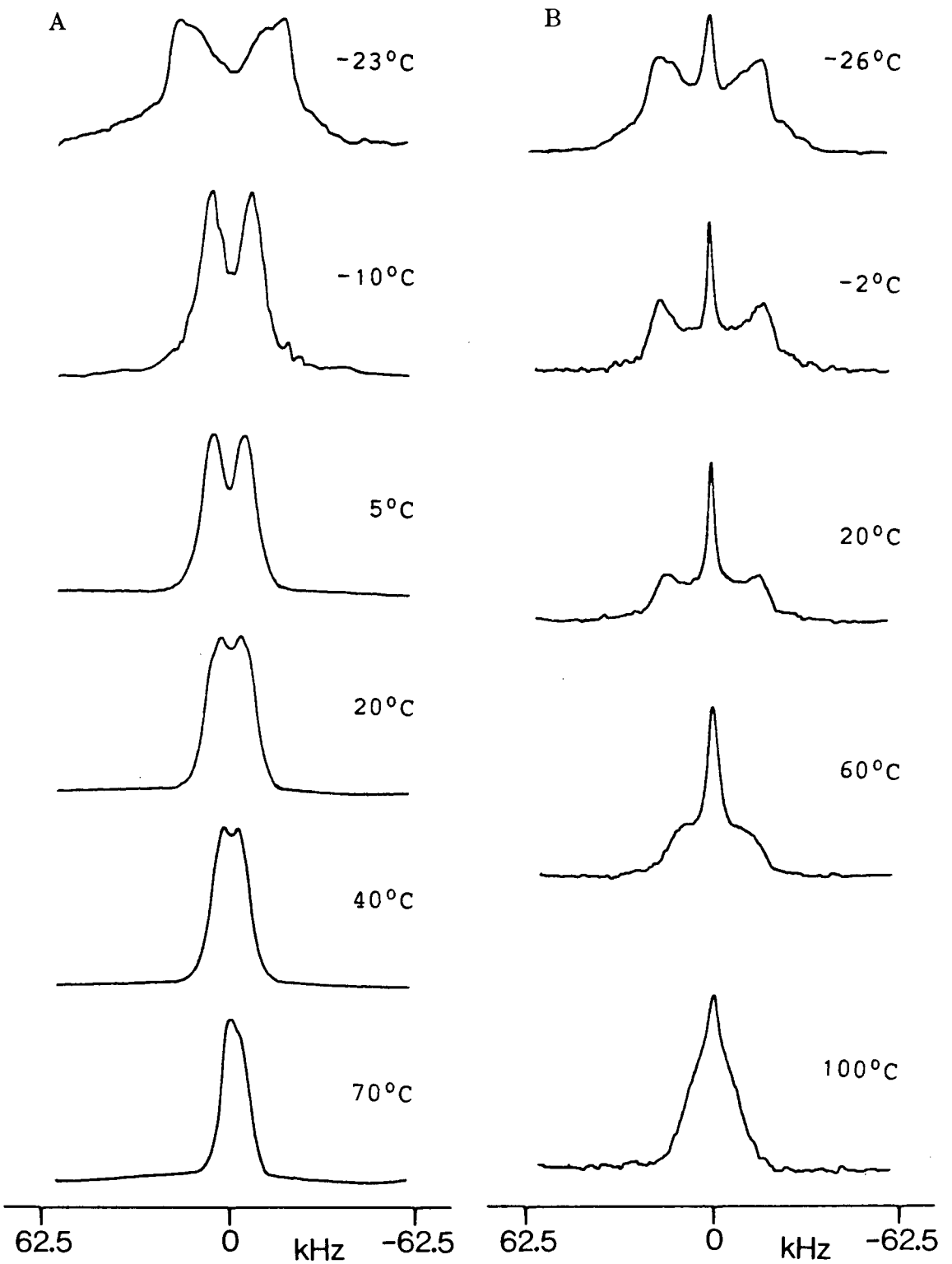

Fig. II-27. ^{2}H-N.m.r. spectra of $(CD_3)_2SO$ in (A) [26] and (B) [28] recorded at the temperatures indicated.

groups. Thus, to account for the small splittings (10 kHz) observed above ambient temperature, the molecule must experience additional anisotropic motion which is fast on the n.m.r. timescale. A possible rotation of the molecule about the axis through the sulfur and oxygen atoms would further reduce the splitting by a factor of $(3\cos^2 107^\circ - 1)/2$, to afford a 13.8 kHz splitting, in not unreasonable agreement with the experimental value. Molecular reorientation about the second axis is reduced or "frozen", with decrease in temperatures; thus, a 38.8 kHz splitting was observed at -23°C, corresponding to a pure C_3 rotation.

The success of this simple model, prompted us to examine the complex [27] of acetone-d_6 with β-cyclodextrin. The observed splitting at 20°C is <5 kHz. Although the acetone molecule is of planar symmetry, rotation about the carbonyl bond would reduce the splitting by $(3\cos^2 123^\circ - 1)/2$, to give a separation of 4.6 kHz. Fast rotation about an axis perpendicular to the plane of the acetone molecule seems unlikely since it would lead to a substantially larger splitting (20 kHz) than that observed experimentally. Thus, these results suggest that both guest molecules behave similarly within the annulus of β-cyclodextrin.

Comparison with the analogous α-cyclodextrin complexes enables an evaluation to be made of the effects of ring-size. The quadrupole splitting for $(CD_3)_2SO$ in the α-CD complex [29] at 20°C is larger (40 kHz) than that of the β-

CD complex (10 kHz), which suggests a substantially tighter fit within the smaller annular space of the former. A further important difference is the presence of a small, sharp isotropic peak, which is indicative of "free" $(CD_3)_2SO$ molecules. Heating the sample to higher temperatures, increased the intensity of the isotropic peak and, concomitantly, decreased the breadth of the large splitting. Furthermore, the former could not be removed even by careful washing of the crystals with cold methanol. The *a*-cyclodextrin complex of acetone [30] also revealed two kinds of guest molecules within the crystal lattice, although in this case the isotropic peak was more intense than that of complex [29]. It is of interest to note that when these complexes were crystallized from methanol/water solution, no significant changes of their lineshapes were observed. Presumably, the methanol and/or water molecules present in the crystal lattice have no substantial influence on the molecular reorientation of the guest molecules.

It has been shown by proton n.m.r.[84] that benzene molecules undergo thermally activated reorientation about their C_6 axis in the solid state; however, the detailed mechanism of the process is still not fully understood. The temperature dependence of the quadrupole splitting of polycrystalline benzene has been reported,[78] and the values of the quadrupole coupling constant are in the range of 177 to 193 kHz. The lineshape can be calculated by transforming

the e.f.g. tensor from the static molecular frame principal axis system to a reference frame rotating about the appropriate fixed axis with a unitary matrix expressed in terms of the Euler angles. Without going into the mathematics of transformation from one coordinate system to another, a qualitative treatment of the effect of molecular reorientation on the powder spectrum governed by e.f.g. tensors is illustrated. For the particular case considered here, the principal elements of the e.f.g. tensor are related to the molecular frame in which the principal axis V_{zz}, lies approximately along the C-D bond. Hence, V_{yy} will either be along or perpendicular to C_6 and $V_{zz}^{(R)}$, which are colinear for rapid reorientation. This can be verified by examining the effect of molecular rotation on the spectrum, using the expressions derived for the chemical shift tensors.[85] The averaged e.f.g. tensor will be axially symmetric with respect to the C_6 axis:

$$V_{xx}^{(R)} = V_{yy}^{(R)} = 1/2(1 - \cos^2\alpha\sin^2\beta)V_{xx} + 1/2(1 - \sin^2\alpha\sin^2\beta)V_{yy} + 1/2\sin^2\beta V_{zz}$$

$$V_{zz}^{(R)} = \sin^2\beta\cos^2\alpha V_{xx} + \sin^2\beta\sin^2\alpha V_{yy} + \cos^2\beta V_{zz} \quad (3)$$

where the Euler angles (α,β) relate the effective axially symmetric tensor to the original tensor. For V_{yy} lying along the rotation axis ($\alpha = 90^\circ$ and $\beta = 90^\circ$), the

principal elements are represented by[86]

$$V_{xx}^{(R)} = V_{yy}^{(R)} = 1/2(V_{xx} + V_{zz}) = -1/2(V_{yy})$$

and (4)

$$V_{zz}^{(R)} = V_{yy} = -1/2(1 + \eta)V_{zz}$$

Therefore, the frequencies for spectral discontinuities are given by

$$\nu_1 = \nu_2 = \pm V_{xx}^{(R)} = \pm V_{yy}^{(R)} = \pm \frac{3}{16} \frac{e^2qQ}{h} (1 + \eta) \quad (5)$$

$$\nu_3 = \pm V_{zz}^{(R)} = \pm \frac{3}{8} \frac{e^2qQ}{h} (1 + \eta)$$

where

$$V_{zz} = \frac{3}{4} \frac{e^2qQ}{h}$$

In the case of V_{yy} lying perpendicular to the rotation axis ($\alpha = 0^\circ$ and $\beta = 90^\circ$), the frequencies are given by

$$\nu_1 = \nu_2 = \pm V_{xx}^{(R)} = \pm V_{yy}^{(R)} = \pm \frac{3}{16} \frac{e^2qQ}{h} (1 - \eta) \quad (6)$$

$$\nu_3 = \pm V_{zz}^{(R)} = \pm \frac{3}{8} \frac{e^2qQ}{h} (1 - \eta)$$

Hence, by measuring the splitting $\Delta\nu_{Q,}$ in the rotationally

averaged spectrum, the correct assignment can be made.

The quadrupole coupling constants previously measured for benzene were 190 ± 3 kHz from polycrystalline n.m.r. and 186 ± 1.6 kHz from single crystal n.m.r.,[87] but the asymmetry parameter was not determined in either case. Barnes and Bloom[88] have obtained the values e^2qQ/h = 180 ± 1.5 kHz and η = 0.041 ± 0.007 at -196°C; the former was found to be independent of temperature between the range of -123 to -23°C. This can also be seen from the quadrupole splittings (refer to Fig. II-28) obtained in this study. By substituting the averaged value of $\Delta\nu_{Q_1}$ = 70.10 ± 1.0 kHz and η = 0.041 ± 0.007 into the Eqs. (5) and (6), the respective e^2qQ/h values are 179.6 ± 2.8 and 194.9 ± 2.8 kHz. Thus, the appropriate assignment should place V_{yy} along the rotation axis as shown on Pg. 155.

The molecular motion of apolar, aromatic molecules within the inclusion channel of cyclodextrin have been discussed earlier in our ^{13}C-c.p.-m.a.s. studies. Recently, Inoue et al.[89] reported similar studies on complexes of α- and β-cyclodextrins with polar, aromatic molecules. Continuation of the work using the deuterium n.m.r. method provides a better understanding of the types of motion executed by the guest molecule. Full analysis of the experimental lineshapes using (a) planar Brownian diffusion[90] and (b) discrete jumps between three equivalent sites[90,91] (symmetric jumps about a diffusion axis of

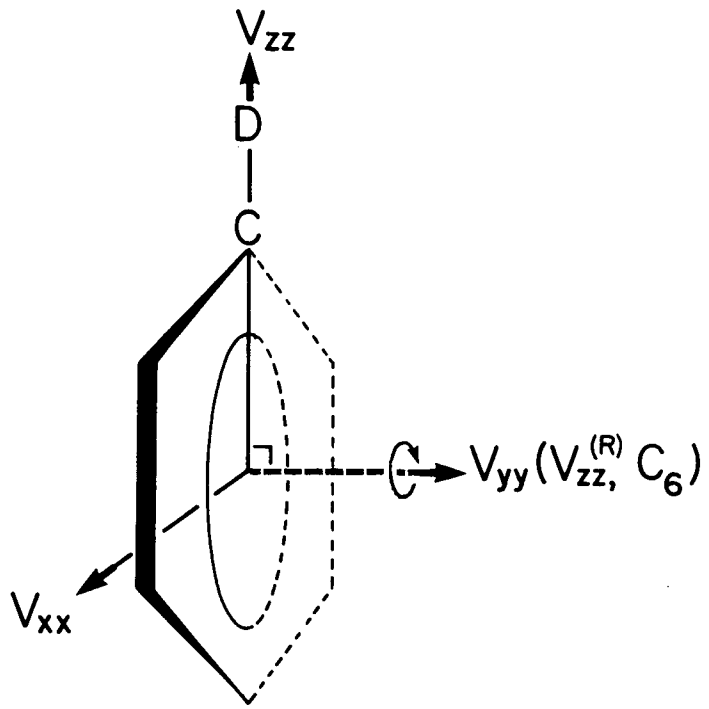

symmetry C_{3v}) models has been presented in the literature. However, it was decided in this study not to simulate the lineshapes based on the above possible models to illustrate the various dynamic modes experienced by the benzene and other aromatic molecules.

The ^2H quadrupole splittings of benzene-d_6 sequestered in the host molecules [3] and [4], clearly illustrate the influence of cavity size on its mobility. The values measured at 20°C for complexes [5] and [23] are 48 and 68.5 kHz, respectively (Figs. II-28 and II-29). For a rigidly bound benzene molecule, a splitting of 141 kHz would be expected; rapid rotation of the benzene about its C_6 axis ($>10^8$ s^{-1}) within the cavity would give an observed splitting of 70 kHz, and about a C_2 axis, a 15 kHz

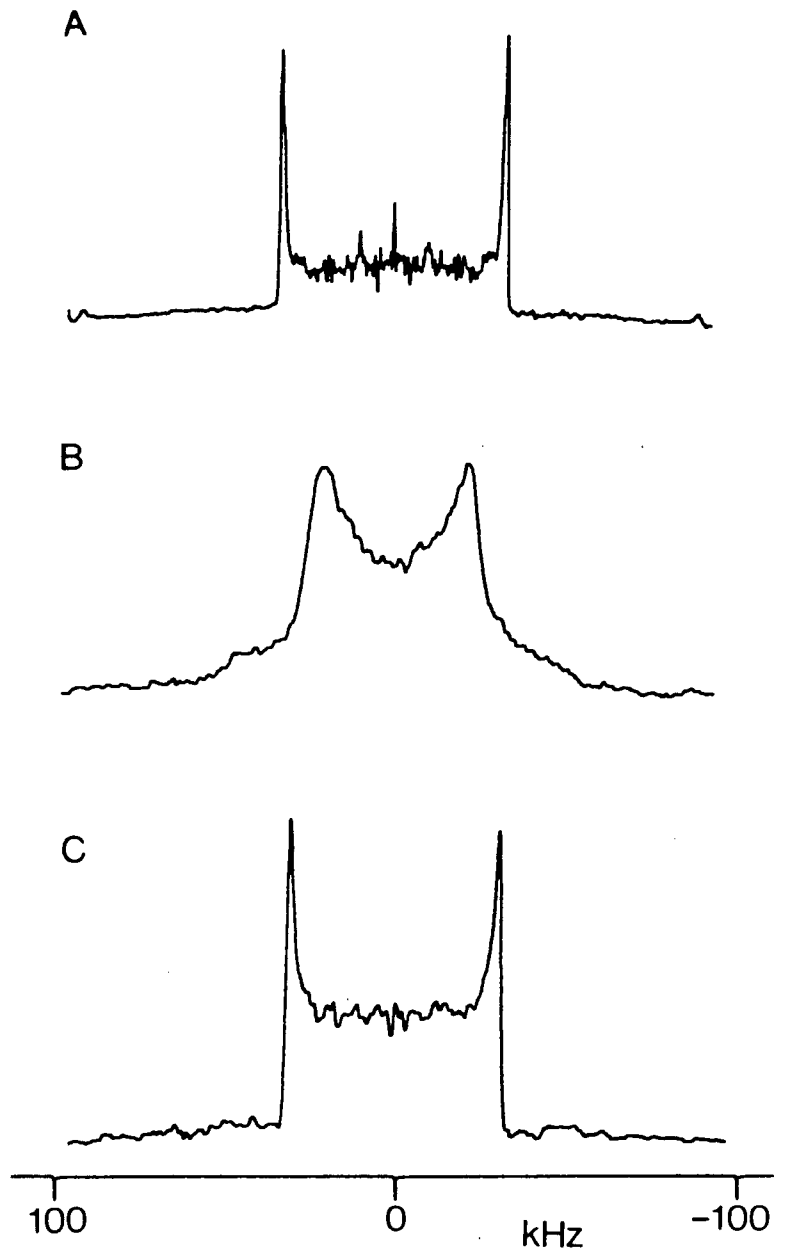

Fig. II-28. ^{2}H-N.m.r. spectra of (A) frozen C_6D_6; (B) C_6D_6 in [5]; (C) C_6D_6 in [23]; {(A) and (B), measured at 20°C}.

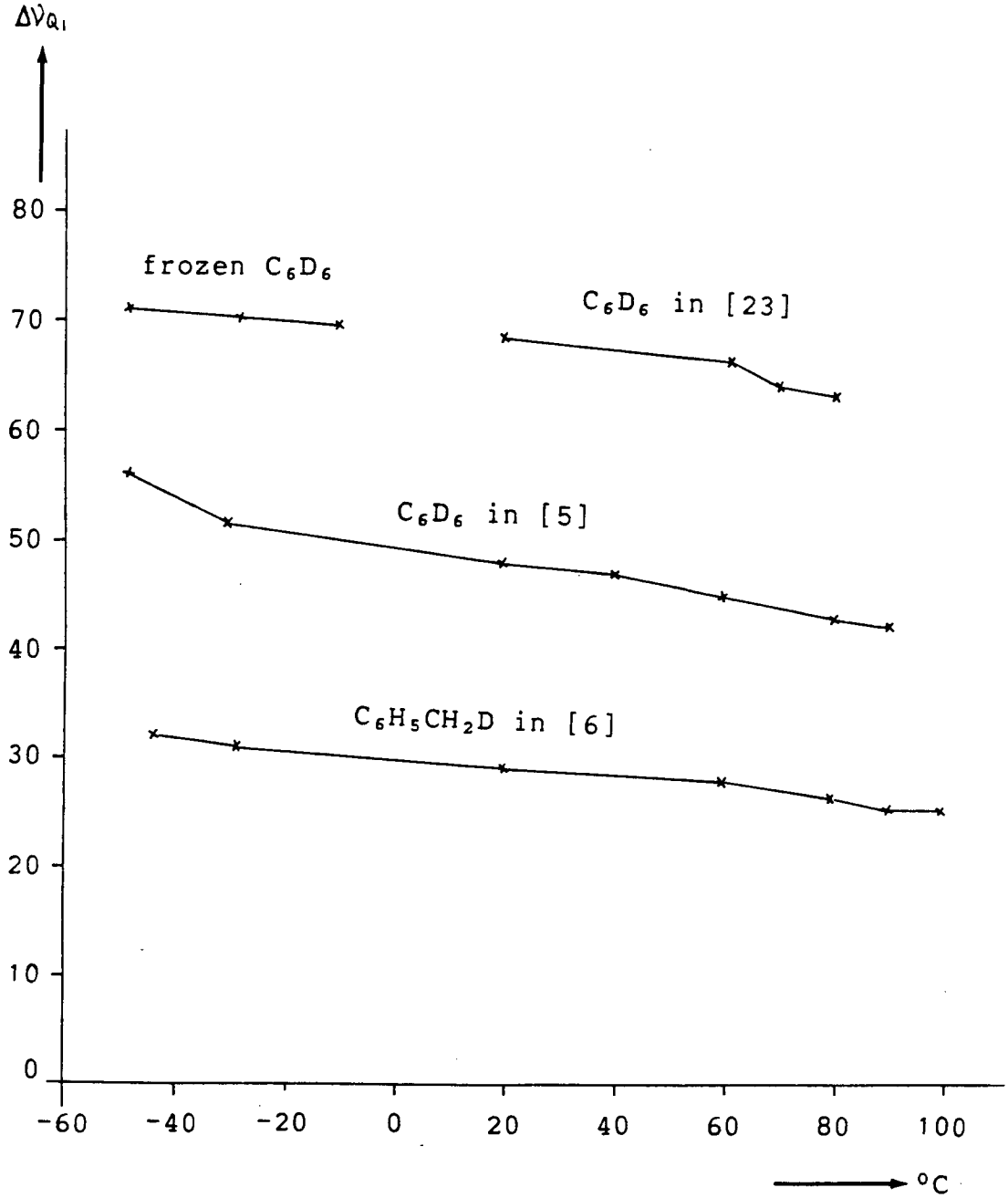

Fig. II-29. Variation of $\Delta\nu_{Q_1}$ with temperature for C_6D_6 in [5] and [23], and $C_6D_5CH_2D$ in [6].

splitting. From these values, it is clear that rapid rotation occurs principally about the C_6 axis; an additional angular fluctuation of the axis would account for the smaller value observed experimentally for complex [5]. Interestingly, it is possible to freeze out this angular fluctuation by decreasing the temperature of sample [5], as indicated by the larger quadrupole splitting values obtained at lower temperatures (Fig. II-30). Furthermore, the molecular motion can also be perturbed further by raising the temperature up to a limit of 90°C. Above this temperature, steady "distillation" of benzene from the annulus makes it difficult to obtain a spectrum. When the experiment is performed in a sealed tube, the free benzene appears as a single peak centered at the Larmor frequency, and a thermal equilibrium exists between the guest and the host.

The axially symmetric powder spectra[81] observed suggest, at least for higher temperatures, that the benzene molecule may also reorient about a second diffusion axis perpendicular to the rapidly rotating C_6 axis. Since the benzene ring assumes an upright position within the inclusion channel, both the channel and the second diffusion axes are likely to be colinear. As a consequence of motional averaging along this axis, the quadrupole splitting observed for the pure C_6 rotation would be further reduced by a geometric factor of $(3\cos^2 90^\circ - 1)/2$, to afford a value of 35.1 kHz. In the case of β-

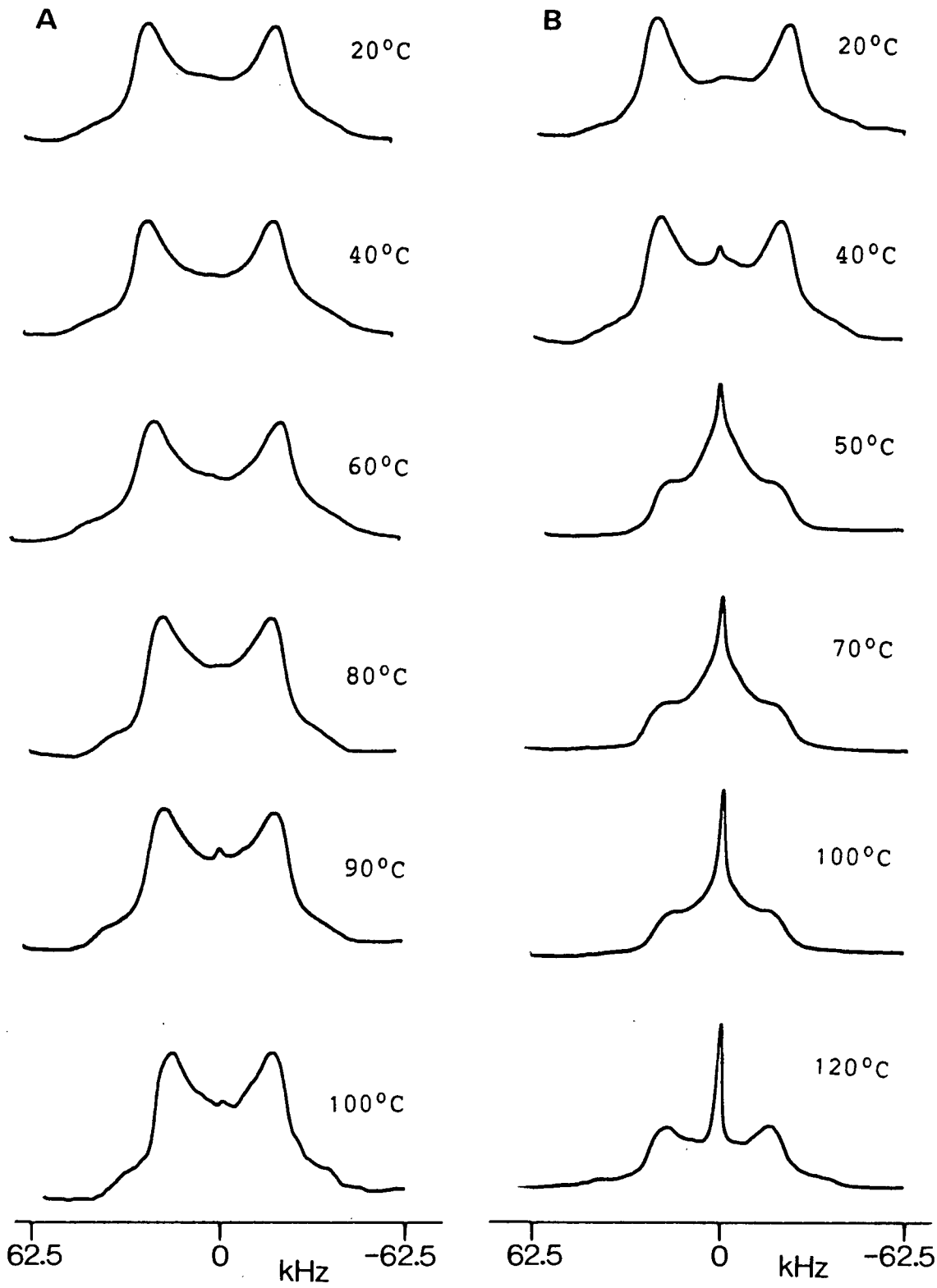

Fig. II-30. ^{2}H-N.m.r. spectra of C_6D_6 in [5]: (A) in unsealed and (B) in sealed tubes, recorded at the temperatures indicated.

cyclodextrin peracetate complex [23], the mobility of the guest molecule is restricted by the cavity size to rotation about its C_6 axis, even at higher temperatures.

A similar differential was found for α-d_1-toluene, $C_6H_5CH_2D$, sequestered in the same two host molecules [3] and [4]. The observed splittings measured at 20°C (Fig. II-31) are 29 and 40 kHz, respectively. The latter value is close to that (45 kHz) expected[88] for fast rotation of a methyl group about its C_3 axis. Additional fast motion about the long molecular axis in which the aromatic ring undergoes molecular reorientation, may be the source of the small additional reduction observed. That same motion would also explain the results described earlier from the dipolar dephasing ^{13}C spectrum of [6]. It should be noted[92] that reorientation of toluene precisely about its long axis would not further alter the powder pattern of the methyl group because the reduction factor corresponding to $(3\cos^2 0^\circ - 1)/2$ is unity. Presumably, the fast motion occurs about an axis, z', which is tilted slightly away from the long molecular axis (Fig. II-32). On heating the sample above ambient temperature, the toluene gradually distilled off and this was accompanied by a decreased quadrupole splitting; a reduction in splitting was not obvious for β-cyclodextrin peracetate complex [24].

Intuitively, it seemed reasonable to expect an increase in motion with increase in distance of the pendant group from the annulus, due to decreased energy barriers to

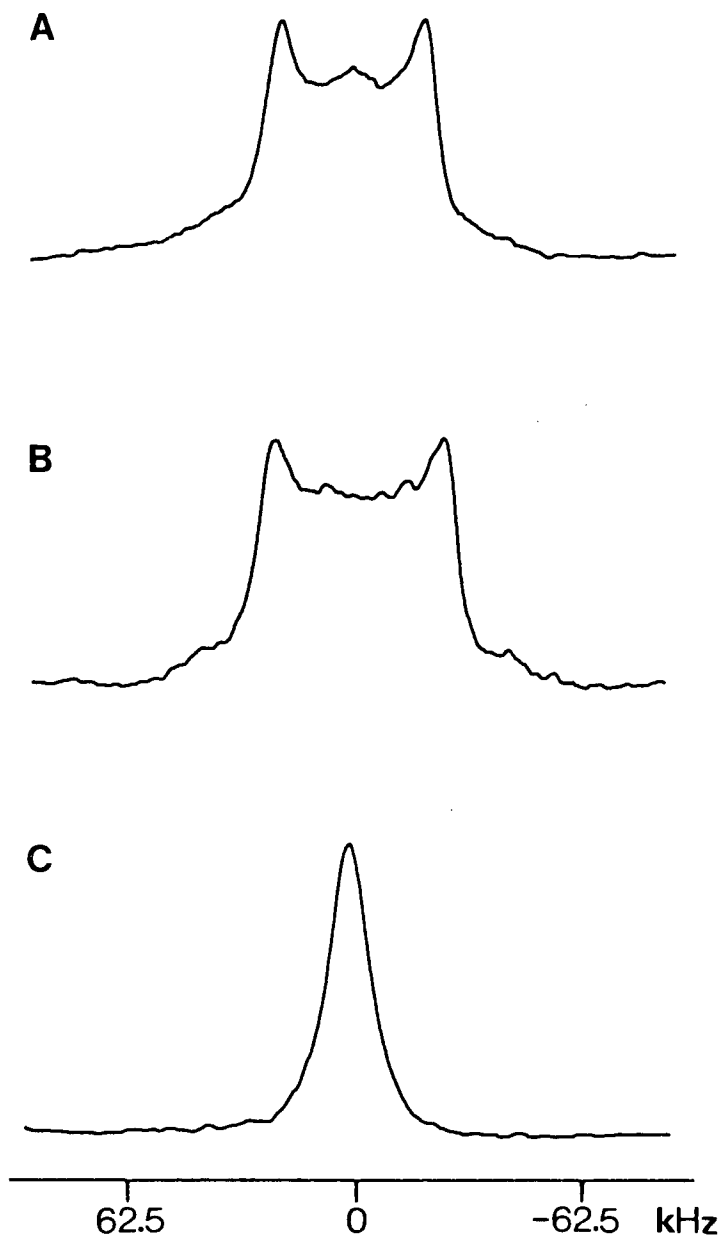

Fig. II-31. ^{2}H-N.m.r. spectra of (A) $C_6H_5CH_2D$ in [6]; (B) $C_6H_5CH_2D$ in [24]; (C) $C_6H_5CH_2CH_2D$ in [7]; (measured at 20°C).

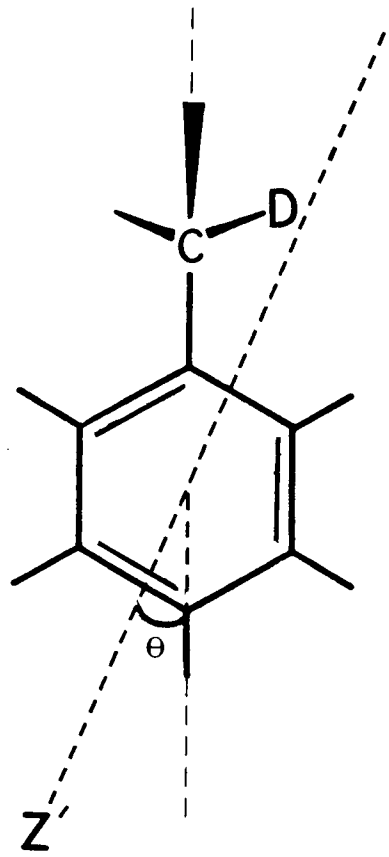

Fig. II-32. Molecular reorientation of toluene along the z'-axis.

aliphatic conformational changes. This is nicely illustrated by the decrease in the magnitude of the quadrupole splitting at 20°C in going from the 2,6-di-O-Me-β-CD complex of $C_6H_5CH_2D$ (29 kHz), to that of $C_6H_5CH_2CH_2D$ (<5 kHz) (Fig. II-33). For fast motion about the long molecular axis, the quadrupole splitting of the methyl group would be reduced by a further factor of $(3\cos^2 109.5^\circ - 1)/2$, to give a value of about 15 kHz. The sharp, isotropic-like, peak observed at ambient temperature for complex [7] suggests that the aromatic ring of

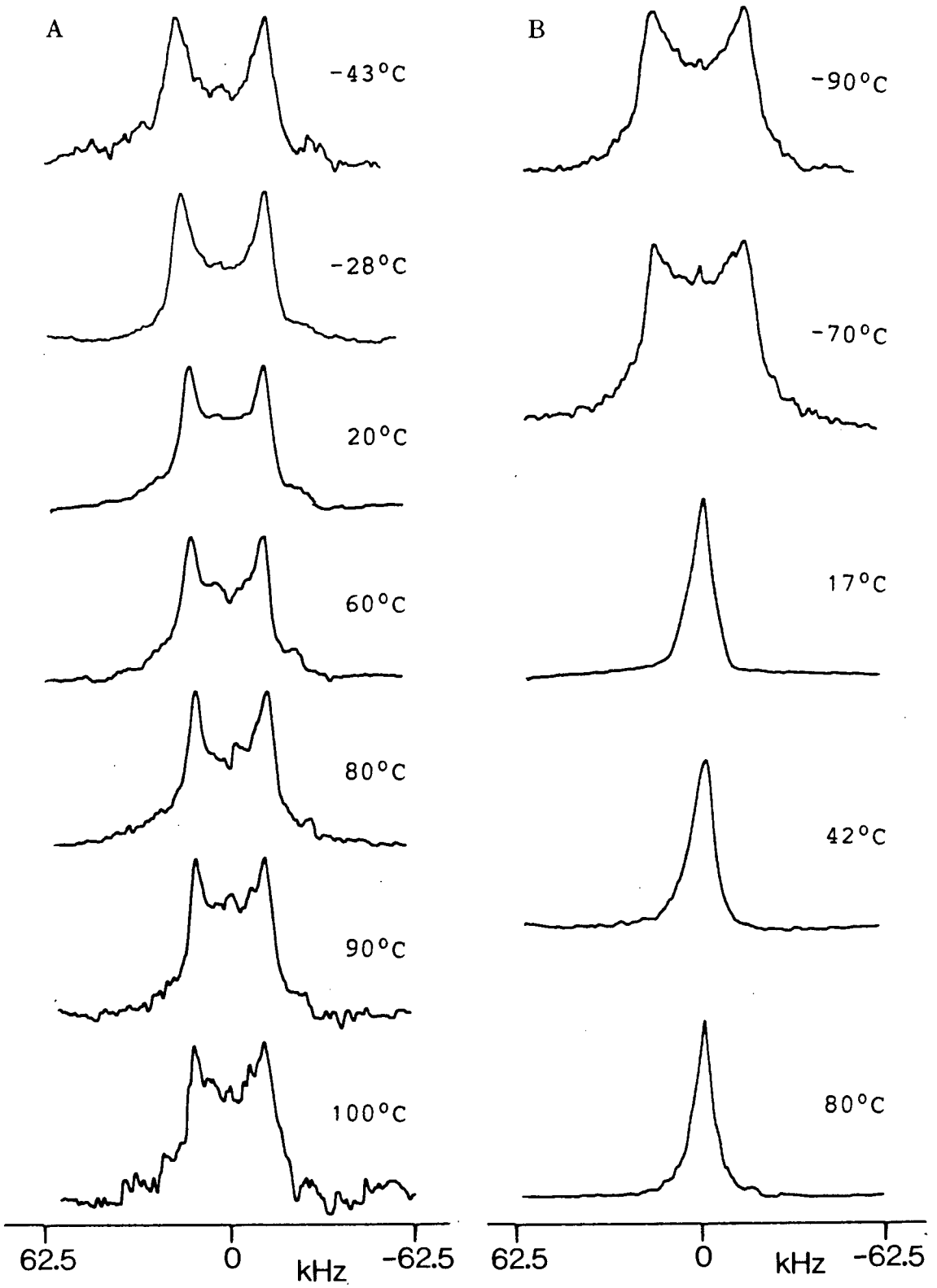

Fig. II-33. ^{2}H-N.m.r. spectra of (A) $C_6H_5CH_2D$ in [6] and (B) $C_6H_5CH_2CH_2D$ in [7] recorded at the temperatures indicated.

ethylbenzene also reorients about a similar axis as toluene. On cooling the sample to -90°C, the observed splitting of complex [7] increased to 37 kHz. This observation indicates that the molecular motion is almost completely confined to the methyl group, with some additional motion of the aliphatic chain being responsible for the slight reduction of the quadrupole splitting from the 44 kHz value expected for a pure methyl rotation.[88]

Dianin's Inclusion Complexes

II.7. Introduction

Dianin's compound [30], which is a nonsugar host molecule, was included in this chapter so that some comparison can be made with the cyclodextrins. It forms crystalline inclusion complexes with a large variety of liquid guest molecules. So, it is rather difficult to find a suitable noncomplexing solvent to dissolve the desired solid substrate which is to be included. Encaged guest molecules such as argon, sulfur dioxide, ammonia, benzene, decalin, and di-tert.-butylnitroxide have been reported.[93] The structure of this host molecule was unambiguously established by Baker et al.[94] in the mid-fifties. A decade and a half later, detailed X-ray studies[95] confirmed the true cage structure for the chloroform, ethanol and 1-heptanol complexes, and for the unsolvated crystal.

As distinct from cyclodextrins where inclusion complexes and the free host have different crystal

structures, the structures of the complexes of Dianin's compound are independent of the encaged organic guests. They belong to space group $\bar{R}3$, with 18 molecules per unit cell.[93]

Six host molecules of compound [30], 4-p-hydroxyphenyl-2,2,4-trimethylchroman, are required to make up the hourglass-shaped cage; the ends of each cage are formed by their hydrogen-bonded hydroxyl groups, with alternate host molecules pointing up and down with respect to the plane of the hexagonal OH ring (Fig. II-34; A and B). The constriction at the middle is formed by six inward-pointing methyl groups, one from each of the six host molecules. For smaller guest substrates such as ethanol or acetone, two molecules are held in the wider parts of the cage, while for larger guests such as benzene, toluene, or p-xylene the cage is singly occupied.

Like the cyclodextrins, the cavity size of this host molecule can be altered. Removal of the protruding methyl groups (Fig. II-34C) could bring about a marked change to the cavity, in which the waist would be completely eliminated. It has been shown[96] that removal of either geminal methyl group of host [30] does not lead to a collapse of the cage structure and, at the same time, the analogues still retain the ability to form inclusion complexes. Hence, it is possible to study the molecular reorientation of a guest molecule within these cavities.

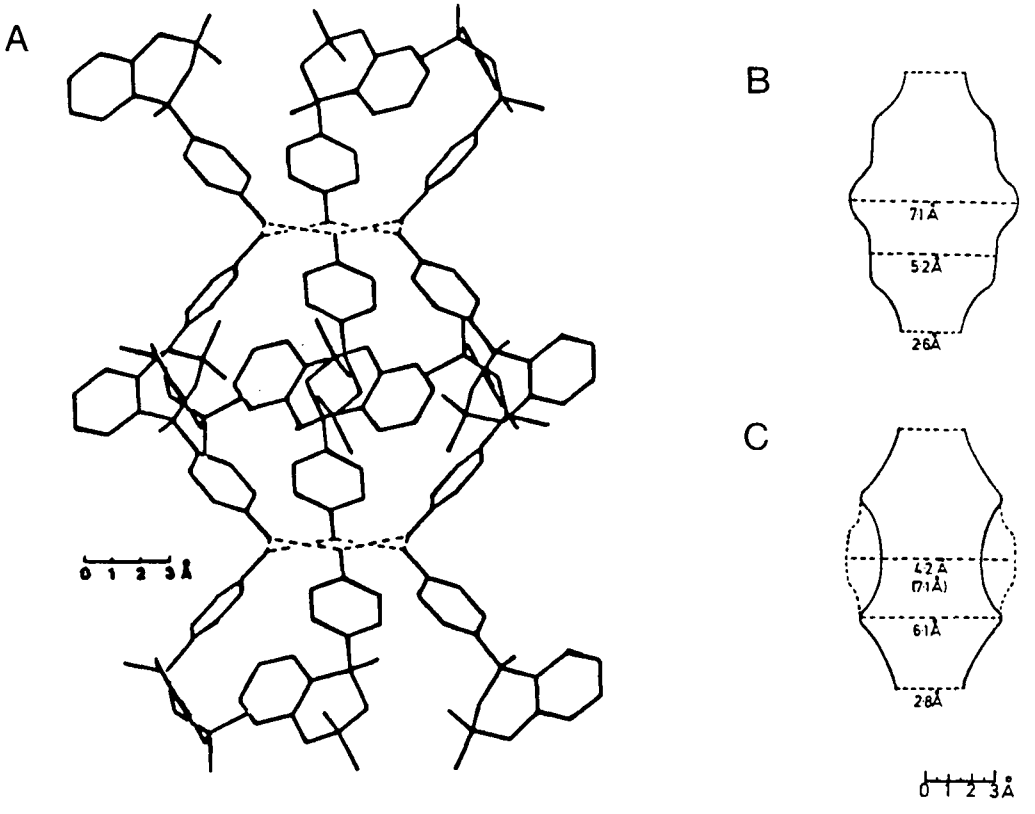

Fig. II-34. The structures of Dianin's compound (A and B) and modified Dianin's compound which lacks the 2-methyl groups trans to the p-hydroxyphenyl substituent (C) (from Ref. [93]).

II.8. Synthesis

In 1914 Dianin[97] discovered that compound [30] could be prepared by condensation of phenol (2 mol) and mesityl oxide (1 mol) as shown below:

$$2C_6H_5OH + (CH_3)_2C{=}CHCOCH_3 \xrightarrow{HCl} \text{[30]}$$

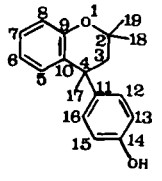

[30]

Subsequently, the formula of this compound was established by Baker and McOmie,[98] who also improved on the synthetic method. The crude product was recrystallized from ethanol which was then removed by vacuum sublimation, to afford the free host material. The inclusion complexes of benzene [31], toluene [32], and p-xylene [33] were prepared by recrystallization of compound [30] from the respective liquid-guest compounds.

II.9. Results and Discussion

Inclusion complexes [31], [32], and [33] were chosen for the study because of their similarity to 2,6-di-O-Me-β-CD inclusion complexes, in which there is one guest molecule per cavity. The solid-state ^{13}C-c.p.-m.a.s. spectra of Dianin's inclusion complexes with nonaromatic guest molecules have been previously reported.[99] Similar results were obtained in this study with aromatic guest molecules, which cause little or no perturbation of the crystal structure of the host (Fig. II-35).

The asymmetric unit in the unit cell is one complete molecule; thus, no more than 18 resolvable resonances are anticipated. It is not surprising that sharp peaks are observed, as the host molecules are merely linked together by hydrogen bonding. This is not true for cyclodextrins where distortion of the glycosidic linkages may cause splittings of the carbon resonances.

According to Ripmeester,[99] partial assignment of the

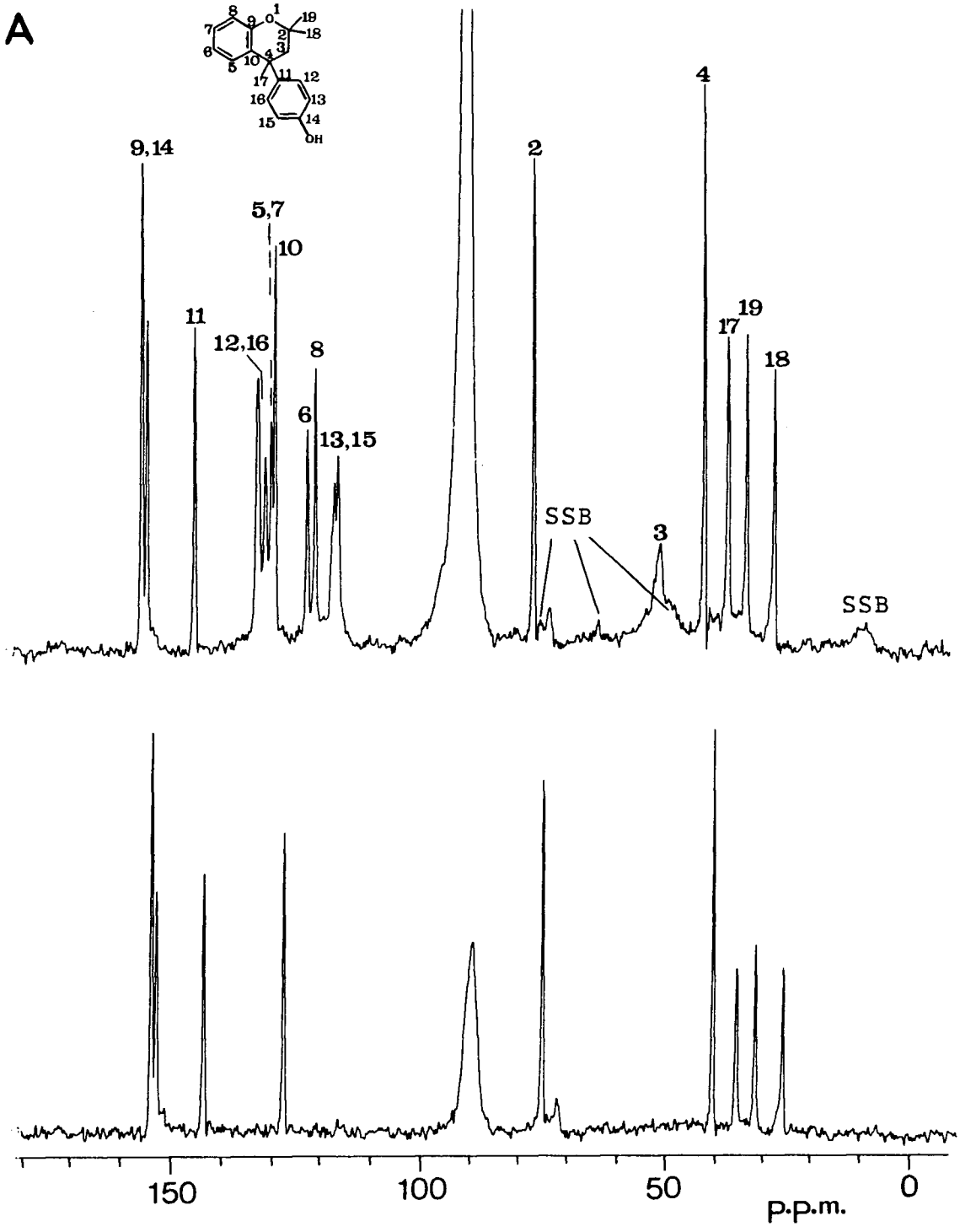

Fig. II-35. ^{13}C-n.m.r. spectra of Dianin's compound and its inclusion complexes, without and with dipolar dephasing (top and bottom spectra, respectively): (A) [30]; (B) [31]; (C) [32]; (D) [33].

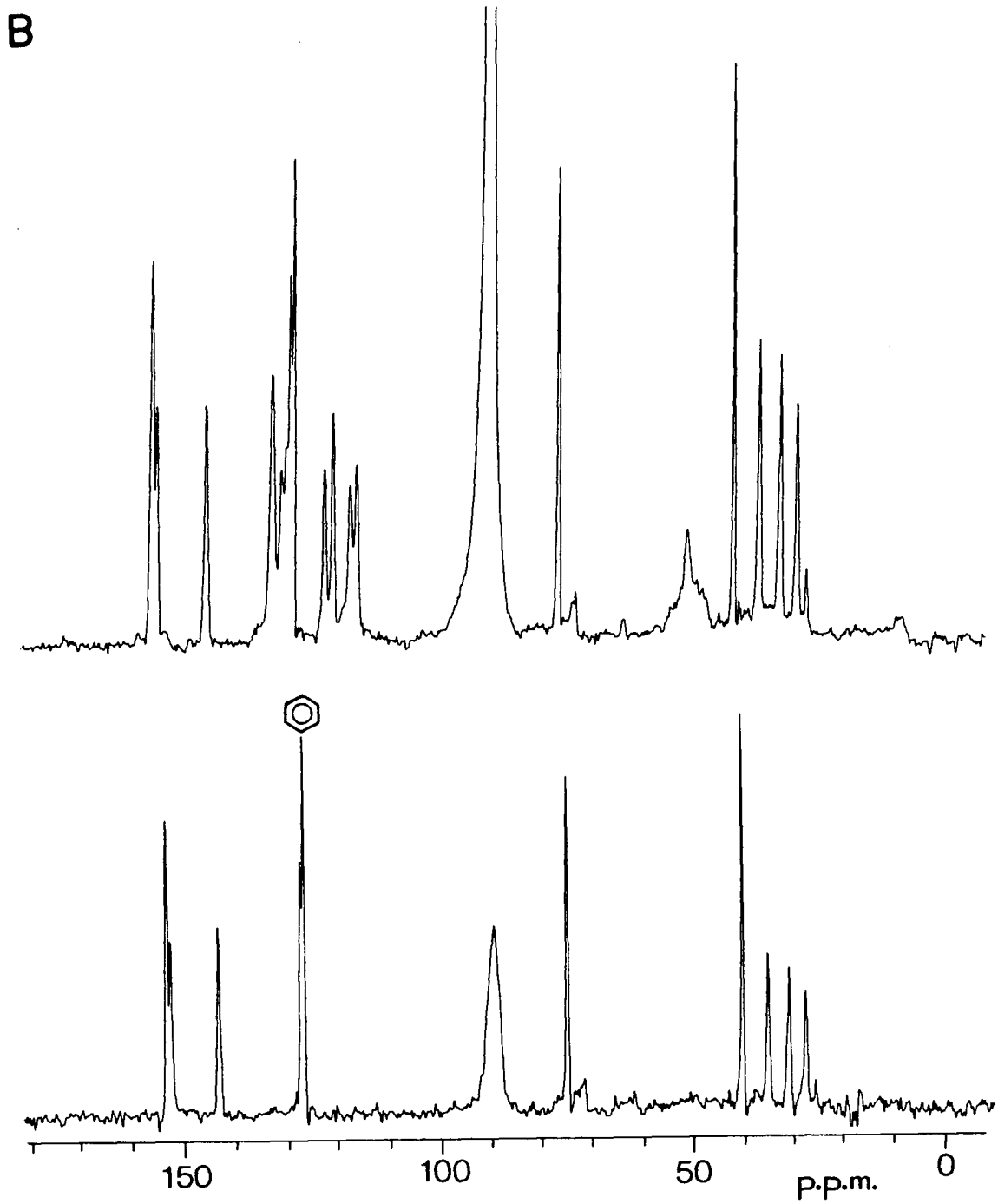

Fig. II-35 cont'd

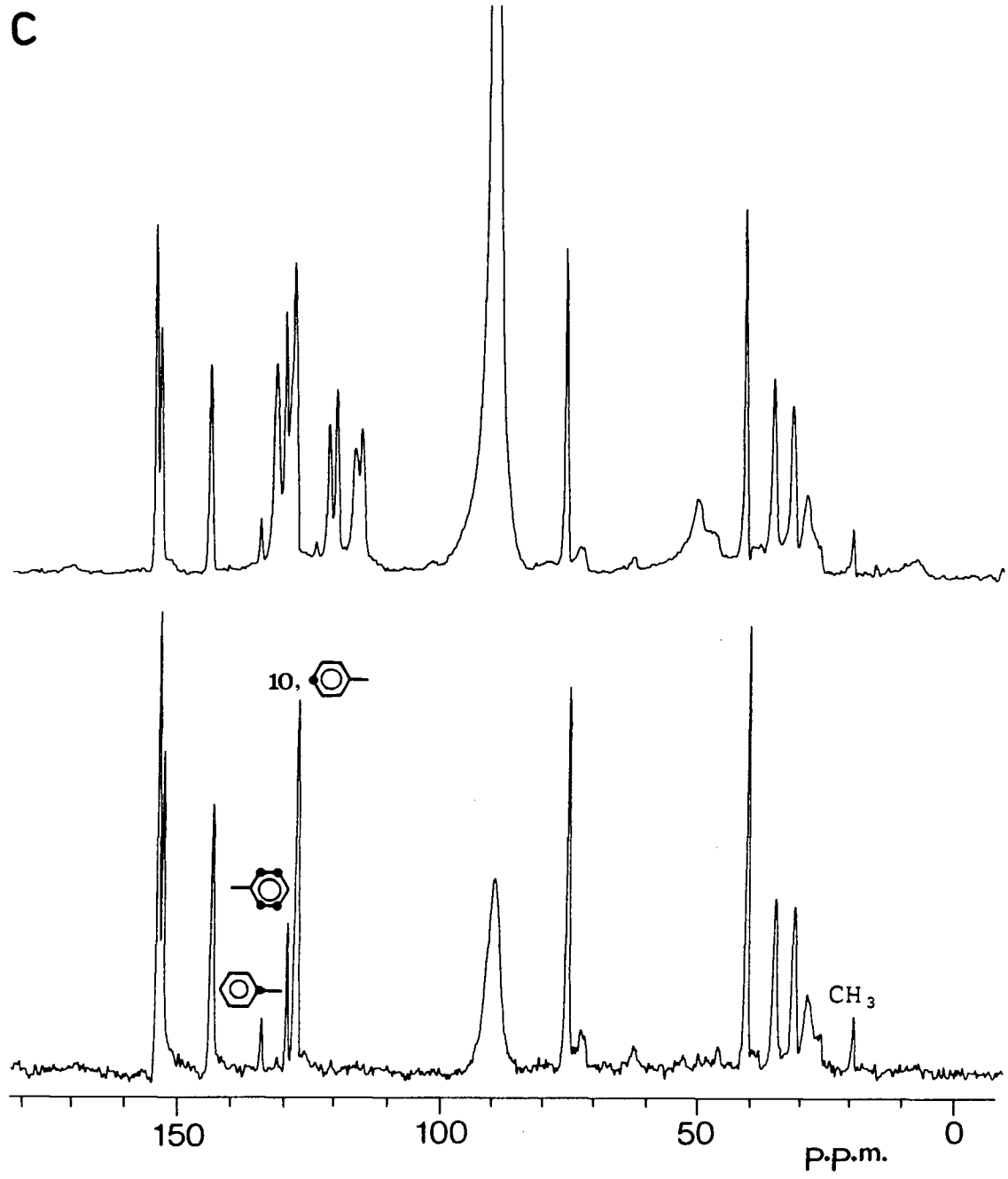

Fig. II-35 cont'd

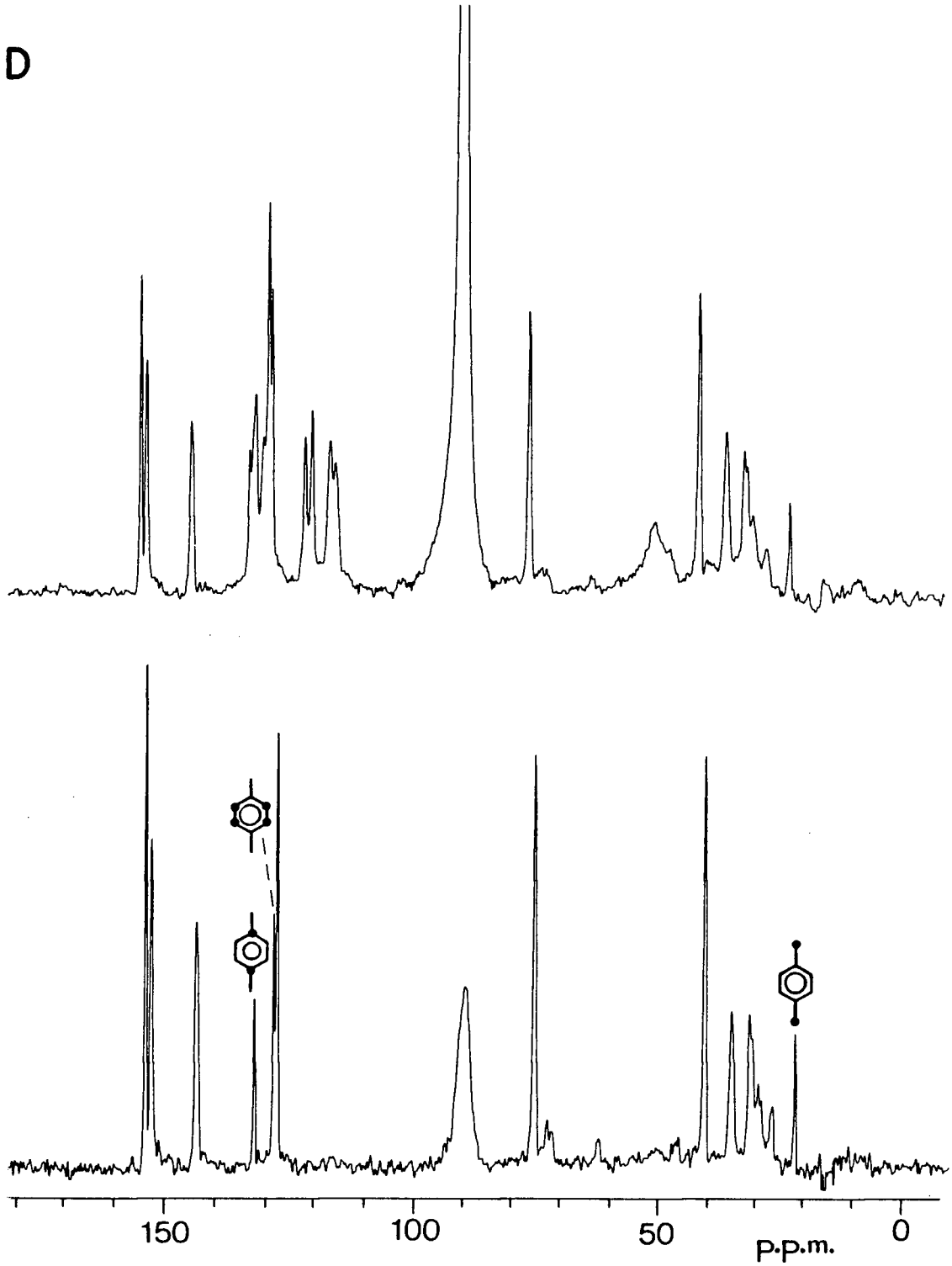

Fig. II-35 cont'd

^{13}C resonances is made possible by the use of the dipolar dephasing technique. The methyl groups (C-17,C-18,C-19) are assigned on the basis of their locations in the crystal lattice. The lowest field methyl carbon resonance can be assigned to C-17, which is situated close to two phenyl rings. Of the two geminal methyl groups, the inward-pointing methyl carbon would be deshielded most by the encaged aromatic substrates. The high field methyl resonance, which is most sensitive to the aromatic π-cloud and ring size, is then assigned to C-18. The remaining eight protonated ring carbons have been assigned[100] by selective deuteration of the molecule (Fig. II-35A).

The spectra of Dianin's complexes reveal a small peak corresponding to C-18 of the free host molecule. Albeit the host to guest ratio is generally 6:1 (i.e., 1 guest molecule per cavity) for larger guest species, a ratio of 7:1 has been reported in the literature for a number of molecules. The method used for the analysis[94] of these three inclusion complexes was by loss in weight on heating, which was found to be less accurate, especially for the borderline cases. Hence, there is a possibility that some cages are completely empty, which would then account for the above observation. This could happen to the analogous cyclodextrin complexes discussed earlier, but the spectra are too complicated to reveal the presence of this phenomenon.

It should be noted that the lineshapes of the geminal

methyl carbons are affected to different extent by the three aromatic guest molecules. The C-18 resonance broadens gradually as the benzene is replaced by toluene, and then by p-xylene. The latter spectrum also shows a slight splitting of the C-19 resonance into a doublet. Therefore, these methyl carbons are most sensitive to changes in local environment.

The ^{13}C resonances of the guest molecules are shifted upfield with respect to their isotropic chemical shift values measured in the "free" state. The aromatic π-cloud of the Dianin's molecules probably generates an area of high electron density in the host cavity and, therefore, imparts a steric compression shift to the guest molecules. This was not seen in the analogous complexes of 2,6-di-O-Me-β-CD, in which the ^{13}C resonances of the guests are not shifted.

The dipolar dephasing spectra of these complexes indicate that the guest molecules are undergoing molecular reorientation within the cavity of the host. A comparison is made, of the molecular motion undertaken by benzene and toluene in the cavities of 2,6-di-O-Me-β-CD and Dianin's compound. Before discussing this study, it would be helpful if the orientations of the guest molecules were known in the latter compounds. Since X-ray data are not available, one has to rely on other related crystal structures to fix the position of the aromatic ring within the cavity. Most likely, the ring would stay in an upright position as shown

in Fig. II-36.

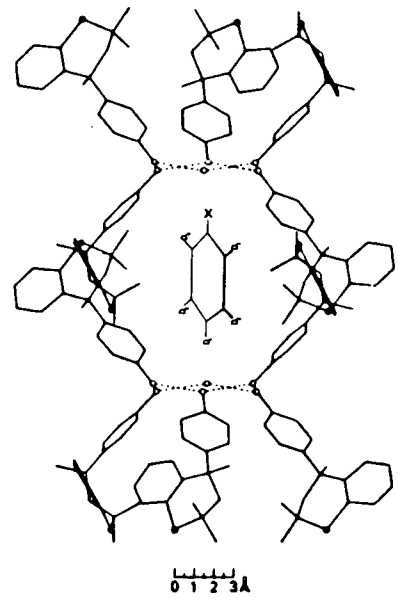

Fig. II-36. Structure of Dianin's compound depicting the orientation of the aromatic guest molecule.

It has been demonstrated earlier that the benzene molecule within the cavity of host [4] is free to rotate about its C_6 axis, with further additional anisotropic motions suggested for inclusion in host [3]. Interestingly, the deuterium n.m.r. spectrum of the Dianin's complex of benzene-d_6 affords a quadrupole splitting of 16 kHz. In this case, the benzene ring would undergo rapid diffusional rotation about its C_2 axis, in which case the C-D bonds would be at 60 ± 1° to the axis of motional averaging. The splitting is then given by (assuming $\eta = 0$)

$$\Delta\nu_{Q_1} = \Delta\nu_Q \frac{(3\cos^2 60^\circ - 1)}{2}$$

which is about 17 kHz. Opella et al.[101] have defined the frequency expressions for the spectral discontinuities to include η (Fig. II-37).

$$\nu_1 = \nu_2 = \pm V_{xx}^{(R)} = \pm V_{yy}^{(R)} = \pm \frac{3}{64} \frac{e^2qQ}{h} (1 - 3\eta)$$

$$\nu_3 = \pm V_{zz}^{(R)} = \pm \frac{3}{32} \frac{e^2qQ}{h} (1 - 3\eta)$$

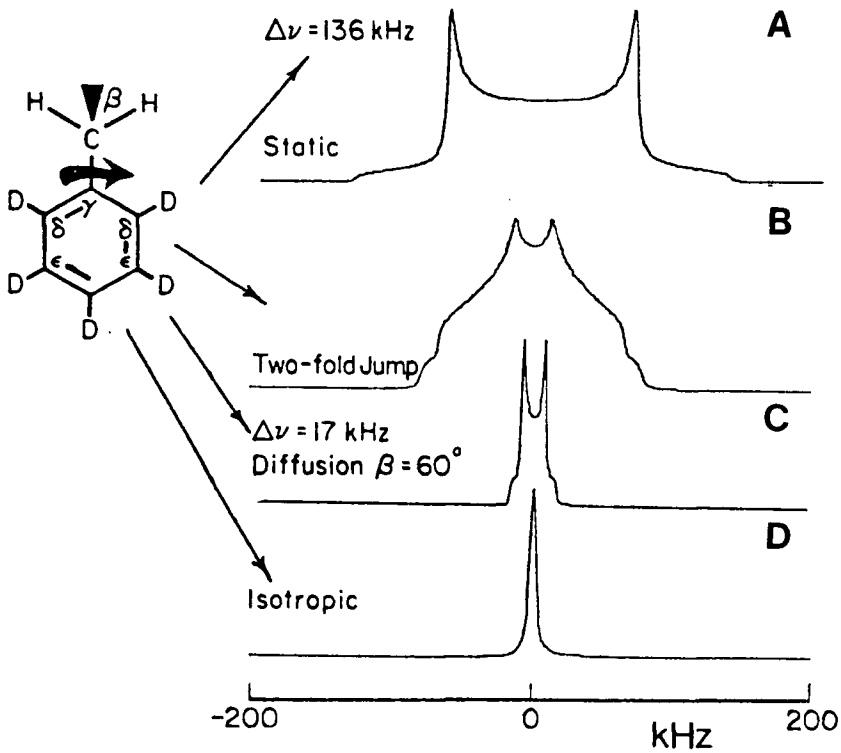

Fig. II-37. Theoretical ^{2}H-N.m.r. spectra of polycrystalline phenylalanine-d_5 where e^2qQ/h = 180 kHz and η = 0.05. (B), powder pattern averaged by fast 180° flips about the C_β-C_γ axis. (C), powder pattern averaged by fast rotation about the C_β-C_γ axis (from Ref. [101]).

Besides the split lineshape, there is also a sharp "isotropic" peak having a width of <2 kHz. This could be due to a residual amount of "free" benzene, which was not

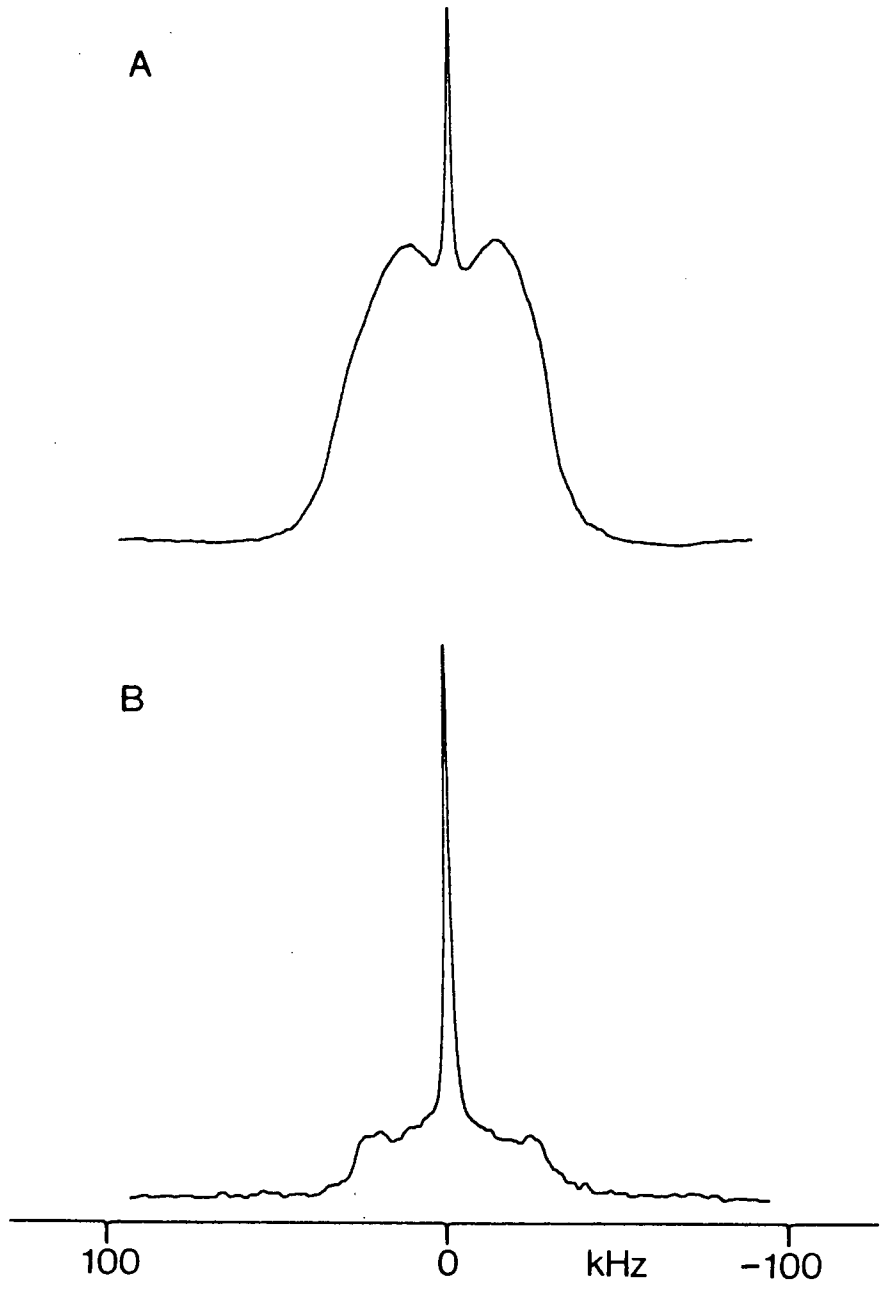

Fig. II-38. ^{2}H-N.m.r. spectra of (A) C_6D_6 in [31]; (B) $C_6H_5CH_2D$ in [32].

removed completely by drying the crystalline sample in vacuo. Since a rapid isotropic motion of benzene would preclude generating its ^{13}C signal in a c.p.-m.a.s. spectrum, it is impossible to verify such a finding by this method.

The deuterium spectrum of the equivalent complex of $C_6H_5CH_2D$ reveals a lineshape of width 35 kHz. It corresponds to fast rotation of the methyl group, with additional fast motion about the long axis. Again, an isotropic peak is present in the spectrum.

II.10. Summary and Conclusions

Cyclodextrins are probably the most important example of compounds that exhibits the "host-guest" relationship. A variety of organic molecules has been used in the synthesis of these complexes with host molecules [3] and [4]. Since crystal structures are not available for either of the two host molecules or for their inclusion complexes, the studies reported here provide new information for these systems as discussed in this chapter. However, the interpretations given here have been facilitated by comparison with the ^{1}H- and ^{13}C-n.m.r. studies of these complexes in solution, and with the X-ray data of the guest molecules themselves and of related guest-host complexes.

It was found that the sugar resonances of cyclodextrins are relatively broad, and are often complicated by the substantial splittings induced by the

presence of the guest molecules. Reciprocal shifts are induced for the guests; those of the smaller guest molecules were found to be least affected by the cavity size of the host molecule [3], and their isotropic chemical shift values are similar to those measured for solutions. Those molecules which undergo anisotropic motion within the cavity, could be detected by the dipolar dephasing technique.

Deuterium quadrupole echo spectroscopy provided direct evidence concerning the molecular motion of the guest molecules and could be interpreted by comparison with results reported in the literature for other systems. The novel aspect of this study is that it draws qualitative conclusions about the anisotropic motional behavior of several guest molecules in the cavities of host cyclodextrins [3] and [4]. It should be noted that interpreting of ^{2}H lineshapes of the guest molecules in some intermediate state of the host/guest environments may, in general, be quite difficult. However, the present study supports previous reports[78,81] that the deuterium quadrupole method can provide useful information pertaining to molecular motion of complex organic systems; this potential is further enhanced by the ease, and low cost with which specific deuteration can be achieved.

As a result of instrumental limitations at U.B.C. during the time of this research, it was not easy to expand this work further to include other interesting inclusion

complexes. Nevertheless, sufficient data of interest have been collected for these cyclodextrins and their inclusion complexes. Since the cavity of host molecule [4] could only trap small aromatic molecules, the number of complexes formed is severely limited. Several potential host molecules (other cyclodextrin derivatives) could have been synthesized whereby the cavity size is changed gradually. For instance, 6-deoxy-β-cyclodextrin may be used to prepare heptakis(6-deoxy-2-O-methyl)-β-cyclodextrin and 6-deoxy-β-cyclodextrin peracetate. Here, the cavities [of the C(6) side] are expected to be larger than those of compounds [3] and [4]. Thus, larger organic molecules, which could not be trapped earlier, would probably find some success with these modified, potential host molecules. The inclusion of data from the resulting complexes would have been a bonus to the discussion on the relationship between motion, structure and stability. Clearly then, cyclodextrins represent carbohydrate systems which can be exciting and valuable to study. It is hoped that more attention will be focussed on the use of modified cyclodextrins in micro-encapsulation of sensitive aromatic substances, pharmaceuticals, herbicides and insecticides.

In conclusion, it is believed that ^{13}C-c.p.-m.a.s. studies have become and will continue to be an integral part of organic n.m.r. spectroscopy.

References

1. A. Villiers, C.R. Acad. Sci., 112, 536(1891).
2. F. Schardinger, Wien. Klin. Wochenschr., 17, 207(1904).
3. F. Schardinger, Zentralbl. Bakteriol. Parasitenkd. Infektionskr. Hyg. II, 29, 188(1911).
4. K. Freudenberg, M. Meyer-Delius, Ber. Dtsch. Chem. Ges., 71, 1596(1938); K. Freudenberg, E. Plankenhorn, H. Knauber, Chem. Ind.(London), 1947, 731; Justus Liebigs, Ann. Chem., 1, 588(1947).
5. R. J. Bergeron, J. Chem. Educ., 54, 204(1977).
6. W. Saenger, Angew. Chem. Int. Ed. Engl., 19, 344(1980).
7. M. L. Bender, M. Komiyama, Cyclodextrin Chemistry, Springer, Berlin, 1978.
8. J. Szejtli, Cyclodextrins and Their Inclusion Complexes, Akademiai Kiado, Budapest, 1982.
9. D. W. Griffiths, M. L. Bender, Adv. Catal., 23, 209(1973).
10. R. K. McMullan, W. Saenger, I. Fayos, D. Mootz, Carbohydr. Res., 31, 211(1973).
11. N. Wiedenhof, Stärke, 21, 163(1969).
12. J. Solms, R. H. Egli, Helv. Chim. Acta, 48, 1225(1965).
13. C. H. Lee, J. Appl. Polym. Sci., 26, 489(1981).
14. J. Boger, R. J. Corcoran, J. M. Lehn, Helv. Chim. Acta, 61, 2190(1978).

15. B. Casu, M. Reggiani, G. G. Gallo, A. Vigevani, Tetrahedron, 24, 803(1968).

16. A. Hybl, R. E. Rundle, D. E. Williams, J. Am. Chem. Soc., 87, 2779(1965).

17. V. S. R. Rao, F. Foster, J. Phys. Chem., 67, 951(1963).

18. B. Casu, M. Reggiani, G. G. Gallo, A. Vigevani, Chem. Soc. Spec. Publ., 23, 217(1968).

19. R. J. Bergeron, M. A. Channning, Bioorg. Chem., 5, 437(1976).

20. R. J. Bergeron, D. M. Pillor, G. Gibeily, W. P. Williams, ibid., 7, 263(1978).

21. P. C. Manor, W. Saenger, J. Am. Chem. Soc., 96, 3630(1974).

22. F. R. Senti, S. R. Erlander, Carbohydrates, Academic Press, New York-London, 1964.

23. S. G. Frank, J. Pharm. Sci., 64, 1585(1975).

24. J. F. Wojcik, R. P. Rohrbach, J. Phys. Chem., 79, 2251(1975).

25. F. Cramer, F. M. Henglein, Angew. Chem., 68, 649(1956).

26. F. Cramer, F. M. Henglein, Chem. Ber., 91, 308(1958).

27. J. Cohen, J. L. Lach, J. Pharm. Sci., 52, 132(1963).

28. F. Cramer, F. M. Henglein, Chem. Ber., 90, 2561(1957).

29. J. N. J. J. Lammers, Stärke, 19, 70(1967).

30. H. Schlenk, D. M. Sand, J. Am. Chem. Soc., 83, 2312(1961).

31. R. K. McMullan, W. Saenger, J. Fayos, D. Mootz, Carbohydr. Res., 31, 37(1973).

32. M. Komiyama, M. L. Bender, Bioorg. Chem., 6, 323(1977).

33. F. Cramer, W. Dietsche, Chem. Ind.(London), 1958, 892.

34. R. L. VanEtten, J. F. Sebastian, G. A. Clowes, M. L. Bender, J. Am. Chem. Soc., 89, 3242(1967).

35. W. Banks, C. T. Greenwood, Starch and its Compounds, University Press, Edinburgh, 1975.

36. M. Noltemeyer, W. Saenger, J. Am. Chem. Soc., 102, 2710(1980).

37. B. Pfannemüller, H. Meyerhöffer, R. C. Schulz, Makromol. Chem., 121, 147(1969).

38. B. Casu, M. Reggiani, G. R. Sanderson, VIIth Int. Symp. Carbohydr. Chem., Bratislava, 1974.

39. L. D. Melton, K. N. Slessor, Carbohydr. Res., 18, 29(1971).

40. K. Takeo, T. Kuge, Stärke, 28, 226(1976).

41. A. Harada, M. Furue, S. Nozakura, Macromolecules, 9, 705(1976).

42. J. Szetjli, E. Fenyvesi, B. Zsadon, Stärke, 30, 1278(1978).

43. P. V. Demarco, A. L. Thakkar, J. Chem. Soc. D, 1970, 2.

44. J. P. Behr, J. M. Lehn, J. Am. Chem. Soc., 98, 1743(1976).

45. J. Sunamoto, H. Okamoto, K. Taira, Y. Murakami, Chem.

Lett., 1975, 371.

46. J. A. Ripmeester, Chem. Phys. Lett., 74, 536(1980).
47. J. Szejtli, Zs. budai, Acta Chim. Acad. Sci. Hung., 99, 433(1979).
48. B. Hingerty, W. Saenger, J. Am. Chem. Soc., 98, 3357(1976).
49. K. Harata, Bull. Chem. Soc. Jpn., 51, 1644(1978).
50. K. Takeo, K. Hirose, T. Kuge, Chem. Lett., 1973, 1233.
51. J. Szejtli, A. Lipták, I. Jodál, P. Fűgedi, P. Nánási, A. Neszmélyi, Stärke, 32, 165(1980).
52. M. L. Wolfrom, M. Konigsberg, S. Soltzberg, J. Am. Chem. Soc., 58, 490(1936).
53. P. J. Stoffyn, R. W. Jeanloz, ibid., 80, 5690(1958).
54. E. T. Lippmaa, M. A. Alla, T. J. Pehk, ibid., 100, 1929(1978).
55. R. H. Atalla, J. C. Gast, D. W. Sindorf, V. J. Bartuska, G. E. Maciel, ibid., 102, 3249(1980).
56. W. L. Earl, D. L. VanderHart, ibid., 3251(1980).
57. H. Saitô, R. Tabeta, Chem. Lett., 1981, 713.
58. J. R. Lyerla, C. S. Yannoni, C. A. Fyfe, Acc. Chem. Res. 15, 208(1982).
59. A. N. Garroway, W. B. Moniz, H. A. Resing, ACS Symp. Ser. No. 103, 67(1979); A. N. Garroway, D. L. VanderHart, W. L. Earl, Phil. Trans. R. Soc. Lond. A, 299, 609(1981).
60. G. E. Balimann, C. J. Groombridge, R. K. Harris, K. J. Packer, B. J. Say, S. F. Tanner, Phil. Trans. R. Soc.

Lond. A, 299, 643(1981).

61. K. Harata, Bull. Chem. Soc. Jpn., 48, 2049(1975); K. Harata, ibid., 49, 2066(1976); K. Harata, ibid., 50, 1416(1977); K. Harata, H. Uedaira, J. Tanaka, ibid., 51, 1627(1978); K. Harata, K. Uekama, M. Otagiri, F. Hirayama, H. Ogino, ibid., 54, 1954(1981).
62. K. Harata, K. Uekama, M. Otagiri, F. Hirayama, ibid., 55, 3904(1982).
63. S. J. Opella, M. H. Frey, J. Am. Chem. Soc., 101, 5854(1979).
64. N. Zumbulyadis, J. Magn. Reson., 49, 329(1982).
65. K. Freudenberg, R. M. Hixon, Ber., 56, 2119(1923).
66. D. L. VanderHart, W. L. Earl, A. N. Garroway, J. Magn. Reson., 44, 361(1981); W. P. Rothwell, J. S. Waugh, J. Chem. Phys., 74, 2721(1981); Y. Inoue, T. Okadu, F. H. Kuan, R. Chûjô, Carbohydr. Res., 129, 9(1984).
67. C. Van Hooidonk, J. C. A. E. Breebaart-Hansen, Rec. Trav. Chim., 91, 958(1972).
68. W. I. Rogers, W. M. Whaley, US Patent, 3,061,444(1962); J. Szejli, L. Szente, R. Kolta, K. Lindner, T. Zilahy, B. Koszegi, Hung. Patent Appl., CI-1753(1977); T. Konishi, J. Komiya, T. Yoneda, Japan Kokai, 78,18,775(1978).
69. Y. Suzuki, H. Ikura, Japan Kokai, 75,58,208(1975).
70. J. Trotter, Acta Cryst., 14, 1135(1961).
71. G. Casalone, C. Mariani, A. Mugnoli, M. Simonetta, Acta Cryst. B, 25, 1741(1969).

72. O. Bastiansen, Acta Chem. Scand., 3, 408(1949).

73. H. Suzuki, Bull. Chem. Soc. Jpn., 32, 1340(1959).

74. J. Scheffer, Y. F. Wong, A. O. Patil, D. Y. Curtin, I. C. Paul, J. Am. Chem. Soc., 107, 4898(1985).

75. D. M. Grant, B. V. Cheney, ibid., 89, 5315(1967).

76. B. S. Magdoff, Acta Cryst., 4, 176(1951).

77. J. Seelig, Quart. Rev. Biophys., 10, 353(1977).

78. J. C. Rowell, W. D. Phillips, L. R. Melby, M. Panar, J. Chem. Phys., 43, 3442(1965).

79. P. J. Bos, J. Pirs, P. Ukleja, J. W. Doane, M. E. Neubert, Mol. Cryst. Liq. Cryst., 40, 59(1977).

80. E. Meirovitch, T. Krant, S. Vega, J. Phys. Chem., 87, 1390(1983).

81. E. Meirovitch, I. Belsky, S. Vega, ibid., 88, 1522(1984).

82. L. D. Hall, T. K. Lim, J. Am. Chem. Soc., 106, 1858(1984).

83. M. Rinne, J. Depireux, Adv. Nucl. Quadrupole Reson., 1, 357(1974).

84. E. R. Andrew, R. G. Eades, Proc. R. Soc. A, 218, 537(1953).

85. M. Mehring, R. G. Griffin, J. S. Waugh, J. Chem. Phys., 55, 746(1971).

86. N. Boden, L. D. Clark, S. M. Hanlon, Faraday Sym. Chem. Soc., 13, 109(1979).

87. F. S. Millett, B. P. Dailey, J. Chem. Phys., 56, 3249(1972).

88. R. G. Barnes, J. W. Bloom, ibid., 57, 3082(1972).

89. Y. Inoue, T. Okuda, R. Chûjô, Carbohydr. Res., 116, C5(1983).

90. R. F. Campbell, E. Meirovitch, J. H. Freed, J. Phys. Chem., 83, 525(1979); E. Meirovitch, J. H. Freed, Chem. Phys. Lett., 64, 311(1979).

91. S. Alexander, A. Baram, Z. Luz, Mol. Phys., 27, 441(1974); A. Baram, Z. Luz, S. Alexander, J. Chem. Phys., 64, 4321(1976).

92. R. Eckman, A. J. Vega, J. Am. Chem. Soc., 105, 4841(1983).

93. D. D. MacNicol, J. J. McKendrick, D. R. Wilson, Chem. Soc. Rev., 7, 65(1978).

94. W. Baker, J. F. W. McOmie, A. S. Weaving, J. Chem. Soc., 1956, 2018.

95. J. L. Flippen, J. Karle, I. L. Karle, J. Am. Chem. Soc., 92, 3749(1970); J. L. Flippen, J. Karle, J. Phys. Chem., 75, 3566(1971).

96. A. D. U. Hardy, J. J. McKendrick, D. D. MacNicol, J. Chem. Soc. Chem. Comm., 1976, 355.

97. A. P. Dianin, J. Russe. Phys. Chem. Soc., 46, 1310(1914).

98. W. Baker, J. F. W. McOmie, Chem. Ind.(London), 1955, 256.

99. J. Ripmeester, J. Inclusion Phenomena, 1, 87(1983).

100. P. Barker, N. E. Burlinson, B. A. Dunell, J. A. Ripmeester, J. Magn. Reson., 60, 486(1984).

101. C. M. Gall, J. A. DiVerdi, S. J. Opella, J. Am. Chem. Soc., 103, 5039(1981); R. A. Kinsey, A. Kintanar, E. Oldfield, J. Biol. Chem., 256, 9028(1981).

CHAPTER III

METAL-CHELATES OF SUGARS

III.1. Introduction

The ability of sugars and their derivatives to sequester metals is of interest to the possible development of novel classes of metal-based affinity chromatography materials,[1] of chiral homogeneous catalysts,[2] of metal-chelators for clinical use,[3] and of models for biologically important chelates.[4] Other ongoing interests include n.m.r. investigations of metal ion binding to sugars. As an extension of a long-standing interest in our own laboratory in high-resolution n.m.r. studies of "metal conjugation" by sugars, it was appropriate then to examine these complexes in the solid state. The metal-complexes involved here can be classified into two classes, those which are diamagnetic and others which are paramagnetic.

The study of paramagnetic molecules by n.m.r. has had a tremendous impact on the chemical and biological sciences. Although this field originated in the early 1950's, there was initially doubt of its potential because it was feared that paramagnetic compounds would furnish n.m.r. spectra that were broadened too extensively to be of any signficance. In 1975, a well-resolved spectrum of nickelocene, $[Ni(C_2H_5)_2]_2$, was reported by McConnell and Holm.[5] Since then, the use of n.m.r. spectroscopy for studying such complexes has surpassed the interest shown for the diamagnetic counterparts. Analysis of paramagnetic shifts and relaxation rates provides useful information about the molecular geometry of the complex, its dynamic

behavior, and/or the distribution of unpaired electrons in the ligand skeleton of paramagnetic metal ion complexes in the solution state. Nevertheless, optimal development of this field has been severely hampered by the evident lack of any source of a clear description of the physical principles of the phenomenon, or of the interpretation of the resulting magnetic resonance parameters.[6] The latter requires knowledge of the ligand field theory, of electron paramagnetic resonance, of magnetic susceptibility, and of the optical properties of transition metal complexes.

In this area of study, the synthesis of specific monomeric, metal-sugar compounds was initially undertaken. Schiff's base ligands were obtained by combining amino sugars with aromatic aldehydes, followed by complexation with suitable metal ions. Subsequently, studies were made of the chelating polymers, chitin and alginate, which can be obtained in enormous quantities from natural sources. Then, following other recent attempts to improve the metal-chelating capability by chemical derivatization of the native polymer,[7] chitosan Schiff's bases were studied. Although this study represents only a beginning, it clearly warrants further evaluation of the merits of using solid-state ^{13}C-n.m.r. methods.

III.2. Paramagnetics in Solution

III.2.1. Relaxation Processes

Considering a paramagnetic ion in solution, the spin energy levels in an external field, B_0, can be written as[6]

$$E_T = g\beta B_0 S_z - g_N\beta_N B_0 I_z + aI_z S_z \qquad (1)$$

where "g" and "β" are the electronic spectroscopic splitting factor and Bohr magneton, respectively, "a" is the hyperfine coupling constant, "g_N" and "β_N" are the nuclear "g" value and magneton, respectively, "S_z" is the z-component of the electron spin, and "I_z" is the z-component of the nuclear spin. The allowed nuclear transitions $\Delta I_z = \pm 1$ and $\Delta I_S = 0$ are shown as vertical arrows in Fig. III-1. The two lines would be observed in the n.m.r. spectrum with frequencies

$$h\nu_1 = g_N\beta_N B_0 - 1/2(a) \qquad (2)$$

$$h\nu_2 = g_N\beta_N B_0 + 1/2(a) \qquad (3)$$

and their separation is equal to "a".

Relaxation of nuclei in this kind of solution is often dominated by the hyperfine interaction between the nuclear spin and the unpaired electron spin. The strong local field produced by the electron can be coupled to the nuclei by simple "dipolar" interaction and the "Fermi hyperfine contact" interaction. Since the electron relaxation or

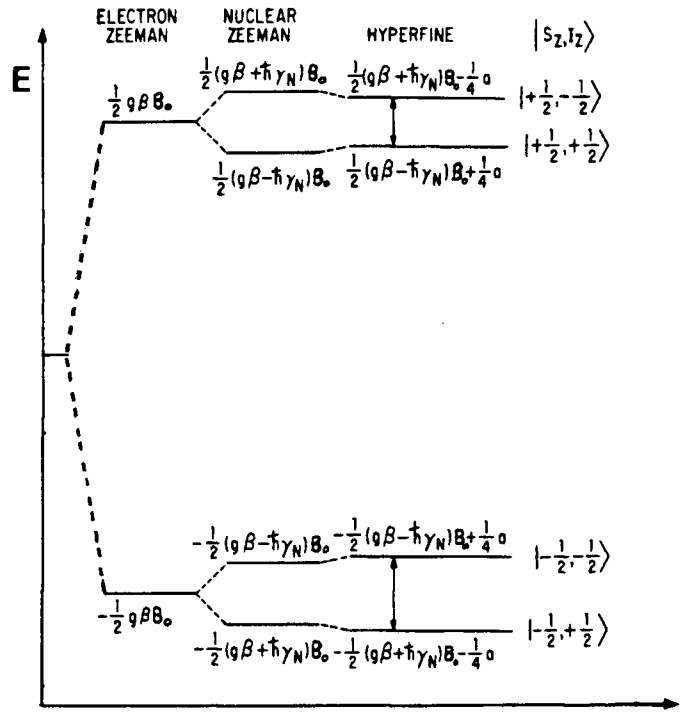

Fig. III-1. Energy levels for a proton with weak hyperfine coupling to an electron. Vertical arrows represent allowed nuclear transitions (from Ref. [6]).

electron exchange is so rapid on the n.m.r. time scale, the doublet should collapse into a single peak. The resultant peak is not centered midway between the components of the doublet, but is slightly shifted due to the unequal populations of the electron spin states, by the contact shift. The expected case of two shifted peaks has never been observed since for such slow electron relaxation, protons magnetically coupled to the electrons will be relaxed very efficiently giving rise to broad resonance lines that could not be detected.

Electrons relaxing with exactly the same frequency as

the hyperfine coupling constant, a/h (in Hz), are most efficient at broadening the spectrum. The lifetime of an electron spin state is related to T_{1e}, the electron-spin relaxation time, which is a measure of the time taken for energy to be transferred between a pair of levels such as the $|+1/2, -1/2\rangle$ and $|-1/2, -1/2\rangle$. T_{1e}^{*}, the electron exchange time, is characteristic of the time spent by the ligand at the particular metal site.[8] If $1/T_{1e} >> a/h$ or $1/T_{1e}^{*} >> a/h$, the resonance signal would appear at a position which is the average of the two frequencies ν_1 and ν_2 weighted by the populations of the two electron spin states. a/h is typically 10^8 Hz, while T_{1e} is generally in the range of 10^{-9} to 10^{-11} s, so that in practice, $1/T_{1e} >> a/h$. Thus, the average transition energy is given by[6]

$$h\nu = f_{+\frac{1}{2}}[(g_N\beta_N B_0) - 1/2(a)] + f_{-\frac{1}{2}}[(g_N\beta_N B_0) + 1/2(a)] \qquad (4)$$

where $f_{+\frac{1}{2}}$ and $f_{-\frac{1}{2}}$ are the fractions of the molecules in the $|+1/2\rangle$ and $|-1/2\rangle$ electron spin states, respectively. Since the nuclei are divided between the levels according to the Boltzmann distribution, it follows that

$$f_{+\frac{1}{2}} = 1 + \left\{e^{(g\beta B_0/kT)}\right\}^{-1} \approx (2 + g\beta B_0/kT)^{-1} \qquad (5)$$

$$f_{-\frac{1}{2}} = 1 + \left\{e^{(-g\beta B_0/kT)}\right\}^{-1} \approx (2 - g\beta B_0/kT)^{-1} \qquad (6)$$

so that Eq.(4) becomes

$$h\nu = \frac{4g_N\beta_N B_o + g\beta B_o a/kT}{(4 - g^2\beta^2 B_o{}^2/k^2T^2)} \approx g_N\beta_N B_o + \frac{g\beta B_o a}{4kT} \qquad (7)$$

since the quantity $g^2\beta^2 B_o{}^2/k^2T^2$ is negligible. The isotropic shift (or contact shift) is then given by

$$\left(\frac{\Delta\nu}{\nu_o}\right)_c = \frac{-ag\beta}{4g_N\beta_N kT} \qquad (8)$$

where $\Delta\nu$ is the shift from the corresponding position in the diamagnetic complex, and ν_o is the irradiating frequency. The direction of the shift depends on the sign of "a".

The relaxation times T_1 and T_2 of nuclei bound to, or near, a paramagnetic center, are usually well represented by the classical Solomon-Bloembergen equations.[9,10] These expressions are based on analysis of the dipole-dipole interaction between the electron and nuclear spins, and of the isotropic nuclear-electron spin exchange interaction. More recently, there have been several developments in the theory of nuclear spin relaxation in paramagnetic systems. Sabirov[11] has reviewed the case by considering all possible transitions caused by electron-nuclear interaction. A similar approach has been developed by Bergen et al.,[12] who have derived analytical expressions for electron and nuclear relaxation times in the general case, where the g-factor may be anisotropic and the nine hyperfine

interaction tensor components may all be different.

III.2.2. Electron-Spin Relaxation

It has been mentioned earlier that T_{1e} should be of the order of 10^{-11} s or less if well-resolved n.m.r. spectra are to be obtained for paramagnetic complexes. However, the observed transitions are not as sharp as those observed for the diamagnetic equivalents. Several factors which can lead to short electron relaxation times were discussed extensively during the 1960s.[13] Only a brief summary of some general observations[6] based on first row transition metal ion systems is given here.

For those species containing a single unpaired electron ($S = 1/2$) such as organic free radicals, broad n.m.r. spectra are observed because there is no zero field splitting (z.f.s.) to cause efficient electron-spin relaxation. Exceptions occur for complexes ($S \geq 1$) with triply degenerate (T) ground states, where the presence of small low-symmetry distortions, or spin-orbit coupling, produces low-lying excited states which greatly diminish T_{1e}. These include octahedral complexes having the following configurations: d^2, low spin-d^4, low spin-d^5, high spin-d^6, and high spin-d^7. When large distortions from octahedral symmetry exist in the complexes, the T states are split and the n.m.r. spectra often become broader. Tetrahedral complexes with T ground states also result in sharp n.m.r. spectra; this is typical of Co^{2+} systems.

Table III-1 summarizes the results presented in earlier investigations on electron relaxation. The entries in this table are generally consistent with the conclusions made on the basis of the anticipated electron-spin relaxation mechanism.

III.2.3. Isotropic Shifts

Interactions between nuclei and unpaired electrons are capable not only of affecting nuclear relaxation times, but also of producing shifts of many orders of magnitude greater than those arising from shielding effects in diamagnetic molecules. It is important to appreciate that the observed shift can have contributions from at least three effects: contact shift,[14] dipolar shift,[15] and complexation (or diamagnetic) shift. Hence, correction for the small diamagnetic shift is necessary beforehand in order to show the presence of a paramagnetic induced shift.

The contact shift, $\Delta\nu_c$, is sometimes referred to as the Fermi or isotropic contact shift. This interaction is generally transmitted through chemical bonds to the appropriate nucleus and, therefore, it is directly related to the amount of unpaired spin that is delocalized onto the ligand. A contact shift is observed when the electronic radial wave function has a finite value at a given nucleus. Assuming an isotropic g value for the system, Eq. (8) can be written in the following form

Geometry	Spin state	d^1	d^2	d^3	d^4	d^5	d^6	d^7	d^8	d^9
O_h	High	0	+	−	+	−	+	+	+	−
	Low				+	+	b	−*		
T_d	High	−*	0*	+*	+	0	+	+	+	+
Planar	High				+	+*	+*	+	c	0
Five-coordinate	High	−*	0*	0*	+	+	+*	+	+	0

Table III-1. Ground states of transition metal ions as a function of d configuration, geometry, and spin state (from Ref. [6]).

Plus (+) indicates T_{1e} is usually short enough to yield narrow n.m.r. lines; minus (-) indicates T_{1e} is generally too long to yield useful n.m.r. spectra; zero (0) indicates borderline cases; asterisk (*) indicates predicted quality of as an yet unobserved configuration.
[b]Diamagnetic.
[c]Low-spin, diamagnetic.

$$\left(\frac{\Delta\nu}{\nu_o}\right)_c = -\left(\frac{A}{\hbar}\right)\frac{g\beta S(S+1)}{3kT\gamma_N} = \left(\frac{A}{\hbar}\right)\frac{1}{\gamma_N B_o}\langle S_z\rangle \qquad (9)$$

where S is the total electron spin, and γ_N is the magnetogyric ratio of the nucleus (derived from $g_N\beta_N = \hbar\gamma_N$). "a", which is for one-electron systems, has been replaced by "A" for the many-electron system. $\langle S_z\rangle$ is the average value of S_z over the spin levels, and it is usually referred to as the averaged electron spin polarization.

Another mechanism, which can produce chemical shifts, is the pseudocontact or dipolar shift, $\Delta\nu_{pc}$; it is a through-space interaction between ligand nuclei and unpaired electrons on the metal ion. This shift is only observed if the magnetic field produced by the latter is not averaged to zero, that is, it is anisotropic. Thus, the equation for this shift depends on the symmetry of the g-factor and takes its simplest form for dissolved complexes with axially symmetric g-tensors (i.e., $g_x = g_y \neq g_z$).[8]

$$\left(\frac{\Delta\nu}{\nu_o}\right)_{pc} = \frac{\beta^2 S(S+1)}{45kT}\,\frac{(1 - 3\cos^2\theta)}{r^3}\,[(3g_{\parallel} + 4g_{\perp})(g_{\parallel} - g_{\perp})] \qquad (10)$$

where $g_z = g_{\parallel}$ and $g_x = g_{\perp}$, r is the electron-nuclear distance, and θ is the angle between the electron-nuclear vector and the symmetry axis of the g-factor. The pseudocontact term contains information relating to

molecular geometry and this has been rigorously evaluated. If the g-factor is isotropic, then there will be no shielding effect arising from the dipolar interactions with the unpaired electron.

The total observed isotropic shift is the algebraic sum of these two shifts:[8]

$$\Delta\nu_{iso} = \Delta\nu_c + \Delta\nu_{pc} \qquad (11)$$

$$\left(\frac{\Delta\nu}{\nu_o}\right)_{iso} = \left(\frac{\Delta\nu}{\nu_o}\right)_c + \left(\frac{\Delta\nu}{\nu_o}\right)_{pc}$$

In most complexes, both $\Delta\nu_c$ and $\Delta\nu_{pc}$ contribute to the total observed shift, but it is possible to design systems such that one of the interactions dominates. For example,[16] octahedral Ni(II) and tetrehedral Co(II) are magnetically isotropic, therefore, the contribution from $\Delta\nu_{pc}$ is small. In the case of lanthanide complexes, the unpaired electrons are deeply buried in the 4f orbitals, with very little delocalization onto the ligands. Hence, the contribution from $\Delta\nu_c$ to the observed shift would be negligible.

Line broadening of ligand signals is commonly associated with paramagnetic metal complexes in solution-state n.m.r. studies. In order to observe these signals, it is necessary, in most cases, to use low concentrations of the paramagnetic ion relative to the ligand. This creates a small number of observed nuclei in the "M" environment (coordination sphere) compared to that in the "O"

environment (outside), and the resultant observed spectrum essentially consists of a single peak for the particular kind of nucleus. Swift and Connick[17] have developed equations for such a situation; the linewidth of this peak, $1/\pi T_{2\,obsd}$, and its frequency shift, $\Delta\omega_M$ (in angular frequency terms), relative to the frequency of the O environment, are given by

$$T_{2p}^{-1} = T_{2\,obsd}^{-1} - T_{2O}^{-1}$$

$$= \frac{pq}{\tau_M^2} \frac{(T_{2M}^{-1} + \tau_M^{-1})T_{2M}^{-1} + \Delta\omega_M^2}{(T_{2M}^{-1} + \tau_M^{-1})^2 + \Delta\omega_M^2} \qquad (12)$$

$$\Delta\omega_p = \Delta\omega_{obsd} - \Delta\omega_O$$

$$= \frac{pq}{\tau_M^2} \frac{\Delta\omega_M}{(T_{2M}^{-1} + \tau_M^{-1})^2 + \Delta\omega_M^2} \qquad (13)$$

where p is the ratio of metal-to-ligand concentrations, q is the number of coordinated ligands per metal ion, and τ_M is the lifetime of the ligand in the coordination sphere. T_{2O} and T_{2M} are the relaxation times of the nuclei in the free ligand and in the coordination sphere, respectively. The latter is derived from the Solomon-Bloembergen equation. The adjusted relaxation rate, T_{2p}^{-1}, and isotropic shift, $\Delta\omega_p$, measure the paramagnetic contribution to these observed parameters.

III.3. Paramagnetics in the Solid State

III.3.1. Characteristics of Paramagnetic Spectra

Introduction of a small amount of a paramagnetic "impurity" has been widely used in the solid state to decrease proton relaxation times.[18,19] The use of paramagnetic reagents to induce chemical shift dispersion is still largely unexplored.[20] This is because a paramagnetic molecule, or ion, has difficulty in diffusing rapidly among molecules of interest to give a fast exchange-averaged resultant shift, the magnitude of which would be governed by the concentration of the paramagnetic species. The same lack of rapid molecular tumbling also allows the full development of various types of magnetic anisotropy in the solid state which can complicate the observed line-shapes and spectral resolution. The competition between paramagnetically induced-shift and -relaxation ultimately decides the resolution obtainable for the spectrum.

Electron spin relaxation is normally rapid in solid transition metal complexes and the nuclear spins experience an averaged electron polarization, $\langle S_z \rangle$.

$$\langle S_z \rangle = \frac{g\beta B_o S(S+1)}{3kT} \qquad (14)$$

Since the dipolar and Fermi contact interactions are proportional to $\langle S_z \rangle$, the observed shifts increase linearly

with the inverse of temperature. Well-resolved spectra are observed when the shifts become large compared with the intrinsic linewidth of the individual transition. Hence, low-temperature n.m.r. investigations can provide valuable information about these interactions.[21] As mentioned earlier, the dipolar interaction depends on the geometric factor $(1 - 3\cos^2\theta)/r^3$; thus, by measuring the dipolar terms, it is possible to determine the relative positions of the nuclei in the ligands with respect to the central paramagnetic ion. Although the dipolar interaction falls off as $1/r^3$, it is still possible for neighboring electron spins to participate in this interaction.

The resonance shift for a dilute paramagnetic solid is given by[6]

$$\left(\frac{\Delta\nu}{\nu_0}\right)_{iso} = -\frac{\langle S_z\rangle g\beta}{B_0}\left(\frac{1 - 3\cos^2\theta}{r^3}\right) + \frac{\langle S_z\rangle}{\gamma_N B_0}\left(\frac{A}{\hbar}\right) \quad (15)$$

where θ is the angle between the vector connecting the electron and nuclear spin, and the external magnetic field B_0. The other symbols have been defined earlier.

In concentrated paramagnetic samples, a given nuclear spin interacts not only with the electron spin on the parent molecule, but also with neighboring electron spins as well. Eq. (15) must then consider all possible intermolecular and intramolecular contributions to the electron-nuclear interactions.[22]

$$\left(\frac{\Delta\nu}{\nu_o}\right)_{iso} = -\frac{\langle S_z\rangle g\beta}{B_o}\sum_i\left[\frac{(1-3\cos^2\theta_i)}{r_i^3}\right] + \frac{\langle S_z\rangle}{\gamma_N B_o}\sum_i\frac{A_i}{\hbar} \quad (16)$$

The first term of Eq. (16) represents the anisotropic contribution to the shift, and it contains a summation over a series of angles and distances. The second term belongs to the Fermi contact interaction, in which the isotropic hyperfine coupling constant is normally dominated by the intramolecular term. However, in some cases, a neighboring molecule may contribute to this coupling constant.

III.3.2. Spectral Assignments

C.p.-m.a.s. ^{13}C-n.m.r. spectroscopy has been applied to paramagnetic complexes, but the spectra are usually broad and more difficult to interpret[20] than their diamagnetic counterparts. It is only in situations where T_{1e} is extremely short that sharp resonances are observed. However, the broadening effects can be of aid in making assignments of ^{13}C resonances. More importantly, if some estimate of the proximity of various nuclei to the paramagnetic center can be derived from the ligand geometry, then assignments may be made on the basis of relative linewidths, provided the differences involved are appreciable. When this is used as an aid to spectral assignments for paramagnetic systems, comparison with the analogous diamagnetic species is often made.

III.4. Synthesis

III.4.1. Schiff's Base Formation

Schiff's bases are compounds which contain the azomethine group; they are usually formed by the condensation of a primary amine with an active carbonyl compound. The compound of the latter type considered here is mainly 2-hydroxybenzaldehyde (salicylaldehyde) [1]. In 1922 Irvine and Earl[23] first reported the synthesis of salicylaldimine compounds (Schiff's bases formed from salicylaldehyde or substituted salicylaldehyde compounds) from glucosamine (2-amino-2-deoxy-α,β-D-glucopyranose) hydrochloride [2].

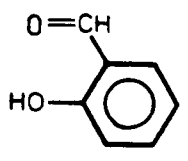

[1]

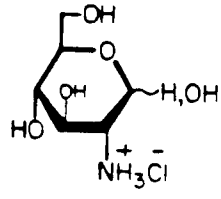

[2]

Not surprisingly, "blocked" glucosamine derivatives such as methyl 3,4,6-tri-O-acetyl-2-amino-2-deoxy-β-D-glucopyranoside hydrobromide [3][24] and 1,3,4,6-tetra-O-acetyl-2-amino-2-deoxy-β-D-glucopyranose [4][25] also react with salicylaldehyde to afford the corresponding Schiff's bases [5] and [6] as shown below.

Compounds [5] and [6] are crystalline, bright yellow, stable derivatives. However, they are acid- and base-labile; for these reasons, aromatic aldehydes are

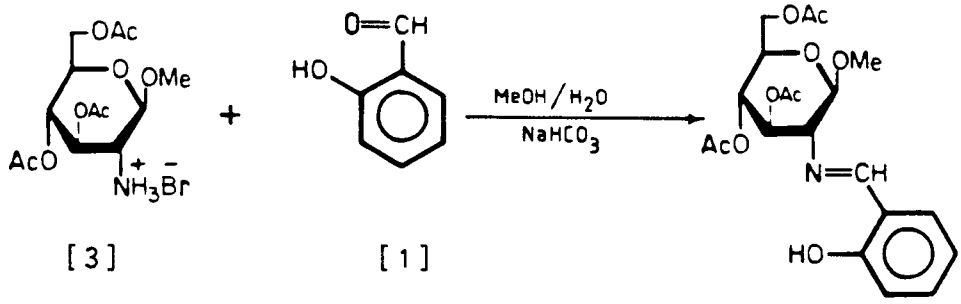

[3] [1] [5]

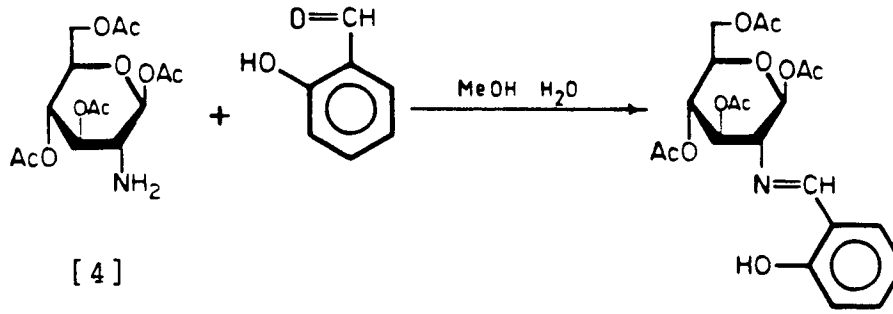

[4] [6]

conveniently used as amino blocking groups for amino sugars. They are stable to cold, anhydrous acylating reagents, and hence the amino sugar [4][25] can be prepared by this approach: anisaldehyde (p-methoxybenzaldehyde) [8] was used as an amino blocking group to yield the Schiff's base [9], which was subsequently acetylated and cleaved as shown (see Pg. 206).

III.4.2. Schiff's Base Metal Complexes

For metal complexation to occur with these Schiff's bases, the hydroxyl function on the aromatic ring must be brought into close proximity with the nitrogen atom of the

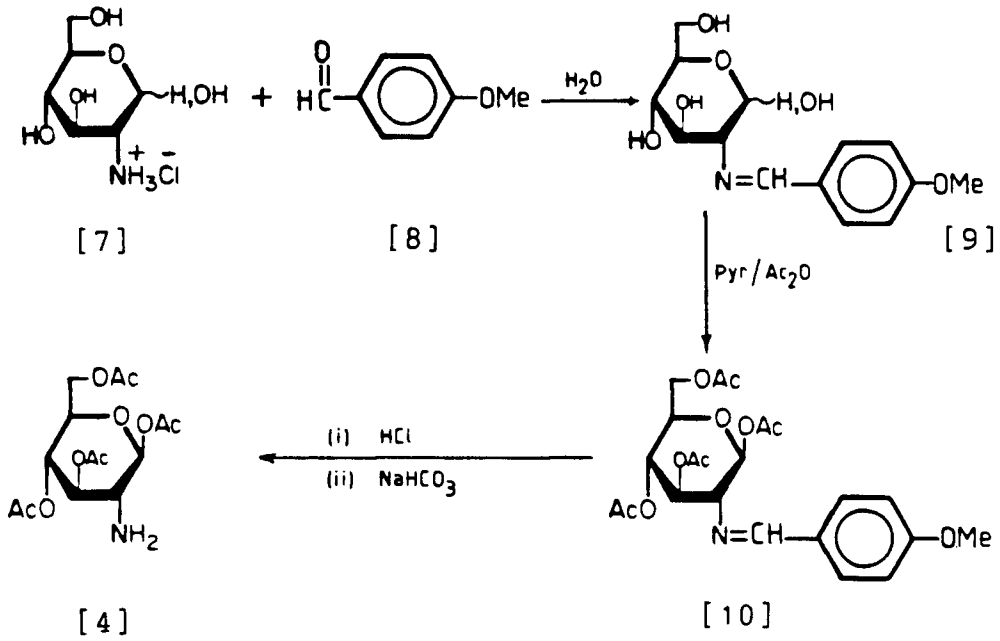

[7] [8] [9]

[4] [10]

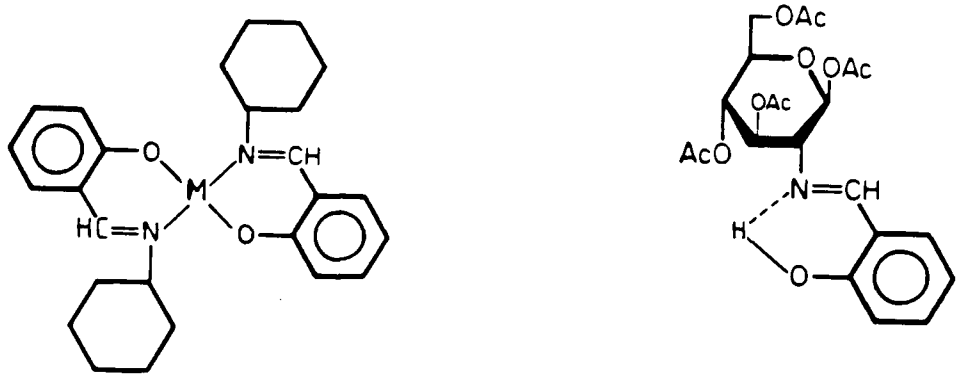

[11] [6]

sugar moiety, preferably by strong hydrogen bonding. It is known[26] that cyclohexyl salicylaldimine can form bis-structure complexes [11] with several divalent metals. The analogous sugar derivatives [5] and [6] were therefore expected to serve as potential ligands as well. When a methanolic solution of cupric acetate was added to a hot

methanolic solution of compound [5], the brown copper(II) sugar complex [12] crystallized readily in good yield.

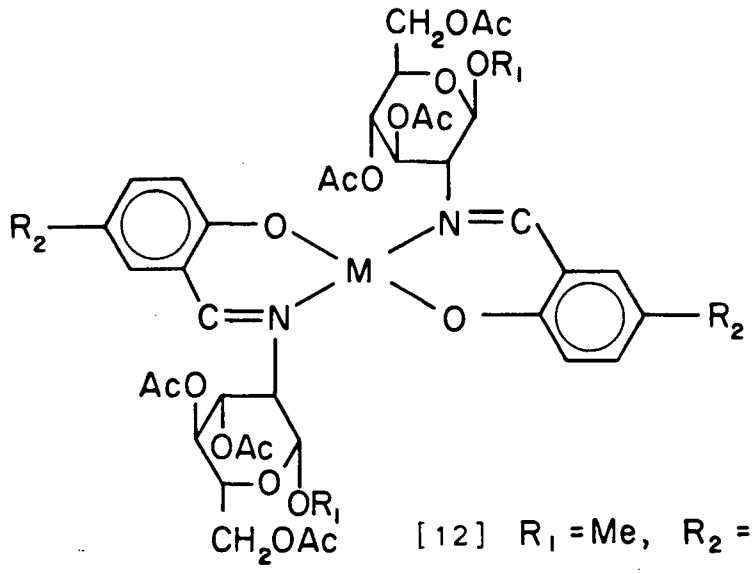

[12] R_1 = Me, R_2 = H, M = Cu

[13] R_1 = Me, R_2 = H, M = Zn

[14] R_1 = Me, R_2 = H, M = Co

[15] R_1 = Ac, R_2 = H, M = Cu

[16] R_1 = Me, R_2 = Br, M = Cu

Similarly, both zinc and cobaltous acetate have been shown to form complexes with ligand [5], but in low yields.[27]

The sugar salicylaldimine ligand [6] also forms a copper(II) complex [15], Cu(Sug II-sal)$_2$; however, attempted complexation of ligand [6] with zinc and cobaltous acetates failed to yield any product. This copper(II) complex was obtained as shiny olive green crystals when hot ethanolic solutions of cupric acetate and ligand [6] were mixed and allowed to cool gradually.

Chitosan [18], a polymer of glucosamine, condenses readily with arylaldehydes following the methods of Nud'ga et al.[28] and Hirano et al.[29] to give the corresponding Schiff's bases. The polymer was first dissolved in a

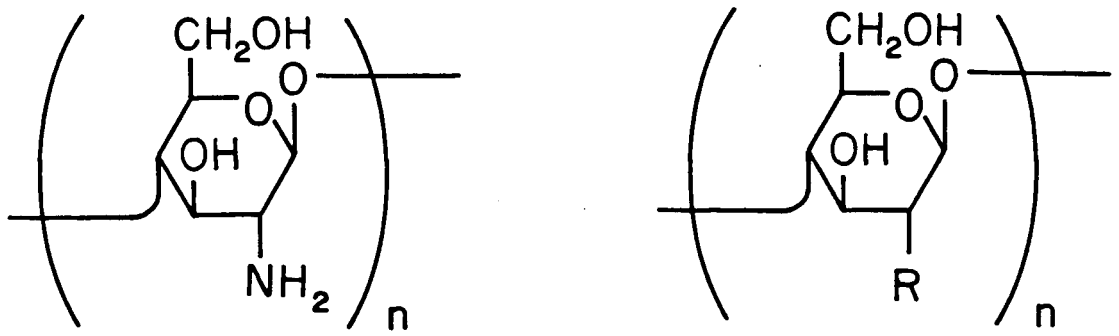

[18]

[19] 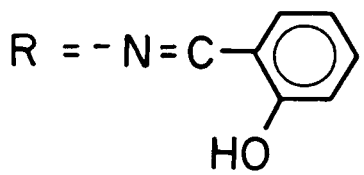

[20] 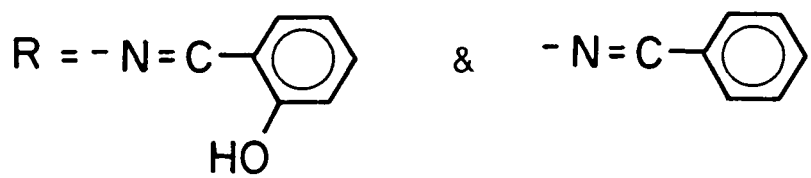

[21] 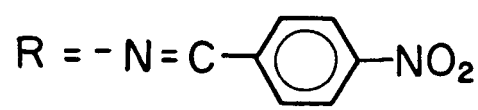

mixture of methanol and 1-10 % aqueous acetic acid at room temperature to afford a viscous solution, which was then treated with a solution of an arylaldehyde. After a few hours, the resultant gel was fragmented, and suspended successively in methanol, ethanol, and ether over a period

of 1 d to remove acetic acid and aldehyde. The filtered gel was air-dried initially and finally in vacuo at 56°C for 1 d.

The N-salicylidenechitosans, like their monomeric counterparts, readily react with copper(II) acetate in methanolic solution to afford colored complexes, which have been characterized by e.s.r. spectroscopy.[30] They are also suitable for chelation of a wide range of metals other than copper.

III.5. Results and Discussion

The c.p.-m.a.s. ^{13}C-n.m.r. spectrum of the zinc sugar complex [13], Zn(Sug I-sal)$_2$, along with that of the parent ligand [5] are shown in Fig. III-2. Although the linewidths of the resonances are narrow and the peaks well resolved, there is still some ambiguity in the assignment of individual resonances in the solid state, even when these assignments are based on solution spectra of these, and related molecules. The presence of the zinc atom nicely disperses the aromatic region, but only the two nonprotonated carbons can be differentiated from the rest by the dipolar dephasing technique.[31] The assignments for the protonated carbons must be considered tentative. Not surprisingly, small changes occur in the sugar region in comparison with that of the free ligand. The broad signal at 75.82 p.p.m. is assigned to C-2, and it is suggested that the broadening is caused by quadrupolar interaction

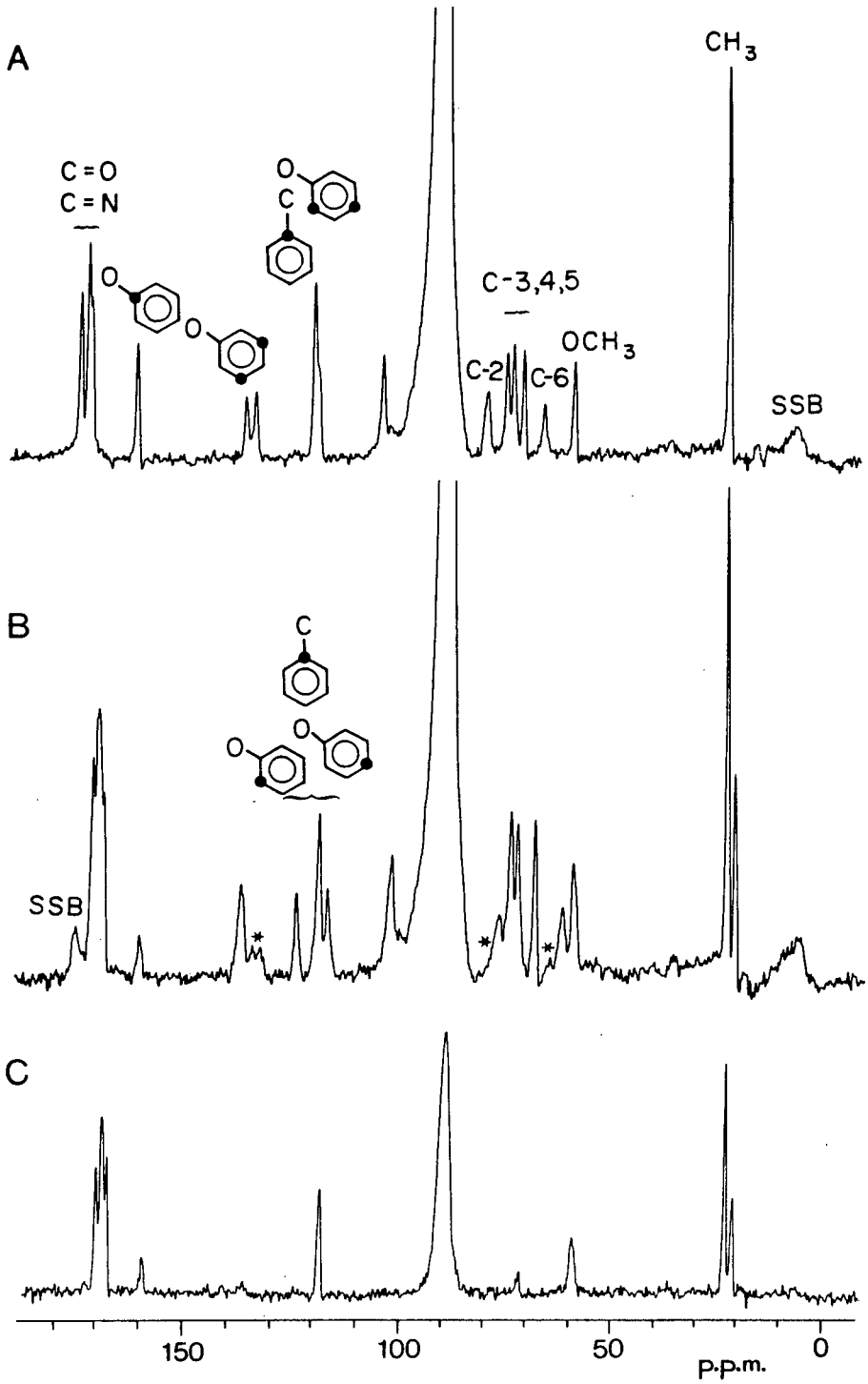

Fig. III-2. ^{13}C-C.p.-m.a.s. spectra of methyl 3,4,6-tri-O-acetyl-2-deoxy-2-salicylideneamino-β-D-glucopyranoside and its complex: (A) free ligand [5]; (B) diamagnetic zinc(II) complex [13]; (C) Dipolar dephasing spectrum of the zinc(II) complex.

with the ^{14}N nucleus, not averaged by magic angle spinning.[32] Surprisingly, metal ion chelation at the C-1 oxygen and the C-2' nitrogen has no pronounced effects on the chemical shifts of C-1 and C-2'. It may be that an up-field steric compression shift[33] counteracts the anticipated low-field shift. The methyl carbon atoms of the

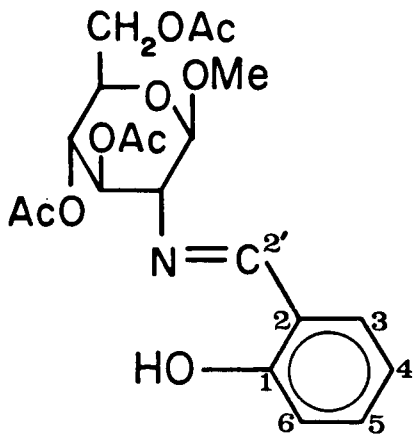

acetoxyl moieties appear as a doublet of approximately 2:1 proportions, one of which is unaffected by metal-induced shifts. Equivalent splittings of the carbonyl resonances may be obscured by the complexity of that spectral region.

It has been reported earlier[27] that the ^{1}H-n.m.r. solution-state spectrum of this complex shows some free ligand which could not be removed by recrystallization, and if this complex decomposes in solution, the proportion of free ligand increases and can be monitored. The signals from the residual, free ligand are marked by asterisks. Microanalysis of the sample used here revealed a negligible amount of free ligand; thus, the splitting of the methyl resonances cannot be attributed to resonances from the free

ligand. Possibly it is due to a crystallographic effect. Apart from these observations, nothing more can be concluded from the spectra of the free ligand or its complex.

As stated earlier, the observed linewidths of the carbon-13 resonance are dependent on T_{1e}, which in turn is dependent on the coordination geometry about the paramagnetic ion.[6] The shorter the T_{1e}, the narrower the linewidth; furthermore, it is known that copper(II) ions with a square planar geometry have a longer T_{1e} than complexes with a more tetrahedral coordination. In general, the former geometry is favored; in that geometry the excited states are well separated as a result of the Jahn-Teller effect. Although the complex Cu(Sug II-sal)$_2$, [15], is closer to a square planar geometry than the Cu(Sug I-sal)$_2$, [12], they are both essentially borderline cases in solution, as evidenced from the i.r. studies reported earlier.[27]

^{13}C-C.p.-m.a.s. spectra of complexes [12] and [15] are shown in Fig. III-3. No signals whatsoever were observed for the square planar complex [15], because the copper(II) electron relaxation rate is so slow. On the other hand, the use of a very short contact time (0.1 ms) in the c.p.-m.a.s. experiment revealed some broad ^{13}C resonances for the pseudotetrahedral complex [12]; only those sugar resonances which are relatively remote from the metal center were observed. The line broadening effect of the

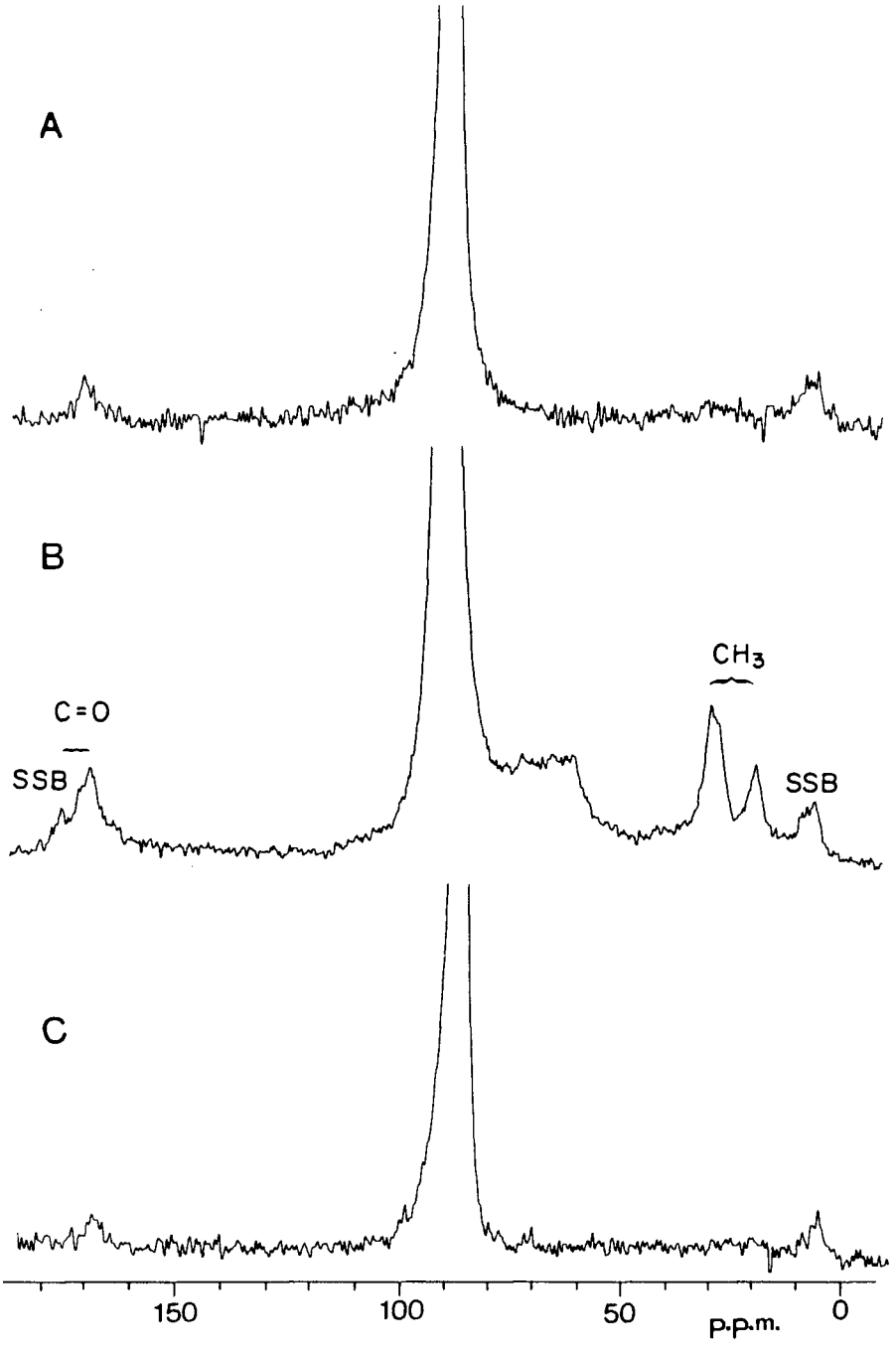

Fig. III-3. ^{13}C-N.m.r. spectra of paramagnetic copper(II) complexes: (A) [15]; (B) and (C) [12], with contact times of 0.1 and 1 ms, respectively.

copper(II) ion is a result of the spin-spin relaxation time, T_2, to which the linewidth is inversely proportional. If the electron-to-carbon-13 dipolar interaction is dominant, T_2 varies directly with the sixth power of the metal-to-carbon distance; hence, resonances of carbon atoms closest to the metal binding sites are broadened most. It should be noted that the isotropic nuclear-electron spin exchange interaction need not be localized to the donor site, but can also extend around the aromatic ring, which could further reduce the T_2 values. Thus, the disappearance of the aromatic resonances indicates extreme broadening and the binding of copper(II) ion to the C-1 oxygen and the C-2' nitrogen. Only the acetyl groups of the sugar rings can be observed clearly, and the other carbon-13 signals appear as a single, broad peak that cannot be assigned. Although the linewidths are relatively broad in comparison with those of the diamagnetic zinc(II) complex [13], the doublets for the carbonyl and methyl carbon atoms of the acetoxyl moieties are well resolved; their separations are approximately 7.3 and 10.2 p.p.m., respectively. The effect of metal ions, paramagnetic or not, on the isotropic shifts is nicely illustrated by these complexes.

When the contact time was increased to 1 ms, all of the sugar signals disappeared; this suggests that the splittings of the acetoxyl resonances are not caused by the presence of free ligands, which should be quite remote from the nearest metal center. This also rules out the

possibility that such splittings are due to paramagnetic anisotropic effects[20] because their separations are comparatively small and, moreover, the integral ratio of the two signals is similar to that measured for the analogous diamagnetic, zinc-sugar complex.

Changing the substituent on the anomeric carbon of the sugar ring, has a very substantial impact on the observed spectrum; compare, for example, complexes [12] and [15]. This is due to a geometric effect on the configuration of the complex. Similarly, broad signals were observed for Cu(Sug I-xsal)$_2$, [16], only for contact times set shorter than those used for complex [12] (i.e. $t_{cp} \leq 0.05$ ms); this suggests that the geometrical structure and $T_{1\rho}$ of [16] are intermediate between those of complexes [12] and [15].

It is appropriate now to review briefly the ways whereby the relaxation induced by the copper(II) ions, result in the observed effects. This is based most appropriately on the matched Hartmann-Hahn condition,[34] according to which, the carbon-13 magnetization grows as

$$M(t_{cp}) = c\lambda^{-1}\{1 - \exp-(\lambda t_{cp}/T_{cH})\}\exp(-t_{cp}/T_{1\rho}^{H}) \quad (17)$$

where

$$\lambda = \left[1 + \frac{T_{cH}}{T_{1\rho}^{C}} - \frac{T_{cH}}{T_{1\rho}^{H}}\right]$$

$T_{1\rho}^{C}$ is the carbon rotating frame relaxation time, and "c" is a proportionality constant. The other symbols have the usual meanings as defined on Pg. 32. Eq. (17) may be simplified to give

$$M(t_{cp}) = c\lambda^{-1}\left[\frac{\lambda t_{cp}}{T_{cH}}\right]\left[1 - \frac{t_{cp}}{T_{1\rho}^{H}}\right] \qquad (18)$$

This expression shows that the carbon magnetization rises with a rate, λ/T_{cH}, and falls off as $1/T_{1\rho}^{H}$. Since T_{cH} is of the order of the carbon-proton T_2 as a result of mutual carbon-proton spin flips under the Hartmann-Hahn condition, this expression is valid when $T_{1\rho}^{C} > T_{1\rho}^{H} >> T_{cH}$.

For a sufficiently long value of T_{1e} (such as for complex [15]), two possible mechanisms may be involved in the course of the ^{13}C-c.p.-m.a.s experiment:

1) The proton magnetization decays so rapidly during the onset of spin locking that none remains for transfer to the carbon nuclei, whose signals are, therefore, eliminated from the spectrum.

2) The $T_{1\rho}^{H}$ is so shortened that cross-polarization between spins occurs rapidly, decaying as a function of $1/T_{1\rho}^{H}$.

A gradual decrease in $T_{1\rho}^{H}$ can result in the appearance of some reasonably broad ^{13}C resonances, observable for very short contact times. Presumably, this long (moderate) T_{1e} modulates the c.p. rate (see Pg. 212), which is subsequently decreased.

For situations where T_{1H} (and T_{1e}) is of intermediate range, conventional single-pulse ^{13}C n.m.r. with high-power, gated decoupling of the proton spins can also be used to obtain the spectrum of complex [12] (Fig. III-4). Its T_{1C} and T_{2C} are reasonably short; the dipolar-carbon-13 dipolar interaction is not complicated by the spin

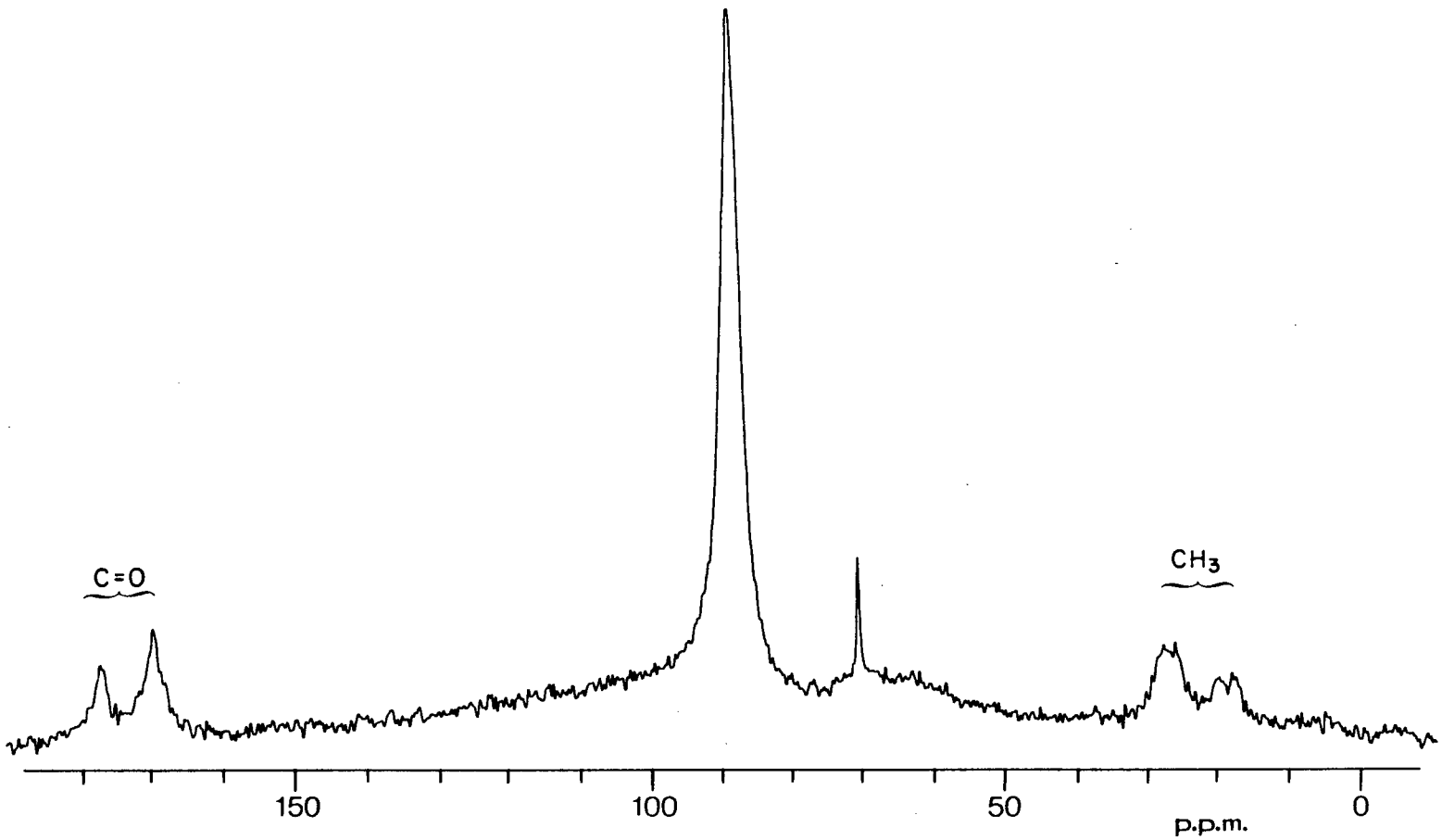

Fig. III-4. High-power, gated decoupling spectrum of copper(II) complex [12].

diffusion effects discussed earlier. However, no signals were observed for complex [15] probably due to extremely short relaxation times.

Cobalt(II) tetrahedral or square planar complexes have the short T_{1e} required to produce narrow n.m.r. lines.[6] However, attempted complexation of ligands [5] and [6] with this metal ion failed to yield the expected products. Although the complex [14] was prepared successfully by Adam,[27] its structure was not examined by n.m.r. spectroscopy. Solid-state n.m.r. studies of this complex would have offered a better evaluation of the behavior of paramagnetic ions with these sugar ligands.

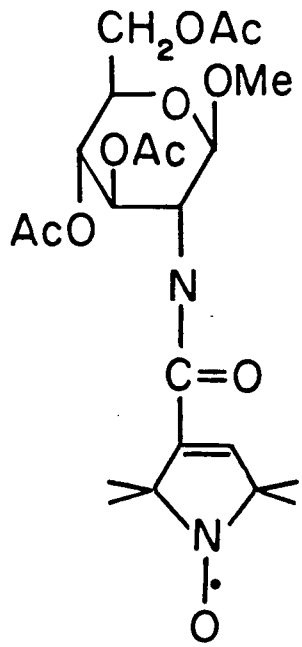

[17]

We have seen in the preceding discussion that T_{1e} governs the resolution of the ^{13}C-n.m.r. spectra of paramagnetic species. Organic free radicals represent a

spin doublet system (S = 1/2) in which T_{1e} is very long, and their e.s.r. spectra are usually well resolved.[6] Most of them possess orbitally nondegenerate ground states, and for those with degenerate ground states, the spin-orbit coupling is still insufficient to greatly diminish T_{1e}. The spin-labelled sugar complex [17], which has a sugar moiety identical to that of complex [12], was chosen to illustrate this point. Like complex [15], no signals can be detected from its c.p.-m.a.s. spectrum.

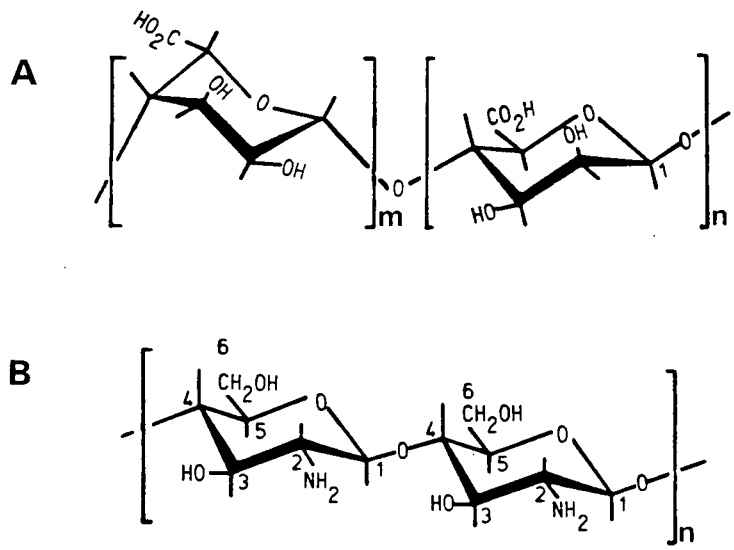

Fig. III-5. Representation of polymeric structures: (A) alginate; (B) chitosan.

Extension of this work in the context of polysaccharides such as chitosan and alginate (Fig. III-5) is most appropriate. First, we note that the metal binding sites can be either closely or distantly spaced, depending on the kind of polysaccharide involved. The carbon atoms of

the polymers which are located close to the metal-locus, should behave similarly to those of the monomeric, metal-sugar complexes. Those of a distant sugar moiety can behave differently, since this moiety may remain far from the metal-binding sites. However, the crystalline or amorphous packing of the sample may bring the two zones into close proximity. Thus, solid-state n.m.r. techniques may be useful not only for studies of paramagnetically induced-shifts and -relaxation phenomena, but also for determination of the primary structure of some polysaccharides and their chemical derivatives.

The ^{13}C-n.m.r. spectra of chitosan [18] and its Schiff's base derivatives are shown in Fig. III-6. Depending on the commercial batch of chitosan used, the residual amount of N-acetyl groups can vary by up to 15 % due to incomplete hydrolysis. A high acetyl-content can easily be detected by the presence of the appropriate carbon resonances; their absence from the spectrum as shown in Fig. III-6A, is indicative of almost complete deacetylation. The ^{13}C-n.m.r. spectrum of an amorphous sample of salicylidenechitosan [19], reveals broad peaks reflecting a dispersion of chemical shifts, and the assignments of its resonances are made by comparison with those for the respective carbon nuclei of the starting materials. The copper(II) salicylidenechitosan complex is analogous to Cu(Sug II-sal)$_2$ in terms of its deep-green color, and its characteristic e.s.r. spectrum which

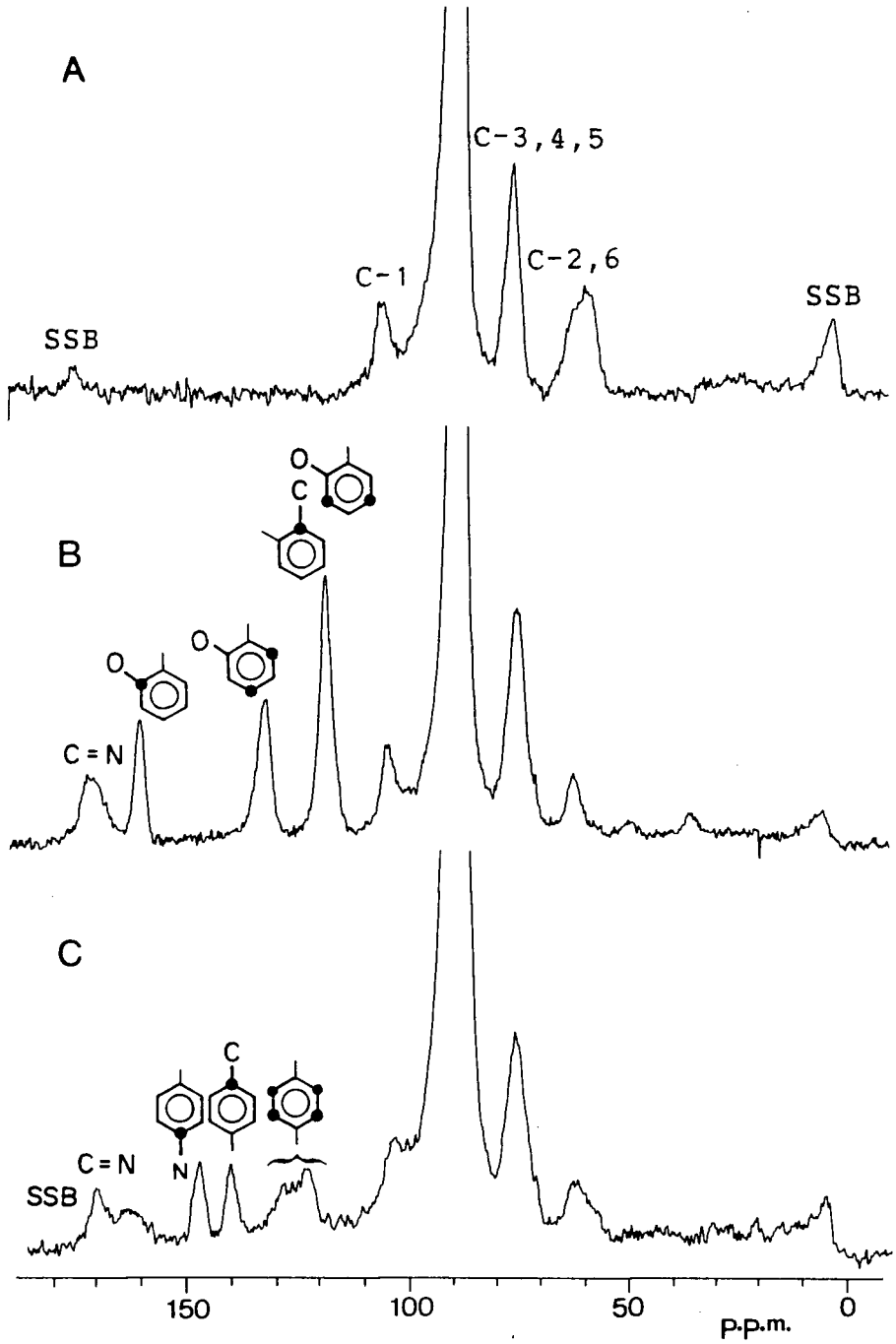

Fig. III-6. ^{13}C-N.m.r. spectra of chitosan and its Schiff's base derivatives: (A) chitosan [18]; (B) salicylidenechitosan [19]; (C) 4-nitrobenzylidenechitosan [21].

indicates a true chelate.[30] A low capacity for chelation was reported earlier for this polymer, in that only 20 % of the binding sites were occupied by copper(II) ions after a 12 h equilibration with these ions. This is presumably due to the low porosity of the polymer and its inability to swell in aqueous or alcoholic solution. In this work, an increase in the copper-chelating capacity was achieved [3.29 mmol of copper(II) per g; 87.4 % of the theoretical value] using the modified reaction procedure given in the Experimental Section. The absence of detectable carbon resonances can be interpreted as arising from the dense dispersion of copper(II) ions in the polymer "matrix"; this causes the resonances of non-metallated monomeric units to experience a T_{1e} comparable to that experienced by those which are metallated.

This point is further illustrated by the substance, [20], prepared by reacting chitosan with a mixture of benzaldehyde and salicylaldehyde. The color of the mixed polymer is lighter, with or without copper(II) ions when compared to salicylidenechitosan. The ratio of benzylidene to salicylidene moieties is estimated to be 2:1 from Fig. III-7. In the presence of copper(II) ions (2.09 mmol of copper(II) per g), the carbon signals of salicylidenechitosan disappeared and those of benzylidene-chitosan were broadened significantly; the latter probably does not participate in metal chelation. By setting a longer contact time (3 ms), reasonably sharp signals were

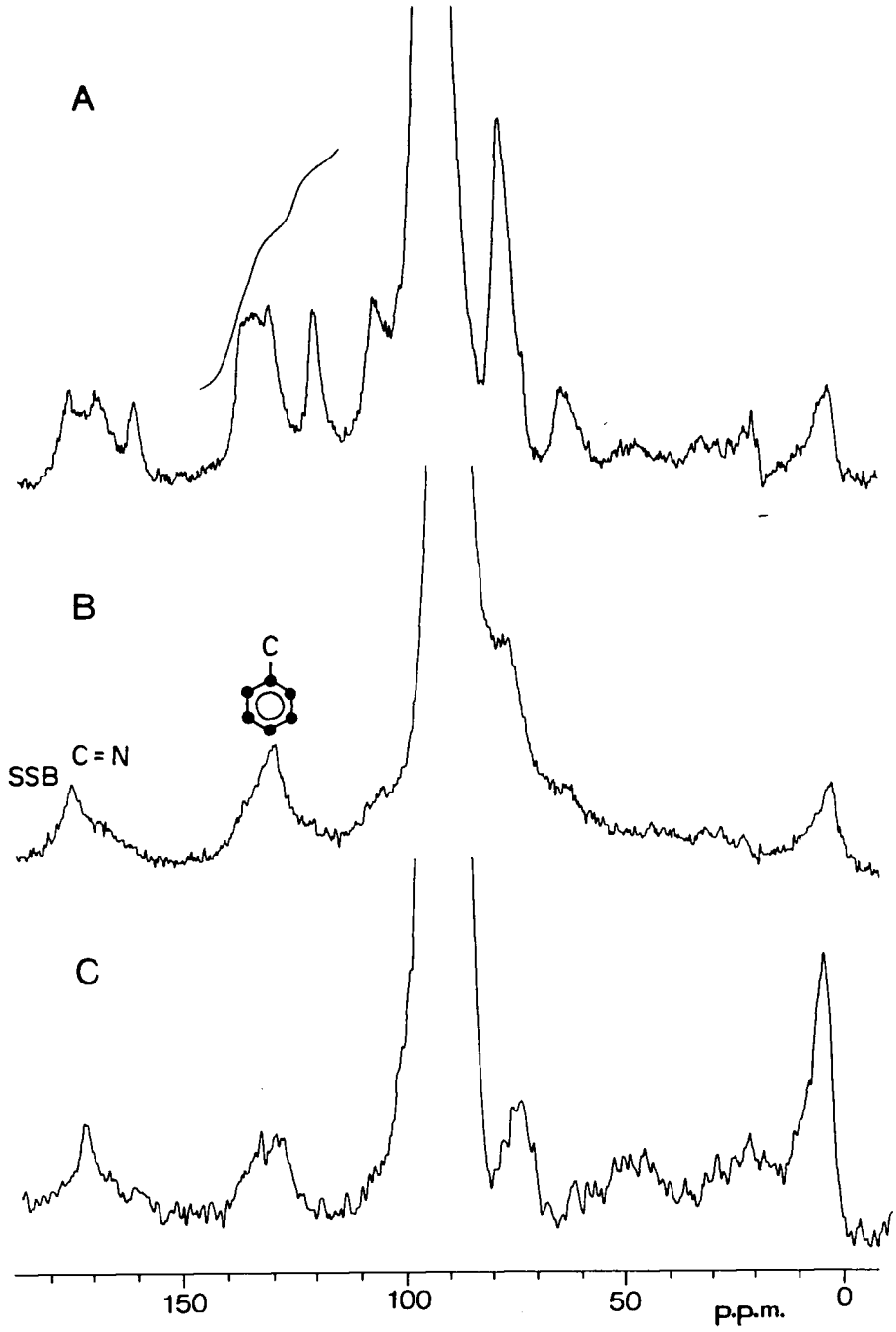

Fig. III-7. ^{13}C-N.m.r. spectra of mixed Schiff's bases of benzylidenechitosan and salicylidenechitosan [20] with and without copper(II) ions: (A) free ligand; (B) and (C) copper complexed, with contact times set at 0.5 and 3 ms, respectively.

obtained, corresponding to "free" benzylidenechitosan unperturbed by the distant paramagnetic ions.

It is now appropriate to consider what effects copper(II) ions have on polymers which lack any major locus for strong metal chelation. For such compounds it has been shown[35] in the solid state that $(1/T_1) \propto N.a.D.$, where "N" is the number of paramagnetic nuclei per unit volume, "a" is the distance between nuclei, and "D" is the spin-diffusion constant derived from the spin flip-flop between nuclei. At low concentrations of copper(II) ions in the polymer matrix, the carbon resonances are expected not to be shifted or broadened to any significant extent. 4-Nitrobenzylidenechitosan, [21], produces a copper(II) complex which is blue, and which binds 0.74 mmol of copper(II) per g of the polymer (21.8 % of the theoretical value). The spectra in Fig. III-8 indicate that the copper(II) ions decrease the relaxation times of the polymer, but to a lesser extent than for the salicylidene-copper(II) complexes discussed above. Slight amounts of line broadening were observed because of the high copper(II) ion concentration, but no measurable shifts were detected for the carbon resonances. Reducing the contact time further, to 0.1 ms only decreased the intensities of the nonprotonated carbon-13 signals of the aromatic ring; this observation would be unlikely for a true metal chelate. Hence, we conclude that the paramagnetic ions are diffused through the matrix, and are weakly bound to the

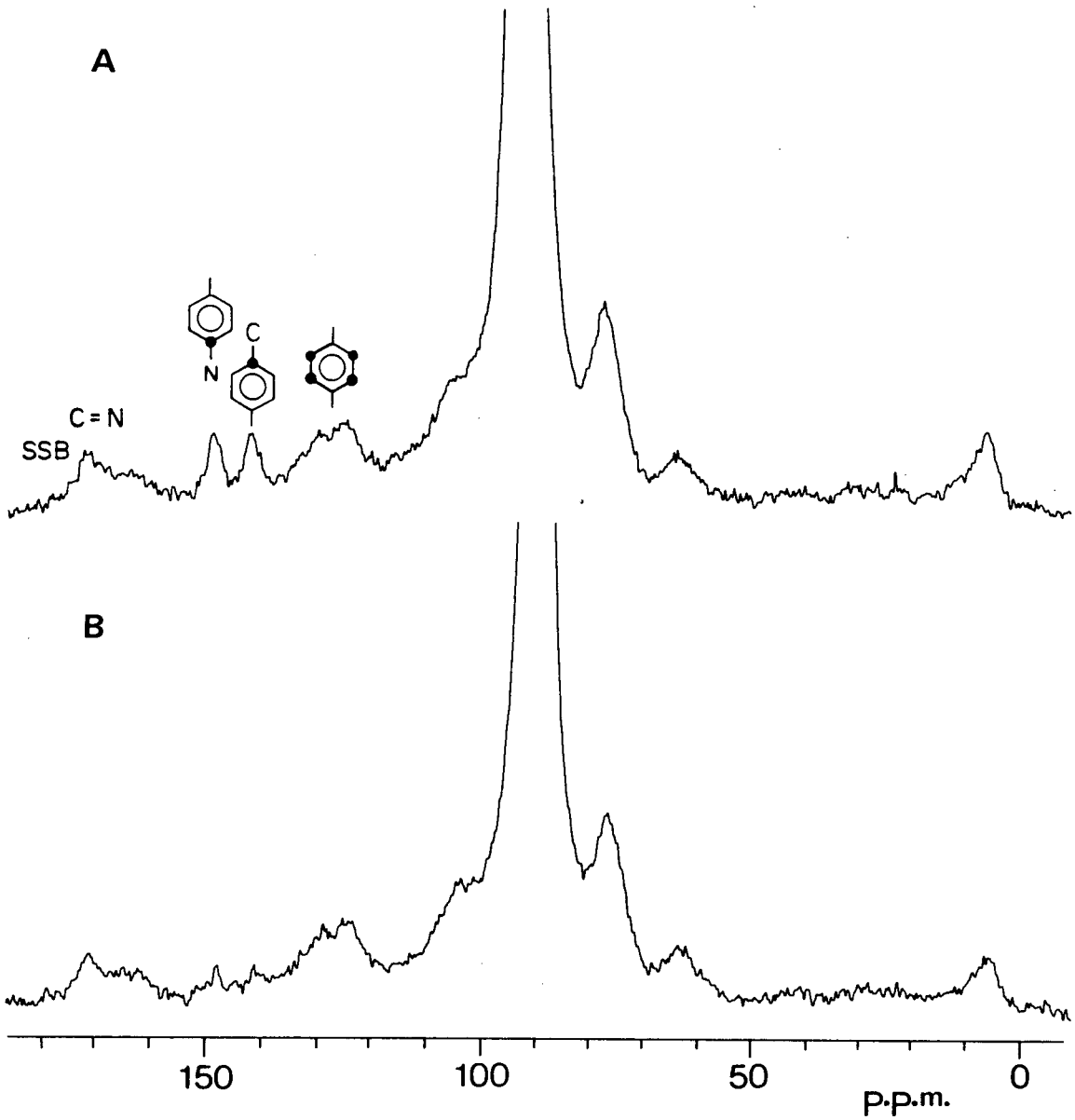

Fig. III-8. ^{13}C-N.m.r. spectra of [21], "doped" with copper(II) ions. Conditions were: (A) 3 ms and (B) 0.1 ms contact times.

matrix by some long-range bonding to the hydroxyl groups.

Alginate may be considered as a linear, block copolymer of β-D-mannuronic acid and α-L-guluronic acid residues, the relative amounts of which vary greatly for alginic acids from different species of algae.[36] The structure consists of three types of blocks: homopolymeric blocks of mannuronic acid (MM) and of guluronic acid (GG), and blocks with an alternating sequence (MG). It has been suggested that the metal ions are selectively bound in the long sequences of GG blocks, and we had hoped that chelation of copper(II) would eliminate the ^{13}C resonances of those blocks, leaving the others still detectable. The absence of carbon signals in the spectrum of the copper-alginate complex (2.58 mmol of copper(II) per g), suggests that not only the copper(II)-complexed regions, but rather the whole polymeric unit experiences a long T_{1e}. This can be explained by two models: the polymer could be rich in L-guluronic acid residues, or the D-mannuronic acid residues could have some affinity for the metal ions and/or have been brought closer to the binding sites by molecular packing. It was decided not to pursue this question further.

II.6. Summary and Conclusions

The amino sugars described in this chapter are biologically significant in their own right and also as models for the amino sugar constituents of a large number

of antibiotics. It might be expected that the combined presence of sugar- and metal-moieties would give these compounds interesting biological properties. Compounds [5] and [6] have been known for over fifty years and were prepared readily in high yield. It was expected that these compounds would form metal sugar complexes; however, this only occurred readily with copper(II) ions. Similarly, amino sugar-containing polysaccharides would be expected to react with the same metal to produce analogs of the monosaccharide complexes. These complexes often have intractable properties, and the solid-state ^{13}C-n.m.r. method has been used to help characterize them. The isotropic shifts of diamagnetic metal-sugar complexes are closely similar to those measured for the uncomplexed sugar-ligands. On the other hand, binding of paramagnetic ions has a profound effect on the obtainable resolution of the ^{13}C spectrum. High concentrations of the paramagnetic metal result in broad featureless spectra. Interpretation of the mechanism for those effects is complicated by spin diffusion of the protons; however, the major factors appear to be the T_{1e} and the inter-moment distances as discussed in this chapter. Since it only represents an extension of the ^{13}C-c.p.-m.a.s. methods to the study of metal chelates, we believe that further investigations are warranted in coming to some general conclusions.

References

1. B. Lönnerdal, J. Carlsson, J. Porath, FEBS Lett., 75, 89(1977); J. P. Lebreton, ibid., 80, 351(1977).
2. W. R. Cullen, Y. Sugi, Tetrahedron Lett., 1978, 1635.
3. M. N. Hughes, The Inorganic Chemistry of Biological Processes, Wiley, New York, 1974.
4. Y. A. Zhdanov, O. A. Osipov, V. P. Grigoriev, A. D. Garnovsky, Yu F. Alexeev, V. G. Alexeeva, N. M. Gontmacher, P. A. Perov, V. G. Zaliotov, V. N. Formina, T. A. Useman, O. N. Nechaeva, V. N. Mirny, Carbohydr. Res., 38, C1(1974).
5. H. M. McConnell, C. H. Holm, J. Chem. Phys., 27, 314(1957).
6. G. N. La Mar, W. D. Horrocks, R. H. Holm, NMR of Paramagnetic Molecules, Academic Press, New York, 1973.
7. R. A. A. Muzzarelli, Chitin, Pergamon, Oxford, 1977.
8. E. Deboer, H. van Willigen, Prog. Nucl. Magn. Reson. Spectrosc., 2, 111(1967); R. S. Drago, J. I. Zink, R. M. Richman, W. D. Perry, J. Chem. Educ., 51, 371(1974).
9. I. Solomon, Phys. Rev., 99, 559(1955).
10. N. Bloembergen, J. Chem. Phys., 27, 572, 595(1957).
11. R. Kh. Sabirov, Paramagn. Rezon., 12, 49(1976).
12. H. A. Bergen, R. M. Golding, L. C. Stubbs, Mol. Phys., 37, 1371(1979).
13. N. Bloembergen, L.O. Morgan, J. Chem. Phys., 34, 842(1961); A. Carrington, G. R. Luckhurst, Mol. Phys., 8, 125(1964); W. B. Lewis, L. O. Morgan, Transition

Metal Chemistry, Vol. 4, Dekker, New York, 1968.

14. H. M. McConnell, D. B. Chestnut, J. Chem. Phys., 28, 107(1958).
15. H. M. McConnell, R. E. Robertson, ibid., 29, 1361(1958).
16. W. D. Horrocks, Inorg. Chem., 9, 690(1970).
17. T. J. Swift, R. E. Connick, J. Chem. Phys., 37, 307(1962).
18. N. Bloembergen, Physica(Amsterdam), 15, 386(1949).
19. P-G. Gennes De, Phys. Chem. Solids, 7, 345(1958).
20. V. P. Chacko, S. Ganapathy, R. G. Bryant, J. Am. Chem. Soc., 105, 5491(1983).
21. T. Sandreczki, D. Onderchin, R. W. Kreilick, ibid., 101, 2880(1979).
22. T. Sandreczki, D. Onderchin, R. W. Kreilick, J. Magn. Reson., 34, 171(1979).
23. J. C. Irvine, J. C. Earl, J. Chem. Soc., 121, 2376(1922).
24. J. C. Irvine, D. McNicoll, A. Hynd, J. Chem. Soc., 99, 250(1911).
25. M.Bergmann, L. Zervas, Chem. Ber., 64B, 975(1931).
26. R. H. Holm, G. W. Everett, Jr., A. Chakravorty, Prog. Inorg. Chem., 7, 83(1966).
27. M. J. Adam, L. D. Hall, J. Chem. Soc. Chem. Comm., 1979, 234.
28. L. A. Nud'ga, E. A. Plisko, S. N. Danilov, Zh. Obshch. Khim., 43, 2752(1973).

29. S. Hirano, N. Matsuda, O. Miura, H. Iwaki, Carbohydr. Res., 71, 339(1979).

30. L. D. Hall, M. Yalpani, Carbohydr. Res., 83, C5(1980).

31. S. J. Opella, M. H. Frey, J. Am. Chem. Soc., 101, 5854(1979).

32. S. J. Opella, J. G. Hexem, M. H. Frey, T. A. Cross, Phil. Trans. Roy. Soc. A, 299, 665(1981).

33. D. M. Grant, B. V. Cheney, J. Am. Chem. Soc., 89, 5315(1967).

34. L. B. Alemany, D. M. Grant, R. J. Pugmire, T. D. Alger, K. W. Zilm, J. Am. Chem. Soc., 105, 2133(1983) and references therein.

35. S. Ganapathy, A. Naito, C. A. McDowell, J. Am. Chem. Soc., 103, 6011(1981).

36. D. W. Drummond, E. L. Hirst, E. Percival, J. Chem. Soc., 1962, 1208.

CHAPTER IV

EXPERIMENTAL

IV.1. Nuclear Magnetic Resonance

IV.1.1. Measurements in the Solution State

Most of spectra were measured at room temperature using a Bruker WH-400 (9.4 T) high resolution spectrometer equipped with an Aspect 2000 computer, operating at 400 MHz for ^{1}H and at 100.6 MHz for ^{13}C, and located in the Department of Chemistry, University of British Columbia. Some of the ^{1}H-n.m.r. spectra were also recorded at 270 MHz with a home-built spectrometer based on a Bruker WP-60 console, a Nicolet 1180 computer (32K), a Nicolet 293B pulse programmer, a Diablo disk drive (model 31), and an Oxford Instruments superconducting solenoid magnet with a 54 mm. bore size.

Samples for n.m.r. spectra were prepared in concentrations of 0.1 to 0.4 M. All deuterated solvents were obtained from Merck Sharp and Dohme Canada Ltd. and tetramethylsilane (TMS) was used as an external standard.

Data were accumulated in quadrature detection mode and stored on 1 Mbyte disks for subsequent processing. Prior to Fourier transformation, all the data were multiplied by an exponential line broadening function (0.1 Hz for ^{1}H and 0.5 Hz for ^{13}C).

IV.1.2. Measurements in the Solid State

All spectra were determined in the Fourier mode using a Bruker CXP-200 spectrometer, operating at the resonance

frequencies of 200 MHz for ^{1}H, 50.3 MHz for ^{13}C, and 30.7 MHz for ^{2}H. An Aspect 2000 computer was used to acquire the data.

^{13}C-C.p.-m.a.s. spectra were obtained at room temperature using a single-coil, doubly tuned probe. Spin-locked cross-polarization was established by the single-contact Hartmann-Hahn procedure, using applied ^{1}H and ^{13}C r.f. fields of 15 and 60 G, respectively. The proton decoupling field was maintained at 15 G using a 1 kW power amplifier. In general, a spectral width of 40 kHz, which sets up a computer-controlled filter bandwidth of 50 kHz, was observed in 16K data points using an approximate pulse angle of 90° (5 μs) and 4K acquisition. For diamagnetic organic solids and solid polymers, contact times were optimized by measuring the magnetization response to variable spin locking times (t_{cp}), when integration of the carbon resonances was desired. The settings, which varied from 0.5 to 5 ms, were much longer than those used for the paramagnetic counterparts ($t_{cp} \leq 0.5$ ms). A waiting time of 12 μs, with concomitant decoupling, between the end of the cross-polarization step and the start of data acquisition was used. The receiver was blanked until the start of data acquisition, and an acquisition time of 50 ms (one dwell time) was employed; at that time, the decoupling power was gated on. In most cases, many acquisitions (1,000-3,000 transients) were required to enhance the signal-to-noise ratio of low intensity peaks, and recycle times of 10-30 s

were used. Quadrature detection and phase alternated pulses ($90°_x$ and $90°_{-x}$) were included in the experiment. The latter technique was used to invert the proton spin temperature so as to eliminate experimental artifacts, and to simplify the data analysis. Magic angle spinning was carried out using an Andrew-Beams rotors made from Delrin. Its spinning frequency, estimated from the spinning sidebands, was 4.2 ± 0.3 kHz. The superconducting solenoid was operated without field-frequency lock because the drift was small enough to give accurate shift measurements. Thus, the ^{13}C-n.m.r. signal of liquid benzene was used as an external reference to determine the chemical shifts, which were subsequently expressed as p.p.m. downfield from TMS (benzene is 128.5 p.p.m. downfield from this reference). For accurate readings, in some cases, corrections were made to the observed chemical shifts by monitoring the drift periodically.

Initially, the nonspinning ^1H f.i.d. of benzene, contained in a 10-mm o.d. sample tube, was properly shimmed to afford a linewidth of 10-15 Hz. The decoupler offset was then set exactly on the proton resonance. Next, the ^{13}C-n.m.r. spectrum of benzene was acquired and stored on a disk. The Hartmann-Hahn condition was adjusted using a nonspinning sample of adamantane. Since this is a small, "spherical" molecule with a high mobility in the crystalline state, narrow linewidths are expected; as a result, adamantane undergoes relatively little cross-

polarization, but its signal is very sensitive to the Hartmann-Hahn match, which is useful for optimizing that condition. Hexamethylbenzene was chosen for the magic angle adjustment because it has two equal sets of carbons. The angle of the sample spinning axis relative to B_0 was adjusted to minimize the linewidth of the aromatic carbons, whose large chemical shift anisotropy makes them more sensitive to magic-angle missetting than the methyl carbons. Two isotropic peaks of almost equal intensity were observed when a longer spin locking time (5-8 ms) was set. Once the c.p.-m.a.s. conditions were satisfied, the rotor containing hexamethylbenzene was replaced. All experimental samples (200-300 mg) were spun with compressed air in the Delrin rotor.

^{2}H-N.m.r. spectra were recorded on the same instrument using a 10-mm o.d. sample tube and a quadrupole echo pulse sequence. The spectrometer was adjusted using a D_2O sample, and the r.f. field was then applied on resonance. In order to ensure minimum distortions of the spectra, phase corrections were alsc carried out. The r.f. pulse width varied between 2.5 and 6.0 μs, depending on the size of the spectral width. A pulse spacing of 100-240 μs, and recycle times of 0.5-1.0 s were used. All data were acquired in quadrature with a 0.25-MHz digitization rate. Since the experiments were performed on resonance, Fourier transformation resulted in the negative frequencies of the symmetric spectrum being folded over on top of the positive

frequencies, thereby increasing the signal-to-noise ratio by a factor of $\sqrt{2}$.[1] Even so, a great number of scans (10,000-50,000) were needed to give a good spectrum.

Most of the experiments were also performed as a function of temperature. The probehead and the air flow heating system provided by Bruker were used. The temperature at the sample was controlled with a flow of compressed air or N_2 gas, and stabilized with a Bruker temperature control unit (model B VT 1000), with a precision of roughly $\pm 1.5^{\circ}C$.

IV.2. General Synthetic Procedures

All melting points were recorded using a Fisher-Johns melting point apparatus and are uncorrected. All solutions were evaporated using a Buchi rotary evaporator. Thin layer chromatography (t.l.c.) was performed on 7.5 x 2.5 cm Baker-flex (J.T. Baker Chemical Co. N.J.) precoated silica gel plates. The following solvent systems were used: (A) 1:3 v/v methanol:ethyl acetate; (B) 1:4 v/v methanol:ethyl acetate; (C) 1:1 v/v toluene:ethyl acetate; (D) 1:4 v/v methanol:benzene. Visualization was effected by spraying with 30 % sulfuric acid in ethanol, and heating. All solvents used were of spectro or reagent grade and, in most cases, were used without further treatment. For reactions requiring anhydrous (dry) solvents, the solvents were dried by standard methods, then distilled and stored under a nitrogen atmosphere.

Microanalyses of the samples were carried out by Mr. P. Borda, Microanalysis Laboratory, University of British Columbia. Copper microanalysis was performed by Canadian Microanalytical Service Ltd. (Vancouver) using nitric acid digestion of the polysaccharides and atomic absorption. All ultraviolet measurements were performed using a Gilford Instrument (model 2530).

IV.3. Chapter II

IV.3.1. Sources of Materials

α- and β-cyclodextrins were purchased from Sigma Chemical Company, St Louis, MO. Sources for the chemicals, which were used as potential guest molecules for ^{13}C measurements, were as follows: benzene (Eastman); toluene (BDH Chemicals); ethylbenzene (Eastman); chlorobenzene (Matheson Coleman and Bell); bromobenzene (Eastman); p-xylene (Matheson Coleman and Bell); p-di-tert.-butylbenzene (Aldrich); biphenyl (Mallinckrodt); 4,4'-dimethylbiphenyl was prepared using the procedure of Gilman and Lichtenwalter;[2] cyclohexane (Matheson Coleman and Bell); methylcyclohexane (Aldrich) p-bromotoluene (Eastman); p-hydroxytoluene (Eastman); p-toluidine (Aldrich); benzoic acid (Mallinckrodt); pyridine (Mallinckrodt); durene (Aldrich); naphthalene (Aldrich). Dianin's compound [30] was kindly donated by Henmi Wong.

IV.3.2. Synthesis

Preparation of 2,6-di-O-Me-β-CD [3].

The title compound was prepared by adapting the procedure of Szejtli et al..[3] To a stirred solution of β-cyclodextrin (9 g) in 1:1 v/v DMSO-DMF (300 ml) was added gradually a mixture of BaO (78 g) and $Ba(OH)_2.8H_2O$ (78 g). The mixture was maintained below 20°C during the addition of dimethyl sulphate (100 ml) in small portions over a period of 2 h with intensive stirring. The mixture was stirred for another 4 d at room temperature and then warmed to 85°C for 30 min. After cooling, concentrated NH_4OH (105 ml) was added to decompose the excess dimethyl sulphate and the mixture was stirred for an additional 4 h at room temperature. The precipitate was allowed to settle into "clumps" overnight before decanting the filtrate. The solid was washed several times with chloroform to ensure maximum recovery of the product. The solution was then evaporated (temperature 60°C) to a thick syrup which crystallized on cooling. The crude product was dissolved in a minimum volume of chloroform and the solution passed through a column of silica gel (Kieselgel 60) previously equilibrated with the eluant, methanol-ethyl acetate (1:1 v/v). The purified compound [3] was then crystallized from hot water (85°C) to produce needle-like crystals in 70 % yield, m.p. 309-311°C (lit. value 310-312°C). Microanalysis, calculated: C 50.50, H 7.42, O 42.06; found:

C 50.50, H 7.50, O 42.00 %.

Preparation of 2,3,6-tri-O-Ac-β-CD [4].

Per-acetylation of β-cyclodextrin was carried out according to the procedure of Stoffyn et al..[4] β-Cyclodextrin (5 g) was added to a solution of acetic anhydride (25 g) in dry pyridine (32.5 g). The suspension was stirred at 48°C until the cyclodextrin had dissolved, and the solution was maintained at this temperature for 18 h. The solution was cooled and then poured with stirring into 100 ml of ice and water; the crude product precipitated out immediately. It was filtered, redissolved in chloroform (50 ml), and washed with saturated copper sulphate solution. The organic layer was then separated, dried over magnesium sulfate, and evaporated to a thick syrup (temperature 35°C). The syrup was dissolved in ethanol (10 ml) and again poured into ice and water to regenerate the pure precipitate. The product was suction filtered, washed with ice-cold water, and finally dried in vacuo at 56°C to achieve a 90 % yield, m.p. 150-152°C. Microanalysis, calculated: C 50.00, H 5.60, O 44.40; found: C 49.75, H 5.56, O 44.69 %.

Preparation of α-d_1-toluene (CH_2D-benzene).[5]

A solution of freshly distilled benzyl chloride (9 ml) in 20 ml of anhydrous ether was added to clean, dry magnesium turnings (2.5 g). The reaction was initiated by a

small crystal of iodine and the mixture was allowed to reflux gently. An additional 20 ml of ether was added and boiling under reflux was continued for 30 min. The reaction mixture was cooled in an ice-bath and deuterium oxide (10 ml) was added cautiously to the stirred mixture, followed by 30 % deuterium chloride-deuterium oxide solution (5 ml) before refluxing for another 1 h. The crude product was obtained by cooling the mixture prior to filtering off the precipitate. The solution was then distilled to give the α-d_1-toluene in a yield of 69.4 %, b.p. 109-111°C (lit. value 110.6°C).

Preparation of β-d_1-ethylbenzene.

(2-Bromoethyl)benzene (14.0 ml, 102 mmol) was used and the yield of β-d_1-ethylbenzene was 75.0 %, b.p. 133-135°C.

Preparation of α-CD-DMSO-d_6-H_2O complex.

Methyl sulfoxide-d_6 (0.5 ml, 7.0 mmol) was added to anhydrous α-cyclodextrin (0.5 g, 0.5 mmol) and with dropwise addition of water (2 ml) and heating, a saturated solution was obtained. Slow cooling at room temperature yielded colorless needle-like crystals which were then filtered by suction. Washing was done thoroughly with ice-cold water to remove the "free" methyl sulfoxide-d_6 molecules and the product was either air-dried for 24 h or dried in vacuo at room temperature.

Preparation of α-CD-DMSO-d_6-MeOH-H_2O complex.[6]

Anhydrous α-cyclodextrin (0.5 g, 5.1 mmol) was added to a solution of methyl sulfoxide-d_6 (1.0 ml, 14.1 mmol) and methanol (2.0 ml, 49.4 mmol). Gradually, water (2 drops) was added to give a saturated solution. The complex was allowed to crystallize in the freezer for 2 d before filtering and washing with ice-cold water. The needle-like crystals were dried by the procedure above.

Preparation of α-CD-Me_2CO-d_6-H_2O complex.

Acetone-d_6 (0.5 ml, 6.8 mmol) was added to the anhydrous α-cyclodextrin (0.5 g, 5.1 mmol) and the procedure for the analogous methyl sulfoxide-d_6 complex was followed.

Preparation of β-cyclodextrin inclusion complex.

β-CD-DMSO-d_6-H_2O complex was prepared from a solution of β-cyclodextrin (0.5 g, 0.4 mmol), methyl sulfoxide-d_6 (0.5 ml, 7.0 mmol) and water (7 ml) by adapting the procedure descibed for α-cyclodextrin. Colorless cubic crystals were formed during storage of the solution at room temperature for 1 d.

Similarly, β-CD-Me_2CO-d_6-H_2O complex was also prepared by this procedure.

Preparation of 2,6-di-O-Me-β-CD inclusion complexes.[7]

2,6-di-O-Me-β-CD-benzene complex was prepared as follows:

1) Benzene (2.5 ml, 28.0 mmol) was added gradually to the sugar (0.5 g, 0.4 mmol) with heating of the mixture. The complex was left to crystallize overnight from the concentrated solution, yielding rod-like crystals. The product was filtered, washed thoroughly with ice-cold methanol and dried in vacuo either at room temperature or at 56°C.

2) Addition of methanol (2.0 ml, 49.4 mmol) to the mixture of host molecule (0.5 g, 0.4 mmol) and benzene (0.5 ml, 5.6 mmol) and heating afforded the same product.

The second method, which is suitable for most guest molecules, was adopted for the synthesis of inclusion complexes with host molecules [3] and [4]. Furthermore, only minimum amounts of guest molecules (especially critical for deuterated samples) are required and the complexes readily separate from the solution as colorless crystals.

Preparation of 1,2:3,4-di-O-isopropylidene-6-O-p-tolylsulfonyl-α-D-galactopyranose.[8]

p-Toluenesulfonyl chloride (5.5 g, 28.8 mmol) was added to a solution of pyridine (15 ml) containing 1,2:3,4-di-O-isopropylidene-α-D-galactopyranose (2.5 g, 9.6 mmol) with stirring at room temperature. The reaction mixture was

allowed to stir for 24 h and then cold 2M-hydrochloric acid (50 ml) was added before extraction of the product with ether. The ethereal extract was further washed with acid (to remove any residual pyridine) followed by sodium bicarbonate solution until it was neutral. The ether was removed to afford a light yellow syrup (4.0 g, 9.7 mmol), which when crystallized from aqueous ethanol, gave colorless crystals in 85 % yield, m.p. 102-103°C (lit. value 104-105°C).

Similarly, 1,2:5,6-di-O-isopropylidene-3-O-p-tolyl-sulfonyl-*α*-D-glucofuranose was prepared in a high yield.

Preparation of 1,2:3,4-di-O-isopropylidene-6-O-p-tolylsulfonyl-*α*-D-galactopyranose-6,6'-d_2.

1,2:3,4-Di-O-isopropylidene-*α*-D-galactopyranose (7.0 g, 26.9 mmol) was oxidized to the corresponding acid (4.8 g, 17.5 mmol) using basic permanganate solution according to a procedure described in the literature.[9] The dried acid (2.0 g, 7.3 mmol) was then reduced by lithium aluminium deuteride in anhydrous tetrahydrofuran using the method of Brown et al.[10] to afford the crude starting material (1.8 g, 6.9 mmol), which is deuterated at the C-6 position. It was used without further purification to prepare the tosylated sugar. Recrystallization of the crude product from aqueous ethanol gave the desired compound (1.7 g, 4.1 mmol), m.p. 102-103°C.

IV.4. Chapter III

IV.4.1. Sources of materials

Materials for the studies described herein were either obtained commercially, or synthesized in this laboratory. Sources for chemicals were as follows: glucosamine hydrochloride (Sigma); carbobenzoxy chloride (Aldrich); anisaldehyde (Eastman); salicylaldehyde (Eastman); 5-bromo-2-hydroxybenzaldehyde (Eastman); zinc acetate (Fisher); cupric acetate (Fisher); chitosan (Sigma); benzaldehyde (Eastman); p-nitrobenzaldehyde (Matheson Coleman and Bell); sodium alginate (Kelco). The spin-labelled sugar complex [17] existed as a pure stock sample in the laboratory.

IV.4.2. Previous Work

The monosaccharide syntheses have either been documented in our own laboratory or reported elsewhere. A brief summary will be given, and any changes in the procedures will be noted.

The glycoside methyl 3,4,6-tri-O-acetyl-2-amino-2-deoxy-β-D-glucopyranoside hydrobromide [3] was prepared by a combination of methods from Chargaff,[11] Gross,[12] and Irvine and Earl.[13] First, the carbobenzoxy derivative of glucosamine was prepared according to the recipe of Chargaff;[11] one equivalent of glucosamine hydrochloride was added to two equivalents of sodium bicarbonate in water, followed by portion-wise addition of one equivalent of

carbobenzoxy chloride (CBZ chloride). The precipitated product was filtered and dried to afford a yield of about 95 %. Next, the glycosyl bromide was prepared by the method of Gross et al..[12] A mixture of acetic acid and acetic anhydride/HBr (3:2 by weight) was added in portions to the CBZ glucosamine at 0°C and, after 30 min, HBr gas was bubbled rapidly through the reaction mixture until the temperature was raised by about 10°C. Ether was added and after refrigeration for a few hours to induce further crystallization, the product was filtered. The glycosyl bromide was then recrystallized from chloroform/ether. The methyl glycoside was finally obtained following the procedure of Irvine and Earl.[13] A 5 % solution of the glycosyl bromide in anhydrous methanol containing 1 % of dry pyridine, was allowed to stand overnight. The mixture was evaporated to a small volume and ether added. Upon refrigeration the crude methyl glycoside was obtained. It was then filtered, dried and used without further purification.

The tetra-O-acetyl-glucosamine derivative [4] was prepared by the method of Bergman,[14] using anisaldehyde as the amino protecting group. The Schiff's base was formed by combining glucosamine hydrochloride and anisaldehyde in water with one equivalent of sodium bicarbonate. The compound precipitated readily on vigorous stirring and was then filtered and dried. The next step involved the acetylation of this material in a 1:1 v/v mixture of acetic

anhydride and pyridine to yield the tetra-acetate. The Schiff's base was then cleaved in a dilute solution of HCl in aqueous acetone. The unhydrolyzed, sugar acetate starting material and anisaldehyde were then extracted with chloroform. Sodium bicarbonate was then added to the aqueous layer until it was neutral before extracting again with chloroform to give the "free" amino sugar. The starting material, which was recovered from the first chloroform extraction, was treated again with acid and the extraction scheme was repeated. The crude product was then recrystallized from aqueous ethanol-water mixture; m.p. 137-139°C.

The sugar salicylaldimines [5] and [6] were readily prepared by adapting the method of Irvine and Earl.[15] Salicylaldehyde was added to the appropriate amino sugar in aqueous methanol, with one equivalent of sodium bicarbonate added in the preparation of the former compound. The reaction mixtures were stirred vigorously for a few hours before filtering the products. Recrystallization from either ethanol or methanol gave the pure compounds in greater than 70 % yield.

Preparation of Schiff's base metal complexes [12], [13], and [15].

The Schiff's base metal complexes from ligands [5] and [6] were readily prepared by the original method of Schiff and repeated by reference to Holm.[16] The ligands were first

dissolved in hot ethanol and an ethanolic solution of the appropriate metal acetate added with stirring. On cooling, the metal-complex separated as fine crystals and the product was then filtered. Recrystallization from either acetone (complex [12]), acetone/chloroform (complex [13]), or ethanol (complex [15]) gave the pure compounds in good yields, except for the Zn(II) sugar complex.

Preparation of bis-{(-N-methyl 3,4,6-tri-O-acetyl-2-deoxy-β-D-glucopyranosyl-2-(4-bromo-salicylaldimino)}Cu(II) [16].

The copper(II) complex [16] was obtained in 85 % yield and was analytically pure when isolated directly from the reaction mixture. Slow crystallization from an acetone/ethanol mixture yielded dark brown cubic crystals, m.p. 243-244°C. Microanalysis, calculated: C 45.06, H 4.35, N 2.60; found: C 45.28, H 4.46, N 2.63 %.

N-Arylidenechitosan gels were prepared by the methods documented in our own laboratory.[17]

Preparation of [N-salicylidene] chitosan [19].

Purified chitosan (2 g, 12 mmol) was dissolved with stirring in a mixture (1:1 v/v, 120 ml) of methanol and 10 % aqueous acetic acid. To the resulting viscous solution was added with vigorous stirring, a methanolic solution (40 ml) of salicylaldehyde (1.4 ml, 14 mmol) followed by saturated sodium bicarbonate solution (8 ml). A thick gel

was formed within minutes and a further equal portion of salicylaldehyde in methanol was added, followed by methanol (320 ml) and sodium bicarbonate solution (4 ml). After 2 h the solvents were decanted and the rigid gel was broken up into smaller pieces. These were suspended in methanol (600 ml), ethanol (300 ml), and diethyl ether (300 ml) over a period of 1 d. The filtered, solid product obtained was first air-dried for several hours and finally dried in vacuo at 56°C. A bright yellow product with d.s. 1.0 was obtained (28 g). Microanalysis for $(C_{13}H_{15}NO_5)$ 0.5 H_2O, calculated: C 56.92, H 5.88, N 5.11; found: C 56.91, H 5.81, N 5.35 %.

Preparation of [mixed(N-benzylidene and N-salicylidene)] chitosan [20].

To chitosan (2 g, 12 mmol), dissolved in a mixture of methanol and 10 % aqueous acetic acid, was added with vigorous stirring, a methanolic solution (40 ml) of benzaldehyde (4 ml, 39 mmol). A saturated sodium bicarbonate solution (8 ml) was added and within minutes a very soft, colorless, and semi-transparent gel was formed. Salicylaldehyde (1.4 ml, 14 mmol) in methanol (40 ml) was added immediately resulting in a further stiffening of the gel, to which was then added methanol (320 ml) and sodium bicarbonate solution (4 ml). The "mixed" gel obtained was lighter in color compared with the pure (N-salicylidene) chitosan. The product, [20], had a

benzylidene-to-salicylidene ratio of 2:1 (estimated from ^{13}C-n.m.r. integration). Microanalysis for $(C_{13}H_{15}NO_5)_{0.33}$ $(C_{13}H_{15}NO_4)_{0.67}$ 0.7 H_2O, calculated: C 58.45, H 6.19, N 5.24; found: C 58.48, H 6.10, N 5.51 %.

Similarly, [N-(4-nitrobenzylidene)] chitosan [21] was prepared by condensing chitosan (2 g, 12 mmol) with p-nitrobenzaldehyde (2.1g, 14 mmol) to give a light brown, rigid gel within minutes (d.s. 1.0). Microanalysis for $(C_{13}H_{14}N_2O_4)$ 1.0 H_2O, calculated: C 50.00, H 5.16, N 8.97; found: C 50.00, H 4.92, N 8.85 %.

Copper complexation reactions

The wet gels (used without drying from the above preparations) were complexed by vigorous stirring overnight in a saturated, methanolic solution of cupric acetate. The fragmented gels were filtered, washed (500 ml methanol) and dried in vacuo at 56°C for 1 d. Copper determinations were obtained by nitric acid digestion of the chitosan samples followed by atomic absorption measurements.

References

1. J. H. Davis, K. R. Jeffrey, M. Bloom, M. I. Valic, T. P. Higgs, Chem. Phys. Lett., 42, 390(1976).
2. H. Gilman, M. Lichtenwalter, J. Am. Chem. Soc., 61, 957(1939).
3. J. Szejtli, A. Lipták, I. Jodál, P. Fügedi, P. Nánási, A. Neszmélyi, Stärke, 32, 165(1980).
4. P. J. Stoffyn, R. W. Jeanloz, J. Am. Chem. Soc., 80, 5690(1958).
5. H. C. Brown, G. A. Russell, ibid., 74, 3995(1952).
6. K. Harata, Bull. Chem. Soc. Jpn., 51, 1644(1978).
7. B. Casu, M. Reggiani, G. R. Sanderson, Carbohydr. Res., 76, 59(1979).
8. K. Freudenberg, R. M. Hixon, Ber., 56, 2119(1923).
9. H. Ohle, G. Berend, ibid., 58, 2577(1925).
10. H. C. Brown, P. M. Weissman, N. M. Yoon, J. Am. Chem. Soc., 88, 1458(1966).
11. E. Chargaff, M. Bovarnick, J. Biol. Chem., 118, 421(1937).
12. G. Fodor, L. Otvos, Ann. Chem., 604, 29(1957).
13. J. C. Irvine, D. McNicoll, A. Hynd, J. Chem. Soc., 99, 250(1911).
14. M. Bergmann, L. Zervas, Chem. Ber., 64B, 975(1931).
15. J. C. Irvine, J. C. Earl, J. Chem. Soc., 121, 2376(1922).
16. R. H. Holm, K. Swaminathan, Inorg. Chem., 2, 181(1963).
17. M. Yalpani, Ph. D. thesis, University of British

Columbia, (1980).

Appendix I

Dipole-Dipole Interaction of Nuclei

It is useful to transform the equation obtained for dipole-dipole interaction to spherical polar coordinates. Eq. [4] (see Chapter I) is obtained, where the six terms A to F are shown below:

$$H_{IS} = r^{-3}\gamma_I \gamma_S h^2 [A + B + C + D + E + F) \frac{\mu_o}{4\pi} \quad [4]$$

$$A = -I_{Iz} I_{Sz} (3\cos^2\theta - 1)$$

$$B = 1/4\{[I_{I+} I_{S-} + I_{I-} I_{S+}](3\cos^2\theta - 1)\}$$

$$C = -3/2\{[I_{Iz} I_{S+} + I_{I+} I_{Sz}]\sin\theta\cos\theta\exp(-i\phi)\}$$

$$D = -3/2\{[I_{Iz} I_{S-} + I_{I-} I_{Sz}]\sin\theta\cos\theta\exp(i\phi)\}$$

$$E = -3/4\{I_{I+} I_{S+} \sin^2\theta\exp(-2i\phi)\}$$

$$F = -3/4\{I_{I-} I_{S-} \sin^2\theta\exp(2i\phi)\}$$

Each of the terms A to F contains a spin factor and a geometrical factor.

Appendix II

The Effects of Rapid Sample Rotation

Several interactions of interest for n.m.r. of solids contain the term $(3\cos^2\theta - 1)$, where θ is the angle between a particular direction **r** (example, the distance between nuclei) and the static magnetic field $\mathbf{B}_o$. An example is the dipolar interaction between two nuclei, in which the expressions for terms A and B are given in Appendix I. It is necessary to know how such functions are affected by rapid sample rotation of about an axis fixed in space relative to $\mathbf{B}_o$.

Consider a unit vector OD in direction **r** rotating about axis **s**, which is inclined at angle β to the direction $\mathbf{B}_o$. Let the angle between **r** and **s** be α and the angle between **r** and $\mathbf{B}_o$ be θ. Then the required cosine is given by OB.

Now $OE = \cos\alpha$

$OA = OE\cos\beta = \cos\alpha\cos\beta$

Also $ED = \sin\alpha$

$EC = \sin\alpha\cos\phi$

$AB = \sin\alpha\sin\beta\cos\phi$ since $AEC = 90^\circ - AEO = EOA = \beta$

[note that the DEC plane is perpendicular to the plane containing $\mathbf{B}_o$ and **s**]

$OB = OA + AB = \cos\alpha\cos\beta + \sin\alpha\sin\beta\cos\phi$

In the case of rotation about **s** at rate ω, the angle $\phi = \omega t$

if **r** is in the plane of $\mathbf{B}_o$ and **s** at time t = 0. Thus $\cos\theta = \cos\alpha\cos\beta + \sin\alpha\sin\beta\cos\omega t$ at time t. Hence

$$\langle\cos^2\theta\rangle = \cos^2\beta\cos^2\alpha + 2\sin\beta\cos\beta\sin\alpha\cos\alpha\langle\cos\omega t\rangle + \sin^2\beta\sin^2\alpha\langle\cos^2\omega t\rangle$$

Now $\langle\cos\omega t\rangle = 0$ and $\langle\cos^2\omega t\rangle = 1/2$

$$\langle\cos^2\theta\rangle = \cos^2\beta\cos^2\alpha + 1/2\sin^2\beta\sin^2\alpha$$

$$= \cos^2\beta\cos^2\alpha + 1/2(1 - \cos^2\beta)(1 - \cos^2\alpha)$$

$$= 1/3 + 1/6(3\cos^2\beta - 1)(3\cos^2\alpha - 1)$$

$$\langle 3\cos^2\theta - 1) = 1/2(3\cos^2\beta - 1)(3\cos^2\alpha - 1)$$

[note that the extrema of the angle θ are clearly $\beta - \alpha$ and $\beta + \alpha$]